HIGH PRESSURE AND TEMPERATURE DEPENDENCE OF THERMODYNAMIC PROPERTIES OF MODEL FOOD SOLUTIONS OBTAINED FROM IN SITU ULTRASONIC MEASUREMENTS

By

ROGER DARROS BARBOSA

A DISSERTATION PRESENTED TO THE GRADUATE SCHOOL
OF THE UNIVERSITY OF FLORIDA IN PARTIAL FULFILLMENT
OF THE REQUIREMENTS FOR THE DEGREE OF
DOCTOR OF PHILOSOPHY

UNIVERSITY OF FLORIDA

2003

To Neila who made me feel reborn, and
To my dearly loved children Marina, Carolina and
especially Artur, the youngest, with whom
enjoyable times were shared through this journey

ACKNOWLEDGMENTS

I would like to express my sincere gratitude to Dr. Murat Ö. Balaban and Dr. Arthur A. Teixeira for their valuable advice, help, encouragement, support and guidance throughout my graduate studies at the University of Florida. Special thanks go to Dr. Murat Ö. Balaban for giving me the opportunity to work in his lab and study the interesting subject of this research.

I would also like to thank my committee members Dr. Gary Ihas, Dr. D. Julian McClements and Dr. Robert J. Braddock for their help, suggestions, and words of encouragement along this research. A special thank goes to Dr. D. Julian McClements for his valuable assistance and for receiving me in his lab at the University of Massachusetts.

I am grateful to the Foundation for Support of Research of the State of São Paulo (FAPESP 97/07546-4) for financially supporting most part of this project. I also gratefully acknowledge the Institute of Food and Agricultural Sciences (IFAS) Research Dean, the chair of the Food Science and Human Nutrition Department, the chair of Department of Agricultural and Biological Engineering at the University of Florida, and the United States Department of Agriculture (through a research grant), for financially supporting parts of this research. I am thankful to Dr. Miriam D. Hubinger, Dr. Florencia C. Menegalli and Dr. Antonio J. A. Meirelles, for the use of their laboratories at the Department of Food Engineering, at the State University of Campinas (UNICAMP), where some of the experiments at atmospheric pressure were conducted. I am indebted

to my colleagues at the Department of Food Engineering and Technology at Paulista State University (UNESP). My accomplishments could not have been achieved without their support.

I would also like to thank the staff and faculty of the Food Science and Human Nutrition Department (FSHN) and of the Department of Agricultural and Biological Engineering (AGEN), in particular the staff members of maintenance support (FSHN), and of the machine shop (AGEN), and the staff of the IFAS network computer office at the University of Florida for their help and support in many difficult situations. I am thankful to all my friends at the University of Florida, in special my friends at Dr. Balaban's lab for their friendship, many helpful discussions, and cooperation.

TABLE OF CONTENTS

page

LIST OF TABLES

LIST OF FIGURES

LIST OF SYMBOLS

a_{ij}	Regression coefficients (units as stated)
$a_{1,2,3}$	Coefficients in Equation 5-2 (units as stated)
A	Specific Helmholtz free energy (J kg^{-1})
A_i	Activity of species i
A_w	Water activity
C	Solute concentration (kg-solute m^{-3})
c_i	Regression coefficients (units as stated)
Cp	Isobaric specific heat capacity (J kg^{-1} K^{-1})
Cp^E	Excess molar heat capacity (J mol^{-1} $^oK^{-1}$)
Cp^m	Molar heat capacity (J mol^{-1} $^oK^{-1}$)
Cp_{ref}	Specific heat capacity of reference material (J kg^{-1} K^{-1})
Cp_{sa}	Specific heat capacity of sample (J kg^{-1} K^{-1})
dH/dt	Heat flow (J s^{-1})
dT/dt	Heating rate (^oC min^{-1})
f	Frequency (Hz)
G	Specific Gibbs free energy (J kg^{-1})
H	Specific enthalpy (J kg^{-1})
k	Reaction rate (s^{-1})
k'	Wave number
K	Reaction constant
$L_{P,T}$	Acoustic path length as a function of P and T (m)
$L_{Po,To}$	Acoustic path length at atmospheric pressure and 0^oC (m)
m	Mass (g or kg)
m_S	Solution molarity (mol kg-$water^{-1}$)
M_w	Molecular weight (kg $kmol^{-1}$)
n	Number of moles
$n_{i,j}$	Number of moles of component *i* or *j* respectively
$n_{1,2}$	Number of moles of component 1 or 2 respectively
P	Pressure (Pa)
P_o	Atmospheric pressure (Pa)
P_w^o	Water vapor pressure (Pa)
Q	General molar thermodynamic property
r_i	Regression coefficients (units as stated)
R	Universal molar gas constant (8.315 J mol^{-1} K^{-1})
S	Specific entropy (J kg^{-1} K^{-1})
$S_{\bar{X}}$	Sample standard deviation
t	Time variable in wave Equation 2-11 (s)
T	Temperature (K, otherwise as stated)

T'	Period (s)
u	Sound velocity (m s^{-1})
u_o	Sound velocity at atmospheric pressure and 0°C(m s^{-1})
U	Specific internal energy (J kg^{-1})
V	Volume (m^3)
$\dot{V}$	Specific volume (m^3 kg^{-1})
$\overline{V}$	Partial molar volume (m^3 mol^{-1})
V^{app}	Apparent molar volume (m^3)
V^E	Excess molar volume (m^3)
V^{id}	Ideal solution volume (m^3)
V^m	Solution molar volume (m^3 mol^{-1})
x	Space variable in wave Equation 2-11 (m)
$x_{i,j}$	Mole fraction of component *i* and *j* respectively
X_S	Solute mole fraction
X_w	Water mole fraction in the liquid phase
Y_w	Water mole fraction in the gas phase
$w_{1,2}$	Mass fraction of component 1 or 2 respectively
Z	Acoustical impedance (Pa s^{-1} m^{-1})

Greek Letters

α	Isobaric thermal expansion coefficient (K^{-1})
α'	Linear thermal expansion coefficient (K^{-1})
β	Coefficient of compressibility (Pa^{-1})
β'	Coefficient of linear compressibility (Pa^{-1})
β_T, β_S	Isothermal and isentropic compressibility respectively (Pa^{-1})
β'_S	Isentropic compression (m^3 kg^{-1} Pa^{-1})
$\overline{\beta}$	Partial compressibility (Pa^{-1})
β^E	Excess compressibility (Pa^{-1})
β^{id}	Ideal solution compressibility (Pa^{-1})
ΔG	Specific Gibbs free energy variation (J kg^{-1})
$\Delta G^{\neq}$	Free energy of activation (J mol^{-1})
$\Delta\overline{V}$	Partial molar volume variation (m^3 mol^{-1})
$\Delta V^{\neq}$	Volume of activation (m^3 mol^{-1})
ΔT	Temperature interval in Equation 4-8 (0.1°C)
Δt	Transit time for the propagation of ultrasound (s)
$\phi_{i,j}$	Molar volume fraction of component *i* or *j* respectively
γ_S	Adiabatic thermal pressure coefficient (Pa K^{-1})
γ_w	Activity coefficient of water
λ	Latent heat of water (J kg^{-1})
λ'	Wavelength (nm)
μ_i	Chemical potential of species i (J mol^{-1})
ξ	Particle displacement in wave Equation 2-11 (m)
ω	Angular frequency (rad)
ρ	Density (kg m^{-3})

Subscripts

$_{air}$	Air
$_{evap}$	Evaporated
$_{i,j}$	Components *i* and *j* of a binary solution
$_{o}$	Atmospheric pressure condition
$_{ref}$	Reference state
$_{S}$	Isentropic condition
$_{sa}$	Sample property
$_{T}$	Isothermal condition
$_{w}$	Water
$_{1,2}$	Components *1* or *2* of a binary solution

Superscripts

^{app}	Apparent property
^{E}	Excess function
^{id}	Ideal condition
^{i,j}	Exponent of mathematical models
^{m}	Molar property
^{o}	Pure component property
$^{\neq}$	Indicates activation state

Mathematical symbols

∂	Partial differential operator
Σ	Summation operator
≡	‘Equivalent to’ or ‘defined as’ operator; used in a mathematical expression to define a property in terms of thermodynamic quantities rather than an equality

Abstract of Dissertation Presented to the Graduate School
of the University of Florida in Partial Fulfillment of the
Requirements for the Degree of Doctor of Philosophy

HIGH PRESSURE AND TEMPERATURE DEPENDENCE OF THERMODYNAMIC PROPERTIES OF MODEL FOOD SOLUTIONS OBTAINED FROM IN SITU ULTRASONIC MEASUREMENTS

By

Roger Darros Barbosa

May 2003

Chair: Dr. Murat Ö. Balaban
Cochair: Dr. Arthur A. Teixeira
Department: Food Science and Human Nutrition

High-pressure treatment has been recognized for over a century as a potential food preservation technique because of its demonstrated ability to inactivate microorganisms without adverse effects on food quality. Recent developments in high pressure processing equipment technology have already brought into practice a number of successful commercial applications. Process development efforts are currently based mainly on observation of end effects from trial-and-error experimentation, and are further confounded by the inability to distinguish temperature from pressure effects because of the thermodynamic temperature rise that accompanies pressurization. The ability to predict such effects is further hampered by the complex composition of foods and by the fact that thermodynamic and transport properties, which govern the reactions and transformations taking place, are highly sensitive to pressure, temperature and food composition. The purpose of this research was to develop methodology for measurement

of sound velocity in liquid foods under high pressure treatments from which a number of important thermodynamic properties could be derived and determined as a function of pressure, temperature and composition.

An ultrasonic high-pressure measurement cell was developed and instrumented for use within the sample chamber of a prototype high-pressure treatment unit equipped with independent temperature- and pressure-monitoring and control instrumentation. Measurements were taken over a range of pressures up to 600 MPa and temperatures between 10^{o} and 30^{o}C with four different simulated liquid food systems (binary aqueous solutions of sucrose, glucose and citric acid at different concentrations, and pure water). The resulting sound velocity data along with atmospheric pressure data on density, specific heat capacity and thermal expansion coefficient were used to derive the important thermodynamic properties of specific volume/density, isentropic and isothermal compressibility and isentropic pressure thermal coefficient at elevated pressures. These results also led to an interpretation of the pressure-, temperature-, and concentration-dependence behavior of each property, allowing prediction of each property as a function of temperature, pressure and composition. The thermodynamic relationships of partial molar properties of solute and solvent in each solution have also led to a better understanding of the interactions between solute and solvent under the influence of pressure, temperature, concentration and solute type in model aqueous food systems. For predictive or numerical application purposes, regression coefficients were determined by fitting data to the appropriate model.

CHAPTER 1
INTRODUCTION

High-pressure treatment has been known as a potential food preservation technique for over a century. However progress has been relatively slow since Hite's first report on the subject (Hite 1899b). Important developments in high hydrostatic pressure equipment made it possible to subject foods to high-pressure treatments resulting in commercial success of the process, first in Japan in the early 1990s, then in Europe, and recently in North America. Despite the capability of high-pressure processing to preserve without compromising physical, nutritional, and sensory quality characteristics, predictions of the effects of high-pressure treatment are difficult. This also applies to generalizations for any particular type of food due to the complexity of foods and the possibility of changes and reactions that can occur under pressure. Yet, mathematical models capable of such predictions are a necessary first step for process design, optimization and control.

The ability of high-pressure treatment to kill vegetative microorganisms is widely known, even at low-temperature processing. The main advantages of high-pressure processing, when compared to other traditional food processing technologies, are retention of flavor, nutrients, and color. This is true only if the process is not conducted at high temperatures. Other important attributes are independence of product size and geometry, and instantaneous and uniform distribution of pressure, which reduces processing time, as opposed to conventional processes (e.g., thermal) where time/mass

dependency for mass and heat transfer are critical process variables and pose limitations. Moreover, there is the possibility of high-pressure processing in low-temperature applications with the same or even enhanced pressure effects, which causes even less heat damage for temperature-sensitive materials. In addition, there is no need for extra energy to maintain pressure once the system reaches a given processing pressure.

Negative aspects of high pressure include a poor understanding of the mechanisms and effects on foods and their constituents, and the generation of heat within the pressure vessel due to adiabatic heating upon pressure buildup. For example, in microorganisms, studies have shown that there is a change in the permeability of cell membranes, accompanied by a reduction in the liquid volume and consequently a decrease in the internal volume of the microbial cell. The physicochemical environment can adversely change the resistance of the microorganisms to pressure; consequently the interactivity of components is of great importance to determine the pressure mechanism and the subsequent reduction of viable cells. Furthermore, despite the effectiveness of high pressure on the destruction of vegetative cells of bacteria, molds, and yeasts, some bacterial spores are strongly resistant to pressure. Also, the effects on enzymes in general are not conclusive. Enzyme activity may increase or decrease, depending on the enzyme, its source, physicochemistry of the environment, and treatment conditions. Temperature variation within the food system during pressure treatment is non-isotropic because of pressure-induced adiabatic heating and depends on pressure, composition, and other factors such as vessel volume and initial and boundary conditions. In many cases, researchers did not examine these issues, which may affect inactivation kinetics and other pressure effects significantly.

Transformations in foods under high pressure can be irreversible or reversible, depending on the process; involved substances; environmental conditions; and the combination of pressure, temperature, and time of exposure. High-pressure treatment effects on food systems are highly dependent on the primary effects of pressure and temperature on the thermodynamic and transport properties of food systems, including their components and interactions. Some of the relevant thermodynamic properties of high-pressure processing are density, compressibility, the adiabatic pressure thermal coefficient, phase transition properties (e.g., boiling and melting point), solubility, and their changes. Pressure is a fundamental state variable that influences the values of those properties.

Pressure-dependence studies reveal information on the volume profile of the process, in the same way that temperature-dependence studies tell us something about the energetics of a process. Applying high pressure hastens reactions that reduce volume (by Le Chatelier's principle) and vice-versa. There is also a thermodynamic relation between volume changes and activation energy, due to changes in free energy. Change in volume for a given substance under an applied pressure depends on its compressibility. Since compressibility, like volume, is determined by the composite effect of intra- and intermolecular interactions, its value can be used to gain insight into these interactions. Compressibility is a macroscopic property, which is sensitive to solute-solvent interactions, and therefore can help to characterize hydration properties of solutes in solutions. In solute molecules, pressure affects ion pairs, hydrogen bonds, and hydrophobic interactions. The mechanism of pressure denaturation of proteins, for example, involves ionization and precipitation. However electrostriction also occurs,

corresponding to charge separation and dissociation of ionic interactions. Thus, solvation and electrostriction effects can be examined using volume-change studies of solutions under high pressure using models, and consequently giving more insight into these phenomena. Compressibility is an important property determined by the balance between attractive and repulsive forces. It enters into many pressure-dependent thermodynamic expressions, and is an essential parameter for the design and use of any high-pressure equipment. In fact, the adiabatic thermal pressure coefficient derived from volumetric and heat-capacity data under pressure supplies very useful information about the magnitude of adiabatic heating generated by the work of compression. Knowledge of this nonisotropic temperature rise is fundamental for optimizing high-pressure processing, especially if it is combined with thermal treatment to maximize safety and quality. Accurate data are needed of pressure and temperature dependence of thermodynamic and transport properties, coupled with reliable kinetic parameters for destruction of microorganisms, enzyme inactivation, nutrient retention or any other quality or safety attribute.

The effect of high pressure in thermodynamic properties such as density, compressibility, and the adiabatic-pressure thermal coefficient of food systems and their constituents are scarcely discussed in the literature. Therefore, the purpose of this study was to develop procedures and instrumentation for *in situ* measurements of thermodynamic properties during the pressurization process in an isostatic high-pressure unit. This study seeks to determine pressure and temperature dependence of thermodynamic expressions for specific volume (or density) and isentropic and isothermal compressibility of food-based model liquids and the effects of temperature

and composition near ambient temperatures. In addition, other thermodynamic expressions for isentropic thermal pressure coefficient, isobaric specific heat capacity, and isobaric expansivity are derived as a function of pressure and temperature. Research on high-pressure processing began as a qualitative trial-and-error process, focused on determining end effects in specific food products. Now it is evolving into a more systematic fundamental approach addressing pressure-dependence kinetics, thermodynamics, thermophysical properties, and modeling aspects, providing a basis for broadening its applicability. We hope that this study, together with numerous other *in situ* measurements, contributes to this endeavor.

CHAPTER 2
BACKGROUND AND LITERATURE REVIEW

Research on high-pressure treatment of foods has dealt almost exclusively with the effects on food systems *after* the pressure treatment. There is a lack of experimental data and basic concepts involving *in-situ* effects on thermodynamic and transport properties. This study deals primarily with modeling the influence of pressure on thermodynamic properties of food components. Therefore, most of the background information focuses on the thermodynamics of high-pressure science and technology and its fundamentals. Moreover, much of the research relevant to this field is related to nonfood systems, which brings about different approaches, equipment, and techniques sometimes difficult or impossible to apply to food materials. For this reason, some of the existing techniques and the fundamentals used to explore the effects of pressure on nonfood materials are highlighted. We also give a brief overview of some of the research on high-pressure technology for food processing and preservation to show some of the difficulties presented by the complexity of food materials.

High-Pressure Food Processing and Technology

Treatment of foods with high pressure is generally accomplished by compressing the medium (usually water mixed with lubricating oil) surrounding prepackaged foods in flexible or semi-rigid vacuum-sealed containers. In this manner, high hydrostatic pressure for food processing in the range of 100 to 1000 MPa (600-800 being considered the maximum for economic feasibility) is generated through direct or indirect

compression (depending mainly on the maximum operating pressure, vessel volume, and frequency of operation) of the pressure transmitting fluid in thick-walled, cylindrical vessels made of low-alloy steel (Deplace and Mertens 1992; Hori et al. 1992; Kanda et al. 1992; Traff and Bergman 1992; Mertens and Deplace 1993; Zimmerman and Bergman 1993; Mertens 1995; Ting and Farkas 1995; Olsson 1997; Vardag and Korner 1997; Freeman 1997, 1998). In the case of direct, piston-type compression, the pressure medium is directly compressed by a low-pressure piston-driven pump at one end. According to the hydraulic principle, the desired high pressure results at the small diameter vessel end of the piston. The indirect concept uses a high-pressure intensifier pump (using the same hydraulic principle) to pump the pressure medium into the closed vessel until the desired pressure is achieved. The direct method delivers very fast compression (a few seconds), but is limited by the high-pressure dynamic seal between piston and internal vessel surface. The indirect compression method requires only a static high-pressure seal in the vessel (Mertens and Deplace 1993). Most industrial and laboratory-scale high-pressure systems use the indirect pressure-generation concept (Traff 1998). A production cycle includes loading the product into the chamber, pressurizing, dwell time (typical range 1 to 30 minutes), depressurizing, and product unloading (Deplace 1995). This process can be made semicontinuous by using alternating cycles in a series of pressurization chambers for greater capacities (Moreau 1995; Bignon and Lebas 1997; Morris 2000). Vessel volumes may vary from a few milliliters in laboratory units to several hundred liters in large commercial systems (Olsson 1995). Indirect heating and cooling capability through an external circulating jacket is possible, although slow thermal responses are expected because of vessel

thermal inertia and the small heat-exchange surface between vessel and pressure medium. Internal cooling/heating sources or conditioning of the pressure medium may be a choice, but sophisticated and complex solutions are more likely (Colman 1997). Only a few reports have been documented on continuous high-pressure systems as prototype equipment (Itoh et al. 1996a; Sionneau et al. 1997).

Although high-pressure technique for food processing and preservation already has a number of commercial applications, limitations related to data comparison and complexity associated with understanding interactive components of the process limit full acceptance of the method (Eley 1992; Mozhaev et al. 1994; Earnshaw et al. 1995; Hayashi 1995; De Cordt et al. 1997; Smelt 1998; Knorr 1999a; Farkas and Hoover 2000; Linton and Patterson 2000; Tewari 2000; Dunne and Kluter 2001; Smelt et al. 2002). Furthermore, predictions of the effects of high pressure are difficult as are generalizations for any particular type of food (Palou et al. 1999). Nevertheless, a considerable amount of information has been generated, and evidence exists on the end effects of high pressure on food systems, including microbial inactivation, chemical and enzymatic reactions, and the structure and functionality of food components.

The Role of Water in Food Systems under Pressure

Water is the major constituent of many food products, which can be described as aqueous solutions; dispersions; or suspensions of proteins, carbohydrates, lipids, inorganic salts, organic acids (etc.) and their mixtures. The characteristics, behavior, and interaction of water with solutes under pressure are very important (Fennema 1996; Palou et al. 1999). Water molecules, consisting of dipoles of two hydrogen atoms attached to an oxygen atom, form a unique, extensively hydrogen-bonded network with localized and structured clustering, with a number of anomalous properties. These anomalies have

been explained by dynamic equilibrium of open low-density and condensed higher-density structure bending, but not breaking, some of the hydrogen-bonds (Chaplin 1999; Symons 2001). This two-state structural model for water, with its interconverting mechanism between a cavity form capable of enclosing small solute molecules and another form able to collapse because of competition of bonded and nonbonded molecules, explains many of water's anomalous properties including its temperature-density and pressure-viscosity behavior; and the solvation and hydration properties of ions, hydrophobic molecules, carbohydrates and macromolecules (Chaplin 1999). Functionality of water is attributed to its two proton donor sites and two proton acceptor sites, while cooperativity is determined by the strength of hydrogen bonds which depends on the number of such bonds (Symons 2001). Many properties of water change with pressure according to an initial breaking of hydrogen-bonded structures, reducing the structure (Bridgman 1931). Water influences the structure, appearance, and taste of foods and their susceptibility to spoilage. From a chemical and physical standpoint, water is an excellent solvent because of its polarity, high dielectric constant and small size; its behavior as a carrier of solutes, a reactant and reaction medium, a lubricant and plasticizer, a diffusion medium, a stabilizer of biopolymer conformation; and because it probably facilitates the dynamic behavior of macromolecules, including their catalytic (enzymatic) properties (Cheftel 1992; Tauscher 1995). Because of the complexity of foods and interactions between food components and preservation or biophysical-chemical-transformation factors, the role of water may not be easily identified in some cases (Palou et al. 1999). Thus, in high-pressure food processing, if pressure and temperature affect water properties, changes in density, compressibility, surface tension,

viscosity, thermal properties, dipole moment, dielectric constant (which are all solute-solvent sensitive) are expected with their related consequences on food structure and stability. The presence of different solutes has varying effects on physicochemical properties of the solution. Solutes interfere with cluster equilibrium by favoring either open or collapsed structures. Any of these effects, which are pressure and temperature sensitive, will cause the physical properties of the solution, such as density, compressibility or viscosity, to change. Also, water is a more reactive environment when the extent of hydrogen bonding is reduced by pressure toward unstructured water (Ludemann 1992). Local clustering will be affected by the presence of solutes, thus changing the nature of water and making solutions to behave non-ideally. However, the extension of these pressure effects on the structure of aqueous solutions and its consequences to pressure processing of foods is still to be determined.

High Pressure as a Preservation Process for Foods

The ability of high pressure to inactivate microorganisms was first demonstrated more than 100 years ago by Roger (1895). A few years later, Hite and co-workers (Hite 1899a; Hite et al. 1914) demonstrated the microbial shelf stability of milk, meat and fruit products by using high pressure as a food preservation method. As a preservation technique high-pressure processing is primarily based on reducing the microbial load to prevent growth in populations of food-spoilage and pathogenic microorganisms. The preservation of other quality attributes is also a concern (Farr 1990; Cheftel 1991; Mertens and Knorr 1992; Tewari et al. 1999; Knorr 1999b; Cano et al. 1999; Palou 2000). Other important applications aim to improve quality and process efficiency by means of pressure-shifting phase transitions (Knorr et al. 1998; Hayashi et al. 1998).

Researchers have shown that high pressure inactivates microorganisms by inducing changes to the morphology, biochemical reactions, genetic mechanisms, and cell membranes (Hoover et al. 1989; Earnshaw et al. 1995; Isaacs et al. 1995; Smelt 1998; Abe et al. 1999; Farkas and Hoover 2000; Smelt et al. 2002; Brul 2002). Resistance of microorganisms to high pressure varies greatly as shown by a number of experimental works, and reduction of microbial loads is directly related to the level of hydrostatic pressure applied (as well as temperature, which is also pressure-dependent due to adiabatic heating), type and growth phase of microorganism, food matrix, and environmental conditions (e.g., physicochemical and synergistic factors) (Aleman et al. 1994; Arroyo et al. 1997; Linton and Patterson 2000; Farkas and Hoover 2000; Furukawa et al. 2002; He et al. 2002; Ludwig et al. 2002). Kinetics of pressure inactivation observed with different microorganisms varies from first order, to a change in slope, to a two-phase pattern, to even more complex kinetics, depending on the food system, microorganism, and experimental conditions (Earnshaw 1995; Heinz and Knorr 1996; Palou et al. 1997b; Ludwig and Schreck 1997; Braddock et al. 1998). Spores of bacteria have been identified as the most resistant form of microorganisms, requiring either higher pressures or combination with other treatments, such as moderately high temperatures (Hayakawa et al. 1994b; Takeo et al. 1994; Balasubramaniam 1999), modified atmosphere containing CO_2 (Enomoto et al. 1997a; Enomoto et al. 1997b; Ballestra and Cuq 1998; Park et al. 2002; Corwin and Shellhammer 2002), lytic enzymes such as lysozyme (Lechowich 1993), freezing pre-treatment, and gamma irradiation (Gould and Sale 1972). These factors would sensitize bacterial spores by induced germination, cell-wall weakening, internal vital solute extraction, and pH decrease (caused by carbonic

dissociation in the case of CO_2), consequently reducing pressure resistance. Inactivation of bacterial spores is of special interest for the sterilization of low-acid foods, as opposed to acid foods (fruit juices and jams, yogurt, and acidified meats) where the low pH would act as inhibitor for bacterial growth.

Studies have shown that some food constituents and their interactions have a positive baro-protective effects on natural microbial flora, as opposed to studies using buffer solutions or laboratory media containing pure cultures (Calik et al. 2002; Castellari et al. 2000; Ganzle et al. 2001). In other studies, substances such as trehalose, sucrose, glucose, and sodium chloride caused enhanced synergistic protective effects; while others like glycerol, citrate salts, and sorbic acid weakened the pressure inactivation of microorganisms (Ogawa et al. 1990; Hayakawa et al. 1994a; Tauscher 1995; Earnshaw et al. 1995; Iwahashi et al. 1997; Palou et al. 1997a). There is also experimental evidence that pressure sterilization conditions can be improved further when processing is done at low temperature, including sub-zero temperatures (Hashizume et al. 1995, 1996; Hayashi et al. 1998). Pulsed pressure treatment has also been used to increase microbial inactivation (Aleman et al. 1996; Itoh 1996; Hayakawa et al. 1997; Yuste 2001). At present, it is difficult to see why and how all these synergistic effects of pressure, temperature, and component interactions may enhance or weaken the pressure inactivation of microorganisms. We lack primary knowledge of how pressure influences physical and chemical properties of food systems and their constituents. Earnshaw (1995) suggests that these compound effects could be partially explained in terms of modification of dissociation properties under pressure, since volume reduction of water causes strong perturbation of electron cloud distribution around ionized molecules (a

phenomenon known as electrostriction). As water is much more densely packed around the ions than around the corresponding undissociated molecules, weak acids ionize, increasing the number of formal charges. So when charges are created, substantial volume contraction occurs due to solvation effects or electrostriction of water molecules around the ions as pressure favors the ionized form (Hui Bon Hoa et al. 1992). This has profound effects on water hydration and ionization. One consequence is a significant shift in pH equilibrium during pressurization. Accurate models relating to microorganisms or other transformations in food systems are yet to be developed (Smelt et al. 2002). In addition, indirect pH measurements reveal discordance in the magnitude of pH shift due to pressure, and direct measurement under pressure presents a number of technical problems that currently prevent this approach (Hayert et al. 1999). For accurate control of the treatment intensity required for the desired microbial reduction, numerical models of heat transfer can be used that must consider the pressure and temperature dependence of thermophysical properties of foods.

End Effects of High Pressure on Foods and Food Components

The effect of high-pressure processing on food itself is another area of interest and concern. High pressure may modify structure/functionality of proteins and alter enzyme activity; induce changes in phase transitions (e.g., reversibly increase the melting point of lipids, or decrease melting point of ice); and break down biomembranes. The behavior of food systems under the influence of high pressure is governed by Le Chatelier's principle, which predicts that the application of pressure shifts equilibrium toward the state that occupies a smaller volume, hence favoring processes associated with negative changes of volume.

Proteins and macromolecules. As early as the beginning of the twentieth century, Bridgman (1914) reported that egg-white albumen coagulated under high pressure just as by the application of heat. However, denaturation of proteins is understood to be distinctly different to that induced by heat treatment. Pressure is thought to break up mainly the hydrophobic and electrostatic (ion pair and polar-group bond) interactions; and hence, at sufficiently high pressure causes the unfolding, either completely or partially, of the proteins (Hayakawa et al. 1996; Mozhaev et al. 1996b; Iametti et al. 1998; Smith et al. 2000). In contrast, heat induced denaturation causes the formation and destruction of covalent bonds potentially producing off-flavors. The type of protein gelling and cross-linking of starches that high-pressure treatment induces may make the process unsuitable for some types of food although these same properties may also be used to enhance products, such as seafood and meat products, or alter macromolecule functionality (Galazka et al. 1995; Douzals et al. 1996; Messens et al. 1997; Hinrichs and Kessler 1997; Fernandes et al. 1998; Hayashi et al. 1998; Stolt et al. 1999; Heremans et al. 1999; Saldo et al. 2000; Lullien-Pellerin et al. 2001). The interplay between macromolecules and high pressure has also driven research into whether it can be used to tenderize/enhance meat/muscle by accelerating reactions of naturally occurring proteases, along with noticeably cooked appearance and other side effects (Ko et al. 1991; Ohshima et al. 1992; Ashie and Simpson 1996; Dumoulin et al. 1998; Ashie and Lanier 1999; Ashie et al. 1999; Hsu and Ko 2001). Apart from a food constituent, the study of proteins under the influence of high pressure has become widespread from a structural and functional point of view, since pressure is considered as an elegant and clever way to disturb their conformational equilibrium without breaking covalent bonds (Isaacs 1981;

Masson 1992; Gekko 1992; Dumay et al. 1994; Funtenberger et al. 1995; Heremans 1995; Paci and Marchi 1996; Kharakoz 1997; Smeller and Heremans 1997b, 1997c; Prehoda et al. 1998; Pares et al. 2000).

Enzymes. Food enzymes may catalyze deteriorative reactions with subsequent loss of quality attributes, such as color (e.g., browning in fruits, vegetables and mushrooms, caused by polyphenoloxidase and peroxidase), appearance (e.g., cloud loss in citrus juice by pectinesterase), nutritional (e.g., destruction of essential fatty acids and production of free radicals by lipoxygenase), and sensory (e.g., flavor and texture changes in meat products by transglutaminase). The effect of high pressure on enzymes and enzyme activity is more complex in that they can be completely and irreversibly inactivated, completely and reversibly inactivated, partially and irreversibly inactivated, and, partially and reversibly inactivated, depending on the enzyme, source, substrate, and environmental conditions such as pressure, temperature, pH, physico-chemistry, presence of salts, sugars (Kunugi 1992; Asaka et al. 1994; Anese et al. 1995; Mozhaev et al. 1996a; Seyderhelm et al. 1996; Cano et al. 1997; Hendrickx et al. 1998; Weemaes et al. 1998b; Indrawati et al. 2000). Only at sufficiently elevated pressure, or combined with moderate temperature, are enzymes completely and irreversibly inactivated. Pressure dependence of enzyme activity differs significantly not only in barostability but also in susceptibility to protective effects (Weemaes et al. 1997; Athes et al. 1998; Ludikhuyze et al. 1998a; Weemaes et al. 1999b; Van den Broeck et al. 1999; Lee and Park 2002). These combined and synergistic effects are not accurately accounted for without the understanding of how pressure influences physical and chemical properties of food systems and their constituents. Kinetics of pressure-temperature enzyme inactivation can

often be described by first order (traditional single step reaction), two or more isozymes (differing in their pressure or thermal resistance following different reaction steps), sometimes identified as biphasic behavior (labile and stable fraction but still first order for each step), consecutive steps (succession of irreversible reaction steps), or fractional conversion models (Ludikhuyze et al. 1997; Goodner et al. 1998; Weemaes et al. 1998a; Ludikhuyze et al. 1998b; Ludikhuyze et al. 1999; Indrawati et al. 1999; Weemaes et al. 1999a; Van den Broeck et al. 2000; Stoforos et al. 2002). The latter model is used when a resistant fraction remains after an inactivation process. There are also situations where antagonistic effects of pressure and/or temperature reveal food quality related problems. In these cases, the remaining enzyme activity is the limiting preservation factor which defines whether refrigeration or other combined preservation technique would be needed. Kinetic parameters describing the pressure and temperature dependence of inactivation rate and constant are of key importance for design and optimization of combined high-pressure/temperature processing for food preservation.

Phase transitions**.** Application of high pressure results in reversible crystallization of certain triglycerides and elevation of the melting point of lipids. For instance, chocolate tempering would be favored by exploiting this effect (Yasuda and Mochizuki 1992). The transition temperature of the lipids depends on the length of the hydrocarbon chain as well as the degree of unsaturation, whereas the rate of change with pressure is almost independent of the length. The freezing and melting point of water can be lowered with increasing pressure to a minimum of -22^{o}C at 207.5 MPa, given that pressure opposes the increase in volume (by the Le Chatellier principle) occurring on the formation of type I ice (regular ice) (Bridgman 1912). At about 900 MPa water may

freeze at room temperature (20^{o}C), forming ice VI with density of approximately 1,310 kg m^{-3} (Wagner et al. 1994). The occurrence of other ice polymorphs involves a similar or smaller increase in density relative to the liquid state which is governed by pressure and temperature conditions along with the water phase diagram. It is possible to obtain certain ice forms with the aid of nucleating agents specific to each form, such as ice III or ice IV (Knorr et al. 1998). It is also important to mention that the presence of solutes in food materials will result in a melting point depression. In addition, high pressure facilitates supercooling, and promotes uniform and rapid ice nucleation and growth throughout the sample upon pressure release, producing smaller ice crystals, rather than a stress-inducing ice moving front in heat transfer driven freezing processes (Kalichevsky et al. 1995). The interplay between the various phase diagram pathways and different pressure and temperature combinations has motivated research on high pressure-assisted freezing and thawing of foods (Deuchi and Hayashi 1992; Fuchigami and Teramoto 1996; Denys et al. 1997; Schlueter et al. 1998; Rouille et al. 2002; Li and Sun 2002). Because of the large heat of crystallization released as ice is formed, freezing has a warming effect, and therefore additional cooling of the sample would be required to enable complete freezing to occur. The opposite effect is expected during decompression, which in turn requires heat supply to prevent recrystallization during pressure-assisted thawing processes (Kalichevsky et al. 1995). Faster freezing and thawing rates are anticipated with the use of high pressure, along with energy savings and quality improvement, especially regarding solid foods for minimal tissue damage and drip loss, although side effects that are difficult to control on certain food components may be of concern (see previous paragraphs) (Fuchigami et al. 1996; Hayashi et al. 1998;

Zhao et al. 1998; Otero et al. 2000; Fernandez-Martin et al. 2000). Better exploitation of phase transitions in high-pressure food processing requires more studies on the kinetics of ice nucleation, crystal size, distribution and growth, recrystallization, and changes of thermodynamic properties during phase transitions.

Thermodynamics of High Pressure

Pressure primarily affects the volume of a system in such a manner that all matter, regardless of its thermodynamic state, suffers a reduction of volume upon application of pressure, even though the effect is much greater for gases than it is for condensed matter, liquids and solids (Bridgman 1931). Expressing this change in volume using thermodynamic notation produces

$$\left(\frac{\partial V}{\partial P}\right) < 0 \qquad [2\text{-}1]$$

Compressibility

The amount of contraction is governed by the compressibility, which is dependent on the intermolecular forces acting within the substance, that is, it is the result of the balance between attractive and repulsive potentials (Isaacs 1981). Compression results in decreasing the average intermolecular distance and reducing rotational and translational motion. Compressibility, an intrinsic physical property of the material defined by Equation 2-2, decreases from gases (order of magnitude 10^{-5} - 10^{-6} Pa^{-1}) to liquids (10^{-6} - 10^{-10} Pa^{-1}) with the greatest variability, to solids (10^{-10} - 10^{-12} Pa^{-1}).

$$\beta \equiv -\frac{1}{V}\left(\frac{\partial V}{\partial P}\right) = \frac{1}{\rho}\left(\frac{\partial \rho}{\partial P}\right) \qquad [2\text{-}2]$$

Compressibility of liquids decreases with pressure, since the initial ‘free volume’ has largely disappeared, and the repulsive potential is stronger than the attractive at high

pressures. For most liquids compressibility increases with temperature given that thermal expansion increases the internuclear distances (increase in 'free' volume). Once more, water is an exception and its isothermal compressibility decreases with temperature passing through a minimum around 46^{o}C (Kell 1974).

Adiabatic Thermal Pressure Coefficient

Upon compression of a liquid, heat is evolved due to the work of compression against repulsive intermolecular forces. Once a substance experiences a positive thermal expansion, this temperature rise increases the volume and affects the value of compressibility. Therefore, compressibility can be obtained either isothermally β_T or isentropically β_S, i.e. reversibly and adiabatically. The magnitude of this temperature rise is given by the adiabatic thermal pressure coefficient (Rowlinson and Swinton 1981). Since the process is reversible and isentropic, it follows that:

$$\gamma_S \equiv \left(\frac{\partial P}{\partial T}\right)_S \qquad [2\text{-}3]$$

Expanding the expression above, since change in entropy with temperature are related to heat capacity, and applying Maxwell's equation (see appendix A for details) and the definition of volumetric thermal coefficient, Equation 2-4 is obtained. Thus, by knowing the amount of compression, isobaric heat capacity and thermal expansion as a function of pressure and temperature, it is possible to quantify the adiabatic heating from a given starting temperature. This temperature rise is accompanied by a dissipation of heat within and through the pressure vessel, which is dependent on the rate of compression, vessel size, initial and boundary conditions, and heat transfer parameters.

$$\gamma_S = -\frac{\left(\frac{\partial S}{\partial T}\right)_P}{\left(\frac{\partial S}{\partial P}\right)_T} = \frac{C_P}{TV\dot{\alpha}} \qquad [2\text{-}4]$$

Isobaric Heat Capacity and Thermal Expansion Coefficient

Equations 2-5 and 2-6 below represent the definitions of the isobaric heat capacity and the coefficient of thermal expansion.

$$C_P \equiv \left(\frac{\partial H}{\partial T}\right)_P \qquad [2\text{-}5]$$

$$\alpha \equiv \frac{1}{V}\left(\frac{\partial V}{\partial T}\right)_P = -\frac{1}{\rho}\left(\frac{\partial \rho}{\partial T}\right)_P \qquad [2\text{-}6]$$

The pressure dependence of the isobaric heat capacity can be derived from basic thermodynamic relationships, differentiation rules, and the definition of isobaric heat capacity; the end result is given by the following expression (see derivation on Appendix A), which can be further combined with the definition of the coefficient of thermal expansion (Equation 2-6).

$$\left(\frac{\partial C_P}{\partial P}\right)_T = -T\left(\frac{\partial^2 V}{\partial T^2}\right)_P = -\frac{T}{\rho}\left[\alpha^2 + \left(\frac{\partial \alpha}{\partial T}\right)_P\right] \qquad [2\text{-}7]$$

The change of isobaric thermal expansion coefficient with pressure is the complement of the change of isothermal coefficient of compressibility with respect to temperature, and then Equation 2-8 is found (see derivation in Appendix A).

$$\left(\frac{\partial \alpha}{\partial P}\right)_T = -\left(\frac{\partial \beta_T}{\partial T}\right)_P \qquad [2\text{-}8]$$

The complex variation of the pressure dependence of isobaric heat capacity is not easily interpreted in terms of physical changes in the liquid, where specific interactions

may occur depending on the nature of the liquid. For some organic liquids, specific heat capacity shows a decrease with pressure up to 200-300 MPa, and beyond this point it behaves erratically; water also behaves irregularly (Isaacs 1981). Thermal expansion of liquids usually decreases with pressure, water below 40^{o}C being an exception besides a very anomalous behavior in the pressure range from atmospheric to 1,000 MPa (Bridgman 1931).

The relationship between isentropic and isothermal compressibility is given by Equation 2-9; the derivation can be found in appendix A. Upon adiabatic compression, the temperature rises and the volume change for unit pressure increases, consequently the compressibility is less than that under isothermal condition.

$$\beta_T = \beta_S + \left(\frac{\alpha^2 T}{C_P \rho} \right) \qquad [2\text{-}9]$$

Speed of Sound

A key thermodynamic property for the present study is the speed of sound, which is linked to isentropic compressibility and density (or specific volume) by means of the Newton-Laplace[1] Equation 2-10. Therefore, a number of thermodynamic functions can be derived by measuring the speed of sound over a range of pressures and temperatures, since it is a simple function of the derivative of density over pressure and, also the second derivative of the free energy over pressure. By measuring $u(P,T)$, one can obtain $\rho(P,T)$, $V(P,T)$, which allows calculation of any thermodynamic function.

[1] **Newton-Laplace equation**. This equation is also called the Wood equation since he first demonstrated in 1941 the independence of the sound velocity to frequency for homogeneous liquid and gases, while others just called it the Laplace equation (Povey 1997). The former is preferred in this text simply because they were the first to describe it (Newton 1686) and to show the adiabatic nature (Laplace 1816) of the relationship between sound velocity and density / compressibility.

$$u^2 \equiv \left(\frac{\partial P}{\partial \rho}\right)_S = -V^2\left(\frac{\partial P}{\partial V}\right)_S = \frac{1}{\beta_S \rho} \qquad [2\text{-}10]$$

The study of sound waves and their propagation, and its prospective applications in food science and technology is still not well acknowledged, despite the effort of several scientists (Povey and McClements 1988; Povey 1989; Povey 1997; McClements 1997; Povey and Mason 1998). What has directed the present research on this subject is not the theory of sound propagation itself but the thermodynamic properties that can be derived from sound velocity and their interpretation.

It should be emphasized that Equation 2-10 defines the speed of sound in terms of isentropic properties, although Newton (1686) in his classical analysis did not distinguish between isothermal and isentropic compressibility. The assertion that the propagation of sound waves was adiabatic (owed to the small thermal dissipation) and reversible was made by Laplace (1816) more than one century later. Propagation of sound requires an elastic medium, so that a longitudinal or compression (contrasting to shear or surface waves) sound wave traveling through a fluid produces a series of compressions and rarefactions. Consequently, planes of molecules perpendicular to the direction of the sound waves are cyclically displaced (although there is no net movement). The particle displacement, or pressure perturbation, depends upon position and time, which can be equated by means of the mass and momentum conservation laws of fluid mechanics yielding the so-called wave equation, expressed below in terms of a one-dimensional, homogeneous, isotropic, non-dispersive propagation (Dowling and Ffwocs-Williams 1983).

$$\frac{\partial^2 \xi}{\partial x^2} = \left(\frac{1}{u^2}\right)\left(\frac{\partial^2 \xi}{\partial t^2}\right) \qquad [2\text{-}11]$$

The solution for the wave equation includes a real and a complex part of waves propagating in the positive direction away from the origin and also in the negative direction. Pressure disturbance or particle displacement as a result of the propagation of a sound wave reveals fundamental properties of the propagation of sound, either in terms of its energy content or in terms of the pressure or amplitude (Dowling and Ffwocs-Williams 1983).

The basic parameters of a continuous wave include the wavelength and the period of a complete cycle. The number of cycles completed in one second is called frequency and is measured in Hertz. The relation between sound velocity, frequency, wavelength and period in a continuous wave is given by the following equation.

$$\lambda = \frac{u}{f} = uT' \qquad [2\text{-}12]$$

The acoustic spectrum breaks down sound into 3 ranges of frequencies, subsonic (< 20 Hz), audible (20 Hz to 20 kHz), and ultrasonic range (> 20 kHz). The ultrasonic range is then broken down further into 3 subsections (low frequency/airborne/high power, conventional/industrial, and high frequency/acoustic microscopy ranges). It is a common practice to express sound velocity in terms of the acoustic impedance *Z* of the medium, a characteristic property, which may give the 'intensity' of the wave propagating through a given medium, expressed as the product of density and sound velocity (Povey 1997). The wave vector *k'* that appears in Equation 2-13 is related to the angular frequency and speed of sound.

$$Z = \rho u = \rho \frac{2\pi f}{k'} = \rho \frac{\omega}{k'} \qquad [2\text{-}13]$$

A piezoelectric[2] transducer, which converts an electric pulse into a sound wave, is needed to generate and detect ultrasonic vibrations. The sound field of a transducer is divided into two zones; the near field and the far field (O'Donnell et al. 1981). The near field is the region directly in front of the transducer where the echo amplitude goes through a series of maxima and minima and ends at the last maximum. The location of the last maximum is known as the near field distance and is the natural focus of the transducer. The far field is the area beyond the natural focus of the transducer where the sound field pressure gradually drops to zero. Because of the variations within the near field it can be difficult to accurately evaluate the signal using amplitude based techniques. The near field distance is a function of the transducer frequency, element diameter, and the sound velocity of the propagation medium. There are a number of sound field parameters that are useful in describing the characteristics of a transducer. In addition to the near field, knowledge of the beam width and focal zone may be necessary in order to determine whether a particular transducer is appropriate for a given application. A transducer's sensitivity is affected by the beam diameter at the point of interest. All ultrasonic beams diverge, or in other words, all transducers have beam spread. In the near field, the beam has a complex shape that narrows, while in the far field the beam diverges. Beam spread from a transducer can be reduced by selecting a transducer with a higher frequency or a larger element diameter or both. However, the smaller the beam diameter, the greater the amount of energy reflected back when using pulse-echo techniques.

---

[2] **Piezoelectricity**. The prefix *piezo* is a Greek word for pressure. The piezoelectricity phenomenon, first discovered in 1880, is the direct result of applying a mechanical stress to most crystalline materials that brings about the appearance of electric charges or inversely strains are generated in certain faces of the crystal due to the application of an electrical field (Beyer and Letcher 1969).

Finally, ultrasound attenuates as it progresses through a medium. Assuming no major reflections, there are three causes of attenuation: diffraction, scattering and absorption. The amount of attenuation through a material can play an important role in the selection of a transducer for a given application. In many liquids, the velocity of ultrasound is a function of frequency, and the liquid is said to be dispersive. If any dispersion occurs it will introduce a systematic error into the velocity measurement (Povey 1997). An important distinction should be made between the use of sound propagation for material characterization, which requires low-intensity (usually pulsed waves) ultrasound, and the use of high-power (> 10 kW m^{-2}, < 100 Hz continuous wave) ultrasound for promoting physical and chemical transformations (e.g., sonochemistry), since they involve different techniques and physical principles, in spite of some similarities. Besides density/compressibility relations, there are a number of applications of low-power ultrasonics in foods taking advantage of its non-invasive, non-destructive and opaqueness-applicability nature, going from quality control (e.g., meat-fat inspection, egg-white quality and shell thickness, fruit ripeness); composition, concentration, and solids content determination; emulsions, dispersions, and particle size characterizations; to the processing plant fluid level and flow measurements, and extraneous matter detection (McClements 1997).

Thermodynamics of Solutions

So far we have treated all thermodynamic quantities as of those regarding pure substances. These expressions hold for solutions since the extensive thermodynamic properties of a pure substance are determined by pressure, temperature and its amount; and its intensive properties by pressure and temperature alone; while for a solution, pressure, temperature, and the amount of each constituent define its extensive properties;

and its intensive properties by pressure, temperature and composition. The question arises as how to separate the composite effect resulting from the combination of different substances as in a real food system, which very often is much more complex than just a solution (homogeneous single phase mixture). Most foods can be seen as dispersions (suspensions, emulsions, foams, colloids, gel, etc) of a dispersed phase (gas, liquid or solid) into a continuous phase, usually liquid, which, besides soluble components, may or may not contain insoluble components or membranes (Walstra 1996). We shall limit our discussion to homogeneous liquid solutions by which many food systems can be approximated (fruit juices, beverages and drinks, milk, liquid egg, etc.). What has driven studies dealing with thermodynamic properties of composite materials (or mixtures of pure substances) is either the 'simple' departure from ideality due to mixing, the original matrix of the studied substances and its significance, or a specific application for the required property (Blandamer 1973; Franks and Reid 1973; Millero 1971; Millero 1980; Hoiland 1986). For instance, the study of proteins in aqueous solutions by means of ultrasonic data is strongly based on the thermodynamics of hydration and its role in modulating structural stability and functional activity, which predominantly depends on the solute-solvent interactions, which in turn can be studied through some sort of apparent or partial thermodynamic expression of derived properties of solution components (Gekko and Hasegawa 1986; Kharakoz 1991; Gekko and Yamagami 1991; Kharakoz and Sarvazyan 1993; Chalikian et al. 1995; Chalikian and Breslauer 1996; Kharakoz 1997; Soto et al. 1998; Prehoda et al. 1998).

There is a thermodynamic relationship between the speed of sound and the inverse of the square root of the product of density and compressibility given by the

Newton-Laplace equation. The compressibility of a fluid is equal to the isothermal or isentropic pressure derivative of volume and, consequently, is a second derivative with respect to pressure of the Gibbs function as for Equation A.10 (refer to Appendix A). Since compressibility, like specific volume (or density), is determined by the composite effect of intra- and intermolecular interactions, its value can be used to gain insight into these interactions (Sarvazyan 1991; Chalikian et al. 1994). It is well known that aqueous solutions of electrolyte and non-electrolyte solutes do not behave ideally at atmospheric pressure since there is considerable interaction, and there is no reason to expect regular behavior of such solutions under elevated pressures. When studying solute-solvent interactions it is convenient to deal not only with the overall compressibility of a solution, but rather with the apparent molar, partial molar, apparent specific, or partial specific compressibility of the solution constituents. For an aqueous solution, the apparent compressibility of a solute is determined by interatomic interactions within the solute molecule itself (intrinsic compressibility of a molecule), solute-solute interactions, and solute-solvent interactions (hydration) (Sarvazyan 1991). A substantial number of compressibility studies of mixtures of non-aqueous systems can be found in the literature (Kiyohara et al. 1974; Kortbeek et al. 1988; Zhang et al. 1992; Nath 1998). The general aim has been to use the composition dependence of the apparent or partial (and sometimes ‘excess’ as will be seen shortly) quantities as a means to understand the nature of the molecular scale processes within those mixtures, even without applying pressure to the system and simply looking into the properties derived from Newton-Laplace equation, since temperature also induces volume changes.

For a binary solution prepared using n_i moles of solute and n_j moles of solvent, the volume of each component is treated as a partial molar property, rather than the volumes occupied by the separate components at the same temperature and pressure before mixing, as follows (Sage 1965).

$$\overline{V}_i = \left(\frac{\partial V}{\partial n_i} \right)_{T,P,n_j} \qquad [2\text{-}14]$$

Hence, for compression of liquid mixtures or solutions, the partial molar compressibility, since it involves volume, of each component can be expressed in terms of its partial molar volume by introducing the definition above into the thermodynamic definition of compressibility given by Equation 2-2; it follows for a given composition at constant temperature,

$$\overline{\beta}_{T,i} = -\frac{1}{\overline{V}_i} \left(\frac{\partial \overline{V}_i}{\partial P} \right)_T \qquad [2\text{-}15]$$

Partial molar properties are intensive properties which depend only on the pressure, temperature, and composition of the mixture. Thus if $(n_i + n_j)$ moles of two substances are mixed, then the total volume is given by Equation 2-16, which holds either for number of moles or mole fraction (Van Ness 1964).

$$V = n_i \overline{V}_i + n_j \overline{V}_j = x_i \overline{V}_i + x_j \overline{V}_j \qquad [2\text{-}16]$$

The isothermal coefficient of compressibility for a binary solution can be expressed as a combination of the volume fraction weighted partial molar compressibilities of the components (Moriyoshi and Inubushi 1977; Nakagawa et al. 1981),

$$\beta_T = \phi_i \overline{\beta}_{T,i} + \phi_j \overline{\beta}_{T,j} \qquad [2\text{-}17]$$

This follows from the fact that the partial molar volumes of each component are functions only of the relative composition of the mixture and not of its total amount. It is seen, therefore, that the partial molar properties of a system provide how much of an extensive property is to be ascribed to each component. However, partial molar volumes cannot be immediately calculated from the measured density (or specific volume) of the solution because both depend on the solution concentration. An alternative form of Equation 2-16 defines solution volume in terms of the apparent molar volume V_j^{app}, according to Equation 2-18 (Blandamer 1998).

$$V = n_i V_i^o + n_j V_j^{app} \qquad [2\text{-}18]$$

The first term of the right hand side of Equation 2-18 is associated with the molar volume of the pure component (solvent), as denoted by the superscript 'o'. Similarly, Gucker (1933) defines an apparent molar compression (change of apparent molar volume with pressure) of a solute by the difference between the product of the measured compressibility of the solution and solution volume, and that of the solvent as expressed by Equation 2-19.

$$\left(\frac{\partial V_j^{app}}{\partial P}\right) = \beta V - \beta_i^o V_i^o \qquad [2\text{-}19]$$

Partial and apparent molar volumes are related by Equation 2-20. Apparent and partial molar thermodynamic properties are similar but only become identical at the limit of infinite dilution (Blandamer et al. 2001).

$$\overline{V}_j = V_j^{app} + x_i x_j \left(\frac{\partial V_j^{app}}{\partial x_j}\right)_{T,P} \qquad (2.20)$$

Apparent molar volume is usually calculated using the density of the pure solvent and the density of the solution at the same pressure and temperature together with the composition of the solution, i.e. the solute concentration being known. It is not uncommon to express the apparent molar volume for dilute solutions, containing neutral solutes as well as electrolyte solutes, by a linear function of the concentration, and using the apparent molar volume at infinite dilution (where solute-solute interactions vanish) as equal to the limiting partial molar volume of the solute (Hoiland and Holvik 1978; Reis 1998; Blandamer et al. 2001). In this context, one approach assumes that the limiting partial molar volume of the solute is given by the sum of two contributions, the intrinsic volume of the solute, which will reflect the 'size' of the solute molecule, and the volume of the co-sphere[3], representing the solute-solvent interactions (in case of aqueous solutions, hydration). Paljk et al. (1990), studying volumetric properties of aqueous solutions of simple sugars at atmospheric pressure, found that the 'empty' volume associated with the solute molecule was small and roughly the same as the empty volume associated with this molecule in the solid state.

An alternative approach is the interpretation of volumetric properties of solutions or liquid mixtures in terms of departures from their ideal values, defined by excess functions. Excess thermodynamic quantities are usually obtained using the general Equation 2-21 for any particular molar thermodynamic property Q.

$$Q^E = Q - Q^{id} \qquad [2\text{-}21]$$

This procedure implies prior knowledge or subsequent determination of the ideal quantity for the solution of the same composition as the reference state. To illustrate this,

[3] **Co-sphere concept**: The general rule is as follows: "Two solutes will attract each other if their structural influences, or their tendencies to orient water molecules, are compatible with each other; conversely, an incompatibility in these structural influences or tendencies will result in repulsive forces" (Millero 1971).

the case for the coefficient of compressibility is chosen since it is probably the most important property in view of the present research and because different criteria and approaches have been used for calculating excess compressibilities in preceding works.

According to Equations 2-2 and 2-21, Douheret et al. (1985) suggested that the excess isentropic compressibility would be expressed as

$$\beta_S^E = \beta_S - \beta_S^{id} = -\frac{1}{V}\left(\frac{\partial V}{\partial P}\right)_S + \frac{1}{V^{id}}\left(\frac{\partial V^{id}}{\partial P}\right)_{S^{id}} \qquad [2\text{-}22]$$

The ideal solution volume as well as ideal solution density is calculated using volume- and mole-fraction averaging, respectively, of the pure component properties. The volume fraction is the mole fraction weighted ratio of the volume of the pure component to the ideal solution volume. Hence, for a binary ideal system, the following set of equations in molar basis applies:

$$V^{id} = x_i V_i^o + x_j V_j^o \qquad [2\text{-}23]$$

$$\rho^{id} = \phi_i \rho_i^o + \phi_j \rho_j^o \qquad [2\text{-}24]$$

$$\phi_{i \text{ or } j} = x_{i \text{ or } j} \frac{V_{i \text{ or } j}^o}{V^{id}} \qquad [2\text{-}25]$$

Prigogine (1957) equated excess compressibility by Equation 2-26. It may be added that the condition of the process was not stated, although later work by Prigogine (1965) explicitly referred to isothermal compressibility. It can be seen that the previous rigorous thermodynamic expression (2.22) cannot be reduced to this single term relation.

$$\beta_T^E = -\frac{1}{V}\left(\frac{\partial V}{\partial P}\right)_T + \frac{1}{V}\left(\frac{\partial V^{id}}{\partial P}\right)_T = -\frac{1}{V}\left(\frac{\partial V^E}{\partial P}\right)_T \qquad [2\text{-}26]$$

By defining an ‘excess volume compressibility’ implicitly in terms of excess volume, and then by expanding in Taylor series with only the first order term, Moelwyn-

Hughes and Thorpe (1964) arrived at the following expression for the excess compressibility, taken to be valid for both isothermal and isentropic conditions. Note that this relation has been adapted from its original form as to have the same notation used here.

$$\beta_T^E = \frac{V^E}{V^{id}}\left[-\frac{1}{V^E}\left(\frac{\partial V^E}{\partial P}\right)_T + \frac{1}{V^{id}}\left(\frac{\partial V^{id}}{\partial P}\right)_T\right] \qquad [2\text{-}27]$$

Missen (1969) proposed a more rigorous thermodynamic expression for the isothermal excess compressibility by formulating the appropriated ideal mixing rule as expressed by Equations 2-19 to 2-21; resulting in the following expression,

$$\beta_T^E = -\frac{1}{V}\left[\left(\frac{\partial V^E}{\partial P}\right)_T + V^E \beta_T^{id}\right] \qquad [2\text{-}28]$$

Similarly, ultrasonic speeds in ideal binary solutions require the ideal isentropic compressibility, in this case using the term deviation (from the ideal value), which is preferable as opposed to excess ultrasonic speed (Douheret and Davis 1993). A number of thermodynamic-based attempts have been made to evaluate ultrasonic speed in a binary system. These proposals differ in complexity starting with some sort of simple weighted average of the ultrasonic speed or density of the pure components, or by considering an intuitive model for the passage of a sound wave through unmixed component layers, to more elaborate ones that take into account the ideal mixing rule (Douheret et al. 2001).

It is clear though, that the use of inexact relationships may lead to discrepancies in the calculation of excess compressibilities as well as with other excess thermodynamic quantities. Douheret et al. (2001) pointed out that it is important to examine the consequences of changes in volumetric properties during the process of mixing and thus

separating isentropic or isothermal conditions as one goes from individual pure components to real and ideal solutions. What is desirable in this context is to define a reference state for a solution so that we may correlate the deviation of all thermodynamic quantities of real solution from those of a common model. One may define the reference state by generating a thermodynamically consistent set of mixing rules. The choice of solution model is not as important as the internal consistency, so that real solution behavior relative to one acceptable model may be translated to give deviations from any other existing or future model.

Equilibrium and Rate Processes

Pressure effects on kinetics of reactions are not intentionally covered in this review. Nonetheless, a few concepts on the principles are given because kinetic parameters are affected by or in some cases can be derived from the properties being investigated in the present research. The same Le Chatelier's principle governs reaction kinetics: a reaction associated with decrease in volume is favored by pressure and vice-versa (Tauscher 1995). The pressure-dependence of the equilibrium constant of a given reaction can be derived from the difference in partial molar volumes of products and those of reactants at constant temperature in the form of Equation 2-29 (Butz and Tauscher 1998). Hence, reaction volumes can be determined provided the density of all components involved is known.

$$\Delta \bar{V} = \left(\frac{\partial \Delta G}{\partial P} \right)_T = -RT \left(\frac{\partial \ln K}{\partial P} \right)_T \qquad [2\text{-}29]$$

Pressure effects on the rate of a given elementary reaction is described by the thermodynamic concept of the transition state, which states that a reaction proceeds by a smooth and gradual rearrangement of molecules between those of reactants to those of

products (Isaacs 1981). The energy of the system increases initially to a maximum before falling to that of products. This maximum corresponds to an intermediate known as the activation complex or transition state. Therefore, the rate of reaction will be the rate at which the transition state is converted to products, and its pressure-dependence may be derived from the differences in partial molar volumes between reactants and transition state, known as the 'activation volume', given by,

$$\Delta V^{\neq} = \left(\frac{\partial \Delta G^{\neq}}{\partial P} \right)_T = -RT \left(\frac{\partial \ln k}{\partial P} \right)_T \qquad [2\text{-}30]$$

Since volumes of reactants and transition states change with pressure and there is no reason for them to have similar compressibilities, besides being temperature dependent, the activation volume is pressure dependent as well. Usually activation volumes are derived from the slope of the logarithm plot of the ratio of reaction rates at different pressures versus pressure (Cheftel 1992). High pressure has long been used as a means to accelerate conversion rates of chemical reactions; though depending on the mechanism a reaction velocity may be also retarded by pressure. As for the expressions given for the pressure-dependence on equilibrium constant K and reaction rate k, a rise in pressure from atmospheric to 100 MPa for a reaction with ΔV of -16 ml mol^{-1} would lead to almost twofold increase in K; and a reaction with $\Delta V^{\neq}$ of -16 ml mol^{-1}, the same pressure increase results in a twofold increase of the reaction rate (Mozhaev et al. 1994). Extensive reviews on activation and reaction volume for thousands of organic and inorganic reactions are given in a series of three papers (Asano and Le Noble 1978; Van Eldik et al. 1989; Drljaca et al. 1998), some of which may be applied for reactions occurring in food systems under the influence of high pressure.

Methods of Measuring Thermodynamic Properties at High Pressure

Reports of development of *in situ* measurement techniques under pressure are almost nonexistent in the food science literature. Nevertheless, a heat source probe was developed to successfully measure thermal conductivity of food materials under pressure (Denys & Hendrickx, 1999)[4]. In general, the thermal conductivity increases for ordinary liquids under a pressure of 1,200 MPa by a factor varying between 2 and 3 (Bridgman 1931). The effect on water is smaller; at 1,200 MPa the increase is only about 50 per cent. A remarkable link between this study and the present exists, since there is a close connection between the effect of pressure on thermal conductivity of normal liquids and the effect of pressure on the velocity of sound in the liquid (Isaacs 1981). That is, thermal conductivity in a liquid is primarily a mechanical process; heat is transferred by microscopic mechanical waves traveling with the velocity determined in the conventional way by the compressibility. Shimada et al. (1996) developed a hot-wire probe to measure gel-setting and gel-melting temperatures of aqueous gelatin and agar solutions for assessing gelation and sol-gel behavior of proteins and polysaccharides under pressurized conditions. Measurements of pH under pressure have been proposed by indirect means such as measuring emf, density and conductivity, optical density of indicators, and spectrofluorometry (Hayert et al. 1999). Although not restricted to non food systems, diamond anvil cell in combination with Fourier transform infra-red, Raman spectroscopy or NMR has been used for *in situ* observation of biomacromolecules (Gekko 1992; Taniguchi and Takeda 1992; Heremans 1995; Yamagushi et al. 1996; Heremans et al. 1996; Van Riel et al. 1997; Vermeulen and Heremans 1997; Smeller and Heremans

[4] **Thermal conductivity at high pressure**. Another probe for thermal conductivity measurement of foods under pressure was developed by Shariary et al. (2000), though the maximum pressure achieved in this case was only 10 MP, therefore the technique and results are applicable for processes at low pressures.

1997a; Snauwaert et al. 1998). Most of these methods were only feasible because of the very small sample size in the μL-range, and the presence of an optical window (typically sapphire). Therefore, the majority of the research studies reviewed in this matter were dedicated to non food systems, and in particular those devoted to density (or specific volume), compressibility, and speed of sound measurements. A distinction must be made between compression and compressibility in order to recognize that there are different techniques for each one, even though they are interdependent by way of Equation 2-2. The first can be seen as the change in volume as a result of application of pressure, and the second expresses how compressible a given material is. Because of this, these two properties, namely density (or specific volume) and compressibility, were grouped to be reviewed co-dependently.

Density or Specific Volume and Compressibility Measurements

It is natural to think of volume compression as the simplest and most fundamental of all the effects of hydrostatic pressure, and for that reason it will be discussed first. It is not, however, the simplest to measure experimentally, because the measurements immediately obtained are relative to the vessel, which is itself distorted. Elaborate procedures may be necessary to eliminate the effect of such distortion. Another complication in dealing with compressibility is that upon compression of a liquid, heat is evolved due to the work of compression, and this temperature rise increases the volume and affects the value of the coefficient of compressibility, which is also temperature dependent. Therefore, either the experiment is performed at constant (equilibrium) temperature to obtain the isothermal compressibility, or the volume change produced by a sudden compression or expansion is measured at constant entropy and the adiabatic-

reversible compressibility is obtained. The isothermal condition is frequently sought in view of the methods described in this sequence, however, this mode is usually difficult to maintain, and early experimental estimates of compressions and compressibilities were often between the isentropic and isothermal values (Douheret et al. 2001).

One experimental approach to evaluate compressibility/density of liquids consists in measuring volume changes as a function of pressure. Various methods have been devised for this; length-measuring techniques such as piezometer (Diaz-Pena and McGlashan 1959; Millero et al. 1969; Millet and Jenner 1970; Millero et al. 1974; Tanaka et al. 1977), piston-displacement method (Bridgman 1931; Levelt-Sengers 1965), syphon-bellows (Hayward 1971b), and hydrometer (Goldman 1958; Dymond et al. 1979; Dymond et al. 1982). Very often, these devices contain the test fluid inside a flexible surface (which can be a meniscus of an immiscible fluid of known density/compressibility), the volumetric deformation of which can be observed and related to the change in fluid density. Problems encountered with these techniques include the fact that the test fluid is contained within a sample volume whose magnitude is both vital to the measurement and dependent on pressure in a manner not always readily predicted or reproducible.

Another experimental approach makes direct measurement of density under pressure. Some of the techniques include oscillating U-tube densimeter[5] (Malhotra et al. 1990; Malhotra and Woolf 1993; Chang and Moldover 1996), by means of measuring the resonant frequency, proportional to the mass/density, of a nominally-fixed volume tube; hydrostatic balance (Machado and Streett 1983; Lainez et al. 1987), which uses a direct-weighting apparatus; and vibrating wire (Dix et al. 1991) based on the relationship

[5] **Densimeter**: This instrument is also referred to as densitometer or density meter.

between the density of the fluid surrounding a magnetically-driven vibrating wire and the fluid motion around it. The same principle was applied by Bett et al. (1989) in the design of a vibrating-rod densimeter. In some of these methods, a negative aspect that has been mentioned is the partially inelastic deformation of the volume under the influence of an internal pressure that must be treated, and this is not an easy task.

Most of these techniques described above are very difficult to implement, especially at higher pressures, and very dependent on the pressure-generating equipment design. For example, some are invasive or need an optical window, and for these reasons not always feasible. Some of them are only possible at low pressures, below 100 MPa. Because of these difficulties accurate experiments are tedious and the literature on this subject is full of contradictory and low precision data (Hayward 1971a; Bett et al. 1989). Finding discrepancies of 5 to 10% is quite common between results on the same substance at the same conditions by different researchers, and may be as large as 20 to 30%. Anisotropic distortion of the measurement apparatus and air entrapment has been reported as the main sources of error.

Sound Velocity Measurement

An alternative approach, a non-invasive technique, inherently capable of yielding higher accuracy, is to measure compressibility/density and their pressure-dependence by acoustic methods (Van Dael and Van Itterbeek 1965). Newton-Laplace Equation 2-10 provides the basis for the experimental determination of isentropic compressibilities of solutions and liquid mixtures. However, the velocity of sound data obtained as such at high pressures must be combined with density, isobaric heat capacity, and thermal expansion coefficient data obtained at atmospheric pressure as a function of temperature in order to compute the values of density and compressibility as a function of pressure

and temperature by means of a thermodynamic approach coupled with numerical techniques similar to that proposed by Davis and Gordon (1967). Other significant thermodynamic properties can be derived from acoustic data as well.

Sound velocity is measured using longitudinal or compression plane waves. Due to thermo-viscous losses in liquids, sonic methods are only effective in the low frequency range (usually 1 to 10 MHz), because the attenuation coefficient varies with the square of the frequency (Kinsler and Frey 1962; Bernasconi 1986). In this context, no special attention will be paid to the absorption of sound. Sound velocity measurement involves generation of ultrasonic vibration, propagation through the fluid sample, and detection either as a function of distance traveled, or by change in line widths (Breazeale and Cantrell Jr. 1981). A piezoelectric transducer generates and detects ultrasonic vibrations. An ultrasonic transducer is made up of an active element, a piezoelectric or single crystal material which converts electrical energy to ultrasonic energy; a backing, a highly attenuated and very dense material to control the vibration and absorbing the energy that radiates from the back of the piezoelectric element; and a wear plate to protect and to serve as an acoustic transformer between the piezoelectric element and the material under investigation (O'Donnell et al. 1981). By varying the backing material in order to vary the difference in impedance between the backing material and that of the piezoelectric element, different resolutions and sensitivities may be achieved. Because of the high characteristic acoustic impedance of liquids compared to air, the vibrating elements of transducers designed for liquids must be capable of producing large forces at small displacements to match the impedance of the liquid efficiently (Van Itterbeek 1965). Commonly used transducers are made of quartz crystals (X-cut discs), inorganic crystals

(such as ammonium dihydrogen phosphate), ceramic materials (e.g., barium titanate), and polymers (usually referred to as PVDF or polyvinylidene fluoride) (O'Donnell et al. 1981). The latter carries certain interesting advantages such as short pulse duration and efficient transfer of energy from the transducer to water-like liquids due to the close impedance match between the polymer element and the liquid (Beyer and Letcher 1969).

The choice of a piezoelectric material is ultimately dictated by the specific application. In general, ceramics exhibit higher electromechanical coupling factors and lower mechanical Q-factor[6] (i.e. higher mechanical losses) than crystalline piezoelements. Consequently, crystalline elements are frequently used in narrowband applications, that requires low ultrasonic losses in the transducer compared to the specimen and weakly coupled piezoelement (e.g., for mechanical properties measurements of the specimen), whereas ceramics are commonly used in broadband applications, which in turn requires high electromechanical conversion efficiencies to achieve acceptable signal-to-noise ratios, and short-duration pulses to meet satisfactory time-domain resolution (e.g., imaging and quantitative measurements of velocity and attenuation over a wide range of frequencies) (O'Donnell et al. 1981).

The experimental techniques used in velocity of sound measurements are the variable path length interferometry, the optical diffraction, and the pulse methods. The latter is considered more suitable for high-pressure measurements (Wilson 1959; Van Dael and Van Itterbeek 1965; Davis and Gordon 1967; Bobik 1978; Daridon 1994). The interferometer method is based upon the detection of the periodic impedance variations of

[6] **Q-factor** represents the mechanical resonance of the piezoelement. Transducers constructed for optimal impulse response usually consist of piezoelectric ceramics that are mechanically backed by high-loss materials exhibiting mechanical impedances approximately equal to that of the piezoelement. This approach yields broad bandwidth and a compact impulse response, but at the expense of sensitivity, which then requires electrical tuning for compensation (O'Donnell et al. 1981).

vibrating piezoelement, when a reflector, parallel to the source, moves in a direction perpendicular to the crystal (Parbrook 1953). At high pressures there are important inconveniences inherent to the construction of this type of apparatus, and volume and pressure changes that accompany the displacement of the reflector and difficult tightening are some of the disadvantages. In the optical diffraction technique, a beam of monochromatic light passes perpendicularly through a sound wave traveling in a fluid; by the diffraction effect of light, the grating constant equals the ultrasonic wavelength (Nozdrev 1963). However, this technique also requires an optical window.

Pulse methods seem to be most suitable for the investigation attempted in this study. This method was first implemented by Firestone and Frederick (1946) for detection of flaws in metals, followed by Lazarus (1949), benefited by the wartime development of pulsed circuits, who a few years later, adapted its use in high-pressure environments to measure elastic properties of solid crystals. The measuring cell can be kept so small that high pressures present no major difficulties as far as the mechanical design is concerned. Further advantages are: no movable parts in the cell, a quasi-continuous reading of the sound velocity (or other proportional output parameter), and a very low scattering level, mainly because fluctuations in temperature and pressure can be avoided more easily than with the preceding techniques (Van Dael and Van Itterbeek 1965; Heydemann 1971).

A number of pulse technique variations have been reported in the literature[7], all of which are variations or combinations of the ones discussed: pulse-echo, sing-around, pulse superposition, gated double-pulse superposition, echo-overlap, pulse-interferometer

[7] **Cited literature on pulse techniques**. Most of the literature cited in the sequence refers to pulse methods that were adapted to the high-pressure environment, while others were simply variations of the method.

(or acoustic resonator), and long pulse buffer rod method (McSkimin 1957; Davis and Gordon 1967; Papadakis 1967; Papadakis et al. 1972; Eggers and Funck 1973; Bobik 1978; Sarvazyan 1982; Muringer et al. 1985; Takagi and Teranishi 1986; Lainez et al. 1987; McClements and Fairley 1991; Eggers 1992; Daridon 1994; Horvath-Szabo et al. 1994). In the basic pulse-echo method, a pulsed radio frequency signal (ηs-μs duration) of given frequency (usually 0.1-100 MHz, but can go up to 5-10 GHz) is converted into a pulsed ultrasonic wave by piezoelectric effect of the transducer, travels through the sample, is reflected between the sample boundaries successively, it develops a pulse-echo decay pattern with a small pulse length compared to a round trip transit time. The velocity of ultrasonic wave propagation is determined by measuring transit time between the reflected pulses and the corresponding pulse propagation distance in a sample.

In the case of acoustic resonators (interferometer), the sound velocity is obtained by measuring the pulse repetition frequency for standing wave formation at which maximum constructive interference occurs. Typically, the electrical signals are amplified, filtered and displayed on an oscilloscope, analyzed, digitized, and processed. The electronic procedure to measure the transit time between pulses, usually in the range of microseconds varies according to the specific method, such as a variable time delay/expanded sweep, repetition rate of a continuous succession of pulses, and a frequency counter. Design variations using one transducer (acting as emitter/receiver) and one reflector or two reflectors (Sun et al. 1987), or two transducers have also been reported (Eggers and Kaatze 1996).

Objectives

The purpose of this study was to develop procedures and instrumentation to conduct experiments for measurements of sound velocity in food-based model liquid solutions during the pressurization process in an isostatic high-pressure unit, as well the subsequent approach to analyze and interpret ultrasonic data and derived properties. This study seeks to determine pressure dependence of thermodynamic expressions for specific volume (or density) and isentropic and isothermal compressibility of model binary aqueous solutions of sucrose, glucose and citric acid, and the effects of temperature and concentration near ambient temperatures. The interaction between solute molecules and water in solution were interpreted in terms of partial molar properties and the appropriate mixing scheme. In addition, other relevant thermodynamic properties were also derived as a function of pressure, temperature and concentration. Mathematical expressions were proposed for predictive or numerical application purposes by fitting data to the appropriate model.

CHAPTER 3
MATERIALS AND METHODS

The sound velocity measurement technique through a fluid sample under high pressure using the pulse-echo ultrasonic method was considered as the appropriate method to determine pressure-dependence of density and compressibility of model liquid solutions and the effects of the components. Figure 3-1 illustrates a schematic of the entire experimental setup. The approach to the proposed research work followed the methodology described below. The pressure generating equipment used to perform high-pressure experiments is described as well. Accordingly, since measurements of density and heat capacity at atmospheric pressure were needed, the methodologies to perform these experiments are also described.

Pressure-Generating System

The high-pressure equipment consisted of a Stansted laboratory scale unit (Stansted Fluid Power, Stansted, Essex, UK) with a pressurization chamber of 114-mm diameter and 243-mm height, providing a usable volume of approximately 2,480 ml. The pressure containment comprised a triplex pressure barrel having stainless steel inner liner, top and bottom flanged end caps that delimit the working chamber, a nickel alloy steel main vessel body, and a ductile steel outer member, which provided protection and an annular cavity for heating or cooling capability. The pressure was applied to the yoke type closure indirectly by the use of twin pressure intensifiers, operating in opposite phase, driven by twin radial pumps that injected the working fluid into the pressurized chamber.

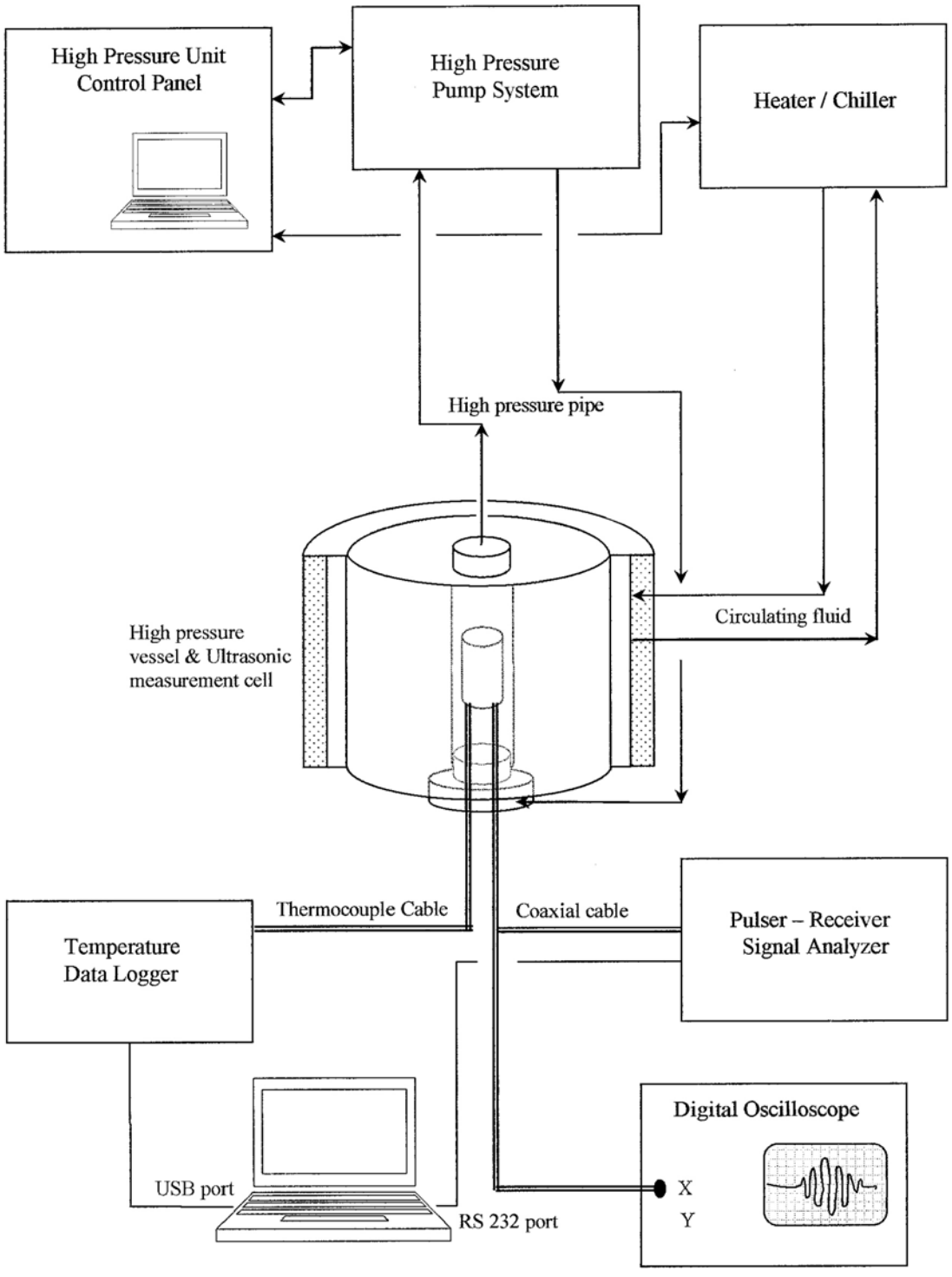

Figure 3-1. Schematic of experimental setup

The intensifiers were sequentially recharged with working fluid by a pre-charge pump which also performed the chamber pre-fill and first stage pressurization functions. The phasing cycle incorporated a short duration overlap on the drive pressure valves at the change over point; this feature allowed the hydraulic pressure driving the intensifier which has completed its stroke to cross flow which 'kick started' the intensifier beginning its stroke. Four sequentially controlled valves backed by graduated capillaries (a Pan-Pipe arrangement) provided a step ramp approximation to a programmed decompression ramp rate. The pressure controller allowed the high-pressure pumping system to step ramp to simulate any programmed ramp rate less than, or equal to, the maximum rate which the pumping system could achieve. The system could reach pressures up to 600 MPa, at rapid compression rates as well as programmable pressurization and decompression cycles through a computerized PLC controller. This system operated at above and below ambient temperatures (-20 to 90^{o}C), by the use of a vessel jacket, with a circulating fluid from an external chiller/heater. The equipment was designed to operate with several pressure transmission fluids, including water; however, for the present investigation it was operated with a mixture of ethanol and castor oil (9:1 ratio), in view of its electrical non-conductivity, since bare wires were inside the pressure chamber immersed within the pressure transmitting fluid (see description below).

A unique feature of this unit was the existence of electrical connections allowing communications between the interior within the pressurized chamber and the outside through electrical leads, which enabled the proposed *in situ* measurements. Originally, two single-wire lead-through connections were built in the bottom plug of the high-pressure vessel, with Stansted proprietary sealing design; basically using a conical plug

that sat in a sealing/insulating cone (pyrophylite ceramic material, Aluminum-hydrated silicate) between the conical plug terminal and the bottom plate of the vessel. The rest of the parallel section was insulated with a heat shrink sleeve; at the base there was a terminal studding and an insulated retaining bush, a fitted lock nut, washers, and a retaining nut for the power cable. After several drawbacks and subsequent failures with the previous described single wires, an additional 8 electrical leads were installed for low power/amperes applications. These were grouped in 4 wires in 2 cables, using Omegaclad 2.0-mm OD (30 AWG copper wires) and 2.35-mm OD (30 AWG K-type thermocouple extension wires) metal sheathed mineral insulated cables (Omega Engineering, Stamford, CT, USA). These cables were sealed with a conical hollow plug soldered outside of each metal 4-wire cable, which also sat in a conical cavity. Figure 3-2 shows details of the bottom plug of the high-pressure unit with the attached electrical leads as seen after modifications.

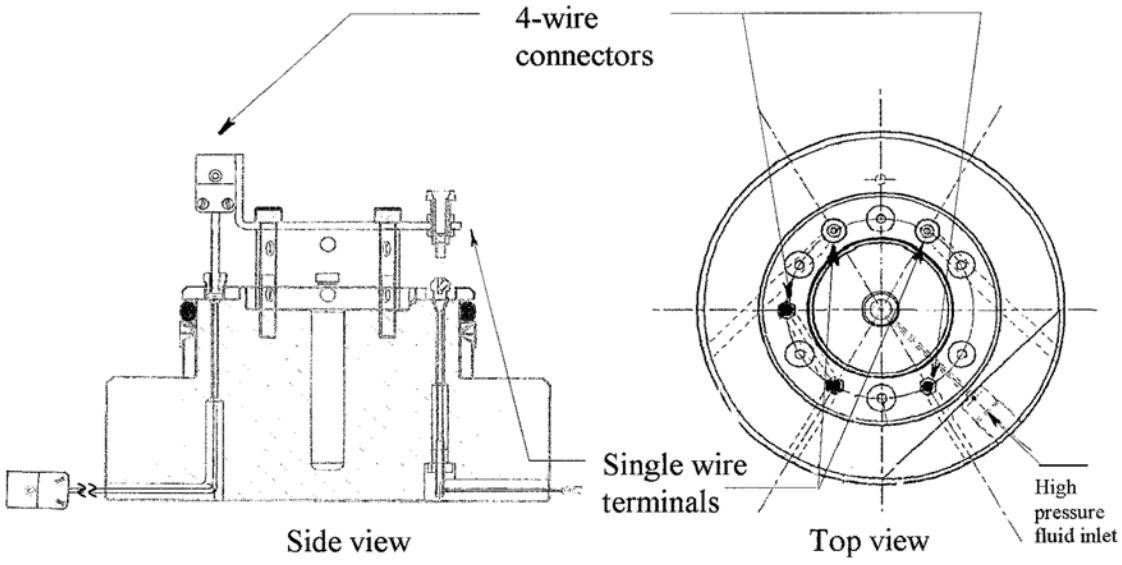

Figure 3-2. High-pressure vessel bottom plug showing details of the electrical leads

The design of this equipment was only suitable for experiments where the sample under investigation is restricted into a flexible or semi-rigid container able to transmit pressure from the pressure transmission fluid inside the working chamber with no other access to the exterior except through electrically communicating devices. The operation of the system was straightforward: by entering compression and decompression cycles setup parameters into the PLC controller with a computer program interface. The system allowed setup operating parameters to be chosen via software interface SCADA-SCAN 1000 (Hexatec Systems, Hexham, Northumberland, UK), or alternatively via PLC data access keypad, which was mainly used for diagnoses purposes or to change the settings of certain permitted timers, counters, and data registers.

The pressure profile settings were divided into six segments, each one comprised of a compression or decompression ramp rate (1 to 350 MPa min^{-1}), a hold level or the pressure set point (up to 600 MPa), and dwell duration (1 second to several hours). All pressure data, supplied by a pressure transducer model HP28 (Barnbrook Systems, Fareham, HA, UK) connected to the high-pressure chamber inlet pipe, was logged and stored at a frequency of one data point every 15 seconds (not programmable) for the specific segment of interest for ultrasound measurements ("stable" pressure and temperature) for further retrieval in the computer hard disk (refer to section concerning experimental procedure for collecting high-pressure ultrasonic data). Gauge pressure data were converted into absolute pressure with the proper barometric pressure at the local altitude (75 ft elevation above sea level) using NOAA daily data as for the Gainesville meteorological station (NOAA 2002). A thermocouple probe provided temperature readings of the working fluid inside the pressure chamber; however our

ultrasonic cell was designed to house a thermocouple probe for temperature sensing within the sample as will be described in the sequence, since accurate temperature measurement is crucial for the ultrasonic data analysis. Although temperature is usually referred to as degrees Celsius [^{o}C] in the text, absolute temperature Kelvin [K] was used throughout the computations. The reason for that is because all experimental temperature data were collected using degrees Celsius.

In spite of the easy operating scheme depicted above, frequent breakdowns and long stops for servicing caused unexpected delays. The pressure generating system did not always deliver pressure as it should have. To list a few events: countless replacements of pressure seals at the top and bottom plugs due to leaks or other problems (aggravated by the not-so-user-friendly task implied); several times electrical leads became grounded (causing loss of electrical communication and rendering impossible any *in situ* measurements; as a result leads had to be repaired, replaced or redesigned); many mechanical and electrical problems (e.g., malfunction of the pre-charge pump, valves, chiller, intensifier); and replacement of the controller computer. As a consequence the experiments to collect high-pressure data were delayed by more than one year, and part of the initially planned experiments had to be significantly reduced. It would have been more constructive to have the necessary time to digest/interpret the acquired data and eventually being able to go back and modify something in the experimental or theoretical approach as it is normally advisable in any research. As a sympathetic supervisor once said, “often the biggest lesson from research is the perversity of nature and the value of diligence.”

Sound-Velocity Measurement at High Pressures

The pulse technique was used to measure sound velocity since it is more suitable for high-pressure conditions. A device was constructed as an ultrasonic sample-holding cell to be inserted into the chamber of the hydrostatic high-pressure unit, containing an ultrasonic probe. Additionally, electronic instrumentation was provided to perform the experiments consisting of a pulser-receiver, a digital oscilloscope, and a signal analyzer.

In the pulse technique, longitudinal (or compression) plane waves were generated at frequencies usually in the range of 0.1 to 10 MHz. This involved power levels (miliwatt region) well below that at which the physical or chemical properties of the material might be altered. The principle is based on measuring the time between a pair of echoes of an ultrasonic wave propagating through the sample fluid in a known fixed acoustic path length.

A schematic of the ultrasonic cell is shown in Figure 3-3. It comprises a Teflon-made semi-rigid container of approximately 300 ml volume capacity, an ultrasonic probe model MP-54 modified (Rhosonics, Baarn, The Netherlands) attached to the top threaded cap of the container, and a type T thermocouple probe. All external parts of the ultrasonic probe were made of 316L stainless steel. The thermocouple probe was positioned as close to the straight sound path as possible but not interfering with it, at mid-point in the vertical direction. The transducer consisted of a highly damped broadband piezoelectric ceramic element, internally housed inside the probe, in such a way that only the stainless steel plate cover made contact with the sample fluid. The whole ultrasonic measurement cell was hermetically sealed to avoid exchange of fluids.

Preliminary tests indicated that the presence of even small air bubbles where the electric circuitry and transducer were housed caused too much stress especially during the

decompression cycle. The original ultrasonic probe was modified in order to equalize pressure at front and rear of the sensor by drilling a hole where a flexible hose could be attached. Then the interior of the ultrasonic cell chamber and the hose were filled completely with glycerol and vacuum applied. In a first attempt a viscous mixture paste of epoxy resin and tungsten powder was used but did not work properly because of the presence of entrapped air. No major pressure gradients were expected once pressure was equalized on both sides by the applied high hydrostatic pressure. Accordingly, maximum care was taken when filling/closing the measurement cell with sample fluid to avoid the presence of air bubbles in the system. This helped to avoid pressure gradients within the container because of differences in compressibilities of air and liquid. Minor pressure gradients were absorbed by the flexible container walls.

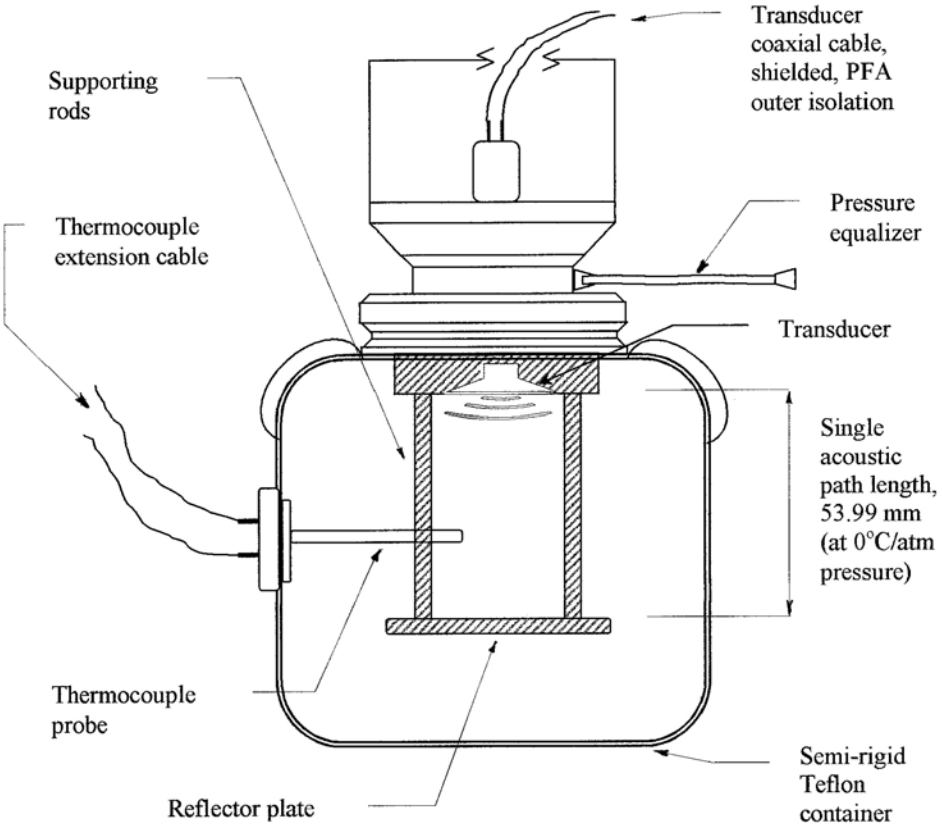

Figure 3-3. Schematic of the ultrasonic high-pressure measurement cell

The transducer of the ultrasonic probe, containing a piezoelectric ceramic element, was excited with a square wave excitation of 75 Volts negative spike short pulse at frequencies of 2 to 4 times per second. Through the piezoelectric effect, this energy was converted to a short sound pulse at the center frequency of the transducer (2 MHz). The pulse duration was about 350 ns and was broadband with a frequency content of about 100 kHz to 10 MHz and a bandwidth around 50% (Q-factor = 2). Figures 3-4 and 3-5 show, respectively, the frequency-domain (obtained by computing the FFT - Fast Fourier Transform of the time-domain waveform) of the transducer response expressed in terms of signal amplitude (dB[1]) versus frequencies, and the time-domain impulse response. Note that there is a decrease in amplitude as frequency increases.

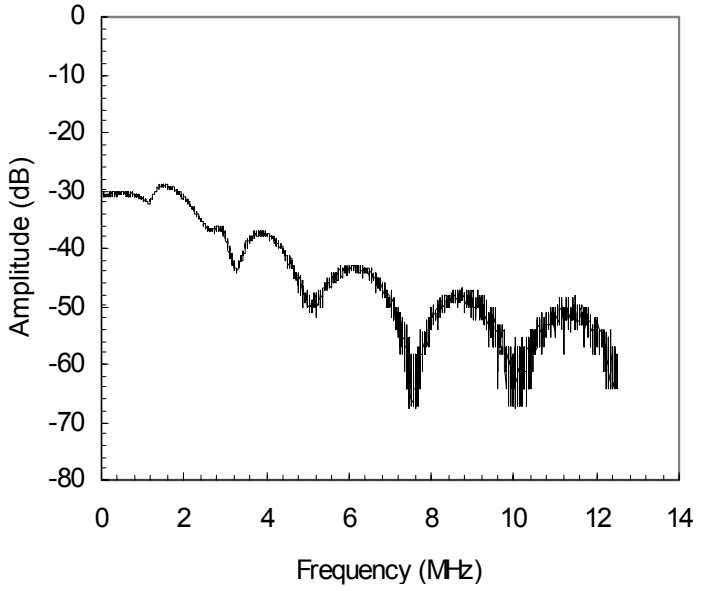

Figure 3-4. Frequency-domain transducer response

This sound pulse was coupled into the fluid sample and propagated through it at a velocity characteristic of the fluid. Ultrasound propagates through a material until the sound wave impinges on an impedance change; an amount of sound energy is reflected

[1] Magnitude is expressed in dB (decibels) relative to 1 Volt (rms) where 0 dB = 1 V_{rms}

dependent on the size of the interface and the relative impedance differences. The wave will continue until it reaches the rear wall of the cell (reflector). Part of the energy of the ultrasound is absorbed and attenuated by the material. Because the transducer is highly damped, the piezoelement can operate as receiver once the reflected waves (echoes) return, converting the wave into an analog signal, having a highly damped waveform with the above characteristics. The reflected signal (echo) was only about 100 to 700 mVolts.

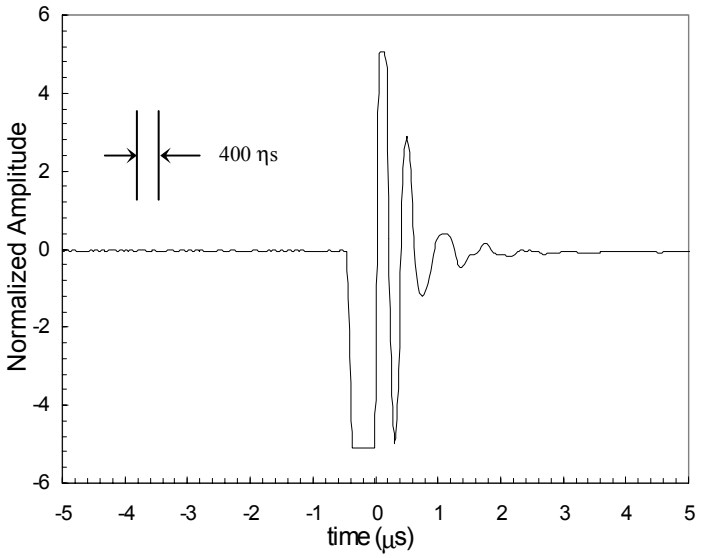

Figure 3-5. Time-domain input negative spike and transducer impulse response

The electrical signal coming from the ultrasonic cell was then amplified and normalized by a signal analyzer model 8100 (Rhosonics, Baarn, The Netherlands). The normalized signal (about 2 Volt peak to peak) was digitized with an 8-bit, 20 MHz A/D converter. A detection algorithm based on the signal waveform, amplitude, frequency content, and the presence of electronic noise, identified the first arrived signal eliminating unwanted signals. The algorithm allowed a down-shift of frequency down to 800 MHz center frequency. In addition, it was possible to compensate the signal in a dynamic range of 60 dB (difference between the strongest and the weakest signal). Through a

digital signal processing technique both signals were analyzed to determine the delay time between the time the transducer was stimulated and the time when the resultant pulse (echo) was detected. The transit time was then diminished from the dead-time (the time through the cable, the probe material, and the delay through the analog electronics). Dead time was determined by calibration using the double/triple transit time method, using pure water at a very constant temperature as the propagation medium. By entering 2x or 3x the one-way sound path (acoustic path length = 2 x reflector distance), the double or triple transit time could be found. This calibration was done at 74^{o}C, since for pure water at this temperature at atmospheric pressure the temperature has no effect on the transit time. At 74.4^{o}C, the sound speed had reached a maximum, and at 74^{o}C the transit time was minimal due to the expansion effect of the reflector standoff. The magnitude of the dead time obtained in this manner was determined to be 1,097 nanoseconds.

Using a standard RS-232 port, the signal analyzer was connected to a PC computer with the primary function of creating a log file in which transit time values were recorded through an interface program. This computer program enabled changes in the settings of file logging, time-span, sample and recording frequency, and also to view the transducer echo in a dialog-box window. Because the wave analysis algorithm dealt with time interval for the measurement, and also because of the intermittent (pulsed) nature of the signal (see previous paragraph), the RS 232 interface sometimes did not handle it correctly. The signal analyzer was primarily focused on measuring and while transferring data to the RS 232 port there were times when the transit time calculation window was too large, resulting in larger echoes, more data points, and longer

calculations, and therefore less time to handle the RS 232 output. For the recording function, the number of communication errors was considered acceptable since real-time measurements were conducted over periods long enough to accommodate eventual interruptions without interfering with the accuracy. Therefore, the interface program was primarily used for recording transit time at a programmable frequency, while the function of monitoring the signal waveform was left for the oscilloscope.

A 400-MHz 2-channel digital oscilloscope model TDS-430A (Tektronix, Beaverton, OR, USA) was used to monitor the input signal and the signal that returned from the ultrasonic cell by using a high impedance x10 probe connected to the signal analyzer. There were important reasons that determined the use of an oscilloscope. First, by monitoring the signal waveform coming from the ultrasonic cell, as the high-pressure experiments were performed, it was possible to verify the transducer response as well as the integrity of the ultrasonic sample-holding cell under such extreme conditions. For instance, since signal strength is inversely proportional to the gain value, the scope was used to monitor attenuation effects to observe specific changes in the process or instabilities. Consequently, it was possible to discontinue the experiment without causing any major irreversible damage, introduce remedies or eventually modify the ultrasonic cell depending on the particular situation. By taking advantage of the digital capability of the oscilloscope, it was also possible to record the signal waveform in a digital format for further analysis in order to test the accuracy of the transit time provided by the signal analyzer as described in the previous paragraph. In this way, samples of waveforms were averaged over 20 readings (to minimize electronic noise), acquired at frequency of 25 MS s^{-1}, and recorded in DAT file format. From these files, data was read line by line and

placed into variables, beginning with four values (header), containing record length, time per sample interval, trigger location, and trigger offset, followed by a linear array of ASCII floating-point amplitude/time values. A typical time-domain echo waveform is shown in Figure 3-6 as seen on the screen of the oscilloscope, shown together with the input signal. It should be mentioned though that it was very difficult to find the returned signal (echo) because the signal amplitude was very small, also due to the presence of electronic noise, multiple reflected echoes (other than the direct one) and reverberations. A very fine tuning was necessary since at high sensitivity the oscilloscope amplifier became saturated.

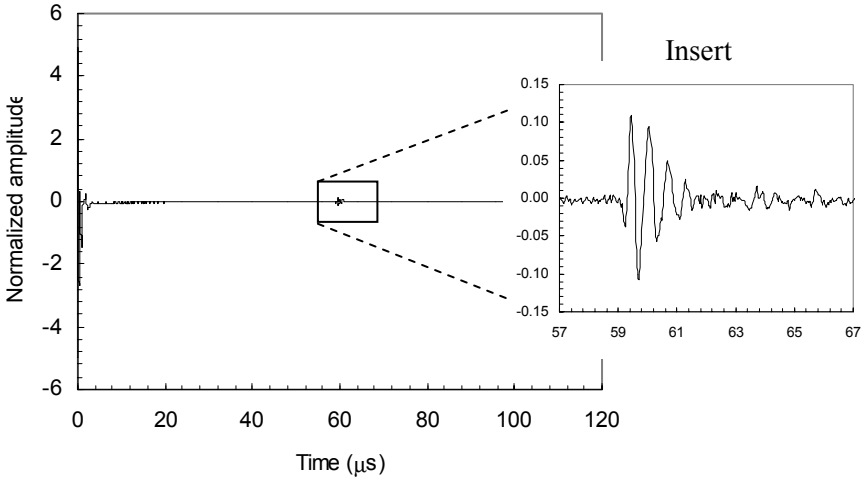

Figure 3-6. Typical reflected (echo) signal waveform at high pressure

The data files containing samples of the waveform were then analyzed in Matlab version 5 (The Math Works, Natick, MA, USA) using a digital signal processing technique via auto-correlation function. With this procedure, only one waveform (i.e. average of 20 waveforms instantly acquired) was recorded each time. Therefore the transit time (or time delay between the input signal and returned echo) values obtained by this technique were only used for comparison purposes in order to evaluate the accuracy

of the transit time obtained with the signal analyzer/interface program, by which any period of time of the experiment could be covered more efficiently with the same accuracy in addition to the inevitable variations due to pressure fluctuations. The accuracy on the transit time provided by the instrumental setup was considered about 1 nanosecond. The difference between the transit time determined from the waveform scope data and the transit time provided by signal analyzer oscillated from 2 to 5 nanoseconds. Considering that there was a time delay, impossible to overcome, between the exact times each datum was acquired, this comparison was deemed excellent.

The time measured, divided by the distance traveled by the pulse gives the velocity of sound. The distance traveled by the sound wave was double the direct straight path since it was the resultant path of the reflected wave. The sound path length measured at $0^{o}C$ and atmospheric pressure was 107.98 mm. Pressure as well as temperature affected this distance because of compressibility and thermal expansivity of the construction material of the ultrasonic probe. Therefore, the acoustic path length had to be corrected by the experimental conditions of the measurement. For 316L stainless steel the coefficient of linear compressibility and coefficient of thermal expansion were taken respectively as 1.9981×10^{11} MPa and $1.602 \times 10^{-5}\ {}^{o}C^{-1}$ (Davis 2000). A data logger model DAQ 56 (Omega Engineering, Stamford, CT, USA) was connected to the type-T thermocouple probe placed in the ultrasonic cell (Figure 3-3) for temperature measurement. The thermocouple probe was calibrated using a standard reference thermistor temperature sensor model 5610 connected to a handheld thermometer model 1521, with $0.01^{o}C$ uncertainty (Hart Scientific, American Fork, UT, USA) and a high precision thermostatic bath model 6035 (Hart Scientific, American Fork, UT, USA) or a

thermostatic refrigerating circulator for low temperatures (model 900, Fisher Scientific), in the temperature range of 5 to 65^{o}C. Temperature data were recorded during high-pressure experiments through a PC computer program at programmable sampling frequency (Balaban 2001).

Procedure for Collecting High-Pressure Ultrasonic Data

Experimental conditions to conduct ultrasonic high-pressure measurements were chosen based on pressure and temperature ranges usually employed in high-pressure processing of foods, pressure generating equipment capability, temperature conditioning availability, ultrasonic cell restrictions, concentration range of major food constituents, as well as by performing preliminary experiments. Therefore, pressure ranged from atmospheric, 200; 400 and 600 MPa and temperatures at 10, 20 and 30^{o}C. These values were taken as set points, but the actual measurements were conducted at equilibrium conditions which are slightly different from the set point values.

Although the high-pressure equipment was fully programmable, once a cycle was started there was no possibility to reset the running time during a cycle. Consequently a set of preliminary experiments were carried out to determine the time for thermal equilibration under acceptable limits. Complete thermal stabilization was not an option, since it was affected by the environmental conditions where the machine was located, which was not under control, and also because only the lateral walls of the vessel were thermally insulated. To exemplify the variation of the ambient temperature, data recorded on selected days are shown in Figure 3-7. Also, there is the effect of adiabatic heating which is pressure as well as pressurization rate dependent. Thus, a series of preliminary experiments was performed at varying conditions of final pressure and temperature, pressurization rates, and initial sample temperature conditioning. It was

concluded that, depending on the pressure/temperature combination after reaching the desired pressure, 2 to 5 hours were needed for thermal stabilization, with the lowest stabilization time at temperature near ambient and at lower pressures, as expected. Accordingly, pressurization rates were adjusted between 50 and 100 MPa min^{-1}.

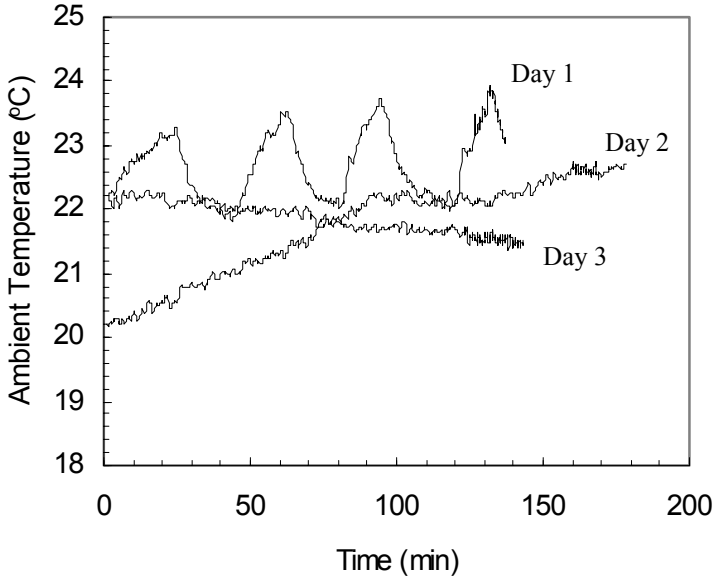

Figure 3-7. Ambient temperature variation during 3 different days

The upper temperature limit (30°C) was imposed since both the pressure generating system and the ultrasonic cell showed signs of weakness facing extreme conditions (pressure, temperature and medium). It should be remembered that, for example, at temperature conditioning of 40°C would result in a final temperature (at the end of pressurization step) over 65°C due to adiabatic heating effects. At this relatively high temperature combined with the effect of ethanol, a strong solvent used as the pressure transmitting fluid, parts such as electrical terminal's insulation or epoxy resins which were used as sealant for parts of the ultrasonic cell would not resist continuous exposure. Consider also that this temperature rise was not far from the boiling point of

ethanol, which at atmospheric pressure is around 77^{o}C. Nonetheless vapor pressure of ethanol increases appreciably, which was of concern as well. The lower temperature limit (10^{o}C) was dictated by the chiller capability and because of possible phase change and its associated volume expansion, which could bring irreversible damage due to material stress. No information was available to attest safety related issues to work at very low temperatures regarding the pressure generating system, such as possible detrimental effects of crystallization of the lubricating oil, although the manufacturer stated otherwise.

Pressure stabilization was totally dependent on the PLC controller and the response of the pump system of the high-pressure generating system as well as system sealing, which was acceptable between certain limits. There was an intrinsic pressure fluctuation around the set point which was pressure dependent, and not exactly invariable from one experiment to another considering experiments under similar conditions. Higher pressures produced larger fluctuations. Care was taken to avoid collecting data during periods when the re-pressurizing process was in progress, even in a short pressure range, since, again, this would promote adiabatic heating, disturb acoustical path, and consequently destabilize system equilibrium. Another important consequence was the disturbance caused by electrical/electronically actuated valves and pumps, which would create a 'noisy' environment, produce interference and end up extremely difficult to analyze and process the signal coming from the ultrasonic measurement cell. Figure 3-8 shows experimental runs with examples of pressure fluctuations around the set point. Decompression rate was kept low (25 MPa min^{-1}) to prevent sudden drop of pressure due to concerns related to the presence of micro pores in the cavity of the ultrasonic cell. In

addition, temperature drop associated with decompression (expansion cooling, which is the reverse effect of adiabatic heating) could possibly cause problems related to phase change.

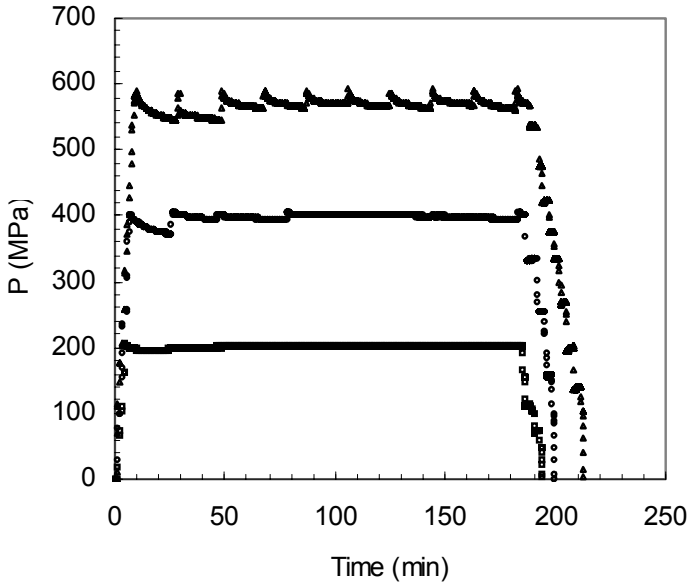

Figure 3-8. Pressure fluctuation of selected experiments at 200, 400 and 600 MPa set points.

Because the effect of adiabatic heating due to compression during the initial pressurization phase and the intrinsic pressure fluctuation which brought about heating or cooling due to the same or reversed effects, changes of temperature were therefore so large that the greater part of the time in performing the experiments under high pressure was consumed in waiting for equalization of temperature after changes of pressure.

In view of the preceding guidelines and observations, the basic procedure for collecting high-pressure ultrasonic data involved the following steps: [1] temperature conditioning of the high-pressure vessel, by setting up chiller or heater according to the desired temperature set point; [2] fluid sample preparation followed by filling up the ultrasonic cell container and its transfer to the high-pressure chamber; [3] set point

configuration of the pressure cycle through PC controller; [4] configuration of temperature data-logger; [5] configuration of signal analyzer interface program for logging and recording transit time; [6] starting pressure cycle and recording all data through PC computer programs at lower data-sampling frequency; [7] pressure and temperature stabilization by monitoring over time; [8] oscilloscope onscreen monitoring and recording signal waveforms; [9] once pressure and temperature reaches equilibrium, starting recording at higher data-sampling frequency (e.g., every 3 seconds) for a 5 to 10 minutes time span. This procedure was applied for collecting high-pressure ultrasonic data for pure water, binary aqueous model solutions, solute combinations, and a food material. Atmospheric pressure ultrasonic data were also collected for the same solutions at the same temperatures following this procedure.

Preparation of Binary Aqueous Solutions

Solutions were prepared with analytical grade reagents (>99% purity) from Fischer Scientific (Fair Lawn, NJ, USA) using deionized water, through ion exchange, activated carbon, and 2 micron filter (USFilter, Warrendale, PA, USA), on a weight by volume of the solution basis, with ±0.1 mg accuracy for mass. Binary solutions of sucrose, glucose, citric acid in water were prepared. The concentrations were 2.5, 10, and 50% (w/v) for sugar solutions, and 1, 5 and 10% (w/v) for organic acid solutions. Other combinations of these compounds in aqueous solutions were tested for component interaction and predictive analysis; simple carbohydrates only, and carbohydrates plus organic acids. This study intended to investigate the concentration range of interest for food science and engineering applications, rather than explore full concentration range as normally seen in physical chemistry studies. In addition, high-pressure ultrasonic measurements in a selected food system were performed in order to test the predictive

ability of the proposed model (see Chapter 4). Pasteurized pulp free orange juice, purchased locally, was chosen for this purpose, since its major components are simple sugars and organic acids, some of which corresponding to the same compounds currently investigated. The major components of this juice were quantified in order to prepare a solution based on this composition (analysis conducted by ABC Research); both juice and emulated juice were then investigated ultrasonically under high pressure at selected conditions.

Density and Heat-Capacity Measurements at Atmospheric Pressure

As will be described in Chapter 4, density, heat capacity, and thermal expansion coefficient data at atmospheric pressure as a function of temperature together with ultrasonic data at high pressures were combined to compute other thermodynamic properties as a function of pressure and temperature. These included density and compressibility computed by means of the appropriate thermodynamic relations and mathematical procedures. Accordingly, density, heat capacity and thermal expansivity data at atmospheric pressure were entered as initial input parameters in the numerical iterative procedure and because of the largely preponderant contribution of the former, in order to obtain reliable pressure dependent data, its accuracy had to be high as well. Accurate density data at atmospheric pressure was then considered the most crucial parameter for the mathematical procedure involved in the calculations of thermodynamic properties at elevated pressures derived from ultrasonic data. Thus, the following sequence describes the experimental procedure employed to determine density and heat capacity[2] at atmospheric pressure as a function of temperature for the same binary

[2] Both density and heat-capacity measurements at atmospheric pressure were performed in the laboratories of Dr. Miriam D. Hubinger, Dr. Florencia C. Menegalli and Dr. Antonio J. A. Meirelles, at the Department

solutions and other solute combinations as described previously. The coefficient of thermal expansion at atmospheric pressure as a function of temperature is subsequently obtained indirectly from density data by taking the first derivative of density with temperature according to Equation 2-6.

Density Measurements

Density measurements were performed using an oscillating tube density meter model DMA 58 from Anton Paar-GmbH (Graz, Austria) coupled to a cooling system. This system measured the period of oscillation, which is dependent on the density of the sample. A hollow U-shaped tube, with calibrated volume (approximately 0.7 cm^3), containing the sample was electro-magnetically excited to undamped oscillation. The calibration constants of the instrument, which comprised the spring constant of the oscillator, the mass of the empty tube, and the volume of the sample, could be calculated from two period measurements when the oscillator was filled with substances of known density. In this case, the instrument was calibrated with dry air and distilled, de-ionized water at the corresponding temperature. The calibration procedure was repeated every three days at each temperature. A semiconductor Peltier element and a resistance-based temperature sensor monitored and controlled the temperature of both sample and tube. An external chiller (Paar Physica-GmbH, Graz, Austria) was used for the low temperature experiments. All samples were thermally equilibrated to a temperature slightly above the instrument set point, in order to avoid formation of water vapor bubbles inside the oscillating tube. After introducing the samples slowly (to avoid formation of invisible gas bubbles), using a plastic-tipped hypodermic glass syringe,

---

of Food Engineering, at the State University of Campinas, SP Brazil; this author gratefully acknowledges their contributions.

totally free of gas bubbles, time was allowed for thermal equilibrium, typically 10-15 minutes. After each measurement, the oscillator was rinsed with water and acetone repeatedly, calibration checked, and dried by a filtered flow of air from a built-in pump.

Density measurements were performed at temperatures of 10^{o}, 20^{o}, 40^{o}, and 60^{o}C. This system provided an accuracy of $\pm 2 \times 10^{-5}$ g cm^{-3} and precision of $\pm 0.5 \times 10^{-5}$ g cm^{-3} on density measurements, and accuracy on temperature reading of $\pm 0.01^{o}$C, which could be controlled within $\pm 0.005^{o}$C.

The accuracy of the density measurements was confirmed based on the measurement of the density of pure water. Results for three such runs and literature values are shown in Table 3-1. The average deviations between the three runs and from literature values were 2.7×10^{-5}, and 4.0×10^{-5} g cm^{-3} respectively (Fine and Millero 1973; Wagner and Pruβ 1993). Thus, the measured density of pure water for temperatures from 10^{o} to 60^{o}C were in good agreement with the density values of Fine & Milleto (1973) and Pruss & Wagner (1993), considered the most accurate data for pure water.

Table 3-1. Results for the calibration of the density meter with pure water

	Density of Pure Water (g cm^{-3})					
T			This work		Fine and Millero	Wagner and Pruβ
(^{o}C)	Run 1	Run 2	Run 3	Average ± S.D.	(1973)	(1993)
10	0.99969	0.99970	0.99965	0.99968 $\pm 2.6 \times 10^{-5}$	0.99969	0.99970
20	0.99831	0.99833	0.99836	0.99833 $\pm 2.5 \times 10^{-5}$	0.99805	0.99821
30	0.99565	0.99572	0.99568	0.99568 $\pm 3.5 \times 10^{-5}$	0.99557	0.99565
40	0.99231	0.99230	0.99226	0.99229 $\pm 2.6 \times 10^{-5}$	0.99227	0.99222
50	0.98806	0.98805	0.98800	0.98804 $\pm 3.2 \times 10^{-5}$	0.98816	0.98803
60	0.98319	0.98319	0.98322	0.98320 $\pm 1.7 \times 10^{-5}$	0.98326	0.98320

Heat-Capacity Measurements

Heat-capacity measurements were performed using a differential scanning calorimeter model DSC-2920 (TA Instruments, New Castle, DE, USA) with cooling system. This system measured the differential heat flow between a sample and an inert reference. The sample and reference were subjected to controlled heating or cooling in a controlled atmosphere. The purge gas was helium with a flow rate of 93 ml min^{-1}. By using the sample-encapsulating press, the liquid sample was prepared within a hermetic sample capsule. The sample mass was in the range 12-14 mg. Sealed capsules containing samples were weighed before and after every run to assure capsule integrity. Based upon a series of preliminary runs, a method was created that held the sample isothermally at -12^{o}C for 5 minutes without freezing the sample (to account for the transient period to reach the desired starting temperature, 5^{o}C), and then heated at a rate of 7^{o}C min^{-1} to 70^{o}C.

The DSC calibrations consisted of the baseline slope (heating an empty cell through the entire temperature range of the experiments), the cell constant and the temperature calibrations (from the run of a calibration material, in this case pure water, through its melting point). To obtain accurate results, the calibrations had to be checked and repeated periodically.

The specific heat of a given sample was then determined by creating a baseline profile, a standard substance (pure sapphire-Al_2O_3) profile, and a sample profile using the same method described above. From the thermograms (resulting heat flow versus time or temperature recorded at 0.2 sec intervals), the heat capacity was calculated by using O'Neill's method (1966). The samples were run in duplicates. The accuracy of the Cp

measurements was estimated to be ±3% on the basis of the measurement of the Cp of pure water.

Summary of Conditions for the High-Pressure Experiments

Table 3-2 shows the range of the experimental conditions of pressure, temperature, and concentration used for collecting ultrasonic high-pressure data for binary aqueous solutions of sucrose, glucose, and citric acid.

Table 3-2. Summary of the experimental range of the high-pressure experiments

Variable	Unit	Experimental Range			
Pressure	(MPa)	0.1	200	400	600
Temperature	(K)	283.15	293.15		303.15
Concentration:					
Sugar Solutions	(kg-solute m^{-3})	25	100		500
Citric Acid Solutions	(kg-solute m^{-3})	10	50		100

CHAPTER 4
DATA PROCESSING AND ANALYSIS

This chapter presents a description of the procedures for processing and analyzing the data collected according to the experimental methods described in Chapter 3. They included: [1] the procedure to calculate speed of sound from transit time data of a sound wave propagating through the fluid sample under elevated pressures at different temperatures; [2] the procedure to determine density and heat capacity as a function of temperature at atmospheric pressure; [3] the procedure to compute thermal expansion coefficient as a function of temperature at atmospheric pressure from density data as a function of temperature; [4] the thermodynamic and numerical approach to derive other thermodynamic properties, such as density and compressibility as a function of pressure and temperature, from speed of sound data as a function of pressure and temperature, and density, heat capacity, and thermal expansion coefficient data as a function of temperature at atmospheric pressure as the initial values in an iterative manner. Predictive equations were also obtained by regression analysis for all thermodynamic properties derived as a means to conduct further mathematical analyses as well as to better interpret such data [5]. Up to this point all thermodynamic properties were derived from binary aqueous solutions properties data. Thus, in order to extend the analysis for multicomponent solutions, [6] a thermodynamic approach was developed to determine the effect and contribution of each component in the binary solutions using a mixing rule, and then this model was tested for combined solutes aqueous solutions and for a real food

system. As a final point, [7] an error analysis was performed in order to estimate the accuracy of the measured experimental data and the subsequent derived properties.

Speed of Sound at High Pressures

From the transit time measurements, or the time delay between the reference input signal and the first reflected echo received by the transducer, the speed of sound by which the ultrasound wave propagated thorough the fluid sample at a given condition was determined. The transit time measured in these experiments was in the range of 45,000 to 75,000 nanoseconds at nominal temperatures from 10^{o} to 30^{o}C at pressures from atmospheric up to 600 MPa. The sound velocity was given by the ratio of the known acoustic path length to the transit time. To carry out this calculation Equation 4-1 below was used, where acoustic path length was double the direct path length, since the reflected echo traveled twice the distance of the direct acoustic path. Since the acoustic path length varied with pressure and temperature, correction to account for the change in this distance was introduced using the thermal linear-expansion coefficient and the coefficient of linear compressibility for the construction material of the ultrasonic probe. Therefore, the acoustic path length had to be corrected by the experimental conditions of the measurement according to Equation 4-2, where $L_{Po,To}$ is the acoustic path length at reference pressure and temperature, 107.98 x 10^{-3} m measured at 0^{o}C and atmospheric pressure, and T and P are respectively the actual measured absolute temperature and absolute pressure of the experiment, respectively in Pascal (Pa) and Kelvin (K). For 316L stainless steel the coefficient of linear compressibility and coefficient of thermal expansion were taken respectively as 1.9981 x10^{11} MPa and 1.602 x10^{-5} $^{o}C^{-1}$ (Davis 2000)

$$u = \frac{L_{P,T}}{\Delta t} \qquad [4\text{-}1]$$

$$L_{P,T} = L_{P_o,T_o}\left[1 + \alpha'(T)\right]\left[1 + \beta'(P)\right] \qquad [4\text{-}2]$$

For prediction purposes as well as for easier and direct use in numerical computations, sound velocity data for each binary solution as a function of pressure P and temperature T at any given concentration were fitted to the following double polynomial model, where u_o is the speed of sound at atmospheric pressure P_o taken as the reference pressure, and a_{ij}'s are regression coefficients of the continuous surface.

$$P - P_o = \sum_{i=1}^{3}\sum_{j=0}^{2} a_{ij}(u - u_o)^i T^j \qquad [4\text{-}3]$$

Density at Atmospheric Pressure

Density of binary aqueous solutions of sucrose, glucose and citric acid at atmospheric pressure and concentration were experimentally obtained from vibrating tube density meter measurements in the temperature range of 5 to 65^{o}C. A total of 74 data points for sucrose solutions were obtained, 60 data points for glucose and citric acid solutions. Again, for prediction purposes as well as for easier and direct use in numerical applications, density data at atmospheric pressure P_o for each binary solution as a function of temperature and concentration were fitted to the following second order model on temperature T and concentration C, where a_{ij}'s are regression coefficients of the continuous surface.

$$\rho_{P_o} = \sum_{i=1}^{3}\left(\sum_{j=0}^{2} a_{ij} C^j\right) T^{i-1} \qquad [4\text{-}4]$$

Isobaric Thermal-Expansion Coefficient at Atmospheric Pressure

Coefficient of thermal expansion at atmospheric pressure was derived from measured density data at atmospheric pressure as a function of temperature using Equation 2-6 rewritten below. The approach included taking the first derivative of density (Equation 4-4) with respect to temperature, through an analytical procedure since not enough experimental data were available to perform this differentiation numerically without loosing precision. Also, the experimental data were not equally spaced with respect to temperature which made the numerical differentiation even more uncertain. The thermal-expansion coefficient for each binary aqueous solution was then obtained by dividing the resulting value by the density at any given temperature and concentration.

$$\alpha_{P_o} = -\frac{1}{\rho_{P_o}}\left(\frac{\partial \rho}{\partial T}\right)_{P=0.1\,\mathrm{MPa}} \qquad [2\text{-}6]$$

$$\alpha_{P_o} = -\frac{1}{\rho_{P_o}}\left[\frac{\partial}{\partial T}\sum_{i=1}^{3}\left(\sum_{j=0}^{2} a_{ij} C^j\right) T^{i-1}\right]_{P=0.1MPa} = -\frac{1}{\rho_{P_o}}\sum_{i=2}^{3}(i-1)\left(\sum_{j=0}^{2} a_{ij} C^j\right) T^{i-2} \qquad [4\text{-}5]$$

Isobaric thermal-expansion coefficients at atmospheric pressure P_o, determined as above, for each binary solution as a function of temperature T at any given concentration were fitted to the following model.

$$\alpha_{P_o} = \sum_{i=1}^{3} a_i T^{i-1} \qquad [4\text{-}6]$$

Isobaric Heat Capacity at Atmospheric Pressure

Heat capacity measured with the differential scanning calorimeter (DSC) was derived from the measured sample and reference heat flow using Equation 4-7, in the temperature range from 5°C to 65°C, calculated at each 0.1°C temperature interval, with a total of 615 data points for each sample, even though the sampling rate used allowed for a

shorter temperature interval. The Cp values were further averaged for two replication runs.

$$\frac{Cp_{sa}}{Cp_{ref}} = \frac{m_{ref}}{m_{sa}} \frac{\left(\frac{dH}{dt}\right)_{sa}}{\left(\frac{dH}{dt}\right)_{ref}} \quad [4\text{-}7]$$

A correction factor has been proposed to account for the effect of water that evaporates into the headspace of the sample capsule due to the exponential increase of water vapor pressure with temperature. By assuming equilibrium between liquid phase and the gas phase (headspace) inside the DSC-capsule, the equilibrium relationship derived from Clapeyron and Clausius-Clapeyron equations for a binary system could be used.

The assumptions are as follows:

- The liquid phase consists of a non-ideal binary solution (solute + water) and the gas phase consists of an ideal mixture of dry air and water vapor, with the equilibrium given by:

$$Y_w P = X_w \gamma_w P_w^o = A_w P_w^o \quad [4\text{-}8]$$

- Water activity of solution was considered a function of solute and water concentrations and activity coefficient, using selected models according to the component (Norrish 1966; Miyawaki et al. 1997; Chen 1989);
- The driving force for water to evaporate was given by the temperature increase, and was computed for each temperature interval;
- The volume of gas phase present inside the capsule was determined by means of an air comparison pycnometer (Multi-Pycnometer, model MVP-5DC, Quanta-Chrome, Boynton Beach, FL, USA);
- The amount of solution (liquid phase) changed over time (as temperature increases) in direct proportion to the amount of water evaporated;

- Enthalpy changes of the liquid solution (as measured by DSC in terms of specific heat flow) were determined by the latent heat of water in proportion to the water evaporated (going to the gas phase);
- Vapor pressure and latent heat of water were functions of temperature;
- There was negligible effect of sensible heat of the evaporated water in the gas phase. Simulation has shown a deviation of less than 0.007% on Cp values.

The correction term that was applied for heat capacity followed Equation 4-9 below:

$$\left(\frac{1}{m_{sample}}\frac{dH}{dt}\right)_{corrected} = \left(\frac{1}{m_{original}}\frac{dH}{dt}\right)_{DSC}\frac{m_{original}}{m_{sample}} - \frac{\Delta H_{evap}}{m_{sample}}\left(\frac{dT}{dt}\frac{1}{\Delta T}\right) \qquad [4\text{-}9]$$

The changing in sample mass due to evaporation is given by:

$$m_{sample} = m_{original} - m_{evap} \qquad [4\text{-}10]$$

Mass of water evaporated by using water mole fraction Y_w calculated using Equation 4-8, was computed with the following expression:

$$m_{evap} = m_{air}\frac{Y_w}{1-Y_w}\frac{Mw_w}{Mw_{air}} \qquad [4\text{-}11]$$

Water activity of solution as a function of composition in Equation 4-8 was calculated using models from Norrish (1966) and Miyawaki et al. (1997) both given by Equation 4-12, and Chen (1989) given by Equation 4-13. Note that Norrish's model differs from that of Miyawaki only by the absence of the cubic term in Equation 4-12.

$$A_w = (1 - X_S)e^{\left(\alpha X_S^2 + \beta X_S^3\right)} \qquad [4\text{-}12]$$

$$A_w = \frac{1}{1 + 0.018\left(\beta_e + Bm_S^n\right)m_S} \qquad [4\text{-}13]$$

Enthalpy carried by water evaporated was determined by multiplying it by the latent heat of water as a function of temperature using Wagner and Pruβ's expression (1993):

$$\Delta H_{evap} = m_{evap}\lambda \qquad [4\text{-}14]$$

$$\lambda = 2500.8 - 2.3293T - 0.0008T^2 \qquad [4\text{-}15]$$

The effect of the variation of the total pressure of the biphasic system along a DSC run, as a function of temperature at constant volume, was computed using:

$$P_2 = P_1\left[\frac{T_2 + 273.15}{T_1 + 273.15}\right] \qquad [4\text{-}16]$$

The Antoine equation was used to determine water vapor pressure as a function of temperature:

$$P_w^o\left(mmHg\right) = \exp\left[18.3036 - \frac{3816.44}{\left(\left(T + 273.15\right) - 46.13\right)}\right] \qquad [4\text{-}17]$$

An example of an outcome by applying the proposed approach for one particular DSC run (heating rate of 7°C min^{-1}, temperature range of 5 to 65°C, for approx. sample mass of 12.000 mg) for 1%-sucrose solution, the calculated amount of water evaporated over the entire run was 0.0115 mg. For this particular run, the calculated amount of water evaporated over each 0.1°C temperature increase was in the range from 2.4 $x10^{-6}$ to 3.7 $x10^{-5}$ mg. This represents about 0.1% of water being evaporated for the entire run relative to the initial sample mass. After applying Equation 4-9, the difference in the heat capacity calculated using Equation 4-7 ranged approximately from 1 to 3% depending on the solute, concentration, and temperature. The greater the concentration of the solution the smaller the deviation due to the effect of solute, which causes a decrease in vapor

pressure of the solution as would be expected. All heat-capacity data presented in this report included the above correction.

The complete set of experimental data of heat capacity determined as indicated above for each binary solution as a function of temperature T and concentration C were then fitted to the following second order model.

$$Cp_{P_o} = \sum_{i=1}^{3}\left(\sum_{j=0}^{2} a_{ij} C^{j}\right) T^{i-1} \qquad [4\text{-}18]$$

From Ultrasonic Data to Thermodynamic Properties at High Pressures. Thermodynamic Approach

Ultrasonic data at high pressures were combined with density, heat capacity, and thermal expansion coefficient data at atmospheric pressure (all functions of temperature as well) to compute other thermodynamic properties as functions of pressure and temperature, including density and compressibility. The latter two properties were the main focus of this research. The work of Davis and Gordon (1967) was taken as reference, and similarities and differences are highlighted where appropriate.

In order to establish the set of thermodynamic expressions to compute these target properties work began with the so-called Newton-Laplace Equation 2-10 together with the definition of compressibility, given by Equation 2-2 expressed isothermically. The relationship between isentropic and isothermal compressibility was also needed since the Newton-Laplace equation defines speed of sound in terms of isentropic compressibility, which has been derived in appendix A, given by Equation 2-9. These three equations are rewritten here for clarity.

$$u^2 = \frac{1}{\beta_S \rho} \qquad [2\text{-}10]$$

$$\beta_T \equiv \frac{1}{\rho}\left(\frac{\partial \rho}{\partial P}\right)_T \qquad [2\text{-}2]$$

$$\beta_T = \beta_S + \left(\frac{\alpha^2 T}{C_P \rho}\right) \qquad [2\text{-}9]$$

These equations were combined to obtain the following first order partial differential equation that expressed the variation of density with respect to pressure at a given constant temperature as being a function of speed of sound, thermal expansion coefficient, heat capacity and temperature.

$$\left(\frac{\partial \rho}{\partial P}\right)_T = \frac{1}{u^2} + \frac{\alpha^2 T}{Cp} \qquad [4\text{-}19]$$

Apart from temperature and pressure which were varied independently, it is recognized that none of the properties incorporated in the right hand side of the expression above, namely speed of sound, thermal expansion coefficient, or heat capacity, can be seen as independent of either pressure or temperature. Consequently, their pressure as well as temperature dependence had to be addressed. The pressure dependence of speed of sound was experimentally determined; therefore it entered into this approach as prior defined as the coefficients of the fitted Equation 4-3. The pressure dependence of the isobaric heat capacity isobaric and thermal expansion coefficient were given by Equations 2-7 and 2-8 (please refer to Appendix A).

$$\left(\frac{\partial C_P}{\partial P}\right)_T = -T\left(\frac{\partial^2 V}{\partial T^2}\right)_P = -\frac{T}{\rho}\left[\alpha^2 + \left(\frac{\partial \alpha}{\partial T}\right)_P\right] \qquad [2\text{-}7]$$

$$\left(\frac{\partial \alpha}{\partial P}\right)_T = -\left(\frac{\partial \beta_T}{\partial T}\right)_P \qquad [2\text{-}8]$$

The right hand side of Equation 2-8 above contains the isothermal compressibility, which can be obtained by combining Equations 2-9 and 2-10 to give:

$$\beta_T = \frac{1}{\rho}\left(\frac{1}{u^2} + \frac{T\alpha^2}{C_P}\right) \qquad [4\text{-}20]$$

Mathematical Solution for the Set of Partial Differential Equations

An iterative simultaneous step-by-step numerical procedure based on the Runge-Kutta 4,5th order, explicit 4,5 pair formula, using an interpolant of order 4 (Shampine and Reichelt 1997), was employed for the solution of the set of partial differential equations proposed above with initial values represented by the properties at atmospheric pressure.

The numerical procedure was applied to the pressure range starting from 0.1 MPa up to 600 MPa at pressure step intervals of 2 MPa, which satisfied the experimental conditions of the available ultrasonic data. This pressure interval was chosen only as a means of balancing an acceptable output accuracy range of values with the program running time, since the precision of the numerical method was internally controlled by convergence criteria. At each pressure interval, the values of density, isobaric heat capacity, and thermal expansion coefficient were computed at elevated pressures for each isotherm in the temperature range of 278.15 to 303.15 K, with temperature step interval of 5 K. The numerical method used variable step size for the iteration which was controlled by convergence, by taking the relative tolerance error of 1 x10^{-6} as the convergence criterion. As a result, the maximum step size for the numerical iteration was 0.2 MPa.

The mathematical procedure was implemented in Matlab version 5 (The Math Works, Natick, MA, USA). All experimental data and derived input properties were entered in the computer program as coefficients of the fitted equations from which

smoothed values were retrieved; hence no instability other than the ones conveyed by the numerical method itself was noticeable. Accordingly, the number of figures presented in the coefficients of those equations ended up playing a major role in the precision of the outcome. The calculations were carried out in the following sequence of operations:

[A] Compute density ρ at atmospheric pressure P_o and temperature T using Equation 4-4, thermal expansion coefficient α at P_o and T using Equation 2-6 and 4-5, heat capacity Cp at P_o and T using Equation 4-17, and sound velocity u at P_o and T using Equation 4-3.

[B] By using the numerical procedure described as above (Runge-Kutta 4,5th order), estimate density ρ at higher pressure $P_1+\Delta P$ at temperature T, by solving for the right hand side of Equation 4-19 with initial values as determined from previous step [A].

[C] Repeat steps [A] and [B] for each isotherm for the entire temperature range. At this point, there is a set of density values at higher pressure P_1 as a function of temperature.

[D] Fit the densities $\rho_{P_1}(T)$ at higher pressure P_1 as a function of temperature to a 2nd degree polynomial according to Equation 4-21 below, and find the coefficients $r_i(P)$.

$$\rho_P = \sum_{i=0}^{2} r_i(P) T^i \qquad [4\text{-}21]$$

[E] Compute thermal expansion coefficient α at higher pressure P_1 for each isotherm for the entire temperature range, by taking the first derivative of the expression just determined above with respect to temperature $(\partial\rho/\partial T)_{P_1}$ at P_1 and with the help of Equation 2-6.

[F] Fit the thermal expansion coefficient $\alpha_{P_1}(T)$ at higher pressure P_1 as a function of temperature to a 2nd degree polynomial according to Equation 4-22 below, and find the coefficients $a_i(P)$.

$$\alpha_{P_1} = \sum_{i=0}^{2} a_i(P) T^i \qquad [4\text{-}22]$$

[G] Compute the first derivative of thermal expansion coefficient $(\partial\alpha/\partial T)_{P_1}$ at higher pressure P_1 with respect to temperature.

[H] Compute isobaric heat capacity C_p at higher pressure P_1 for each isotherm for the entire temperature range, with the help of Equation 2-7, the expression just determined above $(\partial\alpha/\partial T)_{P_1}$, density $\rho_{P_1}(T)$ and thermal expansion coefficient $\alpha_{P_1}(T)$.

[I] Fit heat capacity $Cp_{P_1}(T)$ at higher pressure P_1 as a function of temperature to a 2nd degree polynomial according to Equation 4-23 below, and find thus the coefficients $c_i(P)$.

$$Cp_{P_1} = \sum_{i=0}^{2} c_i(P) T^i \qquad [4\text{-}23]$$

[J] Repeat step [B] taking however, the values of thermal expansion coefficient $\alpha_{P_1}(T)$, first derivative of thermal expansion coefficient with respect to temperature $(\partial\alpha/\partial T)_{P_1}$ and heat capacity $Cp_{P_1}(T)$ just calculated in steps [E]-[F], [G], [H]-[I].respectively, and thus obtaining new, somewhat different values for density for each isotherm for the entire range of temperature $\rho_{P_1}(T)$ which are taken as the final ones.

[K] Repeat steps [C]-[I] taking these new values of $\rho_{P_1}(T)$, thus determining new final values for thermal expansion coefficient $\alpha_{P_1}(T)$ and heat capacity $Cp_{P_1}(T)$, as well as the new coefficients for the fitted equations.

[L] Repeat steps [B] to [K] for the subsequent pressure intervals until the entire pressure range has been computed.

Once the procedure is completed, it is apparent that in the course of calculating density, heat capacity and thermal expansion coefficient values were obtained as a function of pressure and temperature for the entire range covered for the independent variables. It should be recalled that besides pressure and temperature the independent variables also included solute type and solute concentration; consequently this whole calculation process was repeated for each binary solution at different concentrations. The output of this Matlab program was a series of files containing calculated values in binary format for further retrieval.

This method of computation differs from the method of Davis and Gordon (1967) where the pressure dependence of the thermal expansion coefficient is determined by using the additional thermodynamic relation (Equation 2-8), and which therefore requires an additional assumption that the isothermal compressibility is a polynomial function of temperature. In the present method, however, the thermal expansion coefficient is calculated directly from successive density versus temperature isobars, which are found to be described precisely by second degree polynomials in temperature. In addition, the procedure of Davis and Gordon employs the simpler Euler numerical method for the solution of the differential equation, in contrast to the more accurate Runge-Kutta 4,5th order method used in the present procedure.

It should be pointed out that the major contribution to the density increment due to pressure actually comes from the term that contains the reciprocal of the square speed of sound in Equation 4-19 since the difference between the isentropic and isothermal compressibility of the studied solutions is expected to be small, which is the basic source of difference if considering the other term involved according to Equation 2-9. Therefore, the accuracy of speed of sound data plays a major role in the accuracy of the result. As anticipated before, density data at atmospheric pressure has a large influence on the final accuracy of derived properties under high pressure. By running these codes with input thermodynamic properties as those of pure water and then analyzing and interpreting the outcome, it was possible to address these issues. For instance, an uncertainty of 0.1 percent in the density of pure water at atmospheric pressure introduces an error as large as 10 percent in the thermal expansion coefficient at 280 MPa and 20 percent in isobaric heat capacity at 600 MPa. This is because the computation starts at atmospheric pressure and includes calculations of first and second derivatives of density. Furthermore, since the density derivative with respect to temperature is involved in the calculation, the accuracy of the change in density with temperature is more important than that of the density itself. Accordingly, the accuracy of thermal expansion coefficient at atmospheric pressure played a crucial role in the process calculation as well. Generally, at lower and higher temperatures the situation is less satisfactory. Thus, to achieve high accuracy for derived thermodynamic properties at high pressure, it is prudent to carefully examine all atmospheric-pressure measurements for possible systematic errors associated with the results and make all efforts to eliminate them as far as possible.

Additional Thermodynamic Properties Derived

Other thermodynamic properties were computed as well during the calculation process, namely isentropic β_S and isothermal β_T compressibility, isentropic pressure thermal coefficient γ_S as a function of pressure and temperature. The latter property was used to determine and predict the effect of each compound investigated on temperature rise due to adiabatic heating. Isentropic compressibility was calculated directly from the Newton-Laplace Equation 2-10 at any given pressure and temperature. Isothermal compressibility was evaluated using Equation 4-20. Equation 2-4, rewritten here, was used to compute adiabatic pressure thermal coefficient[1] as a function of pressure and temperature (see derivation in the Appendix A, refer to Equation A-10).

$$\gamma_S = \left(\frac{\partial P}{\partial T}\right)_S = \frac{\rho C_P}{T\alpha} \qquad [2\text{-}4]$$

Many other properties can be derived from sound velocity, density, and compressibility data as a function of pressure, temperature, and composition/concentration, for example the ratio between isothermal and adiabatic compressibility and the ratio between heat capacity at constant pressure and heat capacity at constant volume, or even more fundamental thermodynamic properties such as specific entropy or enthalpy, and Gibbs or Helmholtz specific functions (also called 'free energies'). Although these properties may be of interest in other research works at a purely physical chemical level where the entire range of concentrations are usually investigated, they were considered non applicable in the present context.

[1] **Adiabatic pressure thermal coefficient** measures the temperature change produced by an isentropic change of pressure, thus a reversible process; while the so-called Joule-Thomson coefficient is a measure of the temperature change during a throttling (expansion) isenthalpic process, and therefore irreversible.

Thermodynamics of Solution: Mixing Scheme and Solute Effect

The determination of the thermodynamic properties derived from ultrasonic data of dissolved components of solutions must account for every interaction due to the added substance(s). When a solute is introduced into a solvent, it usually 'reacts' in some way resulting in changes in its molar volume (e.g., hydration in the case of aqueous solutions), compressibility, and heat capacity among others. The contributions made by solute and solvent are not promptly identifiable through space occupancy; instead volumetric properties of a solution can be interpreted in terms of partial or partial molar properties from solution density or specific volume. A thermodynamic approach based on the concept of partial properties and their respective summation rule was proposed in order to determine the effect of each component (solute and solvent) and solute concentration on volumetric thermodynamic properties of binary aqueous solutions of sucrose, glucose and citric acid as a function of pressure, temperature and concentration.

Partial Molar Volumes

The volume of a binary aqueous solution, a dependent variable, is described by the set of independent variables given by two intensive variables, pressure and temperature, and the composition variable, solute concentration, expressed in terms of, for example, mole fraction. The procedure starts by defining a solution molar volume, an intensive property, given by the following equation at fixed pressure, temperature and composition, which relates the 'experimentally' obtained solution density, derived from ultrasonic experimental data, and mole fractions of solvent and solute[2].

$$V^m = \frac{1}{\rho}\left(x_1 M_{w1} + x_2 M_{w2}\right) \qquad [4\text{-}24]$$

[2] As a reminder of our notation along this work: subscript 1 is ascribed to solvent and subscript 2 to solute.

The change in volume by mixing of a multicomponent solution, which is not the sum of the volumes of the individual volumes, can be described by the independent variables temperature, pressure, and the amount of each component. In the case of a binary solution, this change is expressed by

$$dV = \left(\frac{\partial V}{\partial T}\right)_{P,n} dT + \left(\frac{\partial V}{\partial P}\right)_{T,n} dP + \left(\frac{\partial V}{\partial n_1}\right)_{P,n_2} dn_1 + \left(\frac{\partial V}{\partial n_2}\right)_{P,n_1} dn_2 \qquad [4\text{-}25]$$

The subscript *n* in the first two partial derivatives indicates that the number of moles for all the components is held constant. The partial molar volumes of each component in solution were then defined as partial derivatives of solution volume and consequently depend on the same variables as *V*, and could be expressed in terms of either number of moles or mole fraction.

$$\overline{V}_1^{\,m} = \left(\frac{\partial V}{\partial n_1}\right)_{T,P,n_2} = \left(\frac{\partial n V^m}{\partial n_1}\right)_{T,P,n_2} \qquad [4\text{-}26]$$

$$\overline{V}_2^{\,m} = \left(\frac{\partial V}{\partial n_2}\right)_{T,P,n_{=1}} = \left(\frac{\partial n V^m}{\partial n_2}\right)_{T,P,n_1} \qquad [4\text{-}27]$$

Using the partial molar volumes as defined by Equation 4-26 and 4-27, *dV* becomes

$$dV = \left(\frac{\partial V}{\partial T}\right)_{P,n} dT + \left(\frac{\partial V}{\partial P}\right)_{T,n} dP + \sum_{i=1}^{2} \overline{V}_i dn_i \qquad [4\text{-}28]$$

Equation 4-28 describes how change in the volume of the solution is related to the partial molar volumes of the individual components. But more useful for the present investigation are the expressions for the thermodynamic properties of the solution rather than only the changes in these properties. With this, we recall that partial molar property quantities obey the summation rule as long as the independent thermal and mechanical

variables of the system are intensive properties of the system (Reis 1982); in this case temperature and pressure are verified.

$$V^m = x_1 \overline{V}_1^m + x_2 \overline{V}_2^m \qquad [4\text{-}29]$$

As seen from Equation 4-29 the solution molar volume is the mole fraction average of the individual components partial molar volumes, in other words, the values of each member on the right hand side of this relationship will provide the answer on how much of the solution molar volume is to be ascribed to each component.

Partial molar volumes cannot be obtained directly from the solution molar volume, using Equation 4-29, because it is not possible to identify the contributions made by the solute and solvent in geometric (i.e. space occupancy) terms since both are concentration dependent and do not change independently as the composition of the solution is changed. Therefore, for the present investigation, these contributions were computed based upon the variation of the solution molar volume with solute mole fraction, since the concentration dependence of solution density and derived volumetric properties can be readily determined. Differentiation of solution molar volume with respect to n_1, as Equation 4-26 suggests, while holding T, P, and n_2 constant gives

$$\left(\frac{\partial n V^m}{\partial n_1}\right)_{T,P,n_2} = V^m + n\left(\frac{\partial V^m}{\partial n_1}\right)_{T,P,n_2} \qquad [4\text{-}30]$$

By making use of the chain rule of differentiation, for the second term of the right hand side of Equation 4-30 becomes,

$$\left(\frac{\partial V^m}{\partial n_1}\right)_{T,P,n_2} = \left(\frac{\partial x_2}{\partial n_1}\right)_{T,P,n_2}\left(\frac{\partial V^m}{\partial x_2}\right)_{T,P} = -\frac{n_2}{(n_1+n_2)^2}\left(\frac{\partial V^m}{\partial x_2}\right)_{T,P} \qquad [4\text{-}31]$$

Combining Equations 4-30 and 4-31 the final equation used to determine the partial molar volume of solvent in solution becomes,

$$\bar{V}_1^m = V^m - (x_2)\left(\frac{\partial V^m}{\partial x_2}\right)_{T,P} \qquad [4\text{-}32]$$

Similarly, it can be shown that the partial molar volume of the solute in solution can be obtained by the following relationship.

$$\bar{V}_2^m = V^m + (1 - x_2)\left(\frac{\partial V^m}{\partial x_2}\right)_{T,P} \qquad [4\text{-}33]$$

Use has been made here of the fact that $x_1 + x_2 = 1$. Hence, x_2 may be regarded as the only independent variable at constant T and P, and the partial derivatives could have been replaced by total derivatives specifically for this analysis, even though the partial derivative notation was kept in regard of the other variables T and P despite the fact that they were held constant in the differentiation. Furthermore, $dx_1 = - dx_2$. It is possible then, to fit the data of solution molar volume $\bar{V}^m$ with an appropriate power series in x_2, and differentiate this mathematical representation directly. A second degree was employed, since the concentration dependence was represented by only three different concentration levels. It is evident that if gram was chosen instead of the mole as unit amount of a substance, the equations would all have been of the same form. Mole fraction would then be replaced by mass fraction, and, in place of the partial molar volume, partial specific volume of a component could be defined as the change in volume of the solution per gram of that component. Thus, in this case, direct differentiation of the specific volume of the solution, which is the reciprocal of solution density, with respect to weight fraction could be performed. This enabled using the data directly as obtained. The results of partial specific volumes multiplied by the molecular weights

give the corresponding partial molar quantities. The equations for the summation rule and partial specific volumes of solute and solvent in solution, respectively, are given by the following expressions.

$$V = w_1\overline{V}_1 + w_2\overline{V}_2 \qquad [4\text{-}34]$$

$$\overline{V}_2 = \left(\frac{\partial mV}{\partial m_2}\right)_{T,P,m_1} = V + (1 - w_2)\left(\frac{dV}{dw_2}\right)_{T,P} \qquad [4\text{-}35]$$

$$\overline{V}_1 = \left(\frac{\partial mV}{\partial m_1}\right)_{T,P,m_1} = V - (w_2)\left(\frac{dV}{dw_2}\right)_{T,P} \qquad [4\text{-}36]$$

Partial Compressibilities

In common with conventional partial molar quantities, partial volume-specific quantities obey the summation rule as well, although because partial isentropic compressibility, like solution isentropic compressibility, has the dimensions of the inverse of pressure, it should not be qualified as a molar quantity; it follows then,

$$\beta_S = x_1\overline{\beta}_{S,1} + x_2\overline{\beta}_{S,2} \qquad [4\text{-}37]$$

Similarly with the development described above for partial molar volumes in conformity with Equations 4-32 and 4-33, it is possible also to compute partial isentropic compressibility from the concentration dependence of solution isentropic compressibility as follows:

$$\overline{\beta}_{S,2} = \left(\frac{\partial n\beta_S}{\partial n_2}\right)_{T,P,n_1} = \beta_S + (1 - x_2)\left(\frac{\partial \beta_S}{\partial x_2}\right)_{T,P} \qquad [4\text{-}38]$$

$$\overline{\beta}_{S,1} = \left(\frac{\partial n\beta_S}{\partial n_1}\right)_{T,P,n_2} = \beta_S - (x_2)\left(\frac{\partial \beta_S}{\partial x_2}\right)_{T,P} \qquad [4\text{-}39]$$

In a similar way, since the concentration dependence was represented by three concentration levels, data of solution isentropic compressibility were fitted to a second degree polynomial in x_2, and differentiated directly with respect to x_2.

Based on the fact that the definition of compressibility involves volume according to Equation 2-2, it is essential to account for changes in molar volume in partial compressibility determination. Following many published works on thermodynamic of solutions (Reis 1998; Blandamer et al. 2001), an alternative approach would be by defining a solution isentropic compression, having dimensions of specific-volume times the inverse of pressure ($m^3kg^{-1}MPa^{-1}$). This s determined simply by dividing the solution isentropic compressibility by the solution density, according to Equation 4-40.

$$\beta'_S = \beta_S V = \frac{\beta_S}{\rho} \qquad [4\text{-}40]$$

The summation rule and the partial specific isentropic compressions can be expressed in terms of mass fractions of the components.

$$\beta'_S = w_1\overline{\beta}'_{S,1} + w_2\overline{\beta}'_{S,2} \qquad [4\text{-}41]$$

$$\overline{\beta}'_{S,2} = \left(\frac{\partial m\beta'_S}{\partial m_2}\right)_{T,P,m_1} = \beta'_S + (1-w_2)\left(\frac{\partial \beta'_S}{\partial w_2}\right)_{T,P} \qquad [4\text{-}42]$$

$$\overline{\beta}'_{S,1} = \left(\frac{\partial m\beta'_S}{\partial m_1}\right)_{T,P,m_2} = \beta'_S - (w_2)\left(\frac{\partial \beta'_S}{\partial w_2}\right)_{T,P} \qquad [4\text{-}43]$$

Water Activity from Solvent Partial Molar Volume: Thermodynamic Approach

The pressure dependence of the Gibbs free energy for a homogeneous material at constant temperature and composition is solely given by the volume (see Appendix A for derivation):

$$\left(\frac{\partial G}{\partial P}\right)_{T,comp} = V \qquad [4\text{-}44]$$

By differentiation with respect to the amount of component 1 n_1, gives

$$\left[\frac{\partial}{\partial n_1}\left(\frac{\partial G}{\partial P}\right)_{T,P,n_2}\right]_{T,P,n_2} = \left(\frac{\partial V}{\partial n_1}\right)_{T,P,n_2} \qquad [4\text{-}45]$$

Recognizing the definition of partial molar volume of the solvent in solution in the above equation, and rearranging by making use of the chain rule of differentiation, we obtain

$$\left[\frac{\partial}{\partial n_1}\left(\frac{\partial G}{\partial P}\right)_{T,P,n_2}\right]_{T,P,n_2} = \left[\frac{\partial}{\partial P}\left(\frac{\partial G}{\partial n_1}\right)_{T,P,n_2}\right]_{T,P,n_2} = \left(\frac{\partial \overline{G}_1}{\partial P}\right)_{T,P,n_2} = \left(\frac{\partial V}{\partial n_1}\right)_{T,P,n_2} = \overline{V}_1^{\,m} \qquad [4\text{-}46]$$

Partial molar free Gibbs energy is identical to the chemical potential of component 1.

$$\left(\frac{\partial \overline{G}_1}{\partial P}\right)_{T,comp} = \left(\frac{\partial \mu_1}{\partial P}\right)_{T,comp} = \overline{V}_1^{\,m} \qquad [4\text{-}47]$$

Moreover, chemical potential of solvent (component 1 in solution) can be expressed in terms of activity of this component in the form of Equation 4-48.

$$d\mu_1 = RTd\ln A_1 \qquad [4\text{-}48]$$

Assuming the chemical potential of the pure component at the highest concentration (water) at the temperature and pressure of the system as the reference standard state (Acree 1984)[3], it follows:

$$\left(\frac{\partial \ln A_1}{\partial P}\right) = \frac{1}{RT}\left[\left(\frac{\partial \mu_1}{\partial P}\right) - \left(\frac{\partial \mu_1^o}{\partial P}\right)\right] = \frac{1}{RT}\left[\overline{V}_1^{\,m} - V_1^{o,m}\right] \qquad [4\text{-}49]$$

[3] Acree argues that for unsymmetrical reference systems, where there is a distinction between solvent and solute molecules, the standard state for the solvent, the component at the highest concentration, is the same as in symmetrical reference systems, meaning the state of the pure component (Acree 1984).

Integrating with respect to pressure at constant temperature T, from P_{ref} (atmospheric pressure 0.1 MPa) to pressure P, for the activity of the component water in solution, and substituting with the usual notation for water activity $A_1 = A_w$

$$\int_{A_{w,\mathrm{Pref},T}}^{A_{w,P,T}} d\ln A_w = \frac{1}{RT}\int_{P_{ref}}^{P}\left(\overline{V}_1^{\,m} - V_1^{o,m}\right)dP \qquad [4\text{-}50]$$

The function $\left(\overline{V}_1^{\,m} - V_1^{o,m}\right)$, which is the difference between the partial molar volume of component water (solvent) in solution, determined as described in the previous section, and the molar volume of pure water (independently determined from experimental sound velocity data), both at the same temperature, can be fitted to a 3rd degree polynomial in P. Ascribing letters for polynomial coefficients A, B, C, and D, which are temperature and concentration dependent, we may write.

$$\ln\frac{A_{w_{P,T}}}{A_{w_{P_{ref}},T}} = \frac{1}{RT}\int_{P_{ref}}^{P}\left(AP^3 + BP^2 + CP + D\right)dP \qquad [4\text{-}51]$$

The integral above can be solved analytically to obtain the final expression for water activity as a function of pressure (from atmospheric to 600 MPa) at a given temperature T, which can be computed for any temperature within the range investigated.

$$A_{w_{P,T}} = A_{w_{P_{ref}},T}\exp\left\{\frac{1}{RT}\left[\frac{A}{4}\left(P-P_{ref}\right)^4 + \frac{B}{3}\left(P-P_{ref}\right)^3 + \frac{C}{2}\left(P-P_{ref}\right)^2 + D\left(P-P_{ref}\right)\right]\right\} \qquad [4\text{-}52]$$

Water activity of the reference state ($A_{w,\,Pref,T}$) is taken as that of the solution, which is solute-type and solute-concentration dependent, at atmospheric pressure at a given temperature calculated using the same model mentioned previously in the text, in conformity with Equations 4-12 and 4-13.

Error Analysis

It has been recognized that a detailed uncertainty analysis of the experimental data obtained for the speed of sound at high pressures is extremely difficult for the present investigation since many of the uncertainties involved in the measurements are unknown. Nonetheless, a qualitative error analysis was given and a quantitative deviation comparison with literature data for pure water was performed which in fact, could be seen as the ultimate figures for the deviations encountered as far as the end results were concerned.

The total errors associated with the measured variables were combinations of systematic (or bias) and random (or precision or repeatability) errors (Coleman and Steele 1999; Bevington 1969), although the ISO Guide categorizes type A uncertainty as those evaluated by statistical analysis of a series of observations, and type B uncertainties as those evaluated by means other than statistical analysis (ISO 1993). The errors associated with the sound velocity measurements were due to the several variables (pressure, temperature, acoustic path length, propagation time, solution concentration and solvent purity).

The uncertainties of the variable pressure, the most important variable in this investigation, were not known; however pressure error was estimated to be as large as 1 to 4 times the magnitude of the atmospheric pressure in absolute terms (up to 4×10^5 Pa). No direct way to check the pressure readings was available, although indirect methods such as comparison-calibration procedures with similar measurements for pure substances, contrasted with literature data, could be a choice, although discrepancies in the literature data at high pressure have also been reported (Hayward 1971b). Moreover, what was considered aggravating, pressure fluctuations, already referred to in the

previous chapter, and made pressure readings even less reliable either in terms of recorded values or for the required process steadiness. For *n* number of observations, the so-called sample standard deviation $S_{\overline{X}}$ of the mean value $\overline{X}$, was calculated using Equation 4-53 (Coleman and Steele 1999). During the data acquisition period, considered to be the state of thermodynamic equilibrium, the overall average standard deviation for pressure was calculated as 0.29 for all experiments. The highest pressure level, around 600MPa, provided the highest average deviation (0.34 MPa). We recall that the sample standard deviation, as obtained, multiplied by the t-value (which approaches 1.96 as *n* approaches infinity), considering these observations to follow the t-distribution at a certain confidence interval (e.g., 95%), it will give the random uncertainty for this measurement.

$$S_{\overline{X}} = \left[\frac{1}{n(n-1)} \sum \left(X - \overline{X} \right)^2 \right]^{1/2} \qquad [4\text{-}53]$$

Temperature equilibration was also greatly influenced by the latter issues, due to adiabatic heating of compression affected by pressure fluctuations. As described in the preceding chapter, although temperature calibration was conducted against standard reference temperature sensor devices, it was performed under atmospheric conditions; consequently no pressure effects were anticipated in this case. Again, similar comparison-calibration procedures, as suggested for pressure measurements, could be performed in the case of temperature. The overall average sample standard deviation for all experiments, calculated using Equation 4-53, was 0.11 K for the temperature measurements. Again, this value multiplied by the t-value gives the random uncertainty for this measurement.

The systematic errors associated to the acoustic path length were tied to pressure and temperature measurements, since it was computed indirectly through ultrasonic measurements conducted at atmospheric pressure in pure water (refer to previous chapter), and then corrected to the increased pressure and temperature effects carried throughout investigation. The errors associated with the determination of the transit time were those resulting from digitizing, sampling, and from the algorithm used for the detection and analysis of the digitized signals, which summed up to 1 ns absolute accuracy. The "random uncertainty" associated with the transit time measurement, computed using the same Equation 4-53, was calculated to be 1.8 ns expressed in terms of the overall average sample standard deviation for the acquisition period considered as that of the thermodynamic equilibrium state.

Solution preparation also contributed to uncertainties as for the purity of the substances involved, water and the various solutes studied (e.g., sugars are highly hygroscopic, absorb moisture from the environment, nonetheless they were used with no further purification), volumetric flasks, balance, which all together may account for less than 0.01% to the overall uncertainty.

Besides the accuracy required for the ultrasonic experimental data at elevated pressures, density, heat capacity and thermal expansivity data at atmospheric pressure, entered as initial input parameters in the numerical iterative procedure and because of the largely preponderant contribution of the former, in order to obtain reliable pressure dependent data, its accuracy had to be attained as well. Accurate density data at atmospheric pressure was then considered the most crucial parameter for the mathematical procedure involved in the calculations of thermodynamic properties at

elevated pressures derived from ultrasonic data. The accuracy of the density measurements, estimated to be better than 0.02%, was confirmed based on the measurement of the density of pure water at atmospheric pressure. The measured densities of pure water in the temperature range studied were in close agreement with literature values (Fine and Millero 1973; Wagner and Pruβ 1993), considered the most accurate data for pure water (see Table 3-1 for details). The accuracy of the heat-capacity measurements was estimated to be ±3% on the basis of the measurement of the Cp of pure water. Since thermal expansion coefficient was determined based on the temperature dependence of solution densities, its contribution to the overall uncertainty followed that of density measurements added to the statistical error of the polynomial fitting and of the first derivative taken of density with respect to temperature.

In addition, the errors due to the numerical iterative procedure carried out to determine density, compressibility, and other thermodynamic properties at high pressures from ultrasonic data at high pressure and density, isobaric specific heat capacity, and thermal expansion coefficient at atmospheric pressure, could not be estimated easily because some of the errors at both atmospheric and high pressure were not known. All these quantities have both random and systematic errors as mentioned before. The error in these calculated values of derived thermodynamic properties could, in principle, be estimated by introducing appropriate perturbations on the input data and recording their effects on the final results. Accordingly, the major contribution to the density increment due to pressure came from the term $1/u^2$ in Equation 4-19, since the difference between the isentropic and isothermal compressibility was small (comprised by the second term in the right hand side of the same equation). Although a systematic error in the density data

at atmospheric pressure only introduced an error of the same magnitude to the density at higher pressures, a random error may affect the precision of all the quantities at higher pressures considerably. The combined contribution of isobaric specific heat capacity and thermal expansion coefficient to the overall uncertainty on derived thermodynamic properties from ultrasonic data was estimated as less than 10%. The influence of a systematic error in the sound velocity data on the calculated values of density and isobaric thermal-expansion coefficient was found to be small. For instance, a systematic error of 0.1% in the sound velocity can introduce a maximum error of 0.02% in the calculated values for density and 0.1% for compressibility at high pressures.

Part of these errors may be caused by the fitting processes, extensively used; on the other hand this procedure can be advantageous for data smoothing, therefore minimizing associated random errors. The standard deviations between the experimental and fitted values were found to be in the order of the accuracy of the measurements showing the validity of the measurements. Many of the errors were possibly eliminated or reduced by the appropriate calibration procedure as described in the experimental section.

Quantitative deviation comparisons with literature data for pure water was conducted for the most representative thermodynamic properties investigated in this study, sound velocity, density and isentropic compressibility, in order to give an estimation of how ‘bad’ or ‘good’ were the data produced. The expression given below, for a general thermodynamic property Q, was used to determine the percentage deviation between the present thermodynamic property, experimentally obtained or calculated, and

those of NIST (National Institute of Standards and Technology), using internationally accepted data and expressions from Saul and Wagner (1989), for pure water.

$$\%Deviation = \frac{(Q_{\exp} - Q_{Lit})}{Q_{\exp}} x100 \quad \text{or} \quad \frac{(Q_{calc} - Q_{Lit})}{Q_{calc}} x100 \qquad [4\text{-}54]$$

Figures 4-1, 4-2, and 4-3 present the percentage deviation between the measured sound velocities (after smoothed out by fitting experimental data of sound velocity in P and T to Equation 4-3), calculated density and isentropic compressibility for pure water and those of NIST, data from Saul and Wagner (1989), plotted as a function of pressure in the temperature range covered in this study.

Although a qualitative error analysis and quantitative deviations from literature data were offered, the lack of information regarding the uncertainties in the measurement of certain variables were used as an excuse for not presenting a detailed uncertainty analysis. Furthermore, the many thermodynamic properties, experimentally determined or calculated, were in close proximity to their true values, as shown by the comparisons made with trusted literature values, although data for pure water were the only possible data available.

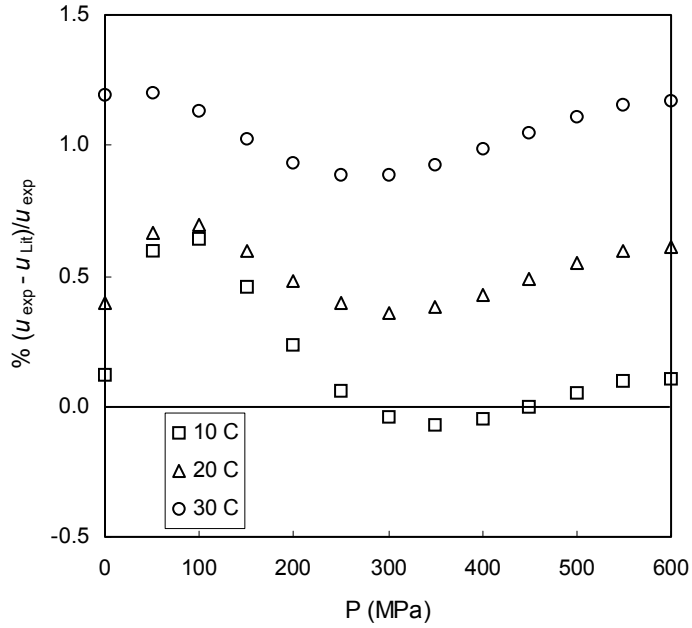

Figure 4-1. Percentage deviation between the measured[4] sound velocities in pure water and those of NIST, data from Saul and Wagner (1989), plotted as a function of pressure at several temperatures

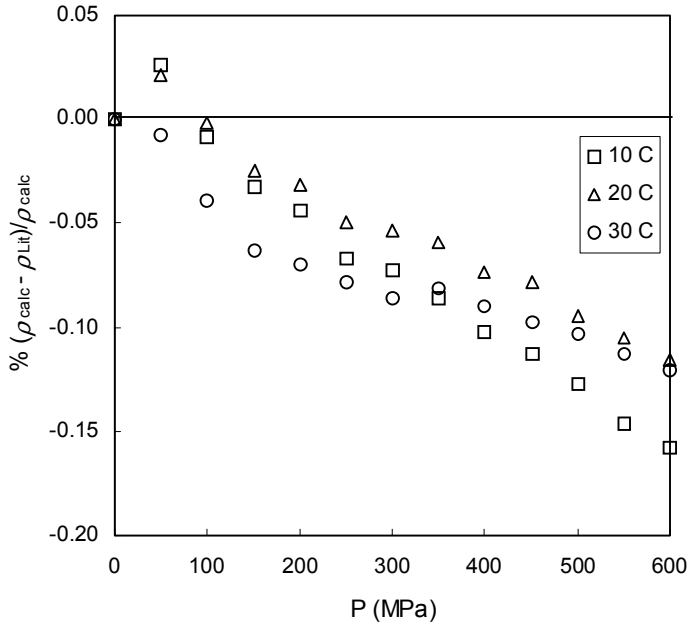

Figure 4-2. Percentage deviation between the calculated densities of pure water and those of NIST, data from Saul and Wagner (1989), plotted as a function of pressure at several temperatures

[4] After smoothed out by fitting experimental data of sound velocity in P and T to Equation 4-3

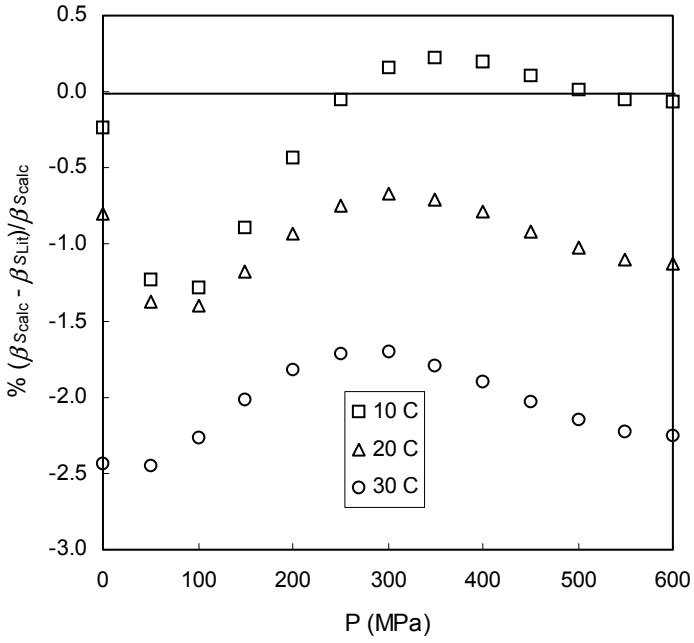

Figure 4-3. Percentage deviation between the calculated compressibilities of pure water and those of NIST, data from Saul and Wagner (1989), plotted as a function of pressure at several temperatures

CHAPTER 5
RESULTS AND DISCUSSION

This chapter presents and discusses the results of the experiments conducted to collect ultrasonic data at elevated pressures and then the calculated properties derived from them as described in the previous chapter. The experimental results of sound velocity as a function of pressure, temperature, and concentration for each binary solution of sucrose, glucose, and citric acid are presented. A brief overview of the thermodynamic properties experimentally determined at atmospheric pressure will be shown as well. In the sequence, thermodynamic properties of density, isentropic and isothermal coefficient of compressibility, and the isentropic pressure thermal coefficient derived from ultrasonic data at elevated pressure combined with density, isobaric specific heat capacity, and thermal expansion coefficient data at atmospheric pressure as a function of temperature and concentration for each binary solution of sucrose, glucose, and citric acid are presented as a result of the application of the numerical iterative procedure. Also presented are the findings of applying the thermodynamic approach proposed for the mixing scheme in terms of partial properties and partial molar volumes of solute and solvent. This section ends with the calculated values of water activity derived from the solvent partial molar volume as a function of pressure, temperature, and concentration for each binary solution of sucrose, glucose, and citric acid.

Sound Velocity at High Pressures

Experimental sound-velocity data for sucrose, glucose, and citric acid aqueous solutions along with that of pure water at different pressures, temperatures, and

concentrations are shown in Figures 5-1 to 5-3. Tables with the numerical values are presented in Appendix B. As described in previous chapters, it should be stressed that these values were obtained at equilibrium conditions of pressure and temperature for each binary solution, which was unique for each experiment. Therefore, each data point, at a given P and T, is the result of the average of a series of measurements of pressure, temperature and transit time over the acquisition period considered as close as possible to the thermodynamic equilibrium state, given the experimental setup available. A total of 36 data points for each binary solution were obtained. It can be observed from these plots that the sound velocity increases as pressure as well as temperature increases, although the effect of temperature is less pronounced in the restricted temperature range investigated. This behavior is expected if we look at Equation 2-10, since it is the result of the balance between the effect of pressure and temperature on both compressibility and density. As pressure increases, the liquid becomes compressed resulting in a volume decrease or an increase in density, but there is thermal expansion associated with temperature rise. Moreover, the liquid becomes less compressible at higher pressures. It is also apparent, from these plots, the sensitivity of the speed of sound with solute concentration, although the smaller concentration range adopted in the case of citric acid solutions makes it not as easy to recognize as it is for sugar solutions. In this regard, as this analysis proceeds a clearer and definite pattern shall be observed for the behavior of other derived thermodynamic properties.

These experimental data were fitted to a double polynomial model expressed by Equation 4-3, rewritten here, for each binary solution as a function of pressure P and temperature T at any given concentration.

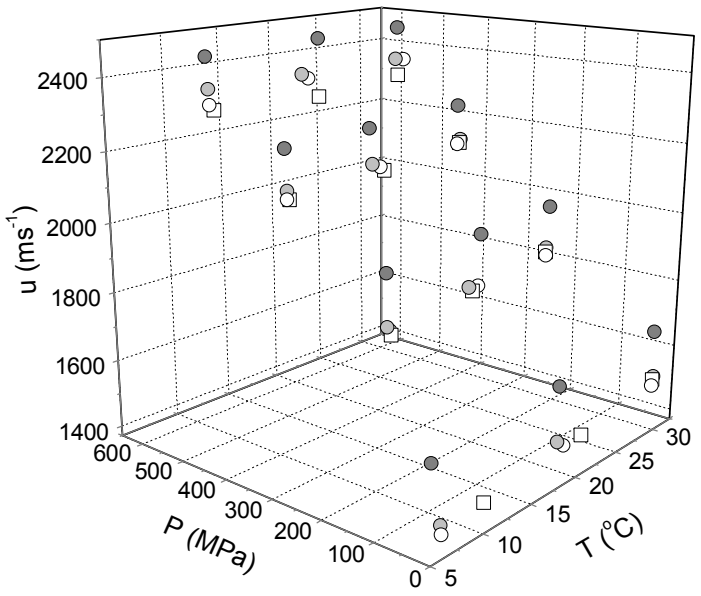

Figure 5-1. Experimental sound velocity in sucrose solutions 2.5% ○, 10% ◍, and 50% ●; and in pure water □

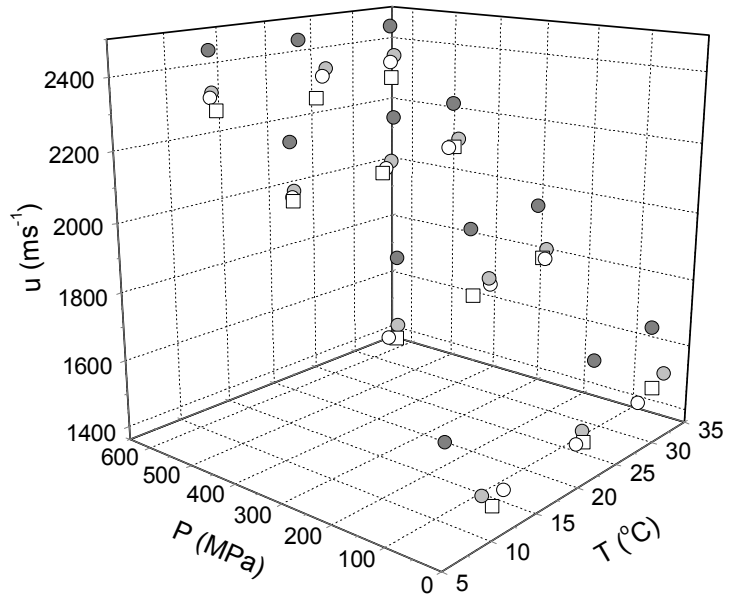

Figure 5-2. Experimental sound velocity in glucose solutions 2.5% ○, 10% ◍, and 50% ●; and in pure water □

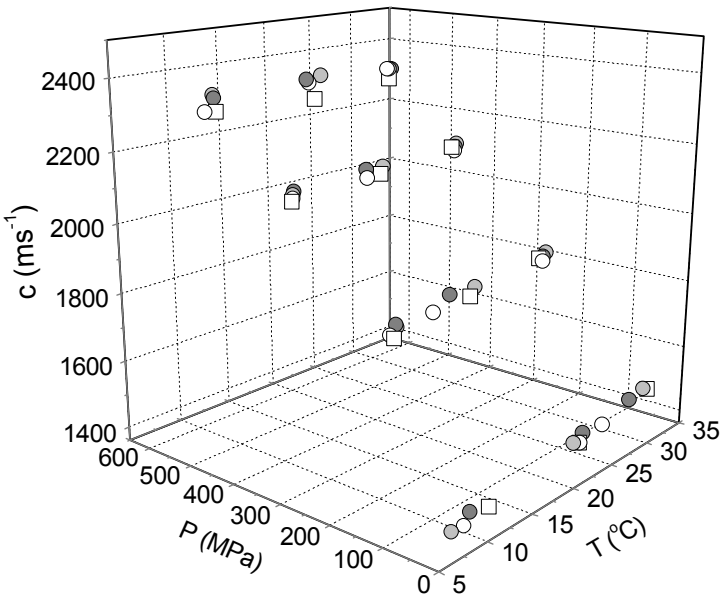

Figure 5-3. Experimental sound velocity in citric acid solutions 1% ○, 5% ◍, and 10% ●; and in pure water □

The resulting regression coefficients of the model a_{ij}'s for the continuous surface are presented in Table 5-1. The average deviation between the best fit and the experimental values was found to be 0.06 ms^{-1} for sucrose solutions, and less than 0.001 ms^{-1} for glucose and citric acid solutions, with a correlation coefficient better than 0.999 for all solutions. These figures confirm our prior error analysis (refer to Chapter 4), which states that the smoothing procedure carried out by fitting experimental data did not increase the error associated with the measurements. On the contrary, it helped to smooth the associated random errors. The standard deviations between the experimental and fitted values are found to be less than the accuracy of the measurements, showing the validity of the procedure. It should be pointed out that the number of significant figures given for the coefficients does not indicate the accuracy, but extra figures are retained in order to accurately calculate the pressure and temperature dependence of this and derived quantities.

$$P - P_o = \sum_{i=1}^{3} \sum_{j=0}^{2} a_{ij} (u - u_o)^i T^j \qquad [4\text{-}3]$$

Density at Atmospheric Pressure

Measured density at atmospheric pressure of binary aqueous solutions of sucrose, glucose, and citric acid as a function of temperature and concentration, together with the surface model are presented in Figures 5-4, 5-5, and 5-6. A total of 74 data points for sucrose solutions were obtained and 60 data points for glucose and citric acid and solutions. Literature values, where available, agreed well with experimental data.

Density of all solutions studied showed a quadratic dependence to temperature and concentration, but a weaker quadratic-dependence to the latter. Coefficients of predictive equations were determined by fitting the experimental data. Table 5-2 shows the parameters for the predictive equations obtained by regression analysis by adjusting experimental data to the mathematical model, given by Equation 4-4 rewritten here. All binary solutions fitted well into the proposed model with correlation coefficients greater than 0.999. Using these equations, the density can be predicted with accuracy better than 5×10^{-5} g cm^{-3}. The standard errors of all fitted predictive equations were in the range from 0.238 to 0.953. The densities obtained in this study are of acceptable accuracy for engineering-design calculations and describe well the temperature and concentration dependence of the solutes investigated. Again, the number of significant figures given for the coefficients does not indicate the accuracy, but extra figures are retained in order to calculate the temperature and concentration dependence of this and derived quantities.

$$\rho_{P_o} = \sum_{i=1}^{3} \left(\sum_{j=0}^{2} a_{ij} C^j \right) T^{i-1} \qquad [4\text{-}4]$$

Table 5-1. Coefficients a_{ij} of Equation 4-3 for binary solutions in Pa $m^{-i}s^{i}K^{-j}$

i→	1	2	3
j		2.5% Sucrose Solutions	
0	$3.466360000 \times 10^{7}$	$-1.022377250 \times 10^{5}$	7.353611539×10
1	$-2.345944600 \times 10^{5}$	$7.008568023 \times 10^{2}$	$-5.045654200 \times 10^{-1}$
2	$4.032456583 \times 10^{2}$	-1.200105120	$8.665580000 \times 10^{-4}$
		10% Sucrose Solutions	
0	$-8.834300000 \times 10^{6}$	$2.986176444 \times 10^{4}$	-3.04915402×10
1	$6.323019296 \times 10^{4}$	$-2.038644640 \times 10^{2}$	$2.06151548 \times 10^{-1}$
2	$-1.062631260 \times 10^{2}$	$3.485954560 \times 10^{-1}$	$-3.47150000 \times 10^{-4}$
		50% Sucrose Solutions	
0	$1.501890000 \times 10^{7}$	$-5.463748860 \times 10^{4}$	4.544403267×10
1	$-9.816235600 \times 10^{4}$	$3.701555794 \times 10^{2}$	$-3.077574600 \times 10^{-1}$
2	$1.665946678 \times 10^{2}$	$-6.245977000 \times 10^{-1}$	$5.215380000 \times 10^{-4}$
		2.5% Glucose Solutions	
0	$-1.599000000 \times 10^{7}$	$7.005462431 \times 10^{4}$	-5.06869120×10
1	$1.195014643 \times 10^{5}$	$-4.959631700 \times 10^{2}$	$3.58318789 \times 10^{-1}$
2	$-2.147794090 \times 10^{2}$	$8.766108510 \times 10^{-1}$	$-6.30770000 \times 10^{-4}$
		10% Glucose Solutions	
0	$-1.0592000000 \times 10^{7}$	$4.105776503 \times 10^{4}$	-2.50614788×10
1	$7.8321602172 \times 10^{4}$	$-2.884169740 \times 10^{2}$	$1.77027337 \times 10^{-1}$
2	$-1.3710340700 \times 10^{2}$	$5.063545360 \times 10^{-1}$	$-3.10670000 \times 10^{-4}$
		50% Glucose Solutions	
0	7.45898000×10^{7}	$-1.947963860 \times 10^{5}$	$1.342149209 \times 10^{2}$
1	$-5.06552635 \times 10^{5}$	$1.331881389 \times 10^{3}$	$-9.168321600 \times 10^{-1}$
2	8.66213236×10^{2}	-2.272779830	$1.565501000 \times 10^{-3}$
		1% Citric Acid Solutions	
0	$3.382720000 \times 10^{6}$	1.38540610×10^{4}	-1.80410091×10
1	$-2.721487240 \times 10^{4}$	-8.39536063×10	$1.16948515 \times 10^{-1}$
2	6.009647687×10	$1.25506041 \times 10^{-1}$	$-1.87500000 \times 10^{-4}$
		5% Citric Acid Solutions	
0	$4.711240000 \times 10^{7}$	$-1.444064020 \times 10^{5}$	$1.310305315 \times 10^{2}$
1	$-3.234463040 \times 10^{5}$	$9.958327126 \times 10^{2}$	$-9.041403200 \times 10^{-1}$
2	$5.608955607 \times 10^{2}$	-1.714321740	$1.559776000 \times 10^{-3}$
		10% Citric Acid Solutions	
0	$7.879600000 \times 10^{7}$	$-1.867349890 \times 10^{5}$	$1.373337113 \times 10^{2}$
1	$-5.342976490 \times 10^{5}$	$1.267277732 \times 10^{3}$	$-9.305151700 \times 10^{-1}$
2	$9.115903125 \times 10^{2}$	-2.148021210	$1.576701000 \times 10^{-3}$

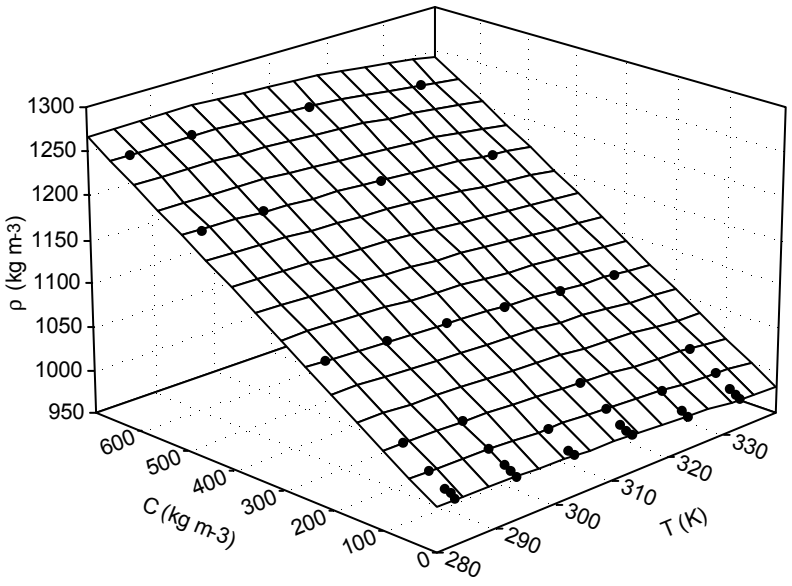

Figure 5-4. Experimental density of sucrose solutions at atmospheric pressure as a function of temperature and concentration

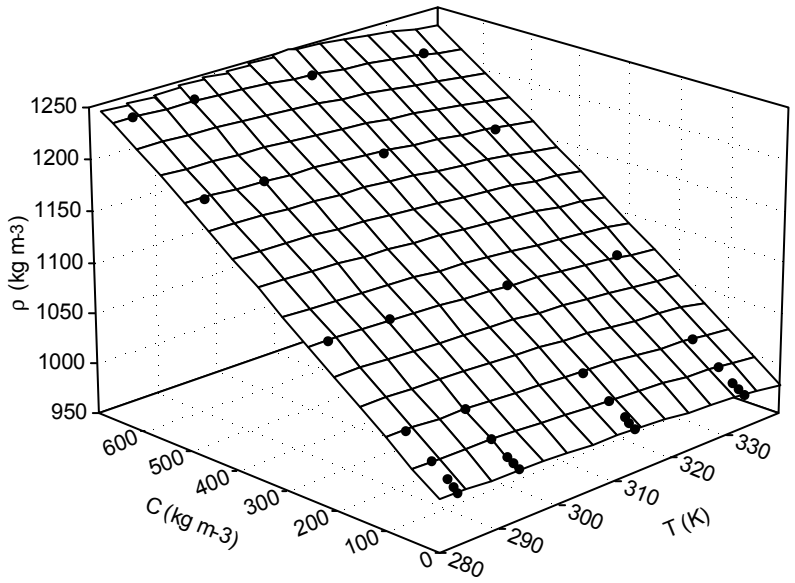

Figure 5-5. Experimental density of glucose solutions at atmospheric pressure as a function of temperature and concentration

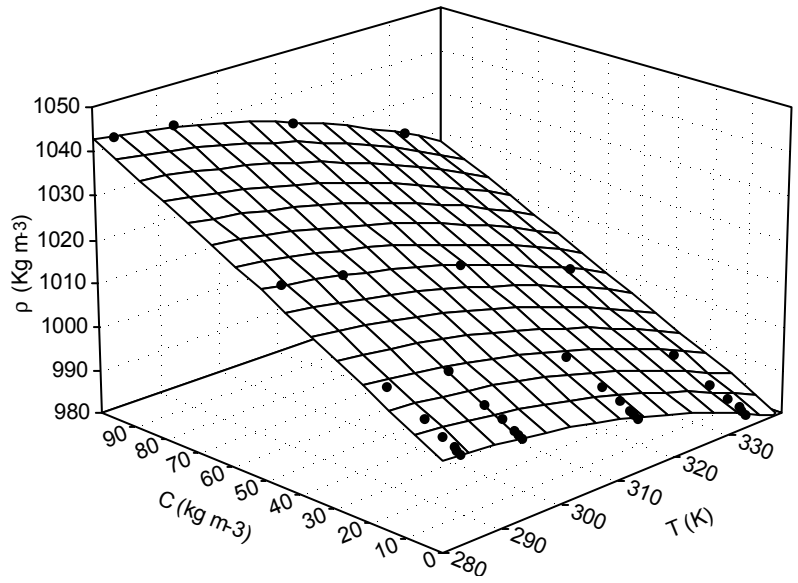

Figure 5-6. Experimental density of citric acid solutions at atmospheric pressure as a function of temperature and concentration

Table 5-2. Coefficients a_{ij} of Equation 4-4 for binary solutions in $[kg^{(1-j)}m^{-3(j-1)}K^{(1-i)}]$

i→	1	2	3
J		Sucrose Solutions	
0	$6.543902625 \times 10^{2}$	1.705422513	$-3.03738000 \times 10^{-3}$
1	2.535927166	$-8.184200000 \times 10^{-3}$	$1.92817000 \times 10^{-5}$
2	$-4.646200000 \times 10^{-3}$	$1.254230000 \times 10^{-7}$	$-3.04250000 \times 10^{-8}$
		Glucose Solutions	
0	$7.084363996 \times 10^{2}$	2.09934391	$-1.88660000 \times 10^{-4}$
1	2.188908665	$1.38762100 \times 10^{-3}$	$9.63030000 \times 10^{-7}$
2	$-4.096960000 \times 10^{-3}$	$-2.62940000 \times 10^{-6}$	$-1.42150000 \times 10^{-9}$
		Citric Acid Solutions	
0	$6.670313285 \times 10^{2}$	3.755891564	$-3.36218800 \times 10^{-2}$
1	2.453599632	$-2.051211000 \times 10^{-2}$	$2.12820000 \times 10^{-4}$
2	$-4.515580000 \times 10^{-3}$	$3.134140000 \times 10^{-5}$	$-3.36780000 \times 10^{-7}$

Heat Capacity at Atmospheric Pressure

Experimental results of isobaric specific heat capacity of binary solutions of sucrose, glucose, and citric acid as a function of temperature and concentration, together with the heat capacity of pure water, are presented in Figures 5-7, 5-8, and 5-9. Tables with the numerical values are presented in Appendix C. Heat capacity increased with increasing water content and increasing temperature for all compounds, with more pronounced effect of temperature for the more concentrated solutions. At low concentrations, heat capacity approached that of pure water, with less pronounced effect of temperature, and similar abnormal behavior of pure water with a minimum around 30°-40°C.

The proposed correction factor in DSC measurements to account for the effect of evaporation of water at higher temperatures appeared to be a reasonable approach for applications on high moisture content samples, such as most food systems. At temperatures above 35°-40°C, the deviation becomes significant, as a consequence of the exponential increase in the water vapor pressure. As stated before, at higher concentrations the deviation becomes smaller due to the effect of solutes lowering the vapor pressure of the solution. For a total of 1,230 data points for each solution, the results showed an average standard deviation of 0.058 for specific heat capacity.

Heat capacity of all solutions showed a quadratic dependence with concentration and temperature. Table 5-3 shows the parameters for the predictive equations obtained by regression analysis by fitting experimental data to the mathematical model, according to Equation 4-18 rewritten below. The fitted surfaces are shown along with experimental results in Figures 5-7, 5-8, and 5-9.

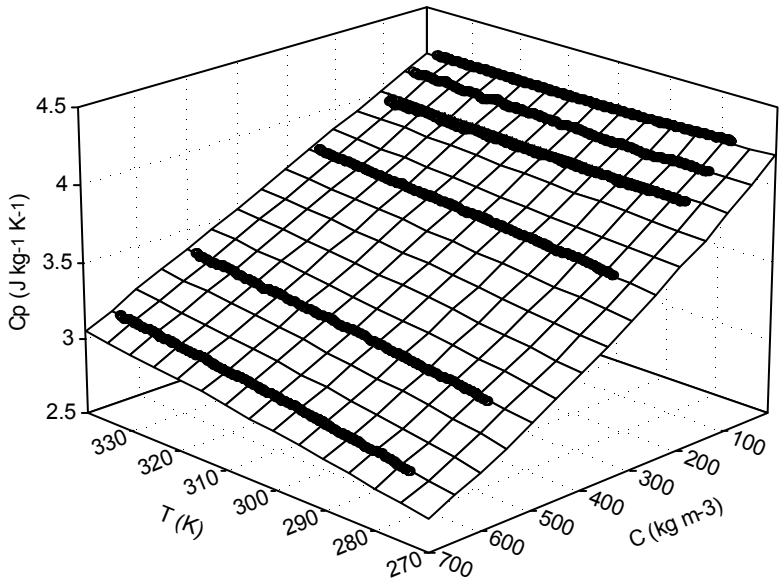

Figure 5-7. Experimental specific heat capacity of sucrose solutions at atmospheric pressure as a function of temperature and concentration

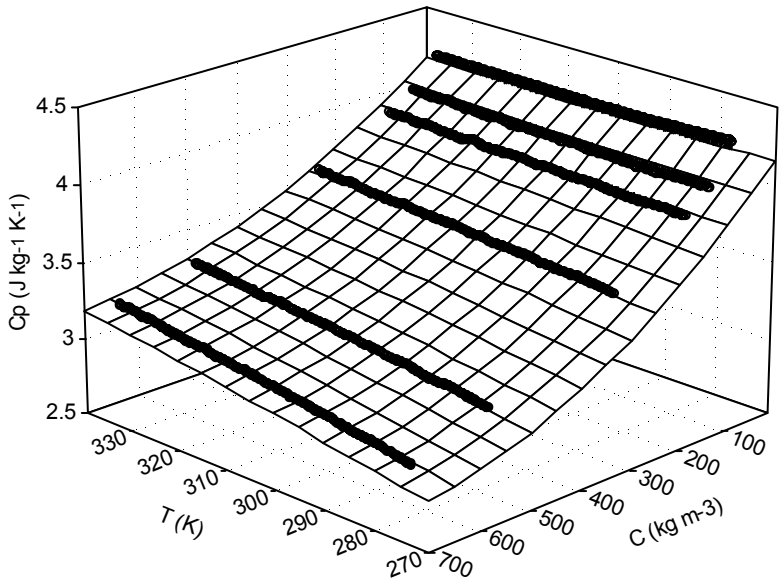

Figure 5-8. Experimental specific heat capacity of glucose solutions at atmospheric pressure as a function of temperature and concentration

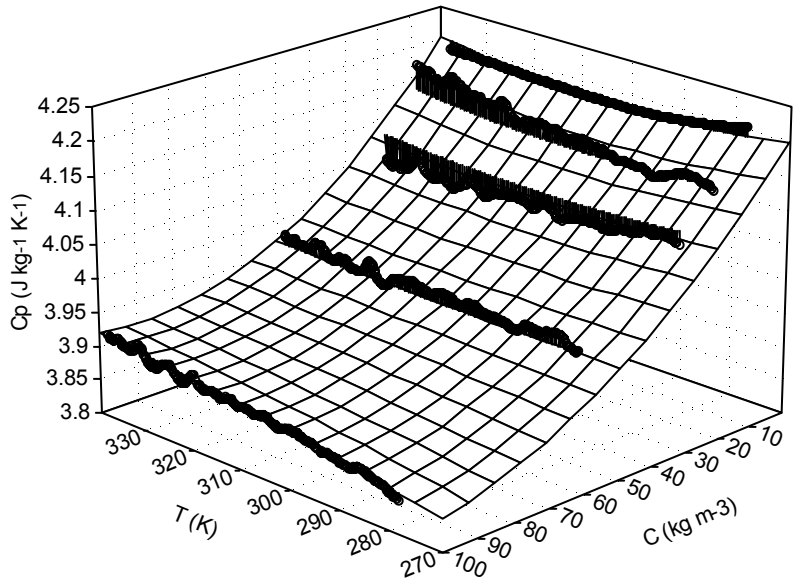

Figure 5-9. Experimental specific heat capacity of citric acid solutions at atmospheric pressure as a function of temperature and concentration

Binary aqueous solutions of all compounds investigated fitted well into the proposed model with correlation coefficients greater than 0.98. The standard errors of all fitted equations were from 0.016 to 0.027. The largest deviations from the model occur at lower concentrations, where the uncertainties in experimental measurements of heat capacity with DSC are greater. This corresponds to smaller differences between the heat capacity of pure water and that of the solution. The relatively high experimental error intrinsic to DSC measurement on heat capacity is because of the notably small changes in heat flow associated with changes in sensible heat as temperature scanning proceeds in contrast with higher heat flow experienced in phase transition studies. Once more, the number of significant figures given for the coefficients does not indicate the accuracy, but extra figures are retained in order to calculate the temperature and concentration dependence of this and derived quantities.

$$Cp_{P_o} = \sum_{i=1}^{3}\left(\sum_{j=0}^{2} a_{ij} C^{j}\right) T^{i-1} \qquad [4\text{-}18]$$

Table 5-3. Coefficients a_{ij} of Equation 4-18 for binary solutions in [$kg^{-j}s^{-2}m^{(2+3j)}K^{-i}$]

i→	1	2	3
j	Sucrose Solutions		
0	5.996787722	-1.200795 x10^{-2}	1.96714 x10^{-5}
1	-1.750330000 x10^{-2}	8.689670 x10^{-5}	-1.18740 x10^{-7}
2	1.248620000 x10^{-5}	-6.861200 x10^{-8}	9.44495 x10^{-11}
	Glucose Solutions		
0	5.741613076	-1.056499 x10^{-2}	1.73814 x10^{-5}
1	-1.856913000 x10^{-2}	9.202260 x10^{-5}	-1.31860 x10^{-7}
2	1.546130000 x10^{-5}	-8.437300 x10^{-8}	1.28382 x10^{-10}
	Citric Acid Solutions		
0	5.916940728	-1.1149346 x10^{-2}	1.89890 x10^{-5}
1	-4.169422000 x10^{-2}	2.4369400 x10^{-4}	-4.12240 x10^{-7}
2	1.309310000 x10^{-4}	-8.4344000 x10^{-7}	1.66411 x10^{-9}

Thermodynamic Properties at High Pressures Derived from Ultrasonic Data

Solving the set of thermodynamic equations starting with the Newton-Laplace expression and Equations that follow 2-7 to 2-10, 4-19 and 4-20, using the numerical procedure described in the previous chapter, density at high pressures was obtained as a function of temperature and concentration for each binary aqueous solution. The input parameters were given by the regression coefficients of equations, as presented above (Table 5-1), obtained by fitting experimental data of speed of sound at elevated pressures as a function of temperature and concentration, and the initial values given by the regression coefficients of equations, also presented above (Tables 5-2 and 5-3), obtained by fitting experimental data of density, heat capacity, and thermal expansion coefficient (derived from density measurements) at atmospheric pressure and also as a function of

temperature and concentration for each binary solution. The calculated values of the density for each binary solution as a function of pressure, temperature and concentration are presented in Figures 5-10 to 5-12. The data are given at round values of pressures between 0.1 and 600 MPa in intervals of 100 MPa and at temperatures of 10°, 20° and 30°C (283.15, 293.15 and 303.15 K), which covers the experimental range investigated, although the numerical solution was performed in pressure steps of 2 MPa and temperature steps of 5°C (5 K). Also, smoothed lines are shown simply to help pattern recognition. Tables with numerical values of thermodynamic properties derived from ultrasonic high-pressure data are presented in Appendix E.

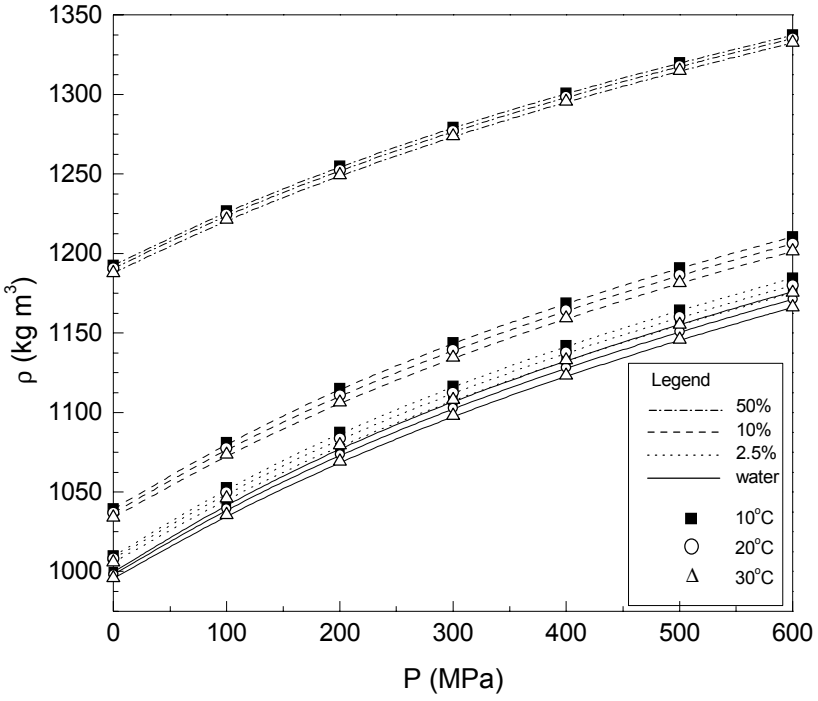

Figure 5-10. Calculated density of sucrose solutions as a function of pressure at different temperatures and concentrations

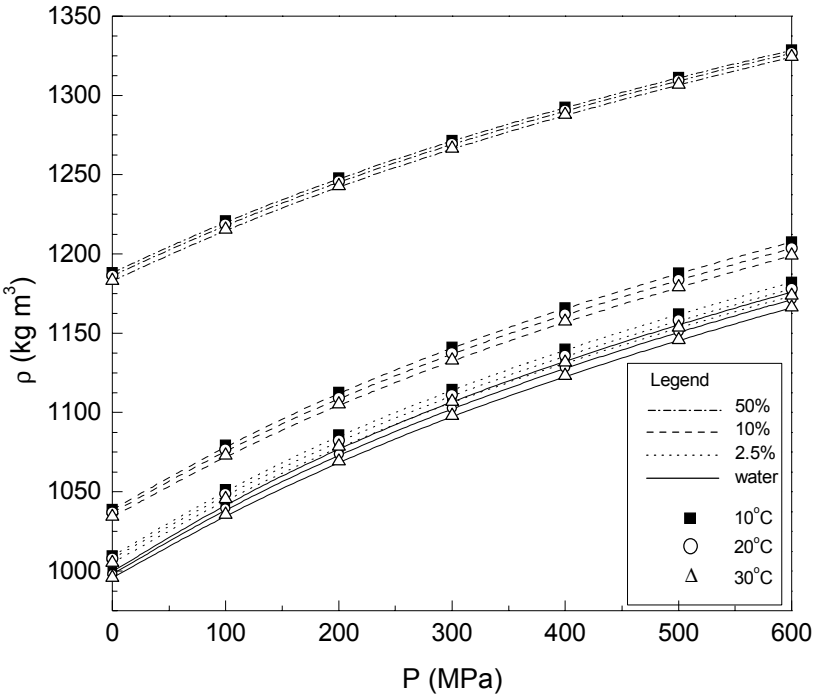

Figure 5-11. Calculated density of glucose solutions as a function of pressure at different temperatures and concentrations

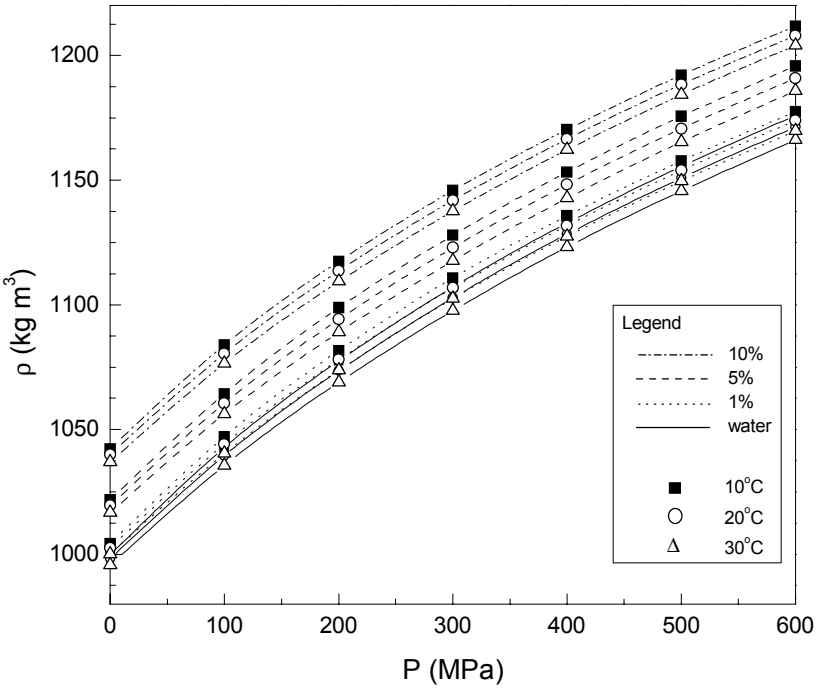

Figure 5-12. Calculated density of citric acid solutions as a function of pressure at different temperatures and concentrations

These plots confirm that the liquid becomes compressed resulting in a smooth increase in density as pressure increases. On the other hand, the effect of the temperature is the reverse because there is thermal expansion associated with temperature rise. Apparently, the concentration dependence of density follows the same behavior as in atmospheric pressure; although a closer look at the concentration dependence of other derived thermodynamic properties shall give more insight on this issue. The effect of pressure on the different solutes in water is not clearly interpreted without separating what is due to the bulk solvent and what is owed to the solute in solution, in other words accounting for solute-solvent and solute-solute interactions. This topic will be discussed later when interpreting the results from the proposed mixing scheme.

Other relevant thermodynamic properties were derived from ultrasonic data at high pressure. Figures 5-13 to 5-27 present the calculated values of the isentropic and isothermal compressibility, isobaric specific heat capacity, thermal expansion coefficient, and isentropic pressure thermal coefficient for each binary solution as a function of pressure, temperature and concentration. In these graphs, the data are given at values of pressures between 0.1 and 600 MPa in intervals of 50 MPa and at temperatures of 10^{o}, 20^{o} and 30^{o}C (283.15, 293.15, 303,15 K). Besides the smaller pressure interval used, an extra point at 10 MPa was added in order to accommodate the observed sharper variation at low pressures for most of these properties. Again, smooth lines are shown simply to help pattern reading.

It is clear from these plots that the isentropic (as well as isothermal) coefficients of compressibility decrease throughout with increased pressure, temperature, and concentration. Another remarkable observation is that the compressibility drops faster at

low pressures than it does at higher pressures. The natural explanation for this is that at low pressures the molecules fit loosely together with considerable free space between them, and the major part of the compressibility at low pressure arises from the occupancy of this free space; whereas as pressure increases, the free space has become limited, the compressibility that remains is that provided by the molecules themselves, which persists with smaller change over comparatively wide ranges of pressure. It is likely becoming asymptotical in the limit at very high pressure.

A striking behavior of these aqueous systems is the effect of temperature on compressibility. For most liquids compressibility increases with temperature since thermal expansion increases the internuclear distance (Bridgman 1931; Isaacs 1981), however for water and aqueous solutions compressibility decreases with temperature as it can be observed from these results within the experimental temperature range investigated[1]. It is likely that temperature affects the nature of structured units present. Breaking of hydrogen bonds on compression results in an unfavorable enthalpy component although this is in part compensated by the entropy. Furthermore, the hydrophilic groups of the solutes investigated match and mismatch into the three dimensionally hydrogen-bonded structure of liquid water. The effect of temperature on compressibility is less pronounced at higher pressures near the limit of our pressure range (600 MPa). This temperature effect can be reasoned by using Bridgman's arguments that at higher pressures, the associated molecules may be thought to be abnormally compressible, in such a way that the volume difference between molecules with different

[1] We recall the fact that the compressibility of pure water at atmospheric pressure passes through a minimum at temperatures about 46.5^{o}C and 64^{o}C for the isothermal and isentropic compressibility respectively (Kell 1974).

degrees of association turns out to be smaller, and the whole effect less pronounced, eventually disappearing at high enough pressures (Bridgman 1931).

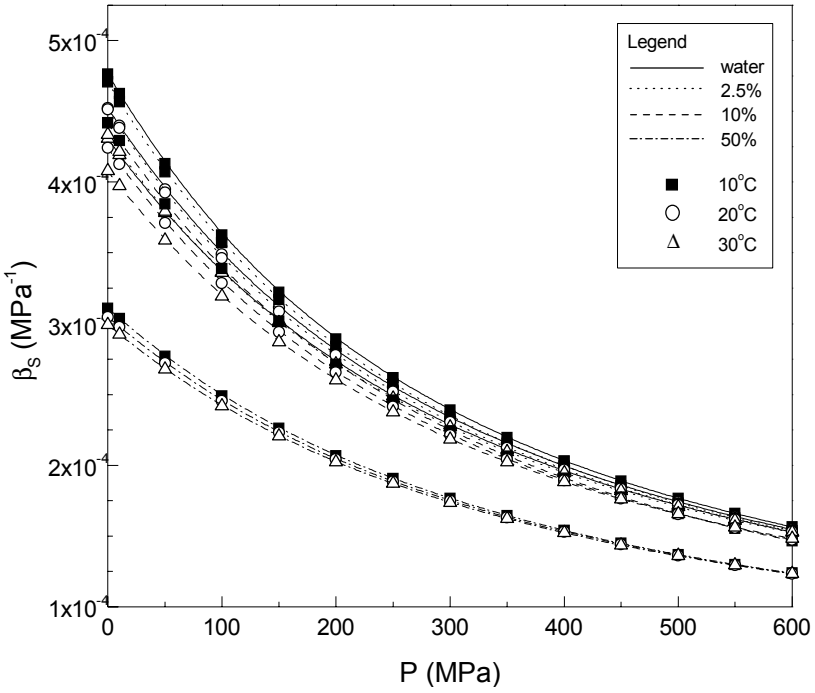

Figure 5-13. Calculated isentropic compressibility of sucrose solutions as a function of pressure at different temperatures and concentrations

It is unambiguous the more sensitivity presented by compressibility (as well as speed of sound) to solute type, concentration and temperature than density with respect to change in pressure. This behavior is attested by the linearity (or parallelism) of the density curves and non-linearity, on the other hand, for the compressibility plots. Similar interpretation was reached by other researchers when analyzing ultrasonic data of sugar solutions, although at atmospheric pressure (Smith and Winder 1983; Contreras et al. 1992). As the density is not markedly affected as compressibility by solute type and concentration with changes in pressure or temperature, it can be inferred that the compressibility is the parameter which is governing the changes in the speed of sound with pressure. The grounds for this are that with increasing pressure and increasing

concentration of solute, sound velocity increases and the product of density and compressibility must decrease to satisfy the inverse in sound velocity relationship (Equation 2-10). Density increases with an increase in pressure and solute concentration (which should decrease sound velocity values according to Equation 2-10), while compressibility decreases to satisfy the inverse relationship. Also, compressibility decreases at a steadily decreasing rate. Thus, compressibility must be more important than density in defining solution sound velocity characteristics with pressure and concentration changes.

It is a well-known fact that even a small amount of a solute decreases compressibility of water, regardless of the solute being more or less compressible than water (Gibson 1937; Newitt and Weale 1951; Moriyoshi and Inubushi 1977; Kubota et al. 1987). This effect can be attributed to the solid-like structure of bound water in such a manner that it loses freedom of mobility, and the free volume contained in the free water is decreased; then the compressibility of bound water is considerably smaller than in normal state causing a net decrease in the compressibility of the solution (Shiio 1958). This is also the case for all solutions investigated here. However, at atmospheric pressure (0.1 MPa) all solutions have a much lower compressibility than pure water (for example, 4.764×10^{-4} MPa^{-1} for pure water against 2.945×10^{-4} MPa^{-1} for 50% glucose solution at $10^{o}C$), but at high pressures the differences are not so great, the corresponding values at pressure of 600 MPa being 1.565×10^{-4} MPa^{-1} and 1.236×10^{-4} MPa^{-1}, respectively. Also, this may be taken as evidence that in aqueous solutions it is the free water, unaffected by the proximity of the solute molecules, which is undergoing compression and not the solute molecules themselves which have a much lower intrinsic compressibility. This

effect was correlated by Tammann and Schwarzkopf (1928) who proposed a theory for solutions on which adding a small quantity of solute increases the internal pressure in the water by chemical affinity (or attraction), in order that the physical properties of the solution at atmospheric pressure, including its compressibility, are the same as the properties of pure water under an external pressure higher than atmospheric by the pressure of chemical affinity. Richards and Chadwell (1925) also correlated this effect with the view that adding a solute to a solvent in which the molecules exist in different states of association (hydrogen bonded structure of clusters in the case of water) changes the equilibrium distribution between the different molecules, in other words, a combination of factors such as affinity, hydration, and the combined effect of several compressibilities of the species is involved.

Figures 5-16 to 5-18 present a comparison between the calculated values of the isentropic compressibility and that of the isothermal compressibility for each binary solution as a function of pressure and concentration at 20^{o}C (293.15 K). Isothermal compressibility data at temperatures other than 20^{o}C are presented in Appendix E. It is interesting to note that the isothermal compressibility is always greater than its isentropic counterpart which is due to the term on the right hand side of Equation 2-9 being proportional to the absolute temperature and the square of thermal expansion coefficient, and the reciprocal of the product of heat capacity and density. Physically, under isentropic (adiabatic[2]) compression, the temperature rises and the volume change for unit pressure rises, consequently the compressibility is less than under isothermal conditions.

[2] The isentropic and the adiabatic conditions can be equated provided that the compression and relaxation process is microscopically reversible (Blandamer et al. 2001).

It can be seen from these plots that this difference is not as significant as it would be expected for other substances, since aqueous solutions present comparatively large values of specific heat capacity and small value of thermal expansion coefficient. In addition, these results show that the increase in density with pressure would be rather compensated by the decrease in specific heat capacity, while the coefficient of thermal expansion does not vary to a great extent with pressure within the temperature range studied (refer to Figures 5-19 to 5-24). As demonstrated from our results, the isentropic and isothermal compressibilities are different numerically; however, when looking for trends the use of either of them is acceptable. Nevertheless, their inter-convertibility was demonstrated by using the pressure dependence of heat capacity and thermal expansion coefficient (Equation 2-9).

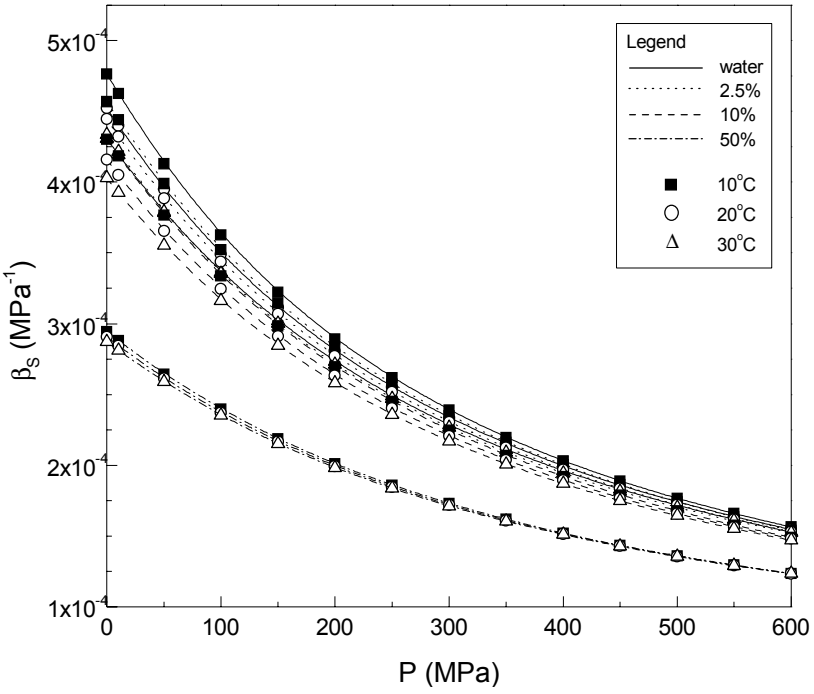

Figure 5-14. Calculated isentropic compressibility of glucose solutions as a function of pressure at different temperatures and concentrations

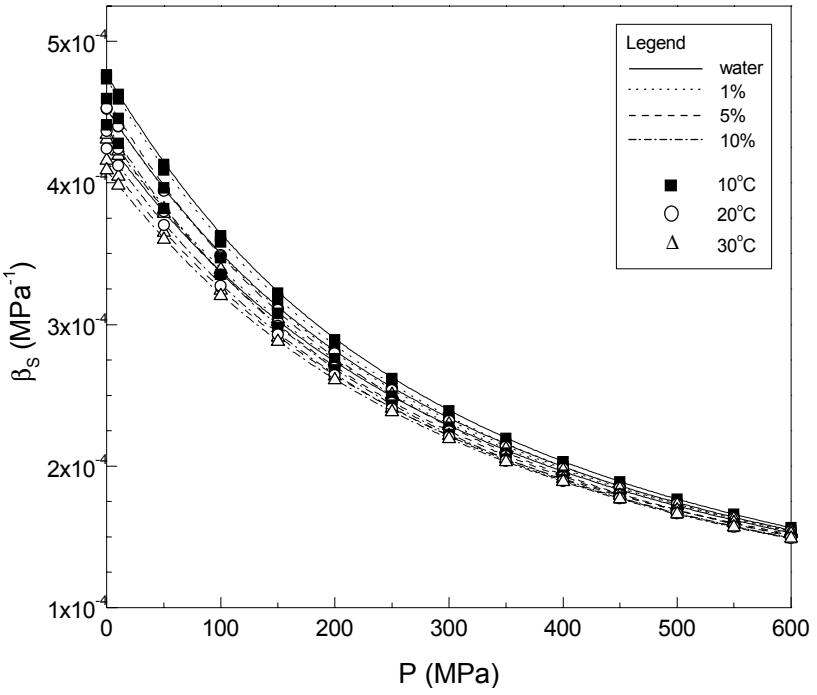

Figure 5-15. Calculated isentropic compressibility of citric acid solutions as a function of pressure at different temperatures and concentrations

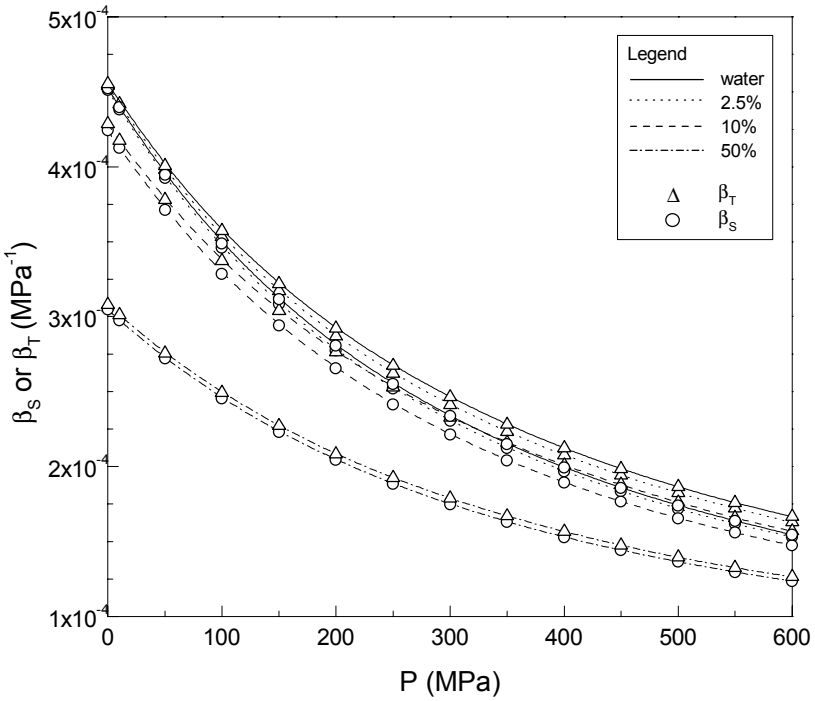

Figure 5-16. Calculated isentropic and isothermal compressibility of sucrose solutions as a function of pressure at different concentrations at 20°C

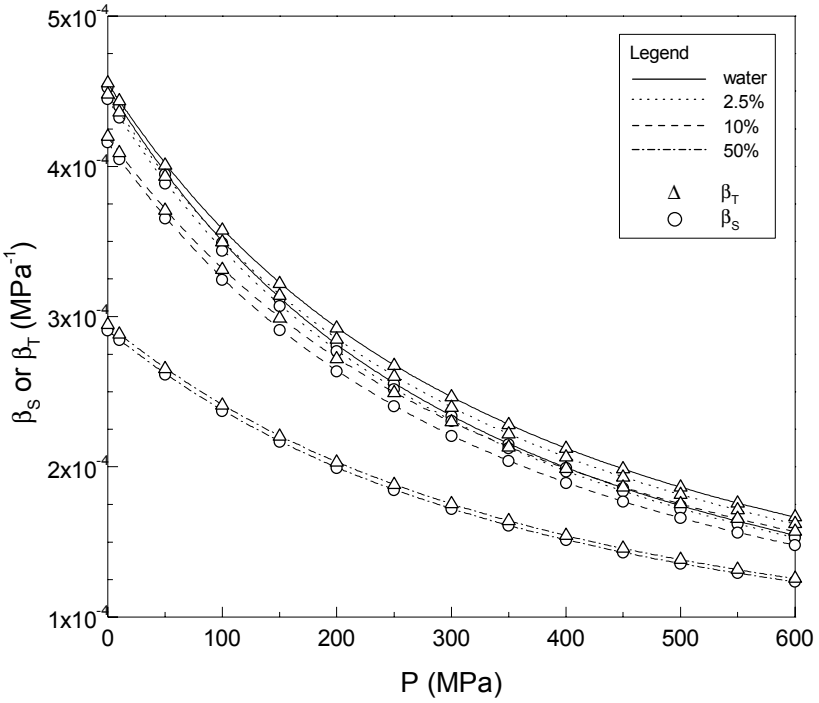

Figure 5-17. Calculated isentropic and isothermal compressibility of glucose solutions as a function of pressure at different concentrations at 20°C

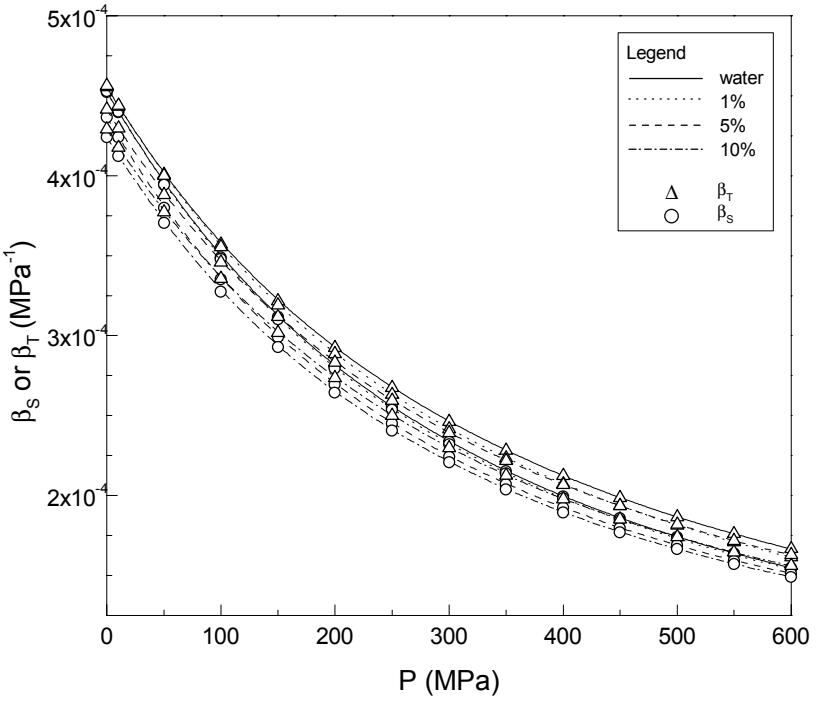

Figure 5-18. Calculated isentropic and isothermal compressibility of citric acid solutions as a function of pressure at different concentrations at 20°C

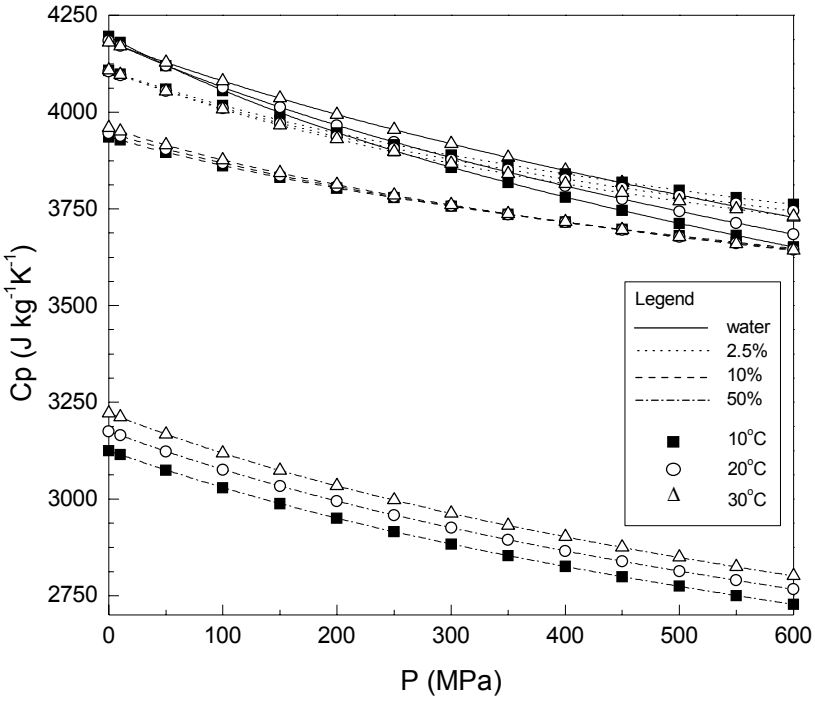

Figure 5-19. Calculated heat capacity of sucrose solutions as a function of pressure at different temperatures and concentrations

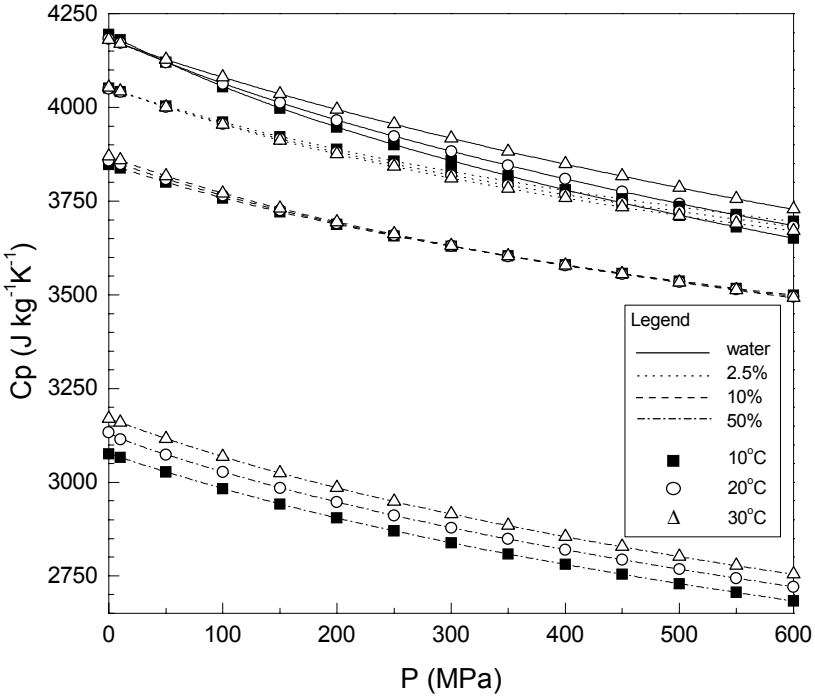

Figure 5-20. Calculated heat capacity of glucose solutions as a function of pressure at different temperatures and concentrations

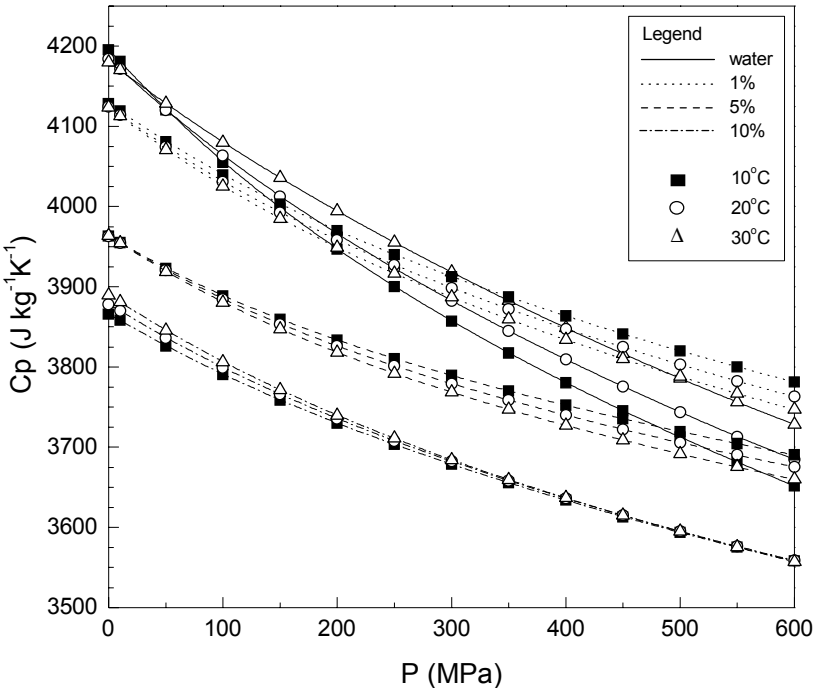

Figure 5-21. Calculated specific heat capacity of citric acid solutions as a function of pressure at different temperatures and concentrations

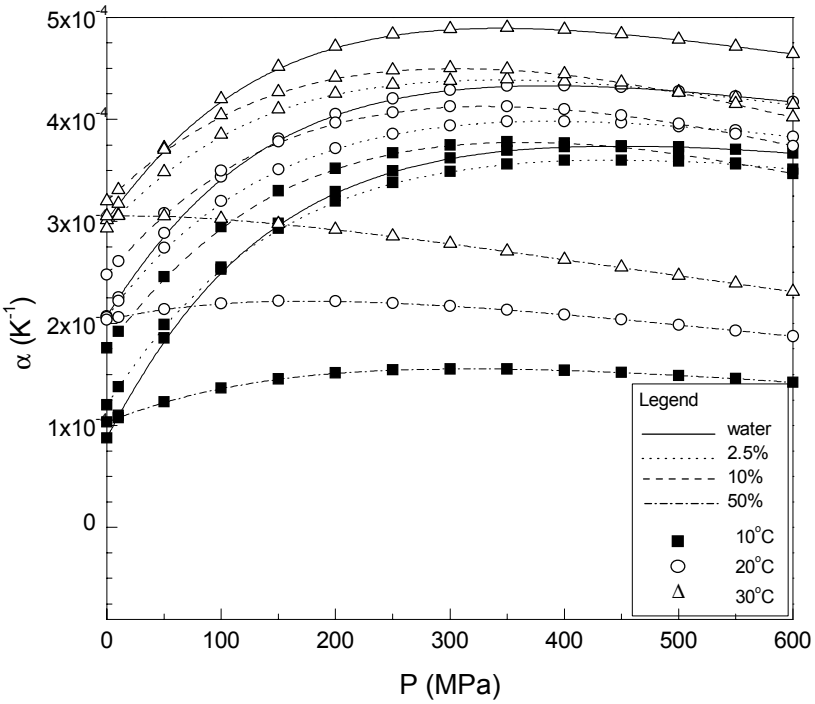

Figure 5-22. Calculated thermal expansion coefficient of sucrose solutions as a function of pressure at different temperatures and oncentrations

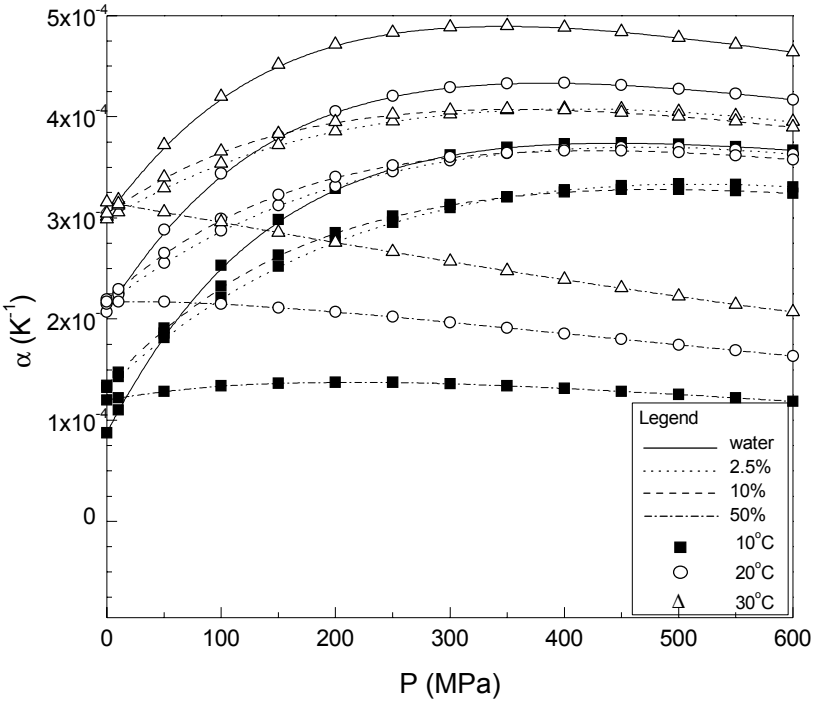

Figure 5-23. Calculated thermal expansion coefficient of glucose solutions as a function of pressure at different temperatures and concentrations

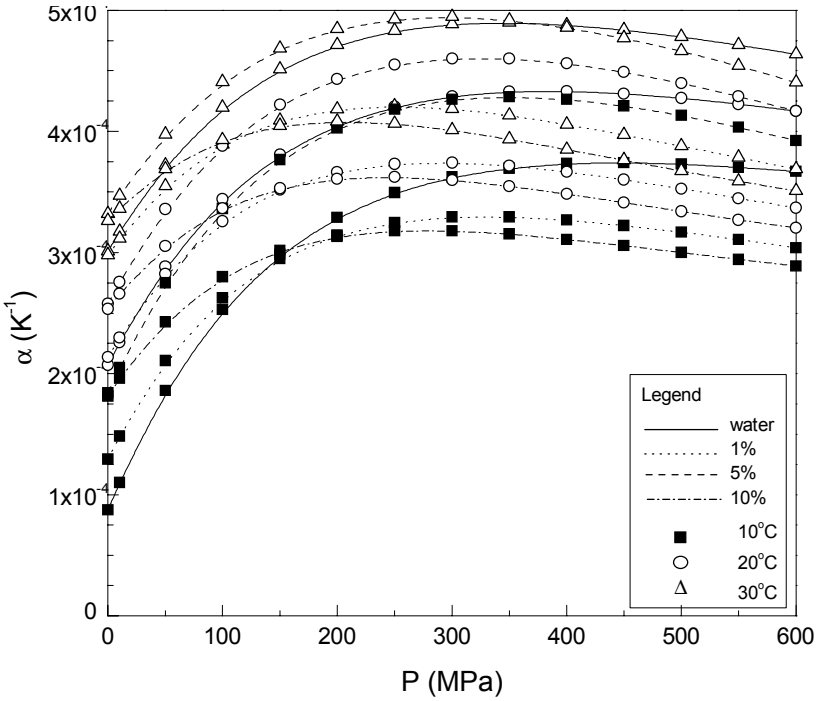

Figure 5-24. Calculated thermal expansion coefficient of citric acid solutions as a function of pressure at different temperatures and concentrations

The thermal expansion of all solutions predominantly increases with increasing pressure up to about 200-300 MPa at least for the low concentration range within the limits of temperature studied, but by an amount materially less than the decrease of compressibility. Again, this can be considered an abnormal behavior, since thermal expansion is expected to decline with pressure (Isaacs 1981). Beyond this pressure threshold, the thermal expansion becomes consistently invariable. Only for the highly concentrated sugar solutions, after a slight increase at low pressures, a certain decrease in the thermal expansion is noted. A mathematical consequence of a decrease of thermal expansion with increasing pressure is an increase of compressibility with increasing temperature, or a decline in the rate of decrease in the compressibility with increasing pressure which is more likely what Figures 5-13 and 5-14 show. As expected, the values of thermal expansion coefficient are positively affected by temperature.

Figures 5-25 to 5-27 show the dependence of the isentropic pressure thermal coefficient on pressure, temperature and concentration for each binary solution. A remarkable feature in these figures is the very sharp decrease in the pressure thermal coefficient with pressure especially pronounced at low pressures and concentrations, meaning that the change in temperature produced by an isentropic (adiabatic) change of pressure is significantly greater in the low pressure range and without the influence of solute.

The importance of this property in the analysis of the effects of high-pressure processing on food materials because it reveals the temperature change accompanied with the rapid compression or release of pressure warrants further discussion. As stressed in the literature review section, many researchers have often neglected this temperature rise

or made precipitated inferences from their results. To better interpret the results reported here, the fact that the isentropic pressure thermal coefficient is a relative (not absolute) expression of the reversible change in temperature as a result of adiabatic compression of the medium must be kept in mind. Therefore, in order to convert these data to a more convenient parameter, the analysis needs to be redirected toward the work done by Rodriguez (1988) with adiabatic heating of some polymers at elevated pressures, and to the classical material science text book of Swalin (1972). The scheme starts by deriving a relationship derived from the Thomson equation, obtained by applying hydrostatic (elastically strained, not plastically) pressure adiabatically to a system, which is equivalent to the reciprocal of the isentropic pressure thermal coefficient as given by Equation 2-4, which was then called thermoelastic coefficient since it calls for a phenomenon that relates temperature change of a system to mechanical stress.

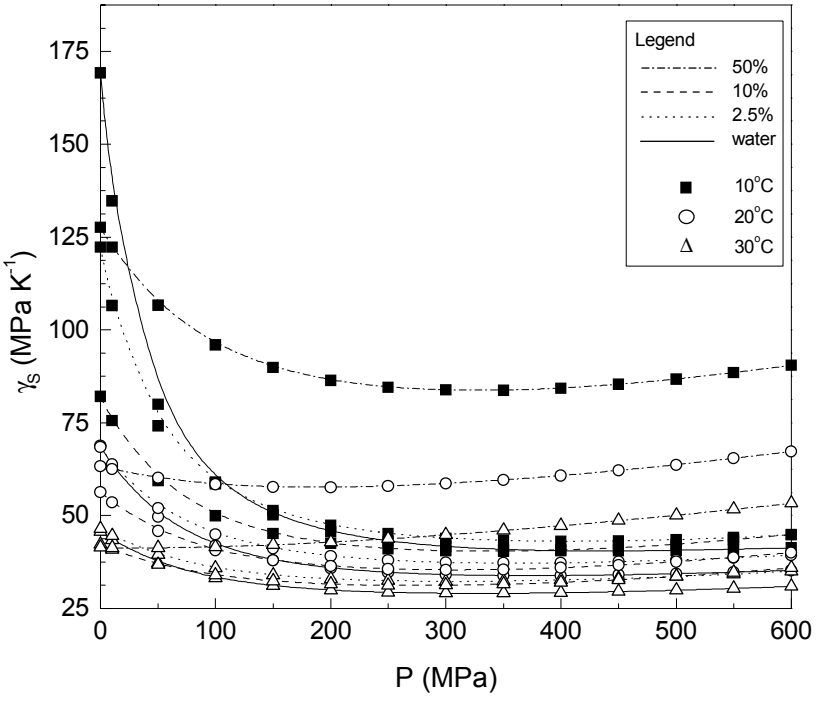

Figure 5-25. Calculated isentropic pressure thermal coefficient of sucrose solutions as a function of pressure at different temperatures and concentrations

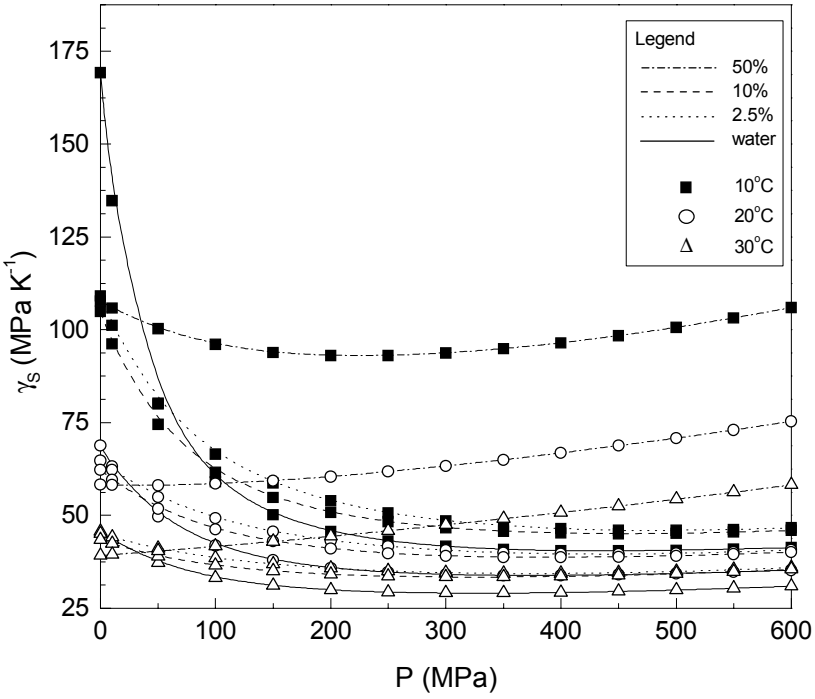

Figure 5-26. Calculated isentropic pressure thermal coefficient of glucose solutions as a function of pressure at different temperatures and concentrations

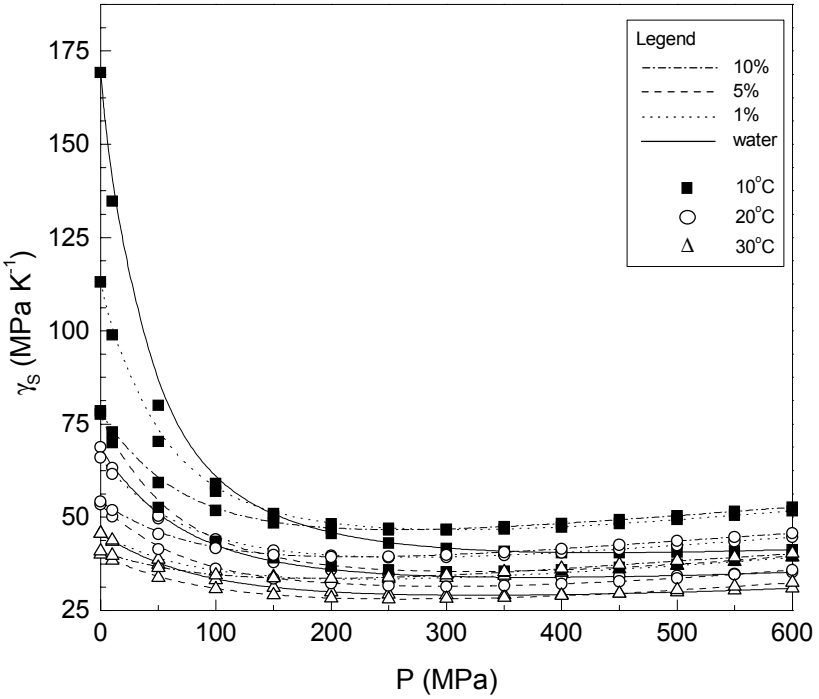

Figure 5-27. Calculated isentropic pressure thermal coefficient of citric acid solutions as a function of pressure at different temperatures and concentrations

$$\frac{1}{\gamma_S} = \left(\frac{\partial T}{\partial P}\right)_S = \frac{T\alpha}{\rho C_P} \qquad [5\text{-}1]$$

A curve fitting analysis has shown that the values calculated by applying this coefficient, as defined by Equation 5-1 above, could be best described through the semi-empirical expression in the form of Equation 5-2, where a_1, a_2 and a_3 are the regression coefficients, $\Delta T = (T - T_o)$ and $\Delta P = (P - P_o)$, where T_o is the reference temperature, P_o is the atmospheric pressure, C is the solution concentration, and n = 1, 2 or 3 depending on the solute and reference temperature.

$$\Delta T = a_1 (\Delta P)^{a_2} \exp\left(a_3 C^n\right) \qquad [5\text{-}2]$$

The thermoelastic coefficient, as defined by Equation 5-1 can then be obtained by differentiating both sides of the above semi-empirical equation with respect to pressure, to give

$$\left(\frac{\partial T}{\partial P}\right)_S = a_1 a_2 \exp\left(a_3 C^n\right)(\Delta P)^{a_2 - 1} \qquad [5\text{-}3]$$

Table 5-4 shows the results of the curve-fitting analysis and the numerical expressions for the thermoelastic coefficient for each binary solution at reference temperatures of 10°, 20° and 30°C (283.15, 293.15, and 303.15 K). These numerical expressions can be used to predict the effect of adiabatic heating upon compression for pure water and aqueous solutions of sucrose, glucose, and citric acid in the concentration range investigated. A simulation of the temperature rise due to adiabatic compression, based on the model just proposed, is shown in Figures 5-28 to 5-30 for each binary aqueous solution at two different concentrations and at reference initial temperatures of 10°C and 30°C.

A comparison of these results with data published in the literature for the effect of the adiabatic heating upon compression for pure water have shown that there is a satisfactory agreement, although no direct numerical comparison was possible since published data were presented only graphically (Makita 1992; Knorr 1999; Ting et al. 2002). Data from the first article mentioned, reported adiabatic heating effects obtained from the equation of state for pure water. Data for aqueous solutions of sucrose, glucose, and citric acid were not found in the literature. Since water is the main ingredient in most food systems, the compression of these foods exhibits temperature changes upon compression similar to that of pure water. However, as it can be seen from these results, depending on the concentration of the different solutes in the food, the temperature rise can be very dissimilar for that of water. It would be extremely desirable to extend the present data set to other food ingredients, such as proteins, lipids, and other carbohydrates. Since compressibility and heat capacity are the main contributing properties to the isentropic pressure thermal coefficient (or derived properties), it is likely that systems with lipids for example, which happen to have higher compressibility and lower heat capacity than water, would have several times larger temperature rise than water and solutions as those studied here.

Thermodynamic Properties of Solution Components at High Pressures

Each type of solute molecule affects the structure of water differently. The mode of action of different classes of solutes on water depends on a series of parameters associated with the chemical structure, polarizing and charge effects, water binding and holding capacity, presence of hydrophilic and hydrophobic groups, packing arrangement of solvent structure around solute molecule, and stereochemistry of the structure, among others. Since most of these parameters are influenced by pressure, temperature and

Table 5-4. Regression coefficients of the Equation 5-2 for binary aqueous solutions (a_1 in [K], a_2 in [K MPa^{-1}], and a_3 in [K $kg^{-2n}m^{3n}$])

Reference Temperature		a_1	a_2	a_3	
(K)	n		Sucrose Solutions		r^2
283.15	3	1.9877013×10^{-2}	1.027912256	-4.3021×10^{-9}	0.994
293.15	2	3.2461409×10^{-2}	$9.729497310 \times 10^{-1}$	-1.8280×10^{-6}	0.993
303.15	2	4.7432288×10^{-2}	$9.320487490 \times 10^{-1}$	-1.4366×10^{-6}	0.991
			Glucose Solutions		
283.15	2	1.3794026×10^{-2}	1.082385459	-2.7440×10^{-6}	0.991
293.15	2	2.5502266×10^{-2}	1.007975485	-2.0714×10^{-6}	0.987
303.15	1	4.2175855×10^{-2}	$9.537546670 \times 10^{-1}$	-9.4451×10^{-4}	0.989
			Citric Acid Solutions		
283.15	3	2.8157127×10^{-2}	$9.75742884 \times 10^{-1}$	-1.1517×10^{-7}	0.961
293.15	3	4.0005153×10^{-2}	$9.41458597 \times 10^{-1}$	-1.1675×10^{-7}	0.970
303.15	3	5.4292011×10^{-2}	$9.12213777 \times 10^{-1}$	-1.1478×10^{-7}	0.975

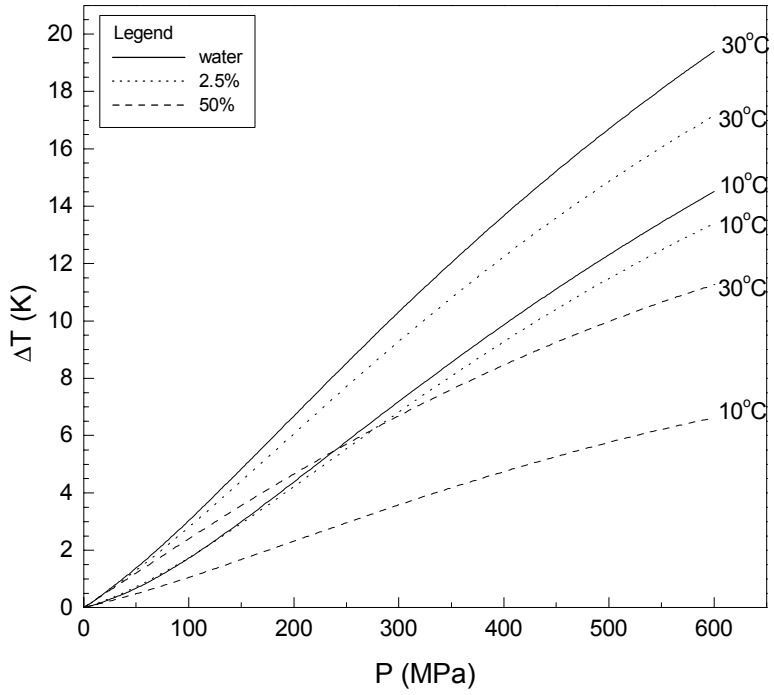

Figure 5-28. Calculated temperature rise by the adiabatic compression of sucrose solutions as a function of pressure at selected concentrations. Temperatures on each curve denotes the reference initial temperatures before compression

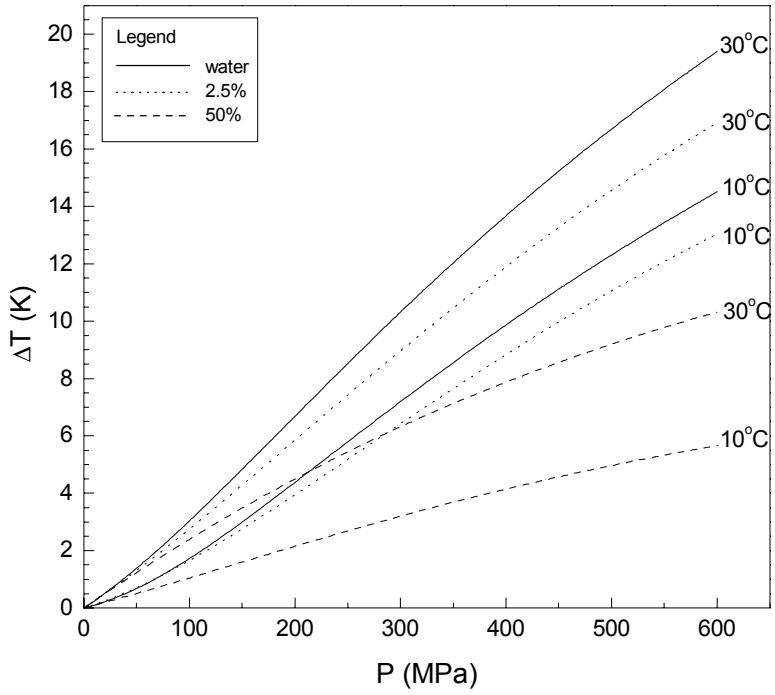

Figure 5-29. Calculated temperature rise by the adiabatic compression of glucose solutions as a function of pressure at selected concentrations. Temperatures on each curve denotes the reference initial temperatures before compression

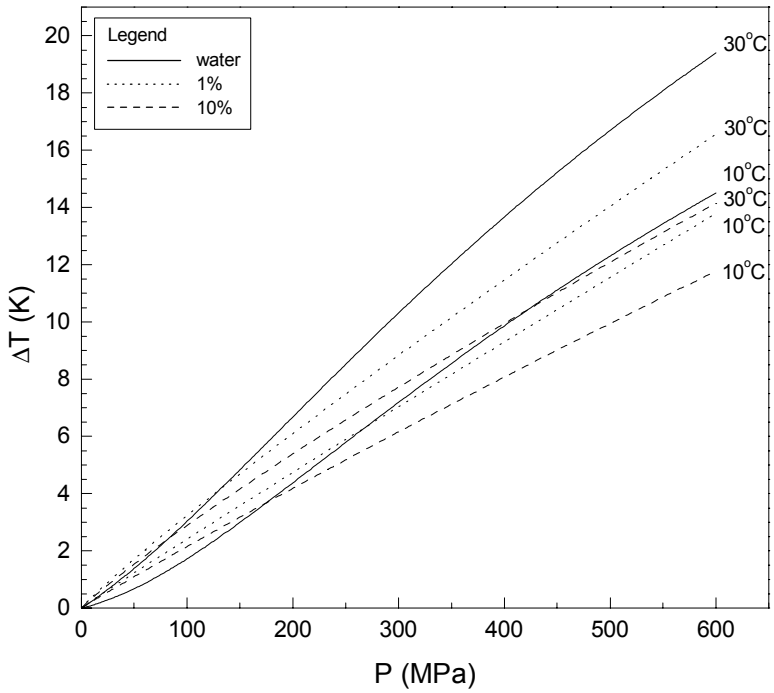

Figure 5-30. Calculated temperature rise by the adiabatic compression of citric acid solutions as a function of pressure at selected concentrations. Temperatures on each curve denotes the reference initial temperatures before compression

concentration, the overall solution structure will be a function of solute type and changes related to these parameters. It is also possible that the phenomena described hereafter may correlate with other physical and functional properties of simple solutions and complex systems in foods under the influence of pressure. Therefore, this section attempts to interpret the contributions made by the dissolved components of the binary solutions investigated to take into account the interactions between solvent and solute molecules through the concept of partial thermodynamic properties of the solutions. Pressure is the main dependent variable to be explored throughout. However, temperature and concentration dependence are also used as convenient, even though their dependence will not be highlighted.

Partial Molar Volumes

Partial molar volumes were obtained by solving Equations 4-32 and 4-33, respectively for the solvent and solute in solution, with the help of the solution molar volume as defined by Equation 4-24 and its concentration dependence with respect to solute mole fraction. Solution molar volumes were calculated from density data as a function of pressure and temperature which in turn were derived from experimental ultrasonic data. Data were treated at constant pressure and temperature for each binary aqueous solution as imposed by the thermodynamic relationships.

Calculated values of partial molar volumes of solute and solvent for each binary solution as a function of pressure at different temperatures and concentrations are shown in Figures 5-31 to 5-33. As in the case of other properties, data are given at values of pressures between 0.1 and 600 MPa at intervals of 100 MPa and at temperatures of 10^{o}, 20^{o} and 30^{o}C (283.15, 293.15 and 303.15 K), covering the experimental range

investigated, also with the help of smooth lines connecting data points for easier pattern recognition.

An analysis of the partial molar volumes of sucrose, glucose, citric acid and those of water in the respective solutions under pressure reveals many interesting features. As the pressure is increased, the partial molar volume of water in solution of any concentration at any temperature decreases by an amount not very different from the decrease in the molar volume of pure water at the same condition (data not shown for clarity: pure water molar volume data are very close to the most dilute solution). In the limit, this would be the behavior of the partial molar volumes of all components in solution if the solution behaves ideally[3]. Considering the partial molar volume of solute in solution under pressure, there is a small increase in the partial molar volumes of solute up to pressures of 100-200 MPa in the low concentration range. The volume increase can be attributed to void space packing of solvent around the solute rather than increase in the size of the solute, since the intrinsic volume of a dissolved solute can be defined as the volume of the cavity in the solvent which accommodates the solute. Above this pressure partial molar volume of solute decreases, and thus at high pressures it behaves as would be expected at all pressures in more normal, and certainly in ideal solutions. There is also a tendency for a less significant temperature effect near the highest pressure limit for the low concentration of sugar solutions.

For the most concentrated sugar solutions, it is more likely to decrease regularly with increasing pressure as for glucose solutions, and more or less invariable in the case

[3] In a solution that at all pressures is ideal in accordance with the well-known thermodynamic definition, it can easily be shown that the components mixture without change of volume; in an ideal solution, therefore, each partial molar volume at any pressure is equal to the molar volume (at that pressure) of the corresponding pure component.

of sucrose solutions. There is also a reversal effect of temperature in the case of sucrose solutions in the sense of a denser packing of sucrose molecules at high temperatures, while for glucose solutions this effect takes place but with the help of increasing pressure. This behavior suggests that the packing of water molecules around a solute molecule leads to an association which is more pressure and thermally stable than the association with water molecules themselves, strengthening the indication that hydrogen bonds between water and the hydroxyl groups of the solute molecules are stronger than water-water hydrogen bonds. At atmospheric pressure, the strength of this association can apparently compensate for the larger number of potentially hydrogen-bonding groups and the larger size of the sucrose molecule than glucose.

Partial molar volumes can also be used to determine the extent of a given reaction. The pressure-dependence of the equilibrium constant of a reaction can be derived from the difference in partial molar volumes of products and those of reactants at constant temperature in the form of Equation 2-28 as mentioned before (refer to Chapter 2). Le Chatelier's principle described previously governs reaction kinetics; accordingly a reaction associated with decrease in volume is favored by pressure and vice-versa. Accordingly, the rate of reaction will be the rate at which the transition state is converted to products, and its pressure-dependence may be derived from the differences in partial molar volumes between reactants and transition state, known as the 'activation volume', given by Equation 2-29. As seen from the results of the present investigation, since partial molar volumes change with pressure and as will be seen shortly their partial compressibilities are pressure dependent as well, besides both being temperature dependent, the activation volume is pressure dependent as well.

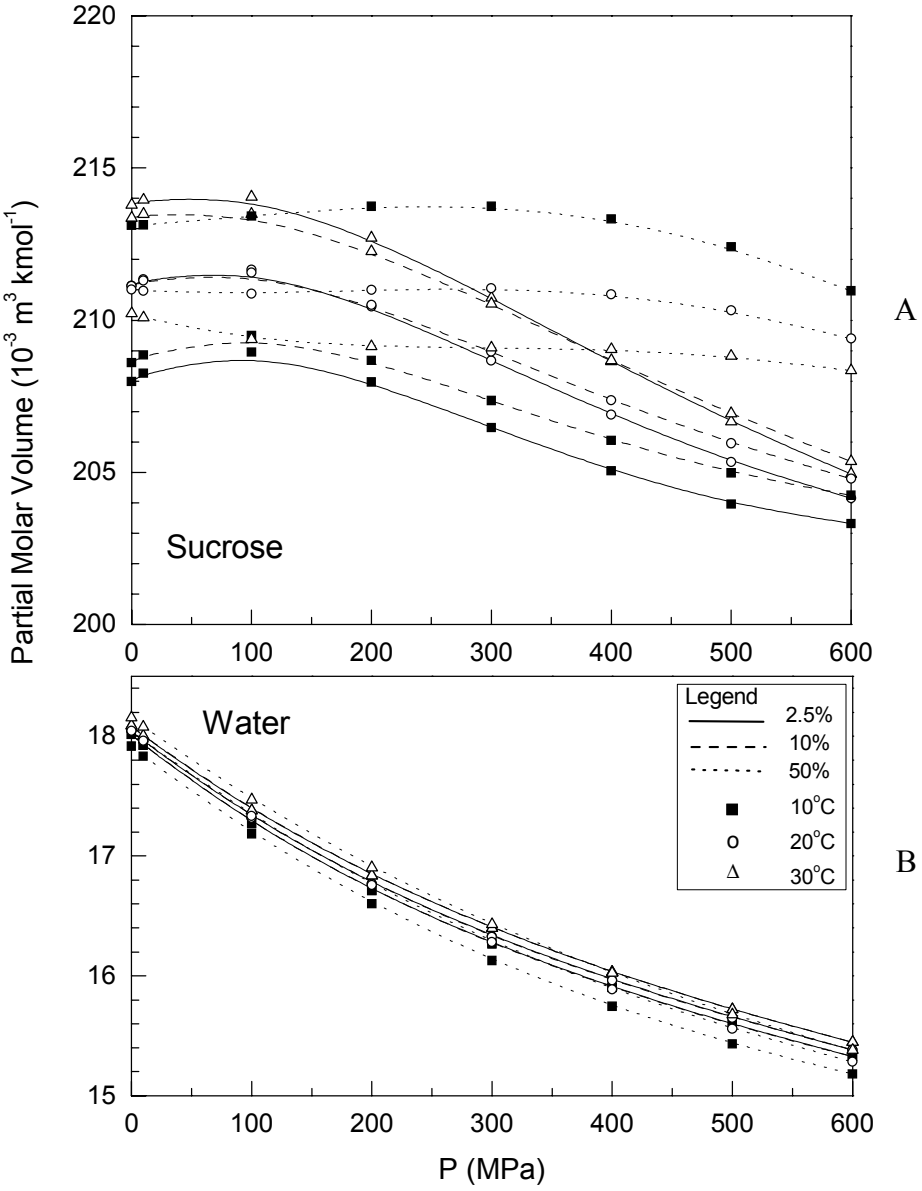

Figure 5-31. Partial molar volumes of solute (A) and solvent (B) in sucrose solutions as a function of pressure at different temperatures and concentrations

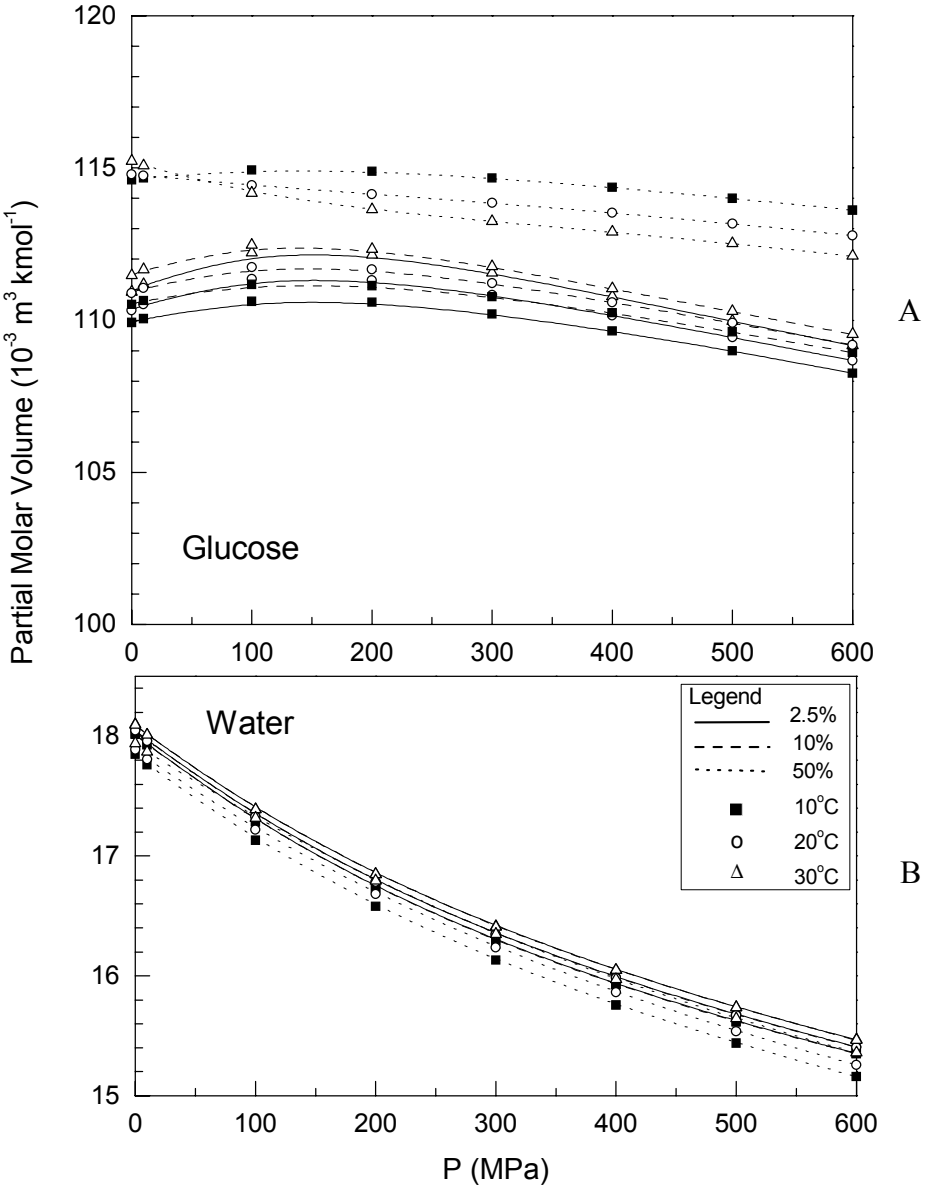

Figure 5-32. Partial molar volumes of solute (A) and solvent (B) in glucose solutions as a function of pressure at different temperatures and concentrations

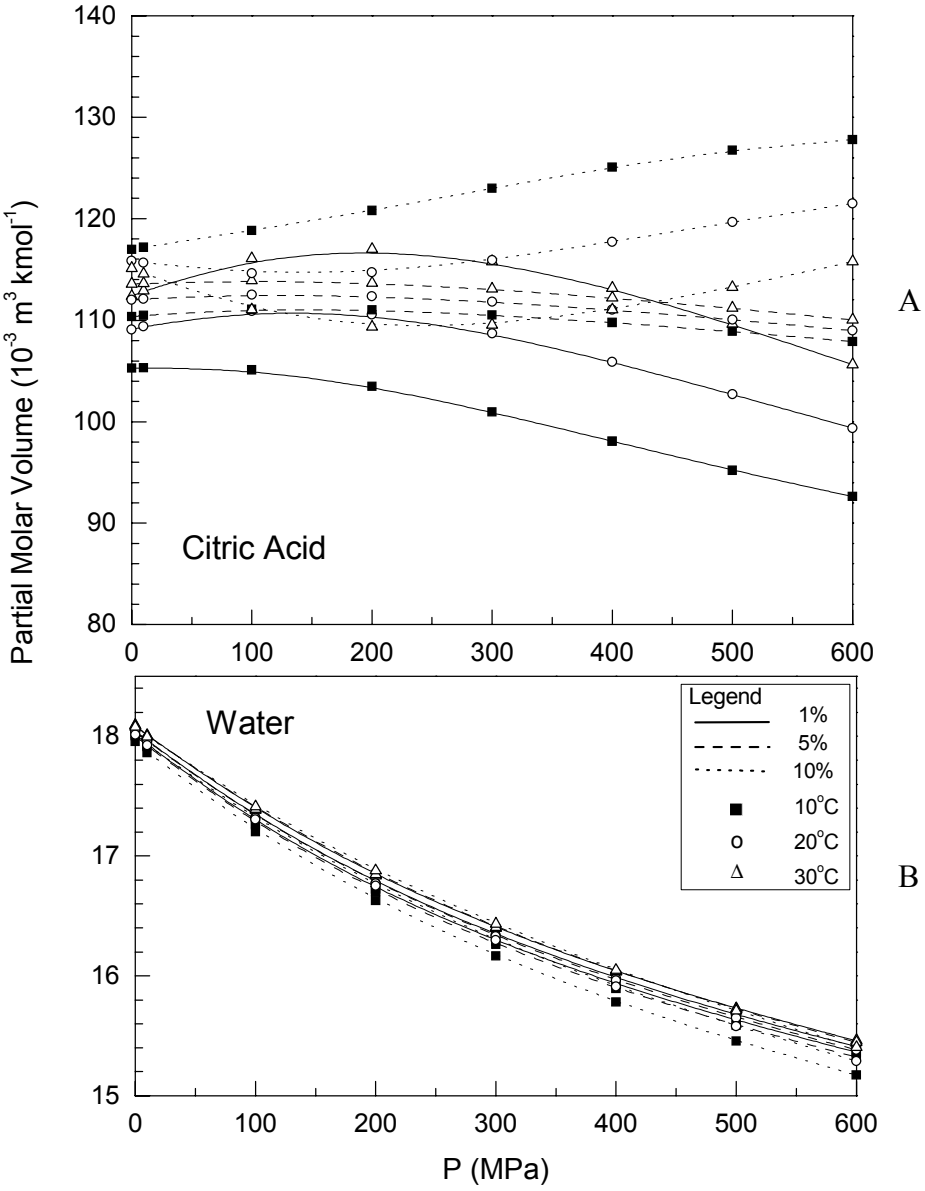

Figure 5-33. Partial molar volumes of solute (A) and solvent (B) in citric acid solutions as a function of pressure at different temperatures and concentrations

Presented next are the results of the pressure-dependence of partial compressibilities of solute and solvent in solution, and the discussion that follows combined with partial molar volume results already shown, since both properties are interconnected. Partial compressibilities are more sensitive than partial molar volumes to solute-solvent interactions; since they are second derivatives of free energy with respect to pressure (refer to Equations 2-2 and A-10). The rationale for this statement is that as the intrinsic volume of the solute molecules can be regarded as almost incompressible comparing with the bulk solvent, the partial compressibility will thus reflect mostly solute-solvent (inter- and not intramolecular) interactions (Banipal et al. 1997).

Partial Isentropic Compressibilities and Partial Specific Compressions

Partial isentropic compressibility and partial specific compression were obtained by solving Equations 4-38 and 4-39, and Equations 4-42 and 4-43, respectively, for solute and solvent in solution, with the help of the solution isentropic compressibility, as derived from ultrasonic data, and its concentration dependence with respect to solute mole fraction. Data were treated at constant pressure and temperature for each binary aqueous solution as imposed by the thermodynamic relationships. In order to simplify the notation from this point on the term 'isentropic' maybe omitted, even though these partial properties were derived from the isentropic compressibility values (not isothermal).

Calculated values of partial isentropic compressibilities and partial specific compressions of solute and solvent for each binary solution as a function of pressure at different temperatures and concentrations are shown in Figures 5-35 to 5-40. Again, data are given at values of pressures between 0.1 and 600 MPa in intervals of 100 MPa and at

temperatures of 10^{o}, 20^{o} and 30^{o}C (283.15, 293.15 and 303.15 K). Smooth lines were drawn connecting data points to facilitate pattern recognition.

The increase in partial molar volume of solute in solution, mentioned above for the low concentration range, obviously means that the partial isentropic compressibility or the partial specific compression of solute is negative in the same pressure range. In dilute solutions, partial compressibility and partial specific compression have a large negative value comparable in magnitude with the compressibility of water, but of the opposite sign. It is apparent from these plots that partial specific compression evidences this behavior more clearly than does partial compressibility property. It can be seen from the former property plots that there is a change in sign at pressures around 100-150 MPa after a sharp increase for sucrose solutions, and a more gradual increase with a change of sign around 200 MPa in the case of glucose solutions, both in the low concentrated range. In the case of citric acid, only near the upper end of pressure does it change sign and acquire a slowly changing positive value.

One of most important characteristic of all solutes investigated is the preponderance of polyhydroxy functional groups in their molecular structure conferring high hydrophilic potential. These are polar groups capable of direct interaction with the solvent water. Different hydration models have been proposed to describe the behavior of hydrophilic solutes in aqueous solutions. In the first approach, by Stokes and Robinson (1966), that of a semi-ideal solution, it is proposed that the solute forms hydrogen-bonded complexes with water molecules, and that each individual complex then behaves ideally in solution, in such a way that the solution properties are explained in terms of a series of well-defined solute-solvent equilibria, and thus no solute-solute

interactions are anticipated. This model provides a useful first approximation when considering simpler thermodynamic functions, but the inadequacies of this theory become important when studying for example derivatives of Gibbs free energy such as partial molar volumes (Franks and Reid 1973). A second approach essentially describes the solution in terms of solute-solute interactions based on the activity concept; which claims a direct relationship between solute functional groups and the extension of the interactions, though failing to accommodate properly the differences in hydrations found in similar solute structures (Kozak et al. 1968). One of the most widely accepted hydration models for hydrophilic solutes is the specific site hydration model which seems to provide a better description of such solutions (Tait et al. 1972). In this model, supported by spectroscopy (magnetic resonance and dielectric relaxation) measurements in aqueous solutions of simple sugars, the absence of long-range interactions in solution is a consequence of an assumed equilibrium between hydration water and the lattice (or bulky) structured solvent water, as the solute will not perturb the solvent water at a distance beyond the hydration layer.

Sucrose and glucose are sugar molecules with hydroxyl and carbonyl groups capable of directly interacting with the solvent by the formation of hydrogen bonds with water molecules. Figure 5.34 shows the chemical structure of these molecules. Sucrose is a nonreducing sugar composed of two monosaccharides-hexoses (6 carbon sugar) units, glucose (α-D-glucopyranosyl) and fructose (β-D-fructofuranosyl), chemically classified, respectively, as aldose (polyhydroxy + aldehyde) and ketose (polyhydroxy + ketone) (BeMiller and Whistler 1996). The effect of hydration can be viewed as the resulting effect of hydrogen bonding of water molecules to specific groups of the solute

molecules. The hydrations of disaccharides (sucrose) are generally smaller than those of monosaccharides as is the case of glucose studied here, because the molecular structure of sucrose is considered to decrease the number of free hydroxyl radicals caused by intramolecular hydrogen bonding and steric hindrance between the two monomers (Shiio 1958). The hydration of both sucrose and glucose decreases as temperature increases since hydrogen bonds are very sensitive to changes in temperature. The higher strength of hydrogen bonding of water molecules with hydrophilic groups of solute molecules than water-water interactions has been demonstrated. Furthermore, there is the effect of the hydrophobic nature of the methyl radicals acting as repulsive forces, but possibly with significantly less influence on the overall solution structure. The partial compressibility of water in solution shows that the state of association of water molecules is effectively nearly the same as in pure water. This may presumably be due to the fact that the effect of hydration on compressibility nearly compensates the effect of the partial destruction of the hydrogen bonds of the associated water molecules by the influence of solute. Different isomeric forms of sugar molecules in aqueous solution seem not be a major effect, since earlier studies have shown that the equilibrium composition of a carbohydrate in water is not strongly affected by pressure (O'Connor et al. 1983). On the other hand, studies have shown that stereochemistry has great influence on hydration properties of the different sugar molecules at atmospheric pressure (Galema and Hoiland 1991). Since partial compressibility is a measure of the protection against compression which the solute molecule imparts to water, the relatively large negative values obtained for sugar molecules, with many hydroxyl groups, would suggest they act as structure preservers. In the case of the most concentrated solutions, it is more likely that the

limiting 'glassy' state[4] of the saccharide is reached, and the probability of water hydrogen-bonded to itself is smaller than water being hydrogen bonded to the hydroxyl groups on the sugar molecules, owed to the higher strength of the former.

Citric acid is chemically classified as hydroxy-tricarboxylic acid with its technical nomenclature being 1,2,3-propanetricarboxylic acid, 2-hydroxy- (see chemical structure in Figure 5.34). The behavior of citric acid is even more complex in the sense that its chemical structure has several functional groups with different properties, hydrophilic hydroxyl groups, hydrophobic methyl groups, and charged carboxylic acid groups. Accordingly, it can be assumed that three limiting types of local water structure near the solute molecule can be distinguished: (i) a solid-like bound water, less compressible than bulk water, (ii) an unbound water, with a higher compressibility, and (iii) electrostricted water, with compressibility lower than (i).

At this point, the electrostriction effect of ions in aqueous solutions may need to be clarified even though this effect is much more pronounced in solutions of strong electrolyte solutes than the weak citric acid currently studied. When ionized, or charged, groups are introduced into water they usually break the water structure by electrostriction. The electric field produced by the ions orientates the water molecules and causes the volume of the water to decrease. It enhances the hydration of ions, principally by increasing the dielectric constant of the solution. The water around these groups is dense and less compressible than bulk water, leading to relatively large negative partial compressibilities depending on the ionic strength. Thus the electrostriction effect

[4] **Glassy state** is a non-equilibrium quasi-stabilized amorphous structure that some aqueous carbohydrate solutions may exhibit at the appropriate condition. It is characterized by very long relaxation times, reduced molecular mobility and if kept at a suitable temperature may remain almost indefinitely in a metastable state. There are also time dependent changes in thermodynamic and physico-mechanical properties associated with this transition state (Kauzmann 1948; Gibbs 1971; Urbani et al. 1997).

of the charged groups of citric acid makes water less compressible around them, leading to partial compressibility less negative than that of the sugar molecules although the number of hydroxyl groups, able to make stronger hydrogen bonds with water molecules than water-water bonds, are very different. The electrostriction effect is evidenced from the partial molar volume and partial compressibility plots of citric acid at high concentration, especially in the higher pressure range (refer to Figure 5-33 and 5-40). The partial compressibility becomes less negative as the concentration increases. The change in volume that is observed when a carboxylic acid molecule dissociates in aqueous solution is mainly a solvent effect (Hoiland 1973). The carboxylic groups become charged causing some water molecules to interact with them, whereas there is little or no interaction with the unchanged acid molecule. The undissociated acid molecules have a lower (intrinsic) compressibility than bulk water, and the ionized molecules tend to behave more or less as water molecules. As the concentration increases, more ionized molecules are formed. Hence, both the partial compressibility and the partial specific compression of solute molecules in solution tend to the values of those of the solvent. Besides being positively affected by pressure, it is also apparent that temperature favors this effect at higher concentration. This evidence seems to support the idea that any weak electrolyte will become strong at sufficiently high pressure. In the case of partial specific compression of citric acid in solution, we have to consider that it refers to a hypothetical state of a purely undissociated acid molecule in solution. The calculated values include dissociative effects which were not taken into account, since degree of dissociation that can be obtained from equilibrium constant, was not available.

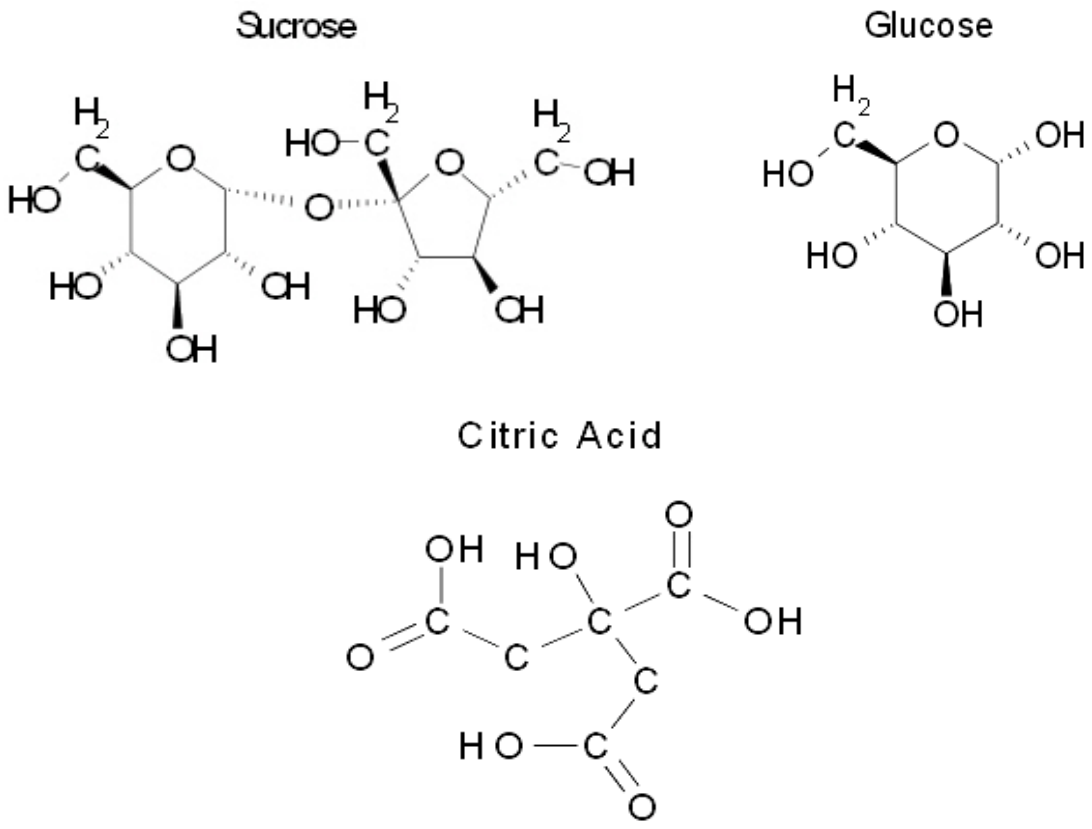

Figure 5.34. Chemical structures of sucrose [$C_{12}H_{22}O_{11}$, M_w = 342.30], glucose [$C_6O_8O_7$, M_w = 180.16] and citric acid [$C_6H_{12}O_6$, M_w = 192.12] molecules

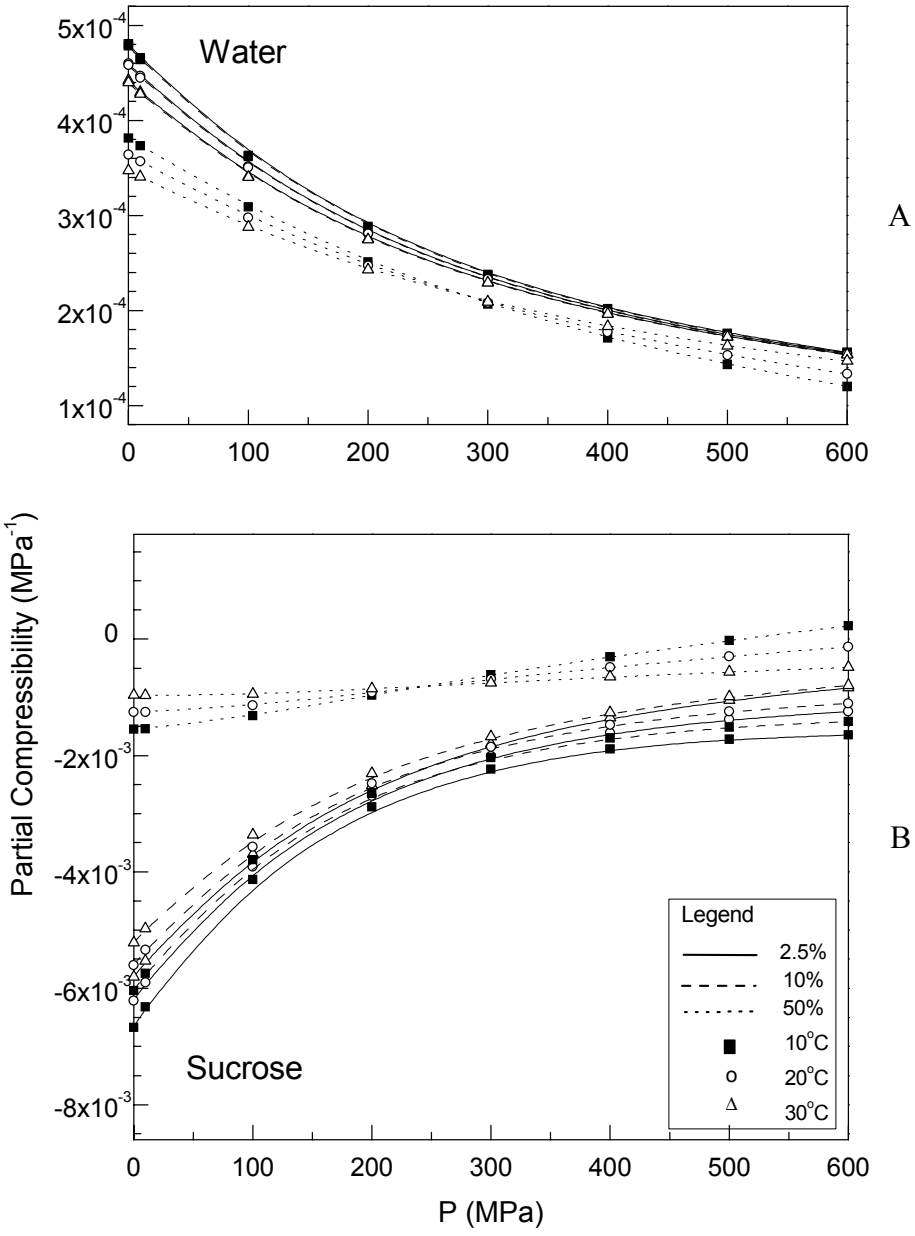

Figure 5-35. Partial isentropic compressibility of solvent (A) and solute (B) in sucrose solutions as a function of pressure at different temperatures and concentrations

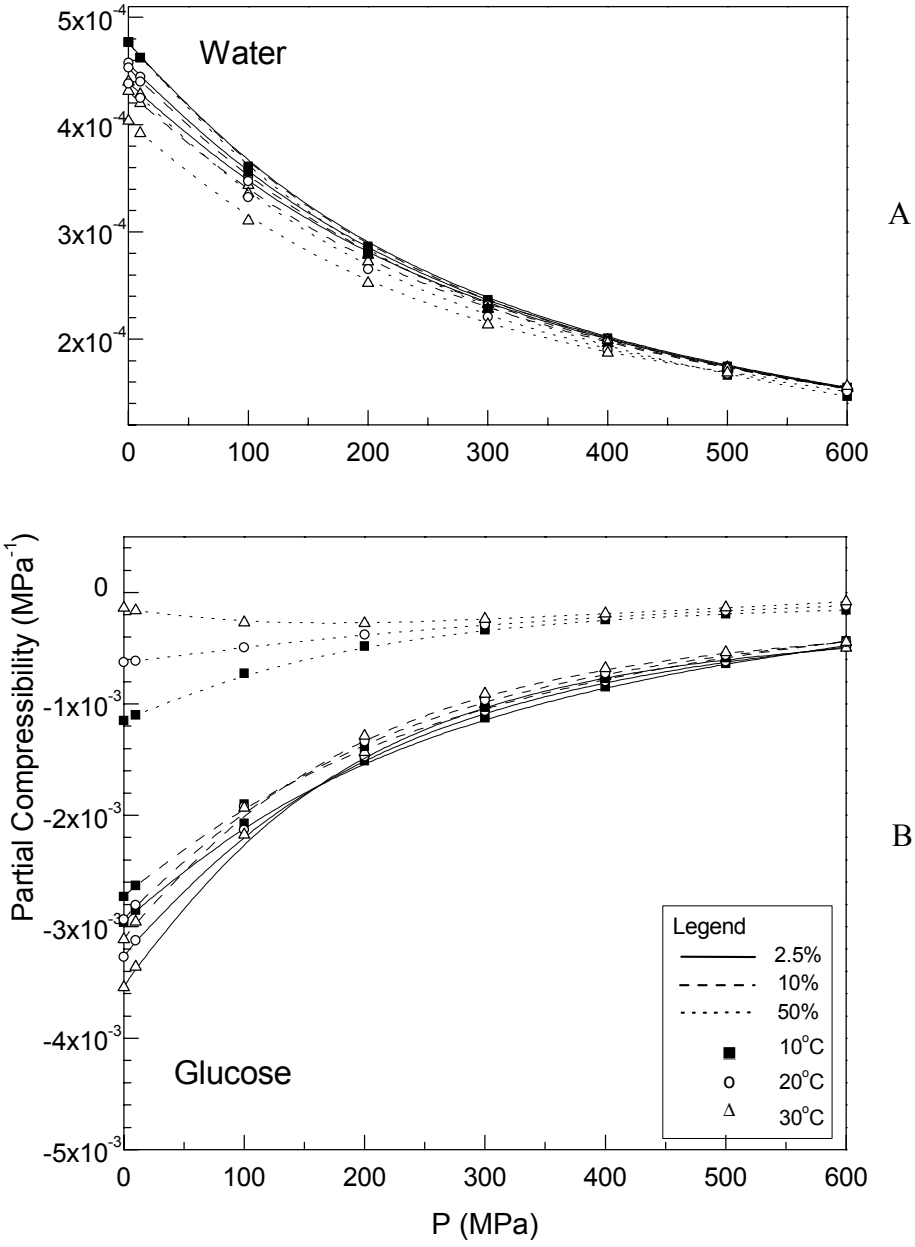

Figure 5-36. Partial isentropic compressibility of solvent (A) and solute (B) in glucose solutions as a function of pressure at different temperatures and concentrations

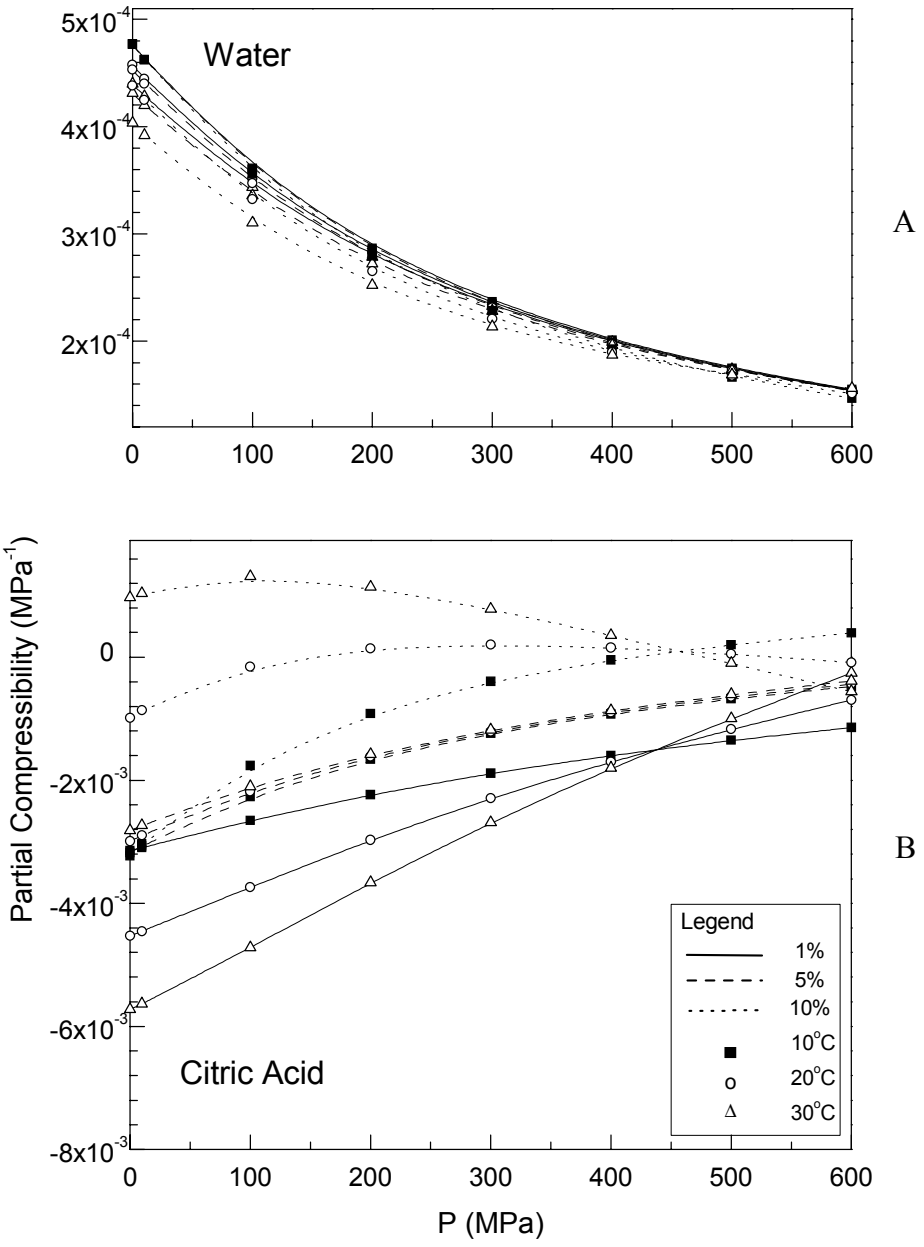

Figure 5-37. Partial isentropic compressibility of solvent (A) and solute (B) in citric acid solutions as a function of pressure at different temperatures and concentrations

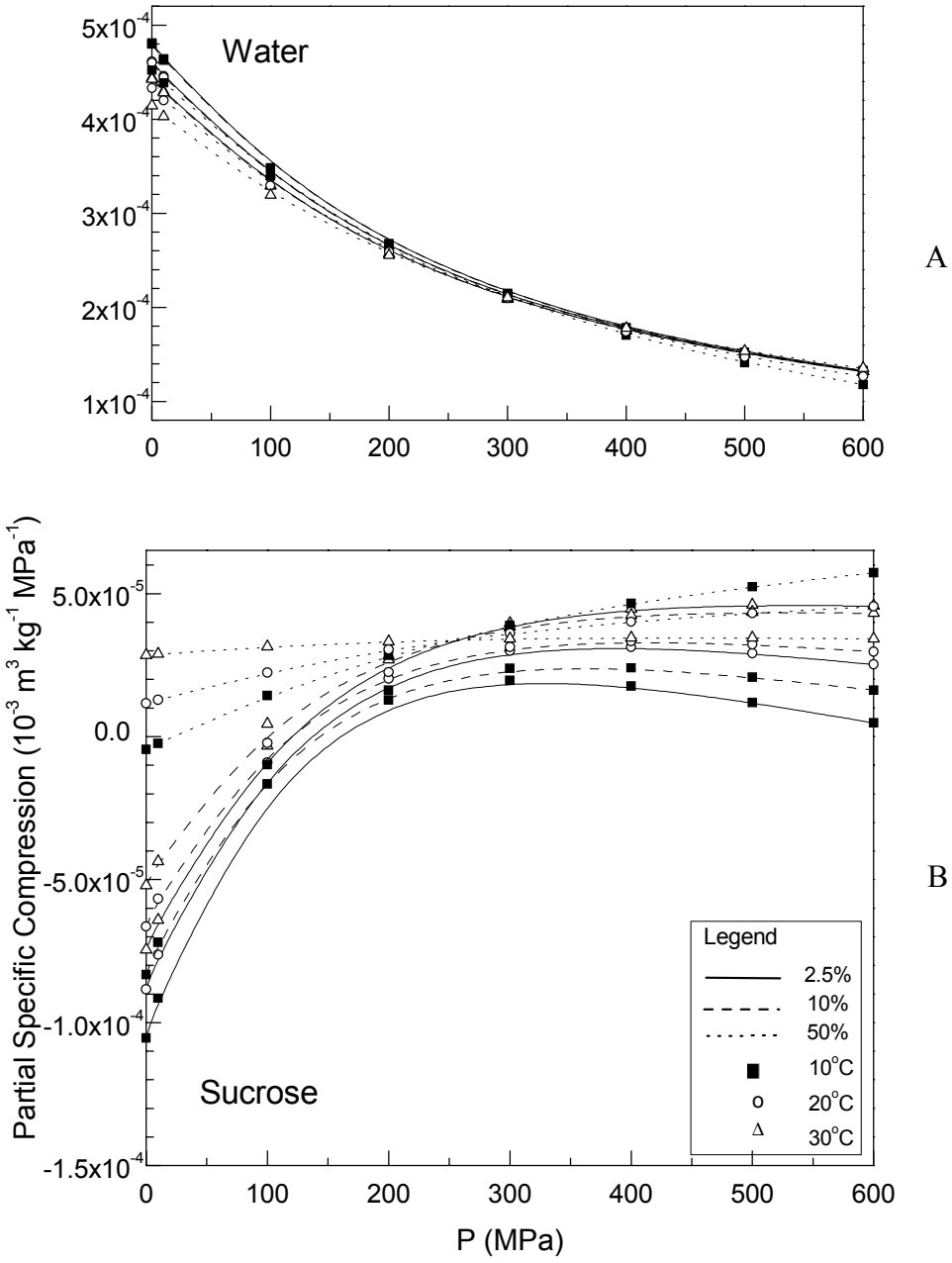

Figure 5-38. Partial specific compression of solvent (A) and solute (B) in sucrose solutions as a function of pressure at different temperatures and concentrations

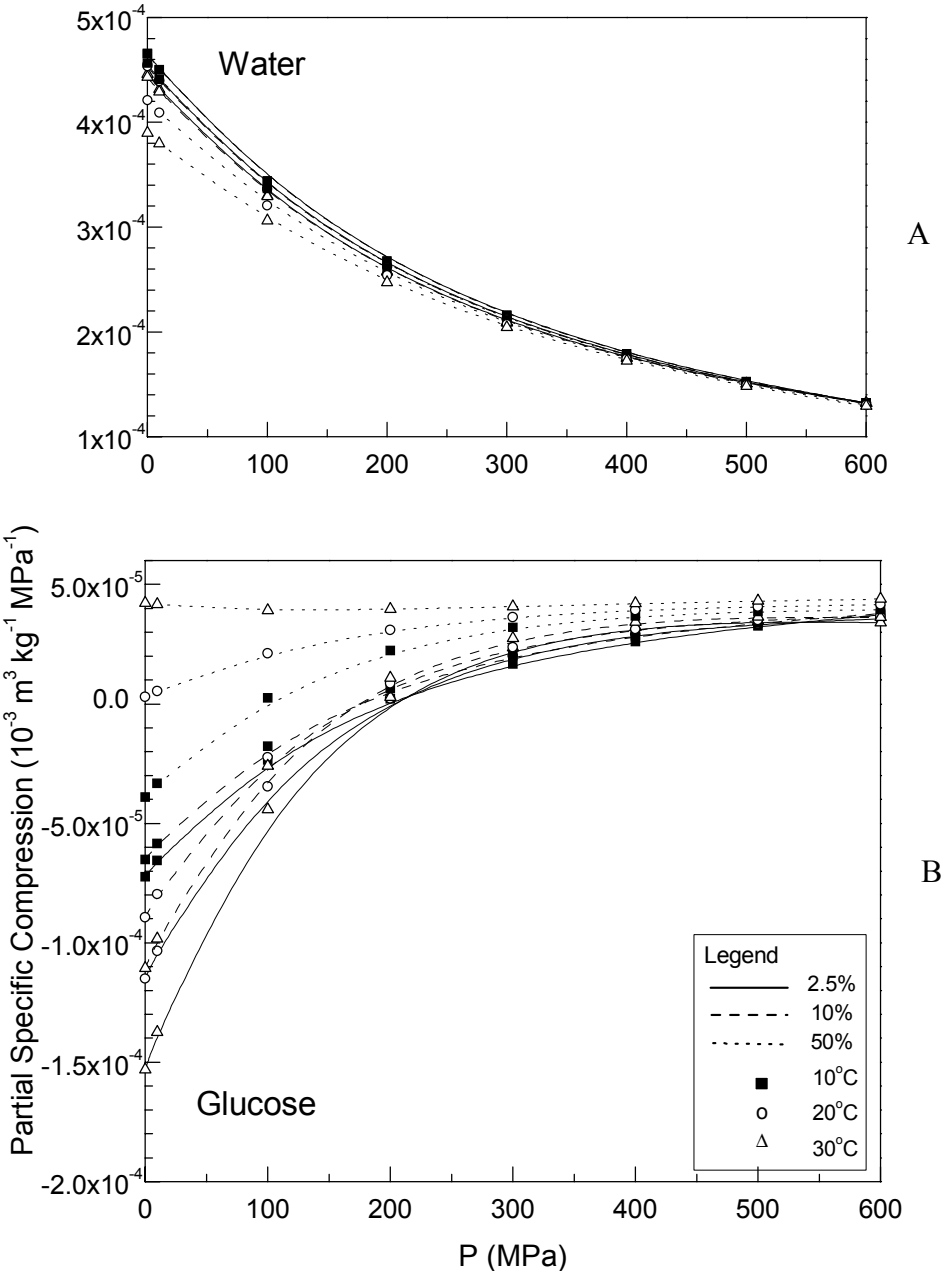

Figure 5-39. Partial specific compression of solvent (A) and solute (B) in glucose solutions as a function of pressure at different temperatures and concentrations

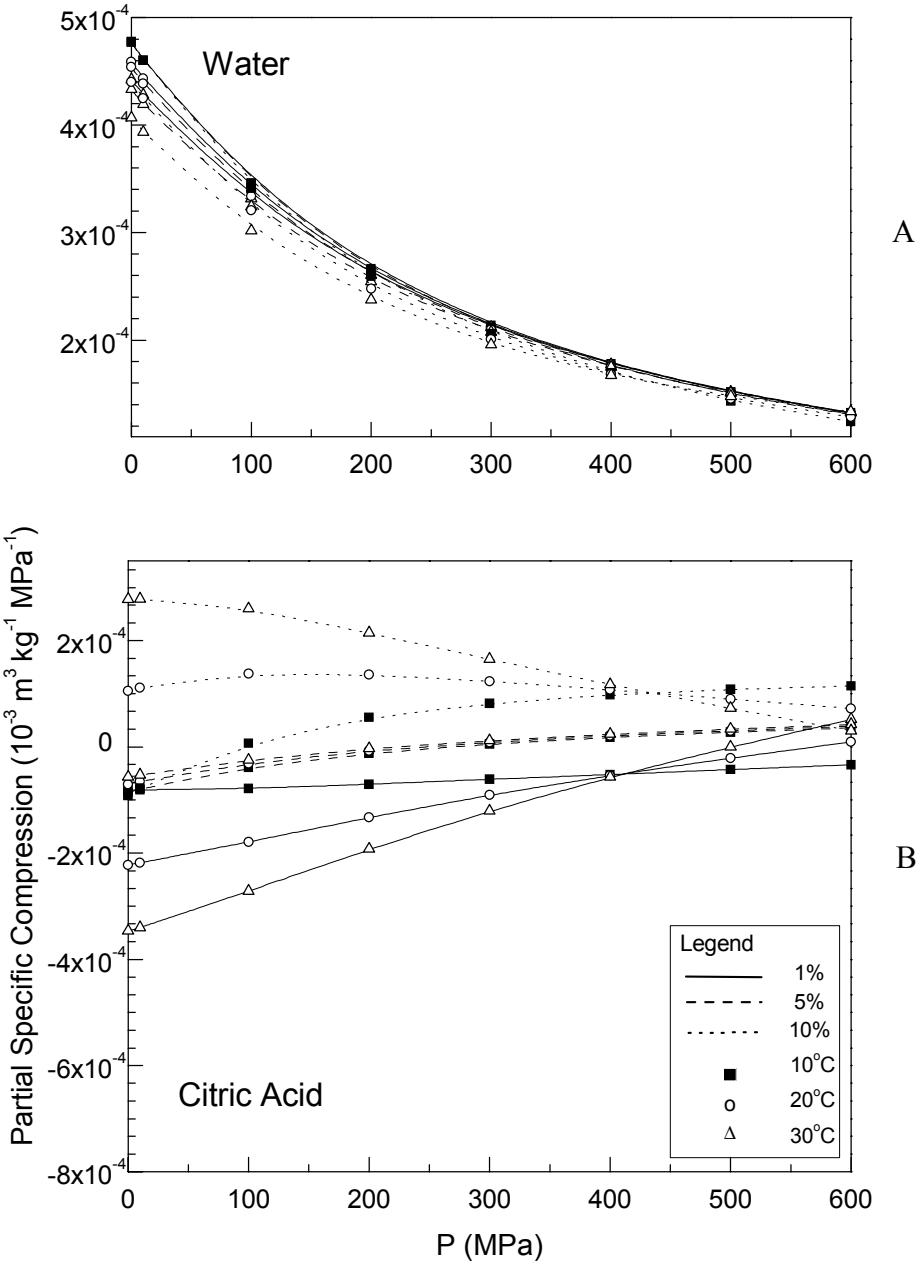

Figure 5-40. Partial specific compression of solvent (A) and solute (B) in citric acid solutions as a function of pressure at different temperatures and concentrations

Water Activity at High Pressures

Water activity of each binary solution was obtained from the difference between the partial molar volume of component water in solution, as presented in the previous section, and the molar volume of pure water, both at the same temperature. From the regression coefficients obtained by fitting $\left(\overline{V}_1^m - V_1^{o,m}\right)$ to a 3rd degree polynomial in *P,* at a given constant temperature, and then inserting these values into Equation 4-52, water activity data were obtained for the experimental range investigated, from atmospheric pressure to 600 MPa at three different temperatures 10°, 20° and 30°C, and at varying concentrations of the solute.

Calculated values of water activity for each binary solution as a function of pressure at different temperatures and concentrations are shown in Figures 5-41 to 5-43. Again, data are given at values of pressures between 0.1 and 600 MPa in intervals of 100 MPa and at temperatures of 10°, 20° and 30°C (283.15, 293.15 and 303.15 K) with the help of smooth lines connecting data points for easier pattern recognition.

Overall the results show a decrease in water activity with increasing pressure, with a more pronounced effect for the high concentrated solutions in the low temperature range. The exceptions for this trend are the most concentrated sucrose and citric acid solutions at the highest temperature (30°C), which show a slight increase in water activity in the low pressure range. The dilute solutions of glucose and citric acid also show a slight increase in water activity with pressure. It is known that at atmospheric pressure, an increase in temperature generally represents a concomitant increase in water activity (an increase in temperature causes a decrease in the amount of adsorbed water); however for sugars and other low molecular weight constituents the effect observed is the

opposite, since these solutes become more hygroscopic at higher temperatures (Kapsalis 1987). Dissolution, an endothermic process, of such solutes uses large amounts of water and is favored by the higher temperature. When these solutes are dissolved in water entropy is reduced as water molecules become organized under the effect of the solute. Our results show that pressure enhances this increasing hygroscopic effect with increasing temperature in the low concentration range. However, for the most concentrated solutions the effect is reversed, i e, the temperature effect of enhancing the hygroscopic potential of these molecules is absent at the elevated pressure; that is, temperature rise becomes unfavorable to water sorption at elevated pressures for low molecular weight solutes in aqueous solutions. Furthermore, pressure enhances temperature effects at high concentration by reversing the hygroscopic potential. It can also be observed from these plots that glucose lowered the water activity of the solution to a greater extent than the other solutions at all pressures, which is consistent with preceding properties' results. In addition, when comparing with sucrose solutions at the same concentration (e.g., in units of weight per volume), glucose solution has a greater molar concentration of sugar molecules per weight, thus the lowering effect on water activity. The reason for this resides on the fact that colligative properties are affected by the number of molecules present in a given quantity rather than by the weight of the quantity (Rosenbaum 1970). It is not clear however, if this hypothesis holds true for both dilute (where the solution becomes more nearly ideal) and concentrated solutions. Water activity itself is not considered a colligative property, although it can be derived from colligative properties like vapor pressure lowering, freezing point depression, boiling point elevation and osmotic pressure. Definitions of colligative[5] properties include those

[5] **Colligative**: from Latin, *co*-, together, + *ligare*, to bind.

properties that are dependent on the properties of the solvent and the total mole fraction of all solutes, but are independent of any particular physico-chemical property of the solutes (Kaufman 2002).

From the definition given by Equation 4-8, it can be seen that activity is equal to the mole fraction multiplied by the coefficient of activity that shows how much more or less "chemically active" the species is than it would be in an ideal solution. From this definition it is clear that for a pure species in an ideal solution the activity coefficient is identically 1 and the activity is equal to the mole fraction. Thus, activity or activity coefficient is a simple dimensionless measure of the departure of the species fugacity[6] (or chemical potential) from ideal solution behavior. Accordingly from the results presented here, all solutions at all pressures have positive deviations from ideality.

Except for the data at atmospheric pressure (which are in satisfactory agreement with literature values), the pressure dependence of water activity cannot be compared or verified because no report was found of any prior 'measurements'[7] (of related properties), description or predictive theoretical approach on this thermodynamic property under the experimental conditions researched, therefore, any attempt at a more detailed interpretation of these results does not appear to be profitable at the moment.

---

[6] **Fugacity** was introduced to overcome the counterintuitive behavior of the chemical potential, which makes it approach minus infinity as the concentration approaches zero. For pure ideal gases the fugacity is the same as pressure, and for ideal gas mixtures the fugacity of one species is equal to that species' partial pressure. Accordingly, activity of a species in a mixture can be defined as the ratio between fugacity of solvent in solution and that of the pure liquid at atmospheric pressure, $A_i = f_i \big/ f_i^o$ (Lewis and Randall 1923).

[7] **Activity** like fugacity or activity coefficient is a computed or estimated quantity; none of them can be measured directly (De Nevers 2002).

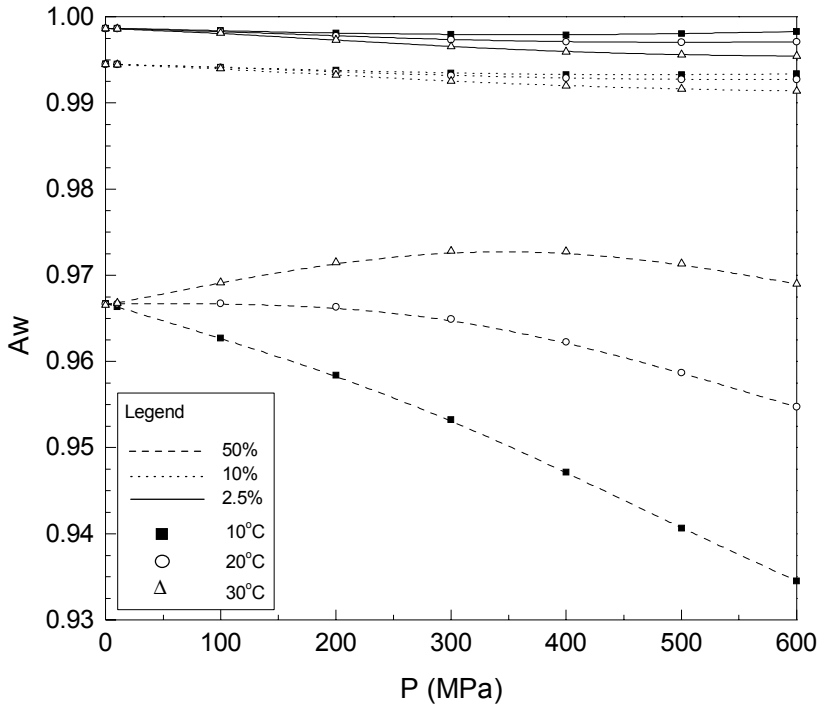

Figure 5-41. Water activity of sucrose solutions as a function of pressure at different temperatures and concentrations

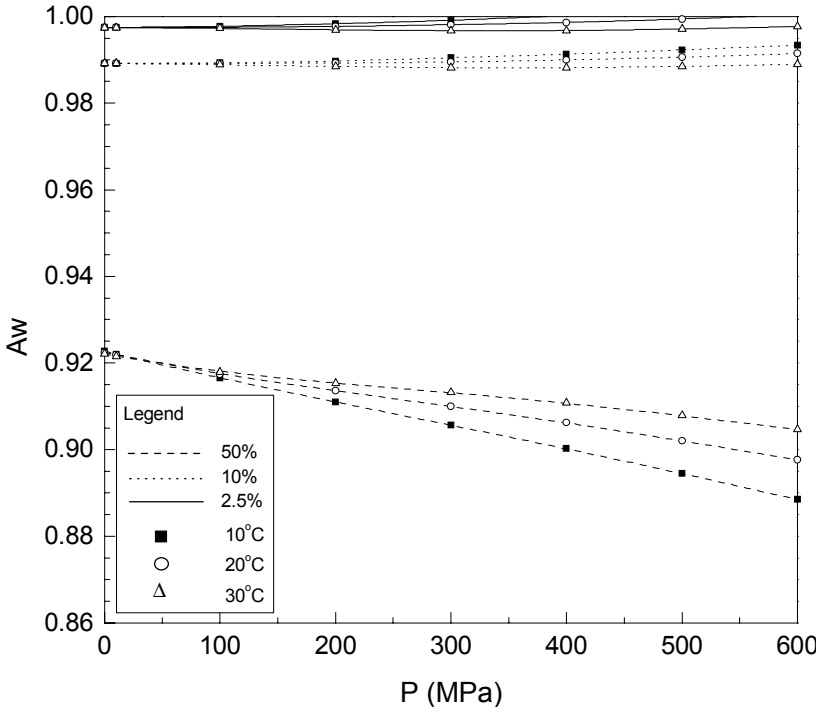

Figure 5-42. Water activity of glucose solutions as a function of pressure at different temperatures and concentrations

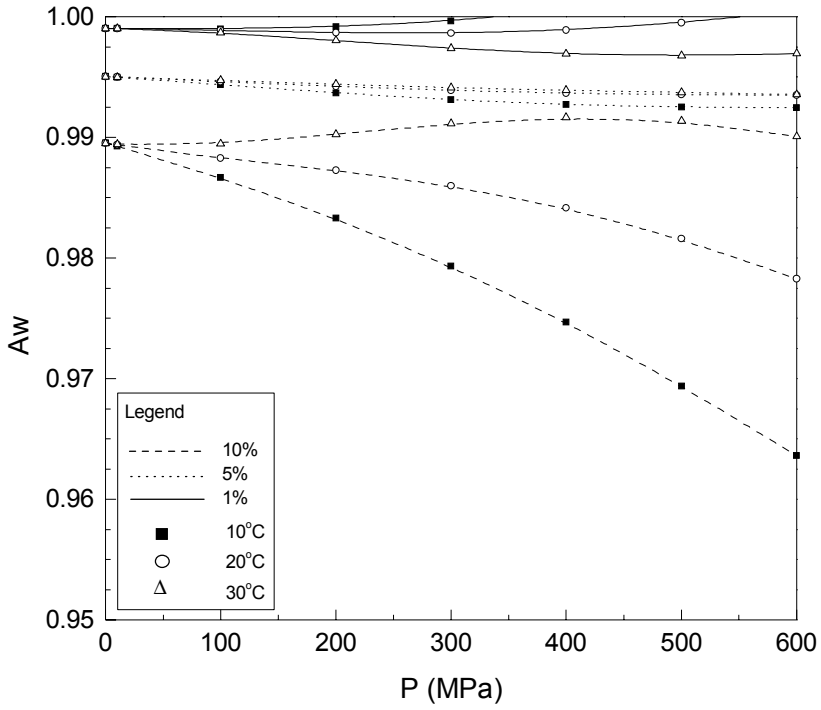

Figure 5-43. Water activity of citric acid solutions as a function of pressure at different temperatures and concentrations

CHAPTER 6
SUMMARY, CONCLUSIONS AND SUGGESTIONS FOR FUTURE STUDY

Experimental *in situ* measurements of sound velocity as a function of pressure, temperature, and concentration for binary aqueous solutions of sucrose, glucose, and citric acid were performed at pressures from atmospheric pressure up to 600 MPa, at temperatures of 10^{o}, 20^{o} and 30^{o}C, and at concentrations of 2.5, 10 and 50% (w/v) for sugar solutions, and 1, 5 and 10% (w/v) for citric acid solutions. An increase of sound velocity as pressure increases was observed as well as an increase with increasing temperature and concentration. Thermodynamic properties of density, isentropic and isothermal coefficient of compressibility, and the isentropic pressure thermal coefficient were determined. They were derived from ultrasonic data at elevated pressure combined with density, isobaric specific heat capacity, and thermal expansion coefficient experimental data at atmospheric pressure as a function of temperature and concentration for each binary solution as a result of the application of a numerical iterative procedure. Pressure- temperature- and concentration-dependence behavior of each property was interpreted accordingly. Predictive equations were proposed for the adiabatic heating effect upon compression for aqueous solutions within the experimental range investigated. A thermodynamic approach was proposed for the mixing scheme in terms of partial properties, partial molar volumes, and partial compressibility of solute and solvent. The findings of applying this approach revealed some of the intricacies of describing the interactions between solute and solvent under the influence of pressure,

temperature, concentration and solute-type. In addition, water activity values were obtained from the partial molar volume of the component water (solvent) in solution as a function of pressure, temperature, and concentration for each solution investigated. For predictive or numerical application purposes, where applicable, regression coefficients were determined by fitting experimental or calculated data to the appropriate model. A qualitative error analysis was given and a quantitative deviation comparison with literature data for pure water was performed. We believe that the many thermodynamic properties, experimentally determined or calculated, are close to their true values, as demonstrated by comparisons with literature values, although data for pure water was the only one available.

The developed high-pressure ultrasonic measurement cell, associated electronics, and the pulse-echo technique have shown to be appropriate choices for *in situ* measurements of sound velocity in a liquid sample during compression. The main advantages of ultrasound are that it is nondestructive, noninvasive, can be applied to systems that are concentrated and optically opaque, and can provide valuable information about fundamental physical and chemical properties of food materials that are difficult to obtain using other techniques. However, a lot of information about the thermophysical properties of the solution components is needed to interpret ultrasonic data using thermodynamic theories. Especially to interpret ultrasonic data at high pressures, since the properties related to the speed of sound, through Newton-Laplace equation, are also pressure dependent, a numerical-iterative procedure with initial value was necessary to solve the partial differential equation set to determine other thermodynamic properties at high pressure. We found appropriate the proposed procedure based on Runge-Kutta 4,5th

order, coupled with properties (density, heat capacity, and thermal expansion coefficient) determined at atmospheric pressure as initial input values.

The present investigation demonstrated that thermodynamics is a powerful tool for the study of the physical and chemical interactions between solutes and water in aqueous solutions under high pressure, and provides many insights into the nature of these interactions. However, the methods of thermodynamics have an intrinsic limitation. Due to the average nature at the macroscopic level the information provided by thermodynamic properties derived, they are unable to give any direct information on the microscopic structure and properties of the systems. Thus, their interpretation must be consistent with the microscopic behavior of these systems in cases any is available; otherwise a consistent model must be accounted for. On the other hand, a thorough understanding of the behavior of such aqueous solutions under the influence of pressure, temperature, composition, and concentration must be based on information gained from a broader variety of experimental techniques before an assessment can be attempted. The availability of experimental techniques that can be applied at high pressures is still in its infancy. Therefore the development of other experimental techniques for *in situ* measurements under elevated pressures is desirable. For instance, the use of ultrasonic spectroscopy, which combines velocimetry with attenuation measurements as a function of frequency, would be very useful to obtain information about relaxation mechanisms. Measurements of the frequency dependent of the absorption of ultrasound have been used to study a number of important relaxation phenomena such as proton transfer equilibria (e.g., electrostriction effects), hydration equilibria (e.g., equilibria between bound and unbound water), and conformational equilibria (e.g., aggregation of macromolecules).

Moreover, it would be extremely advantageous to develop such devices such as for viscosity measurements, since studies on pressure dependence of viscosity, as a reversible process in the same way as the ones investigated presently may reveal important aspects of physical chemical, thermodynamic, and kinetic mechanisms of pressure-induced transformations experienced by food components during high-pressure food processing. This would also contribute to help quantitatively interpret the cause and effect relationship between pressure and physicochemical and structural properties, and mobility of fluid particles and molecules and thus complementing the present study. The overall expectations of high-pressure processing as an alternative technology for food processing will not be satisfied without the basic concepts and the knowledge of thermodynamic and transport properties of foods and their constituents under pressure as those determined in the present investigation.

The thermodynamic properties determined, experimental or calculated and their pressure, temperature and concentration dependence are considered as the first step toward an accurate evaluation of the effects of pressure applied during conventional batch high-pressure processing of foods. Obviously experiments with other materials, their combinations, extended condition ranges, and broader scope of properties should be performed to cover the various food materials of interest for high-pressure processing. Besides pressure dependence, it was considered important to determine the temperature dependence as well, since high-pressure processing does not escape the classical limitations imposed by heat transfer, either because the pressure process is intrinsically accompanied by adiabatic heating or simply because of process combination with mild heat. This has been recognized to be useful in several applications where pressure is not

enough to inactivate some baroresistant spores of microorganisms or certain enzymes. Heat transfer is then caused by the resulting temperature gradients and can lead to large temperature differences, especially in large-volume industrial vessels, with the consequent non-uniform distribution of the desired pressure/temperature effect. In every case, pressure process design, modeling and optimization must rely on pressure-temperature dependence data of nonlinear and non-isotropic food material properties coupled with kinetic parameters of safety- or quality-related component. The effects of adiabatic heating can be now predicted and introduced in kinetic studies as far as the components presently studied are concerned.

Despite the fact that most of the literature dealing with thermodynamics of solutions and their components uses the approach based on the calculation of apparent (molar) properties, it was instead more appropriate to employ a thermodynamic treatment in terms of partial (molar) properties to the high-pressure data. Apparent properties, which attribute all the changes, upon mixing, to the solute species, are calculated directly from the experimental data on a point-by-point basis, and are usually more suitable to determine properties at infinite dilution using extrapolating procedures. On the other hand, the partial properties have to be obtained by some sort of fitting procedure that give estimates of the mole fraction derivatives, which indeed concurred with the mathematical treatment and experimental data in this study. In addition, the treatment involving calculation of apparent properties requires combining with data for pure components and more refined experimental data at low concentrations which were not entirely available in this case. Moreover, the formulation usually employed to derive apparent properties of

the components in solution suffers from inaccuracies due to the mathematical operations involving large quantities.

The features discussed in this dissertation regarding the effects of high pressure in these binary solutions are certainly not small scale effects since the arguments went to broader physicochemical properties and their interpretation. But superposed to these effects there are other features concerning the complexity and irregularities of such molecules in solution. Examples of virtually every conceivable type of behavior may be found; the compressibility, heat capacity, thermal expansion, thermal pressure coefficient, and partial properties may increase or decrease with increasing pressure or temperature, and the curves for different temperatures or concentration may cross and recross in the most confounding way. The reason doubtless is that the different molecules, especially water with solutes, are very complicated structures when details of their behavior and interacting forces are taken into account and the nature of the complications are not the same for any two kinds of molecule, even considering two similar simple sugars such as sucrose and glucose. Additionally, the effect of these local complexities at the molecular level may be expected to become important when molecules are forced into close proximity by high pressure, but is comparatively less important when the molecules are "free" to move as they please at low pressures.

The thermodynamic relationships and equations have illustrated the power of thermodynamics in drawing together the properties of solutions and their components, and in particular of aqueous systems under the influence of high pressure. It can be inferred from the results that the effects of each compound on acoustic and derived properties are a combination of the hydrogen-bonded structure of the bulk water, the

solute ability in alter this structure, intermolecular forces, and property relationships. A convincing argument can be made that the continuation of the present study would gain considerably from the determination of mixing properties of aqueous solutions, such as partial properties of solutes other than sugars and organic acids, for example macromolecules (proteins, starch, pectin, etc.) and strong electrolyte compounds (inorganic salts) and their combinations, by more closely emulating food systems, and their pressure, temperature and concentration dependence. In fact, experimental data have also been collected of different combinations of some of these solutes as well as other binary solutions and combined solutions and are still under investigation. However, because of time constraints due to difficulties in keeping the high-pressure unit operating, these data could not be included in this dissertation. Interesting patterns would emerge pointing to the complexity of both solute-solvent and solute-solute interactions of these systems. Many of the solutes evoked may have limited solubility in water, and therefore phase change may take place in these solutions depending on the combination of pressure, temperature and concentration used. Crystallization and metastable states resulting from supersaturation or supercooling may occur due to pressure shift freezing point effects. The key to describing the water relations in these materials under elevated pressures will depend on the availability of a reasonable model that reflects our understanding of the interaction of water with soluble components, on which some insight were brought from the present investigation.

Water and aqueous solutions of carbohydrates and organic acids, as studied in the present research, and other food constituents (e.g., proteins, lipids, and minerals), are the most important chemical compounds and the most fascinating substances not only in the

food science and technology field but also in scientific research in biophysical-chemistry and other areas. It is hoped that besides reporting many important thermodynamic properties of these systems under high-pressure conditions, some additional facets have also been presented in this research. Research on water and aqueous solutions at high pressure will remain of primary interest and importance in the future. It will continue and develop in many directions because of the primary importance of water for nature, life, biology, medicine, biochemistry, oceanography, meteorology, environmental problems, technological processes, etc. Along the development of this research, in every phase of it, we acknowledge the use of theories, approaches, and ideas from many distinct disciplines. And so, it is reasonable to believe that some barriers which often arise between different fields of knowledge due to otherwise converging approaches must be overcome. Such barriers are wasteful and can no longer be afforded since traditional boundaries between disciplines no longer have much meaning and the understanding of a given phenomenon will benefit from and involve the participation of scientists of many different types of background.

APPENDIX A
SELECTED THERMODYNAMIC RELATIONSHIPS AND DERIVATIONS

Basic thermodynamic functions. By using Legendre differential transformations,[21] change of variables of thermodynamic state functions, yield other fundamentally important thermodynamic state functions in more convenient forms, according to any preferred particular situation. Starting with the first law of thermodynamics ($dU = dW + dQ$) for a closed (constant mass) hydrostatic system with heat expressed in terms of temperature and entropy.

$$dU = -PdV + TdS \qquad [A.1]$$

This equation is convenient for situations involving variations in internal energy U, with changes in volume V and entropy S. Now, from that we can define a new characteristic function enthalpy H, using the Legendre transformation, giving:

$$H \equiv U + PV \qquad [A.2]$$

In differential form,

$$dH = VdP + TdS \qquad [A.3]$$

Enthalpy is a convenient function for problems involving heat quantities, such as heat capacities, latent heat, and heats of reactions, when pressure is the variable being controlled.

[21] **Legendre transformation**: If the state of a system is described by a function of two variables f(x,y), which satisfies df=udx+vdy, and we wish to change the description to one involving a new function g(u,y), satisfying a similar equation in terms of du and dy, then we must define the Legendre transform as g ≡ f-ux, which satisfies dg = -xdu+vdy.

Similarly relationships can be derived for other state functions, namely Helmholtz A and Gibbs G functions.

$$A \equiv U - TS \qquad [A.4]$$

$$dA = -SdT - PdV \qquad [A.5]$$

$$G \equiv H - TS \qquad [A.6]$$

$$dG = VdP - SdT \qquad [A.7]$$

The latter is of special interest in the context of the present work since G is a state function characterized by situations where pressure and temperature are the convenient independent variables. All these characteristic state functions U, H, A, and G are known as thermodynamic potential functions, because they have the property that if the functions are expressed in terms of the appropriate thermodynamic variables, then all the thermodynamic properties of a system can be calculated by differentiation only.

Pressure dependence of isobaric heat capacity. Based on the previous statements and relations, for instance, if the enthalpy function H is known as a function of P and T for a system, then we can calculate all the other thermodynamic properties of the system by differentiation, and no new constants or functions appear in the calculation. Therefore, we may write,

$$dH = \left(\frac{\partial H}{\partial T}\right)_P dT + \left(\frac{\partial H}{\partial P}\right)_T dP \qquad [A.8]$$

The first partial derivative of the right-hand side of Equation [A.8] is promptly identified as the isobaric heat capacity, whereas the second partial derivative deserves extra attention. If we derive Equation [A.6] with respect to pressure at constant temperature and solving for the enthalpy term, we have,

$$\left(\frac{\partial H}{\partial P}\right)_T = \left(\frac{\partial G}{\partial P}\right)_T + T\left(\frac{\partial S}{\partial P}\right)_T \qquad [A.9]$$

From Equation [A.7], solving for Gibbs function, both at constant temperature and at constant pressure, we obtain

$$\left(\frac{\partial G}{\partial P}\right)_T = V \qquad [A.10]$$

$$\left(\frac{\partial G}{\partial T}\right)_P = -S \qquad [A.11]$$

By taking the second derivative with respect to temperature and pressure, of Equation [A.10] and [A.11] respectively, and using the cross partial differentiation rule,[22] it follows

$$\left[\frac{\partial}{\partial T}\left(\frac{\partial G}{\partial P}\right)_T\right]_P = \left(\frac{\partial V}{\partial T}\right)_P \equiv -\left(\frac{\partial S}{\partial P}\right)_T = \left[\frac{\partial}{\partial P}\left(\frac{\partial G}{\partial T}\right)_P\right]_T \qquad [A.12]$$

Combining Equations [A.9] and [A.12], we obtain

$$\left(\frac{\partial H}{\partial P}\right)_T = V - T\left(\frac{\partial V}{\partial T}\right)_P \qquad [A.13]$$

By introducing the definition of isobaric heat capacity and Equation [A.13] into Equation [A.8], becomes

$$dH = C_P dT + \left[V - T\left(\frac{\partial V}{\partial T}\right)_P\right] dP \qquad [A.14]$$

---

[22] **Cross partial differentiation rule**: If x and y are independent variables, and $u = u(x,y)$ is a single-valued function, then $du = \left(\partial u/\partial x\right)_y dx + \left(\partial u/\partial y\right)_x dy$ and $\left[\partial\left(\partial u/\partial x\right)_y/\partial y\right]_x = \left[\partial\left(\partial u/\partial y\right)_x/\partial x\right]_y$

Since dH is an exact differential,[23] we may directly write

$$\left(\frac{\partial C_P}{\partial P}\right)_T = \left\{\frac{\partial\left[V - T\left(\partial V/\partial T\right)_P\right]}{\partial T}\right\}_P \qquad [A.14]$$

Or, the final format of the pressure dependence of isobaric heat capacity.

$$\left(\frac{\partial C_P}{\partial P}\right)_T = -T\left(\frac{\partial^2 V}{\partial T^2}\right)_P \qquad [A.15]$$

Maxwell's relations. As the enthalpy function H, U, A, and G are actual functions of S, V, T and P, their differentials are exact differentials as pointed out before. Therefore, we can apply the same condition to obtain the Maxwell's relations, shown below. These equations do not refer to a process but express relations that hold at any equilibrium state of a hydrostatic system. The reciprocals of Maxwell's relations are also valid equations.

$dU = -PdV + TdS$ ➔ $\left(\frac{\partial T}{\partial V}\right)_S = -\left(\frac{\partial P}{\partial S}\right)_V$ [A.16]

$dH = VdP + TdS$ ➔ $\left(\frac{\partial T}{\partial P}\right)_S = -\left(\frac{\partial V}{\partial S}\right)_P$ [A.17]

$dA = -SdT - PdV$ ➔ $\left(\frac{\partial S}{\partial V}\right)_T = -\left(\frac{\partial P}{\partial T}\right)_V$ [A.18]

$dG = VdP - SdT$ ➔ $\left(\frac{\partial S}{\partial P}\right)_T = -\left(\frac{\partial V}{\partial T}\right)_P$ [A.19]

---

[23] **Condition for an exact differential**: If a relation exists among x, y, and z, then we may imagine z expressed as a function of x and y; whence, $dz = \left(\partial z/\partial x\right)_y dx + \left(\partial z/\partial y\right)_x dy$. If we let $M = \left(\partial z/\partial x\right)_y$ and $N = \left(\partial z/\partial y\right)_x$, then $dz = Mdx + Ndy$, where z, M, and N are all functions of x and y. Partially differentiating M with respect to y, and N with respect to x, we get $\left(\partial M/\partial y\right)_x = \partial^2 z/\partial x\partial y$ and $\left(\partial N/\partial x\right)_y = \partial^2 z/\partial y\partial x$. Since the two second derivatives of the right-hand terms are equal, it follows that $\left(\partial M/\partial y\right)_x = \left(\partial N/\partial x\right)_y$.

Maxwell's relations as well as other thermodynamic expressions derived here are very useful, because they provide relationships between measurable quantities and those which either cannot be measured or are difficult to measure. In particular, it should be noted that pressure, temperature, and specific volume (or density, indirectly calculated through measured speed of sound as in the present study) can be measured by experimental techniques.

Pressure dependence of the thermal expansion coefficient. The change of isobaric thermal expansion coefficient with pressure is the complement of the change of isothermal coefficient of compressibility with respect of temperature. Hence,

$$\left[\frac{\partial}{\partial P}\left(\frac{\partial \dot{V}}{\partial T}\right)_P\right]_T = \left[\frac{\partial}{\partial T}\left(\frac{\partial \dot{V}}{\partial P}\right)_T\right]_P \qquad \text{[A.20]}$$

By applying the cross differentiation rule mentioned before, we then obtain,

$$\left(\frac{\partial \alpha}{\partial P}\right)_T = -\left(\frac{\partial \beta_T}{\partial T}\right)_P \qquad \text{[A.21]}$$

Relationship between isentropic and isothermal compressibility. We now seek the difference between isentropic and isothermal compressibility. Starting with their thermodynamic definitions $(\partial V/\partial P)_S$ and $(\partial V/\partial P)_T$, respectively, and by applying the rule of partial differentiation for changing variable held constant, [24] we find,

$$\left(\frac{\partial V}{\partial P}\right)_T - \left(\frac{\partial V}{\partial P}\right)_S = \left(\frac{\partial V}{\partial P}\right)_T - \left[\left(\frac{\partial V}{\partial P}\right)_T + \left(\frac{\partial V}{\partial T}\right)_P \left(\frac{\partial T}{\partial P}\right)_S\right] \qquad \text{[A.22]}$$

---

[24] **Rule of partial differentiation for change variable held constant**: If $u = u(x,y,z)$, then the complete differential of u is $du = (\partial u/\partial x)_{y,z}\, dx + (\partial u/\partial y)_{x,z}\, dy + (\partial u/\partial z)_{x,y}\, dz$, and
$(\partial u/\partial x)_z = (\partial u/\partial x)_y + (\partial u/\partial y)_x (\partial y/\partial x)_z$

If we apply the minus 1 rule[25] of partial differentiation to the isentropic pressure dependence on temperature (last) term of the right-hand side of the equation above, we find,

$$\left(\frac{\partial T}{\partial P}\right)_S = -\left(\frac{\partial T}{\partial S}\right)_P \left(\frac{\partial S}{\partial P}\right)_S \qquad [A.23]$$

Equation [A.22] becomes,

$$\left(\frac{\partial V}{\partial P}\right)_T - \left(\frac{\partial V}{\partial P}\right)_S = \left(\frac{\partial V}{\partial T}\right)_P \left(\frac{\partial T}{\partial S}\right)_P \left(\frac{\partial S}{\partial P}\right)_T \qquad [A.24]$$

Now, combining Equations [A.06] and [A.11], we get,

$$H = G - T\left(\frac{\partial G}{\partial T}\right)_P \qquad [A.25]$$

By differentiating above expression with respect to temperature at constant pressure,

$$\left(\frac{\partial H}{\partial T}\right)_P = -T\left(\frac{\partial^2 G}{\partial T^2}\right)_P \qquad [A.26]$$

By differentiating the expression for Gibbs function at constant pressure (Equation [A.11]) with respect to temperature at constant pressure, and then combining the result with Equation [A.26], we have,

$$\left(\frac{\partial S}{\partial T}\right)_P = -\left(\frac{\partial^2 G}{\partial T^2}\right)_P = \frac{1}{T}\left(\frac{\partial H}{\partial T}\right)_P = \frac{C_P}{T} \qquad [A.27]$$

[25] **Minus 1 partial differentiation rule**: If x and y are independent variables, and $u = u(x,y)$ is a single-valued function, then $(\partial u/\partial x)_y (\partial x/\partial y)_u (\partial y/\partial u)_x = -1$ or $(\partial u/\partial x)_y = -(\partial u/\partial y)_x (\partial y/\partial x)_u$

Now, introducing the above expression (Equation [A.27]) and one of the Maxwell's relations (Equation [A19]) into Equation [A.24], after rearrangement becomes,

$$\left(\frac{\partial V}{\partial P}\right)_T - \left(\frac{\partial V}{\partial P}\right)_S = -\frac{T}{C_P}\left[\left(\frac{\partial V}{\partial T}\right)_P\right]^2 \qquad \text{[A.28]}$$

And finally, after reintroducing the definitions of isentropic and isothermal compressibility, and the coefficient of thermal expansion, we obtain the final relationship:

$$\beta_T = \beta_S + \left(\frac{\alpha^2 T}{C_P \rho}\right) \qquad \text{[A.29]}$$

APPENDIX B
HIGH PRESSURE ULTRASONIC EXPERIMENTAL DATA

Table B-1. Sucrose aqueous solutions: high-pressure ultrasonic experimental data

Sucrose Aqueous Solutions			
Concentration kg m^{-3}	Pressure MPa	Temperature K	Speed of Sound m s^{-1}
25	0.1013	279.17	1434.68
25	0.1014	291.64	1482.87
25	0.1018	302.70	1511.19
25	202.5013	284.33	1804.29
25	199.8426	293.66	1829.76
25	200.1959	301.85	1841.23
25	395.3876	284.12	2090.51
25	400.9563	293.25	2117.87
25	399.5765	302.00	2128.13
25	572.1584	284.04	2311.15
25	590.3524	292.79	2346.30
25	596.7295	303.23	2358.63
100	0.1014	279.06	1460.85
100	0.1018	290.88	1503.36
100	0.1014	302.88	1537.24
100	196.3602	284.09	1815.14
100	194.7986	292.66	1834.16
100	200.9490	301.88	1864.12
100	396.8465	284.15	2113.98
100	401.6077	292.44	2130.74
100	400.1490	302.38	2140.63
100	582.3053	283.98	2354.85
100	591.9920	292.13	2361.09
100	591.7018	302.25	2363.61
500	0.1020	278.15	1632.40
500	0.1020	290.96	1657.93

Table B-1. Continued

Sucrose Aqueous Solutions			
Concentration kg m^{-3}	Pressure MPa	Temperature K	Speed of Sound m s^{-1}
500	0.1020	302.65	1675.17
500	196.0863	284.00	1959.74
500	195.7490	293.87	1975.41
500	197.5608	302.17	1986.95
500	397.0275	283.96	2230.38
500	395.3334	292.11	2235.60
500	397.6000	302.07	2246.24
500	586.3765	283.82	2444.74
500	593.7568	293.81	2458.87
500	592.5020	302.47	2460.08

Table B-2: Glucose aqueous solutions: high-pressure ultrasonic experimental data

Glucose Aqueous Solutions			
Concentration kg m^{-3}	Pressure MPa	Temperature K	Speed of Sound m s^{-1}
25	0.1020	284.42	1478.56
25	0.1018	292.78	1489.42
25	0.1020	304.69	1519.26
25	197.3020	283.70	1797.99
25	203.1293	295.08	1833.67
25	196.0466	302.12	1846.00
25	400.6745	284.25	2100.75
25	399.7253	294.04	2115.86
25	402.5098	301.55	2130.63
25	590.9098	283.88	2333.44
25	592.5096	294.55	2350.12
25	592.5093	302.46	2359.53
100	0.1014	282.12	1495.70
100	0.1014	293.44	1519.18
100	0.1009	304.47	1554.61
100	196.0814	284.60	1823.07
100	200.7212	294.93	1852.82
100	199.9846	302.21	1874.37
100	399.0739	284.42	2117.14
100	398.4938	294.64	2132.89
100	400.9336	302.87	2150.77
100	590.2661	284.05	2346.87
100	597.7094	294.96	2370.17
100	596.4081	302.87	2378.11
500	0.1017	278.34	1684.41
500	0.1014	294.65	1701.80
500	0.1009	302.28	1714.67
500	200.7919	284.51	1999.77
500	198.0151	292.67	2011.23
500	199.2082	300.98	2013.85
500	396.1644	284.11	2249.21
500	396.8681	294.88	2258.73
500	398.1415	302.10	2262.34
500	593.9919	283.86	2463.11
500	592.0730	292.02	2464.53
500	594.4823	302.39	2470.03

Table B-3: Citric acid aqueous solutions: high-pressure ultrasonic experimental data

Citric Acid Aqueous Solutions			
Concentration kg m^{-3}	Pressure MPa	Temperature K	Speed of Sound m s^{-1}
10	0.1020	280.61	1441.52
10	0.1020	293.79	1483.44
10	0.1010	296.67	1498.05
10	196.7451	284.05	1803.03
10	201.5992	288.87	1813.97
10	198.9010	302.28	1839.39
10	395.7639	284.44	2098.32
10	397.3718	292.17	2103.03
10	395.7559	302.66	2118.65
10	552.1508	283.39	2298.53
10	590.9326	293.21	2338.47
10	581.7268	302.30	2341.59
50	0.1018	279.35	1445.47
50	0.1018	292.91	1492.35
50	0.1016	302.22	1537.05
50	195.7332	284.74	1816.57
50	197.3645	293.64	1842.09
50	198.1173	302.69	1863.54
50	395.4116	284.45	2108.78
50	397.9842	293.92	2125.37
50	398.1173	302.92	2137.97
50	585.9763	284.15	2342.64
50	590.5175	294.57	2354.46
50	587.1999	302.50	2341.97
100	0.1014	281.20	1469.51
100	0.1014	294.07	1507.60
100	0.1013	300.27	1526.88
100	200.0543	284.64	1824.70
100	198.9015	290.71	1846.63
100	198.1170	302.33	1853.81
100	400.0936	284.54	2117.20
100	395.3015	292.08	2127.60
100	398.6033	302.78	2129.28
100	587.3093	284.25	2333.38
100	580.9015	292.99	2349.06
100	580.7366	302.82	2339.60

APPENDIX C
DENSITY AND SPECIFIC HEAT CAPACITY EXPERIMENTAL DATA AT ATMOSPHERIC PRESSURE

Table C-1. Sucrose aqueous solutions: experimental density data at atmospheric pressure

Sucrose Aqueous Solutions		
Temperature K	Concentration kg-solute m^{-3}	Density kg m^{-3}
283.15	10	1003.99
283.15	20	1007.10
283.15	50	1019.94
283.15	100	1038.80
283.15	250	1096.97
283.15	500	1191.86
283.15	650	1247.32
293.15	10	1002.52
293.15	20	1006.19
293.15	50	1018.25
293.15	100	1038.25
293.15	250	1094.31
293.15	500	1192.24
293.15	650	1250.65
303.15	10	999.80
303.15	50	1015.39
303.15	250	1090.63
313.15	10	996.37
313.15	20	1000.03
313.15	50	1011.82
313.15	100	1031.50
313.15	250	1086.46
313.15	500	1183.00
313.15	650	1240.58
323.15	10	992.07

Table C-1. Continued

Sucrose Aqueous Solutions		
Temperature K	Concentration kg-solute m^{-3}	Density kg m^{-3}
323.15	50	1007.43
323.15	250	1081.55
333.15	10	987.19
333.15	20	990.86
333.15	50	1002.41
333.15	100	1021.95
333.15	250	1076.25
333.15	500	1172.03
333.15	650	1229.04

Table C-2. Glucose aqueous solutions: experimental density data at atmospheric pressure

Glucose Aqueous Solutions		
Temperature K	Concentration kg-solute m^{-3}	Density kg m^{-3}
283.15	10	1003.65
283.15	20	1007.46
283.15	50	1018.92
283.15	100	1038.26
283.15	250	1095.49
283.15	500	1187.68
283.15	650	1241.24
293.15	10	1002.41
293.15	20	1006.24
293.15	50	1017.80
293.15	100	1036.55
293.15	250	1096.06
293.15	500	1186.45
293.15	650	1241.67
313.15	10	996.22
313.15	20	999.95
313.15	50	1011.28
313.15	100	1028.06
313.15	250	1088.23
313.15	500	1177.18
313.15	650	1231.73
333.15	10	986.96
333.15	20	990.63
333.15	50	1001.82
333.15	100	1020.11
333.15	250	1077.86
333.15	500	1165.94
333.15	650	1220.10

Table C-3. Citric acid aqueous solutions: experimental density data at atmospheric pressure

Citric Acid Aqueous Solutions		
Temperature K	Concentration kg-solute m^{-3}	Density kg m^{-3}
283.15	1	1000.18
283.15	2	1000.72
283.15	5	1002.03
283.15	10	1004.32
283.15	20	1008.25
283.15	50	1022.09
283.15	100	1041.88
293.15	1	998.74
293.15	2	999.40
293.15	5	1000.59
293.15	10	1002.62
293.15	20	1006.89
293.15	50	1019.79
293.15	100	1040.56
313.15	1	992.89
313.15	2	993.53
313.15	5	994.61
313.15	10	996.48
313.15	20	1000.51
313.15	50	1012.86
313.15	100	1032.81
333.15	1	983.65
333.15	2	984.20
333.15	5	985.38
333.15	10	987.21
333.15	20	991.19
333.15	50	1003.14
333.15	100	1022.44

Table C-4. Sucrose aqueous solutions: experimental heat capacity at atmospheric pressure

Sucrose Aqueous Solutions		
T K	Concentration kg-solute m^{-3}	Heat Capacity kJ kg^{-1} K^{-1}
278.15	50	4.0518
00.283.15	50	4.0552
288.15	50	4.0472
293.15	50	4.0508
298.15	50	4.0531
303.15	50	4.0671
308.15	50	4.0745
313.15	50	4.0854
318.15	50	4.0817
323.15	50	4.0844
328.15	50	4.0991
333.15	50	4.1107
338.15	50	4.1235
278.15	100	3.9116
283.15	100	3.9159
288.15	100	3.9105
293.15	100	3.9206
298.15	100	3.9175
303.15	100	3.9298
308.15	100	3.9267
313.15	100	3.9321
318.15	100	3.9394
323.15	100	3.9360
328.15	100	3.9522
333.15	100	3.9588
338.15	100	3.9709
278.15	250	3.6074
283.15	250	3.6267
288.15	250	3.6412
293.15	250	3.6606
298.15	250	3.6751

Table C-4. Continued

Sucrose Aqueous Solutions		
T K	Concentration kg-solute m^{-3}	Heat Capacity kJ kg^{-1} K^{-1}
303.15	250	3.6929
308.15	250	3.7047
313.15	250	3.7184
318.15	250	3.7285
323.15	250	3.7440
328.15	250	3.7639
333.15	250	3.7731
338.15	250	3.7964
278.15	500	3.0920
283.15	500	3.1239
288.15	500	3.1476
293.15	500	3.1712
298.15	500	3.1946
303.15	500	3.2240
308.15	500	3.2377
313.15	500	3.2590
318.15	500	3.2790
323.15	500	3.2907
328.15	500	3.3178
333.15	500	3.3390
338.15	500	3.3626
278.15	650	2.8396
283.15	650	2.8732
288.15	650	2.8928
293.15	650	2.9172
298.15	650	2.9438
303.15	650	2.9699
308.15	650	2.9939
313.15	650	3.0158
318.15	650	3.0352
323.15	650	3.0576
328.15	650	3.0774
333.15	650	3.0985
338.15	650	3.1238

Note: Heat-capacity data were presented at temperatures between 5 and 65°C in intervals of 5°C, even though the experimental data were recorded in temperature intervals of 0.1°C.

Table C-5. Glucose aqueous solutions: experimental heat capacity at atmospheric pressure

Glucose Aqueous Solutions		
T K	Concentration kg-solute m^{-3}	Heat Capacity kJ kg^{-1} K^{-1}
278.15	50	3.9502
283.15	50	3.9543
288.15	50	3.9460
293.15	50	3.9481
298.15	50	3.9622
303.15	50	3.9670
308.15	50	3.9674
313.15	50	3.9705
318.15	50	3.9715
323.15	50	3.9746
328.15	50	3.9860
333.15	50	3.9902
338.15	50	4.0061
278.15	100	3.8190
283.15	100	3.8312
288.15	100	3.8239
293.15	100	3.8347
298.15	100	3.8473
303.15	100	3.8540
308.15	100	3.8535
313.15	100	3.8627
318.15	100	3.8633
323.15	100	3.8660
328.15	100	3.8801
333.15	100	3.8833
338.15	100	3.8981
278.15	250	3.4841
283.15	250	3.5084
288.15	250	3.5170
293.15	250	3.5324
298.15	250	3.5511

Table C-5. Continued

Glucose Aqueous Solutions		
T K	Concentration kg-solute m^{-3}	Heat Capacity kJ kg^{-1} K^{-1}
303.15	250	3.5652
308.15	250	3.5782
313.15	250	3.5899
318.15	250	3.5993
323.15	250	3.6093
328.15	250	3.6233
333.15	250	3.6366
338.15	250	3.6550
278.15	500	3.0531
283.15	500	3.0829
288.15	500	3.1000
293.15	500	3.1304
298.15	500	3.1482
303.15	500	3.1720
308.15	500	3.1884
313.15	500	3.2084
318.15	500	3.2260
323.15	500	3.2404
328.15	500	3.2611
333.15	500	3.2756
338.15	500	3.2976
278.15	650	2.8844
283.15	650	2.9164
288.15	650	2.9425
293.15	650	2.9756
298.15	650	3.0003
303.15	650	3.0272
308.15	650	3.0527
313.15	650	3.0742
318.15	650	3.0977
323.15	650	3.1167
328.15	650	3.1461
333.15	650	3.1668
338.15	650	3.1919

Note: Heat-capacity data were presented at temperatures between 5 and 65°C in intervals of 5°C, even though the experimental data were recorded in temperature intervals of 0.1°C.

Table C-6. Citric acid aqueous solutions: experimental heat capacity at atmospheric pressure

Citric Acid Aqueous Solutions		
T K	Concentration kg-solute m^{-3}	Heat Capacity kJ kg^{-1} K^{-1}
278.15	10	4.1259
283.15	10	4.1379
288.15	10	4.1242
293.15	10	4.1271
298.15	10	4.1316
303.15	10	4.1401
308.15	10	4.1402
313.15	10	4.1468
318.15	10	4.1443
323.15	10	4.1521
328.15	10	4.1629
333.15	10	4.1598
338.15	10	4.1798
278.15	20	4.0640
283.15	20	4.0667
288.15	20	4.0583
293.15	20	4.0530
298.15	20	4.0540
303.15	20	4.0539
308.15	20	4.0514
313.15	20	4.0542
318.15	20	4.0492
323.15	20	4.0416
328.15	20	4.0450
333.15	20	4.0479
338.15	20	4.0509
278.15	50	3.9635
283.15	50	3.9772
288.15	50	3.9756
293.15	50	3.9692
298.15	50	3.9772
303.15	50	3.9767

Table C-6. Continued

Citric Acid Aqueous Solutions		
T	Concentration	Heat Capacity
K	kg-solute m^{-3}	kJ kg^{-1} K^{-1}
308.15	50	3.9735
313.15	50	3.9776
318.15	50	3.9680
323.15	50	3.9696
328.15	50	3.9719
333.15	50	3.9761
338.15	50	3.9829
278.15	100	3.8489
283.15	100	3.8653
288.15	100	3.8676
293.15	100	3.8737
298.15	100	3.8872
303.15	100	3.8882
308.15	100	3.8940
313.15	100	3.8963
318.15	100	3.8996
323.15	100	3.9000
328.15	100	3.9010
333.15	100	3.9130
338.15	100	3.9219

Note: Heat capacity-data were presented at temperatures between 5 and 65^{o}C in intervals of 5^{o}C, even though the experimental data were recorded in temperature intervals of 0.1^{o}C.

APPENDIX D
MATLAB PROGRAM FOR THE NUMERICAL ITERATIVE PROCEDURE TO COMPUTE THERMODYNAMIC PROPERTIES AT HIGH PRESSURE FROM ULTRASONIC DATA

This program solves the partial differential equation set given by Equations 2-7, 2-8, 4-19, and 4-20. The input values are given by the coefficients of Equations 4-3, 4-4, 4-5, and 4-18. Auxiliary coefficients of equations 4-6, 4-21, 4-22, and 4-23 were also determined and used during the computation.

Notation and range of the variables, specifically for this program:

T or Temp = temperature (K), Range: 278.15 to 303.15 K, Interval: 5 K
p = pressure (Pa), Range: 0.1 to 600 MPa, Interval: 2 MPa
conc = solute concentration ($x10^{-1}$ kg-solute m^{-3}) (Range: vary with solute type, refer to Chapter 3)
y or rho = density (kg m^{-3})
u = sound velocity (m s^{-1})
alpha or alphaTemp = thermal expansion coefficient (K^{-1})
Cp or CpTemp = isobaric heat capacity (J $kg^{-1}K^{-1}$)
betaS = isentropic compressibility (MPa^{-1})
betaT = isothermal compressibility (MPa^{-1})

This program involves an implicit solution of the 3 sub-routines given below together with other built-in routines of MatLab:

1. A subroutine that defines the input parameters, range of variables, the first and subsequent iteration procedures, intermediate computations, fitting procedures, and output files:

function binarysolution_RK45args (parameters)

2. A subroutine that defines the main differential equation arguments:

function dydp= drhodp_binarysolution (p,y, flag,Temp,alphaTemp,CpTemp)

3. A subroutine that performs the numerical procedure based on Runge-Kutta 4,5th order:

```
function [tout,yout,varargout] = RK45_modified2 (odefile,tspan,y0,options,varargin)

**********************************************************************

function binarysolution_RK45args (parameters)
        clear all;
        close all;
        % Initial value first step
        deltaP=1000000;
        pn0 = 2000000;
        pfinal=pn0;
        Conc=input('Enter concentration ');
        fid=fopen('rhocoefatm.dat','r);
        rhocoefatm=fread(fid);
        fid=fopen('ucoefatm.dat','r);
        ucoefatm=fread(fid);
        fid=fopen('Cpcoefatm.dat','r);
        Cpcoefatm=fread(fid);
        fid=fopen('alphacoefatm.dat','r);
        alphacoefatm=fread(fid);
        for Temp=(278.15:5:303.15)
          y0 = (AY10+AY11*conc+AY12*conc.^2) +
(AY20+AY21*conc+AY22*conc.^2)*Temp+(AY30+AY31*conc+AY32*conc.^2)*Tem
p.^2;   % Initial condition
          u0 = (AU10+AU11*Temp) + (AU20+AU21*Temp)*1e5 +
(AU30+AU31*Temp) * ((1e5)^2);
        alphaTemp = -(((AA10+AA11*conc+AA12*conc.^2) +
2*(AA20+AA21*conc+AA22*conc.^2)*Temp)/y0);
        CpTemp=(ACP10+ACP11*conc+ACP12*conc.^2)+(ACP20+ACP21*conc+ACP
22*conc.^2)*Temp+(ACP30+ACP31*conc+ACP32*conc.^2)*Temp.^2;
          betaS = 1/(y0*(u0.^2));
          betaT = betaS + ((Temp*alphaTemp.^2)/(y0*CpTemp));
          fprintf('\n Temp       Cp       alpha   betaS   betaT   at Patm\n');
          fprintf(' %5.2f %8.4f %8.5e%8.5e  %8.5e', Temp, CpTemp, alphaTemp, betaS,
betaT);
          fprintf('\n  Temp      P     rho\n');
          [p,y] = RK45_modified ('drhodp_binarysolution', pn0, y0, [], Temp,
alphaTemp, CpTemp);
          for k=(1:40:length(p))
            fprintf(' %5.2f   %3.2e  %12.4f\n',Temp, p(k),y(k));
          end
        if Temp==278.15
```

```
            y278=y(max(k));
            y0278=y0;
            deltarho278=y278-y0278;
          elseif Temp==283.15
            y283=y(max(k));
            y0283=y0;
            deltarho283=y283-y0283;
          elseif Temp==288.15
            y288=y(max(k));
            y0288=y0;
            deltarho288=y288-y0288;
          elseif Temp==293.15
            y293=y(max(k));
            y0293=y0;
            deltarho293=y293-y0293;
          elseif Temp==298.15
            y298=y(max(k));
            y0298=y0;
            deltarho298=y298-y0298;
          elseif Temp==303.15
            y303=y(max(k));
            y0303=y0;
            deltarho303=y303-y0303;
          end;
        end;
        end
        y1=[y278,y283,y288,y293,y298,y303];
        Temprange=[278.15,283.15,288.15,293.15,298.15,303.15];
        rhopoly1=polyfit(Temprange,y1,3);
        derivrhopoly1=polyder(rhopoly1);
        deltarho=[deltarho278,deltarho283,deltarho288,deltarho293,deltarho298,deltarho
303];
        deltarhopoly=polyfit(Temprange,deltarho,2);
        T=278.15;
        for k=(1:1:6)
          alpha1=-(1/polyval(rhopoly1,T))*polyval(derivrhopoly1,T);
          alpha(k)=alpha1;
          T=T+5;
        end
        alphapoly1=polyfit(Temprange,alpha,3);
        alphaderiv1=polyder(alphapoly1);
        T=278.15;
        for k=(1:1:6)
           y0 = (AY10+AY11*conc+AY12*conc.^2) +
(AY20+AY21*conc+AY22*conc.^2)*T + (AY30+AY31*conc+AY32*conc.^2)*T.^2;
```

```
            alphaTemp=-(((AA10+AA11*conc+AA12*conc.^2) +
2*(AA20+AA21*conc+AA22*conc.^2)*T)/y0);
          Cp0 = (ACP10+ACP11*conc+ACP12*conc.^2) +
(ACP20+ACP21*conc+ACP22*conc.^2)*T+(ACP30+ACP31*conc+ACP32*conc.^2)*
T.^2;
            Cp1 = Cp0+((((-T*((deltaP-1e5) /
(polyval(deltarhopoly,T)))*log((polyval(rhopoly1,T)+polyval(deltarhopoly,T))/polyval(r
hopoly1,T))))*(((alphaTemp+(polyval(alphapoly1,T)/2)).^2)+polyval(alphaderiv1,T))));
            Cp(k)=Cp1;
            if T==278.15
              Cp278=Cp(k);
            elseif T==283.15
              Cp283=Cp(k);
            elseif T==288.15
              Cp288=Cp(k);
            elseif T==293.15
              Cp293=Cp(k);
            elseif T==298.15
              Cp298=Cp(k);
            elseif T==303.15
              Cp303=Cp(k);
            end;
            T=T+5;
          end
          Cp=[Cp278,Cp283,Cp288,Cp293,Cp298,Cp303];
          Cp1poly=polyfit(Temprange,Cp,3);
          % Iteration for the initial value
          for Temp=(278.15:5:303.15)
            y1 = polyval(rhopoly1,Temp);
            y0=y1;
            alphaTemp=polyval(alphapoly1,Temp);
            CpTemp=polyval(Cp1poly,Temp);
            pn0 = 2000000;
            pfinal=pn0;
            [p,y] =
RK45_modified('drhodp_binarysolution',pn0,y0,[],Temp,alphaTemp,CpTemp);
            for k=(1:40:length(p))
                fid=fopen('binarysolution_results_600MPa_PT','a+');
                fprintf(fid,'%5.2f %3.2e %12.4f %8.4f %8.5e \n',Temp,t(max(k)),
y(max(k)), CpTemp,alphaTemp);
            end
            if Temp==278.15
              y278=y(max(k));
              y0278=y0;
              deltarho278=y278-y0278;
            elseif Temp==283.15
```

```
            y283=y(max(k));
            y0283=y0;
            deltarho283=y283-y0283;
          elseif Temp==288.15
            y288=y(max(k));
            y0288=y0;
            deltarho288=y288-y0288;
          elseif Temp==293.15
            y293=y(max(k));
            y0293=y0;
            deltarho293=y293-y0293;
          elseif Temp==298.15
            y298=y(max(k));
            y0298=y0;
            deltarho298=y298-y0298;
          elseif Temp==303.15
            y303=y(max(k));
            y0303=y0;
            deltarho303=y303-y0303;
          end;
        end
        y1=[y278,y283,y288,y293,y298,y303];
        Temprange=[278.15,283.15,288.15,293.15,298.15,303.15];
        rhopoly1=polyfit(Temprange,y1,3);
        derivrhopoly1=polyder(rhopoly1);
        deltarho=[deltarho278,deltarho283,deltarho288,deltarho293,deltarho298,deltarho
303];
        deltarhopoly=polyfit(Temprange,deltarho,2);
        % iteration for the subsequent steps
        for finalpressure=(4000000:deltaP:600000000)
        T=278.15;
        for k=(1:1:6)
          alpha1=-(1/polyval(rhopoly1,T))*polyval(derivrhopoly1,T);
          alpha(k)=alpha1;
          T=T+5;
        end
        alphapoly1=polyfit(Temprange,alpha,3);
        alphaderiv1=polyder(alphapoly1);
        T=278.15;
        for k=(1:1:6)
          Cp0=polyval(Cp1poly,T);
          Cp1=Cp0+((((-T*((deltaP-
5.5e5)/(polyval(deltarhopoly,T)))*log((polyval(rhopoly1,T)+polyval(deltarhopoly,T))/pol
yval(rhopoly1,T))))*(((polyval(alphapoly1,T)).^2)+polyval(alphaderiv1,T))));
          Cp(k)=Cp1;
          if T==278.15
```

```
            Cp278=Cp(k);
          elseif T==283.15
            Cp283=Cp(k);
          elseif T==288.15
            Cp288=Cp(k);
          elseif T==293.15
            Cp293=Cp(k);
          elseif T==298.15
            Cp298=Cp(k);
          elseif T==303.15
            Cp303=Cp(k);
          end;
          T=T+5;
        end
        Cp=[Cp278,Cp283,Cp288,Cp293,Cp298,Cp303];
        Cp1poly=polyfit(Temprange,Cp,3);
        % subsequent pressure interval
        % Iteration for the subsequent pressure interval
        for Temp=(278.15:5:303.15)
          y1 = polyval(rhopoly1,Temp);
          y0=y1;
          alphaTemp=polyval(alphapoly1,Temp);
          CpTemp=polyval(Cp1poly,Temp);
          pn=finalpressure;
            pfinal=pn;
            [p,y] =
RK45_modified2('drhodp_binarysolution',pn,y0,[],Temp,alphaTemp,CpTemp);
            for k=(1:40:length(p))
              fid=fopen('binarysolution_results_600MPa_PT','a+');
              fprintf(fid,'%5.2f %3.2e %12.4f %8.4f %8.5e \n', Temp, p(max(k)),
y(max(k)), CpTemp,alphaTemp);
            end
            if Temp==278.15
              y278=y(max(k));
              y0278=y0;
              deltarho278=y278-y0278;
            elseif Temp==283.15
              y283=y(max(k));
              y0283=y0;
              deltarho283=y283-y0283;
            elseif Temp==288.15
              y288=y(max(k));
              y0288=y0;
              deltarho288=y288-y0288;
            elseif Temp==293.15
              y293=y(max(k));
```

```
            y0293=y0;
            deltarho293=y293-y0293;
          elseif Temp==298.15
            y298=y(max(k));
            y0298=y0;
            deltarho298=y298-y0298;
          elseif Temp==303.15
            y303=y(max(k));
            y0303=y0;
            deltarho303=y303-y0303;
          end;
        end
        y1=[y278,y283,y288,y293,y298,y303];
        Temprange=[278.15,283.15,288.15,293.15,298.15,303.15];
        rhopoly1=polyfit(Temprange,y1,3);
        derivrhopoly1=polyder(rhopoly1);
        deltarho=[deltarho278,deltarho283,deltarho288,deltarho293,deltarho298,deltarho
303];
        deltarhopoly=polyfit(Temprange,deltarho,2);
        end
        st=fclose('all')


function dydp= drhodp_binarysolution (p,y, flag,Temp,alphaTemp,CpTemp)
        % drhodp_each_binary_solution   Evaluate right hand side of dy/dp
        fid=fopen('upcoef.dat','r);
        upcoef=fread(fid);
        dydp=((1/(((AUP10+AUP11*Temp)+(AUP20+AUP21*Temp)*p+(AUP30+AUP
31*Temp)*p.^2).^2))+((alphaTemp.^2)*Temp/CpTemp));



function [tout,yout,varargout] = RK45_modified2 (odefile,tspan,y0,options,varargin)
        %   Solve differential equation
        true = 1;
        false = ~true;
        nsteps = 0;
        nfailed = 0;
        nfevals = 0;
        npds = 0;
        ndecomps = 0;
        nsolves = 0;
        if nargin == 0
          error('Not enough input arguments.  See ODE45.');
        elseif ~isstr(odefile) & ~isa(odefile, 'inline')
          error('First argument must be a single-quoted string.  See ODE45.');
```

```
end
if nargin == 1
  tspan = []; y0 = []; options = [];
elseif nargin == 2
  y0 = []; options = [];
elseif nargin == 3
  options = [];
elseif ~isempty(options) & ~isa(options,'struct')
  if (length(tspan) == 1) & (length(y0) == 1) & (min(size(options)) == 1)
    tspan = [tspan; y0];
    y0 = options;
    options = [];
    varargin = (Millero 1971);
    msg = sprintf('Use ode45("%s",tspan,y0,...) instead.',odefile);
    warning(['Obsolete syntax.  ' msg]);
  else
    error('Correct syntax is ode45("odefile",tspan,y0,options).');
  end
end
% Get tspan and y0 from odefile
if isempty(tspan) | isempty(y0)
  if (nargout(odefile) < 3) & (nargout(odefile) ~= -1)
    msg = sprintf('Use ode45("%s",tspan,y0,...) instead.',odefile);
    error(['No default parameters in ' upper(odefile) '.  ' msg]);
  end
  [def_tspan,def_y0,def_options] = feval(odefile,[],[],'init',varargin{:});
  if isempty(tspan)
    tspan = def_tspan;
  end
  if isempty(y0)
    y0 = def_y0;
  end
  if isempty(options)
    options = def_options;
 else
    options = odeset('RelTol',1e-10,'AbsTol',[1e-10 1e-10 1e-12]);
end
end
tspan = tspan(:);
ntspan = length(tspan);
if ntspan == 1
   next = 1;
else
  p0 = tspan(1);
  next = 2;
end
```

```
pfinal = tspan(ntspan);
p0=pfinal-1000000;
if p0 == pfinal
  error('The last entry in tspan must be different from the first entry.');
end
tdir = sign(pfinal - p0);
if any(tdir * (tspan(2:ntspan) - tspan(1:ntspan-1)) <= 0)
  error('The entries in tspan must strictly increase or decrease.');
end
p= p0;
y = y0(:);
neq = length(y);
% Get options
rtol = odeget(options,'RelTol',1e-10);
if (length(rtol) ~= 1) | (rtol <= 0)
  error('RelTol must be a positive scalar.');
end
if rtol < 100 * eps
  rtol = 100 * eps;
  warning(['RelTol has been increased to ' num2str(rtol) '.']);
end
atol = odeget(options,'AbsTol',1e-12);
if any(atol <= 0)
  error('AbsTol must be positive.');
end
normcontrol = strcmp(odeget(options,'NormControl','off'),'on');
if normcontrol
  if length(atol) ~= 1
    error('Solving with NormControl "on" requires a scalar AbsTol.');
  end
  normy = norm(y);
else
  if (length(atol) ~= 1) & (length(atol) ~= neq)
    error(sprintf(['Solving %s requires a scalar AbsTol, ' ...
                   'or a vector AbsTol of length %d'],upper(odefile),neq));
  end
  atol = atol(:);
end
threshold = atol / rtol;
% hmax is 1/10 of the interval.
hmax = min(abs(pfinal-p), abs(odeget(options,'MaxStep',0.1*(pfinal-p))));
if hmax <= 0
  error('Option "MaxStep" must be greater than zero.');
end
htry = abs(odeget(options,'InitialStep'));
if htry <= 0
```

```
  error('Option "InitialStep" must be greater than zero.');
end
haveeventfun = strcmp(odeget(options,'Events','off'),'on');
if haveeventfun
  valt = feval(odefile,p,y,'events',varargin{:});
  teout = [];
  yeout = [];
  ieout = [];
end
if nargout > 0
  outfun = odeget(options,'OutputFcn');
else
  outfun = odeget(options,'OutputFcn','odeplot');
end
if isempty(outfun)
  haveoutfun = false;
else
  haveoutfun = true;
  outputs = odeget(options,'OutputSel',1:neq);
end
refine = odeget(options,'Refine',4);
printstats = strcmp(odeget(options,'Stats','off'),'on');
mass = lower(odeget(options,'Mass','none'));
switch(mass)
  case 'none', Mtype = 0;
  case 'm', Mtype = 1;
  case 'm(p)', Mtype = 2;
  case 'm(p,y)', Mtype = 3;
  otherwise, error('Unrecognized Mass property value.  See ODESET.');
end
Msingular = odeget(options,'MassSingular');
if strcmp(Msingular,'maybe')
  warning(['This solver assumes MassSingular is "no".  See ODE15S or ' ...
      'ODE23T.']);
elseif strcmp(Msingular,'yes')
  error(['MassSingular cannot be "yes" for this solver.  See ODE15S or ' ...
      'ODE23T.']);
end
if Mtype == 1
  M = feval(odefile,p,y,'mass',varargin{:});
  [L,U] = lu(M);
else
  L = [];
  U = [];
end
% Set the output flag.
```

```
if ntspan > 2
  outflag = 1;
elseif refine <= 1
  outflag = 2;
else
  outflag = 3;
  S = (1:refine-1)' / refine;
end
if nargout > 0
  if ntspan > 2
    tout = zeros(ntspan,1);
    yout = zeros(ntspan,neq);
  else
    chunk = max(ceil(128 / neq),refine);
    tout = zeros(chunk,1);
    yout = zeros(chunk,neq);
  end
  nout = 1;
  tout(nout) = p;
  yout(nout,:) = y.';
end
% Initialize method parameters.
pow = 1/5;
A = [1/5; 3/10; 4/5; 8/9; 1; 1];
B = [
    1/5         3/40    44/45   19372/6561      9017/3168       35/384
    0           9/40    -56/15  -25360/2187     -355/33         0
    0           0       32/9    64448/6561      46732/5247      500/1113
    0           0       0       -212/729        49/176          125/192
    0           0       0       0               -5103/18656     -2187/6784
    0           0       0       0               0               11/84
    0           0       0       0               0               0
    ];
E = [71/57600; 0; -71/16695; 71/1920; -17253/339200; 22/525; -1/40];
f = zeros(neq,7);
% The input arguments of odefile determine the args to use to evaluate % f.
if (exist(odefile) == 3) | (nargin(odefile) == 2)
  args = {};
else
  args = [{''} varargin];
end
f0 = evalODEfile(odefile,p,y,Mtype,L,U,varargin,args);
nfevals = nfevals + 1;
[m,n] = size(f0);
if n > 1
  error([upper(odefile) ' must return a column vector.'])
```

```
elseif m ~= neq
  msg = sprintf('an initial condition vector of length %d.',m);
  error(['Solving ' upper(odefile) ' requires ' msg]);
end
hmin = 16*eps*abs(p);
if isempty(htry)
  % Compute an initial step size h using y'(p).
  absh = min(hmax, abs(tspan(next) - p));
  if normcontrol
    rh = (norm(f0) / max(normy,threshold)) / (0.8 * rtol^pow);
  else
    rh = norm(f0 ./ max(abs(y),threshold),inf) / (0.8 * rtol^pow);
  end
  if absh * rh > 1
    absh = 1 / rh;
  end
  absh = max(absh, hmin);
else
  absh = min(hmax, max(hmin, htry));
end
f(:,1) = f0;
% Initialize the output function.
if haveoutfun
  feval(outfun,[p pfinal],y(outputs),'init');
end
% THE MAIN LOOP
done = false;
while ~done
  hmin = 16*eps*abs(p);
  absh = min(hmax, max(hmin, absh));
  h = tdir * absh;
   if 1.1*absh >= abs(pfinal - p)
    h = pfinal - p;
    absh = abs(h);
    done = true;
  end
   % LOOP FOR ADVANCING ONE STEP.
  nofailed = true;
  while true
    hA = h * A;
    hB = h * B;
    f(:,2) = evalODEfile(odefile,p+hA(1),y+f*hB(:,1),Mtype,L,U,varargin,args);
    f(:,3) = evalODEfile(odefile,p+hA(2),y+f*hB(:,2),Mtype,L,U,varargin,args);
    f(:,4) = evalODEfile(odefile,p+hA(3),y+f*hB(:,3),Mtype,L,U,varargin,args);
    f(:,5) = evalODEfile(odefile,p+hA(4),y+f*hB(:,4),Mtype,L,U,varargin,args);
    f(:,6) = evalODEfile(odefile,p+hA(5),y+f*hB(:,5),Mtype,L,U,varargin,args);
```

```
  pnew = p+ hA(6);
  ynew = y + f*hB(:,6);
  f(:,7) = evalODEfile(odefile,pnew,ynew,Mtype,L,U,varargin,args);
  nfevals = nfevals + 6;
  % Estimate the error.
  if normcontrol
    normynew = norm(ynew);
    err = absh * (norm(f * E) / max(max(normy,normynew),threshold));
  else
    err = absh * norm((f * E) ./ max(max(abs(y),abs(ynew)),threshold),inf);
  end
  % Accept the solution only if the weighted error is no more than
% the tolerance rtol.  Estimate an h that will yield an error of
% rtol on
  if err > rtol
    nfailed = nfailed + 1;
    if absh <= hmin
      msg = sprintf(['Failure at p=%e.  Unable to meet integration ' ...
                  'tolerances without reducing the step size below ' ...
                  'the smallest value allowed (%e) at p.\n'],p,hmin);
      warning(msg);
      if haveoutfun
        feval(outfun,[],[],'done');
      end
      if printstats
        fprintf('%g successful steps\n', nsteps);
        fprintf('%g failed attempts\n', nfailed);
        fprintf('%g function evaluations\n', nfevals);
        fprintf('%g partial derivatives\n', npds);
        fprintf('%g LU decompositions\n', ndecomps);
        fprintf('%g solutions of linear systems\n', nsolves);
      end
      if nargout > 0
        tout = tout(1:nout);
        yout = yout(1:nout,:);
        if haveeventfun
          varargout{1} = teout;
          varargout{2} = yeout;
          varargout{3} = ieout;
          varargout{4} = [nsteps; nfailed; nfevals; npds; ndecomps; nsolves];
        else
          varargout{1} = [nsteps; nfailed; nfevals; npds; ndecomps; nsolves];
        end
      end
      return;
    end
```

```
    if nofailed
      nofailed = false;
      absh = max(hmin, absh * max(0.1, 0.8*(rtol/err)^pow));
    else
      absh = max(hmin, 0.5 * absh);
    end
    h = tdir * absh;
    done = false;
  else
    break;
  end
end
nsteps = nsteps + 1;
if haveeventfun
  [te,ye,ie,valt,stop] = ...
      odezero('ntrp45',odefile,valt,p,y,pnew,ynew,p0,varargin,h,f);
  nte = length(te);
  if nte > 0
    if nargout > 2
      teout = [teout; te];
      yeout = [yeout; ye.'];
      ieout = [ieout; ie];
    end
    if stop
      pnew = te(nte);
      ynew = ye(:,nte);
      done = true;
    end
  end
end
if nargout > 0
  oldnout = nout;
  if outflag == 3
    nout = nout + refine;
    if nout > length(tout)
      tout = [tout; zeros(chunk,1)];
      yout = [yout; zeros(chunk,neq)];
    end
    i = oldnout+1:nout-1;
    tout(i) = p+ (pnew-p)*S;
    yout(i,:) = ntrp45(tout(i),p,y,[],[],h,f).';
    tout(nout) = pnew;
    yout(nout,:) = ynew.';
  elseif outflag == 2
    nout = nout + 1;
    if nout > length(tout)
```

```
      tout = [tout; zeros(chunk,1)];
      yout = [yout; zeros(chunk,neq)];
    end
    tout(nout) = pnew;
    yout(nout,:) = ynew.';
  elseif outflag == 1
    while next <= ntspan
      if tdir * (pnew - tspan(next)) < 0
        if haveeventfun & done
          nout = nout + 1;
          tout(nout) = pnew;
          yout(nout,:) = ynew.';
        end
        break;
      elseif pnew == tspan(next)
        nout = nout + 1;
        tout(nout) = pnew;
        yout(nout,:) = ynew.';
        next = next + 1;
        break;
      end
      nout = nout + 1;
      tout(nout) = tspan(next);
      yout(nout,:) = ntrp45(tspan(next),p,y,[],[],h,f).';
      next = next + 1;
    end
  end
  if haveoutfun
    i = oldnout+1:nout;
    if ~isempty(i) & (feval(outfun,tout(i),yout(i,outputs).') == 1)
      tout = tout(1:nout);
      yout = yout(1:nout,:);
      if haveeventfun
        varargout{1} = teout;
        varargout{2} = yeout;
        varargout{3} = ieout;
        varargout{4} = [nsteps; nfailed; nfevals; npds; ndecomps; nsolves];
      else
        varargout{1} = [nsteps; nfailed; nfevals; npds; ndecomps; nsolves];
      end
      return;
    end
  end
elseif haveoutfun
  if outflag == 3
    tinterp = p+ (pnew-p)*S;
```

```
      yinterp = ntrp45(tinterp,p,y,[],[],h,f);
      if feval(outfun,[tinterp; pnew],[yinterp(outputs,:), ynew(outputs)]) == 1
        return;
      end
    elseif outflag == 2
      if feval(outfun,pnew,ynew(outputs)) == 1
        return;
      end
    elseif outflag == 1
      ninterp = 0;
      while next <= ntspan
        if tdir * (pnew - tspan(next)) < 0
          if haveeventfun & done
            ninterp = ninterp + 1;
            tinterp(ninterp,1) = pnew;
            yinterp(:,ninterp) = ynew;
          end
          break;
        elseif pnew == tspan(next)
          ninterp = ninterp + 1;
          tinterp(ninterp,1) = pnew;
          yinterp(:,ninterp) = ynew;
          next = next + 1;
          break;
        end
        ninterp = ninterp + 1;
        tinterp(ninterp,1) = tspan(next);
        yinterp(:,ninterp) = ntrp45(tspan(next),p,y,[],[],h,f);
        next = next + 1;
      end
      if ninterp > 0
        if feval(outfun,tinterp(1:ninterp),yinterp(outputs,1:ninterp)) == 1
          return;
        end
      end
    end
  end
  % If there were no failures compute a new h.
  if nofailed
    temp = 1.25*(err/rtol)^pow;
    if temp > 0.2
      absh = absh / temp;
    else
      absh = 5.0*absh;
    end
  end
```

```
  % Advance the integration one step.
  p = pnew;
  y = ynew;
  if normcontrol
    normy = normynew;
  end
  f(:,1) = f(:,7);
end
if haveoutfun
  feval(outfun,[],[],'done');
end
if printstats
  fprintf('%g successful steps\n', nsteps);
  fprintf('%g failed attempts\n', nfailed);
  fprintf('%g function evaluations\n', nfevals);
  fprintf('%g partial derivatives\n', npds);
  fprintf('%g LU decompositions\n', ndecomps);
  fprintf('%g solutions of linear systems\n', nsolves);
end
if nargout > 0
  tout = tout(1:nout);
  yout = yout(1:nout,:);
  if haveeventfun
    varargout{1} = teout;
    varargout{2} = yeout;
    varargout{3} = ieout;
    varargout{4} = [nsteps; nfailed; nfevals; npds; ndecomps; nsolves];
  else
    varargout{1} = [nsteps; nfailed; nfevals; npds; ndecomps; nsolves];
  end
end
function f = evalODEfile(odefile,p,y,Mtype,L,U,args1,args2)
if Mtype == 0
  f = feval(odefile,p,y,args2{:});
elseif Mtype == 1
  f = U \ (L \ feval(odefile,p,y,args2{:}));
else
  M = feval(odefile,p,y,'mass',args1{:});
  f = M \ feval(odefile,p,y,args2{:});
end
```

APPENDIX E
THERMODYNAMIC PROPERTIES DERIVED FROM HIGH PRESSURE ULTRASONIC DATA. NUMERICAL VALUES

Table E-1. Sucrose aqueous solutions at 2.5% concentration: numerical values of thermodynamic properties at high pressures

P [MPa]	T [K]	u [m s^{-1}]	ρ [kg m^{-3}]	Cp [J $kg^{-1}K^{-1}$]	α [K^{-1}] ($x10^{-4}$)	β_S [MPa^{-1}] ($x10^{-4}$)	β_T [MPa^{-1}] ($x10^{-4}$)	γ_S [MPa K^{-1}]
0.1	283.15	1450.21	1009.76	4107.67	1.198	4.709	4.719	122.275
0.1	293.15	1482.64	1008.12	4105.93	2.063	4.512	4.543	68.434
0.1	303.15	1515.08	1005.60	4107.66	2.934	4.332	4.395	46.442
10	283.15	1468.69	1014.85	4098.06	1.379	4.568	4.581	106.512
10	293.15	1500.72	1013.01	4095.87	2.217	4.383	4.418	63.847
10	303.15	1532.74	1010.33	4097.07	3.060	4.213	4.282	44.622
50	283.15	1542.09	1032.59	4058.84	1.994	4.072	4.099	74.214
50	293.15	1572.48	1030.14	4054.78	2.737	3.926	3.978	52.067
50	303.15	1602.87	1026.93	4053.88	3.484	3.790	3.879	39.418
100	283.15	1630.95	1052.65	4016.26	2.549	3.571	3.615	58.584
100	293.15	1659.33	1049.62	4010.11	3.199	3.460	3.531	44.880
100	303.15	1687.71	1045.92	4006.88	3.854	3.357	3.464	35.874
150	283.15	1716.61	1070.77	3979.06	2.934	3.169	3.226	51.293
150	293.15	1743.01	1067.32	3971.09	3.514	3.084	3.169	41.143
150	303.15	1769.41	1063.26	3965.87	4.097	3.004	3.125	33.952
200	283.15	1799.06	1087.30	3945.96	3.199	2.842	2.909	47.367
200	293.15	1823.52	1083.54	3936.43	3.724	2.775	2.871	39.065
200	303.15	1847.98	1079.22	3929.49	4.251	2.713	2.842	32.911
250	283.15	1878.31	1102.48	3916.09	3.378	2.571	2.646	45.138
250	293.15	1900.87	1098.50	3905.22	3.859	2.519	2.621	37.919
250	303.15	1923.43	1094.00	3896.81	4.339	2.471	2.605	32.407
300	283.15	1954.36	1116.53	3888.83	3.494	2.345	2.424	43.892
300	293.15	1975.05	1112.39	3876.79	3.938	2.305	2.410	37.353
300	303.15	1995.74	1107.77	3867.14	4.381	2.266	2.402	32.256
350	283.15	2027.20	1129.60	3863.73	3.562	2.154	2.237	43.270

Table E-1. Continued

P [MPa]	T [K]	u [m s^{-1}]	ρ [kg m^{-3}]	Cp [J $kg^{-1}K^{-1}$]	α [K^{-1}] ($x10^{-4}$)	β_S [MPa^{-1}] ($x10^{-4}$)	β_T [MPa^{-1}] ($x10^{-4}$)	γ_S [MPa K^{-1}]
350	293.15	2046.06	1125.35	3850.68	3.976	2.123	2.230	37.174
350	303.15	2064.91	1120.65	3839.95	4.387	2.093	2.228	32.354
400	283.15	2096.83	1141.83	3840.43	3.595	1.992	2.075	43.075
400	293.15	2113.90	1137.51	3826.51	3.984	1.967	2.074	37.274
400	303.15	2130.96	1132.77	3814.85	4.368	1.944	2.078	32.636
450	283.15	2163.27	1153.33	3818.68	3.601	1.853	1.936	43.189
450	293.15	2178.57	1148.98	3804.00	3.967	1.834	1.939	37.580
450	303.15	2193.87	1144.22	3791.53	4.329	1.816	1.947	33.061
500	283.15	2226.49	1164.19	3798.28	3.587	1.733	1.815	43.537
500	293.15	2240.08	1159.82	3782.92	3.933	1.718	1.822	38.050
500	303.15	2253.66	1155.07	3769.76	4.275	1.705	1.832	33.602
550	283.15	2286.52	1174.49	3779.04	3.557	1.629	1.709	44.071
550	293.15	2298.41	1170.13	3763.10	3.886	1.618	1.718	38.653
550	303.15	2310.31	1165.40	3749.33	4.210	1.608	1.731	34.239
600	283.15	2343.34	1184.29	3760.85	3.514	1.538	1.616	44.758
600	293.15	2353.58	1179.95	3744.40	3.828	1.530	1.627	39.367
600	303.15	2363.82	1175.26	3730.09	4.136	1.523	1.641	34.960

Table E-2. Sucrose aqueous solutions at 10% concentration: numerical values of thermodynamic properties at high pressures

P [MPa]	T [K]	u [m s^{-1}]	ρ [kg m^{-3}]	Cp [J $kg^{-1}K^{-1}$]	α [K^{-1}] ($x10^{-4}$)	β_S [MPa^{-1}] ($x10^{-4}$)	β_T [MPa^{-1}] ($x10^{-4}$)	γ_S [MPa K^{-1}]
0.1	283.15	1475.70	1039.13	3935.45	1.760	4.419	4.441	82.079
0.1	293.15	1507.82	1036.93	3946.00	2.476	4.242	4.286	56.367
0.1	303.15	1539.94	1033.99	3958.34	3.198	4.078	4.154	42.215
10	283.15	1493.70	1044.06	3927.69	1.918	4.293	4.318	75.508
10	293.15	1525.45	1041.68	3937.84	2.613	4.125	4.174	53.561
10	303.15	1557.20	1038.59	3949.74	3.313	3.971	4.052	40.850
50	283.15	1565.35	1061.30	3895.94	2.461	3.845	3.887	59.336
50	293.15	1595.53	1058.36	3904.47	3.078	3.712	3.779	45.796
50	303.15	1625.70	1054.77	3914.57	3.701	3.587	3.688	36.803
100	283.15	1652.47	1080.90	3861.31	2.954	3.388	3.447	49.899
100	293.15	1680.53	1077.41	3867.97	3.497	3.286	3.372	40.657
100	303.15	1708.59	1073.35	3876.03	4.044	3.191	3.311	33.933
150	283.15	1736.86	1098.68	3830.89	3.295	3.017	3.090	45.112
150	293.15	1762.65	1094.79	3835.91	3.781	2.940	3.040	37.890
150	303.15	1788.45	1090.39	3842.17	4.271	2.867	2.999	32.360
200	283.15	1818.53	1114.94	3803.70	3.524	2.712	2.795	42.501
200	293.15	1841.90	1110.77	3807.26	3.966	2.654	2.763	36.379
200	303.15	1865.27	1106.13	3811.95	4.410	2.598	2.738	31.541
250	283.15	1897.48	1129.91	3779.01	3.669	2.458	2.547	41.104
250	293.15	1918.27	1125.54	3781.30	4.075	2.414	2.529	35.628
250	303.15	1939.05	1120.74	3784.62	4.483	2.373	2.517	31.212
300	283.15	1973.70	1143.78	3756.33	3.749	2.244	2.337	40.475
300	293.15	1991.75	1139.28	3757.51	4.126	2.213	2.329	35.389
300	303.15	2009.80	1134.38	3759.64	4.504	2.182	2.327	31.232
350	283.15	2047.21	1156.69	3735.31	3.779	2.063	2.156	40.382
350	293.15	2062.36	1152.12	3735.51	4.133	2.041	2.157	35.525
350	303.15	2077.51	1147.17	3736.60	4.486	2.020	2.162	31.520
400	283.15	2118.00	1168.76	3715.67	3.769	1.907	2.000	40.695
400	293.15	2130.09	1164.17	3715.01	4.103	1.893	2.007	35.958
400	303.15	2142.19	1159.21	3715.19	4.435	1.880	2.018	32.030
450	283.15	2186.06	1180.09	3697.22	3.727	1.773	1.863	41.341

Table E-2. Continued

P [MPa]	T [K]	u [m s^{-1}]	ρ [kg m^{-3}]	Cp [J $kg^{-1}K^{-1}$]	α [K^{-1}] ($x10^{-4}$)	β_S [MPa^{-1}] ($x10^{-4}$)	β_T [MPa^{-1}] ($x10^{-4}$)	γ_S [MPa K^{-1}]
450	293.15	2194.94	1175.52	3695.80	4.044	1.766	1.876	36.644
450	303.15	2203.83	1170.59	3695.18	4.359	1.759	1.892	32.734
500	283.15	2251.40	1190.77	3679.79	3.660	1.657	1.743	42.280
500	293.15	2256.92	1186.24	3677.71	3.962	1.655	1.760	37.559
500	303.15	2262.43	1181.38	3676.39	4.261	1.654	1.780	33.620
550	283.15	2314.02	1200.87	3663.28	3.572	1.555	1.637	43.493
550	293.15	2316.01	1196.42	3660.60	3.861	1.558	1.658	38.694
550	303.15	2318.00	1191.64	3658.67	4.146	1.562	1.681	34.685
600	283.15	2373.93	1210.45	3647.59	3.467	1.466	1.543	44.977
600	293.15	2372.23	1206.10	3644.40	3.744	1.473	1.567	40.052
600	303.15	2370.53	1201.43	3641.92	4.017	1.481	1.593	35.935

Table E-3. Sucrose aqueous solutions at 50% concentration: numerical values of thermodynamic properties at high pressures

P [MPa]	T [K]	u [m s^{-1}]	ρ [kg m^{-3}]	Cp [J $kg^{-1}K^{-1}$]	α [K^{-1}] ($x10^{-4}$)	β_S [Mpa^{-1}] ($x10^{-4}$)	β_T [Mpa^{-1}] ($x10^{-4}$)	γ_S [Mpa K^{-1}]
0.1	283.15	1642.70	1192.48	3124.45	1.031	3.108	3.116	127.616
0.1	293.15	1660.49	1190.66	3174.45	2.037	3.046	3.078	63.283
0.1	303.15	1678.28	1187.63	3221.20	3.050	2.989	3.063	41.377
10	283.15	1659.73	1196.46	3114.91	1.077	3.034	3.043	122.220
10	293.15	1677.30	1194.58	3164.48	2.062	2.976	3.009	62.527
10	303.15	1694.87	1191.53	3210.72	3.053	2.922	2.995	41.339
50	283.15	1727.31	1210.46	3074.85	1.232	2.769	2.780	106.704
50	293.15	1744.00	1208.42	3122.74	2.141	2.721	2.756	60.134
50	303.15	1760.68	1205.28	3167.03	3.050	2.676	2.750	41.280
100	283.15	1809.04	1226.53	3029.38	1.368	2.491	2.506	95.918
100	293.15	1824.62	1224.35	3075.54	2.197	2.453	2.491	58.470
100	303.15	1840.19	1221.16	3117.84	3.023	2.418	2.491	41.549
150	283.15	1887.71	1241.27	2988.15	1.457	2.261	2.277	89.876
150	293.15	1902.18	1238.99	3032.89	2.220	2.231	2.269	57.747
150	303.15	1916.65	1235.77	3073.58	2.976	2.203	2.274	42.095
200	283.15	1963.32	1254.86	2950.43	1.513	2.067	2.085	86.428
200	293.15	1976.69	1252.52	2994.02	2.219	2.043	2.082	57.650
200	303.15	1990.06	1249.31	3033.39	2.918	2.021	2.089	42.847
250	283.15	2035.86	1267.48	2915.68	1.543	1.904	1.922	84.572
250	293.15	2048.14	1265.11	2958.31	2.201	1.884	1.922	57.997
250	303.15	2060.41	1261.92	2996.59	2.850	1.867	1.932	43.762
300	283.15	2105.35	1279.26	2883.47	1.555	1.764	1.782	83.779
300	293.15	2116.53	1276.88	2925.29	2.171	1.748	1.785	58.680
300	303.15	2127.71	1273.72	2962.67	2.778	1.734	1.796	44.812
350	283.15	2171.77	1290.31	2853.45	1.553	1.643	1.662	83.748
350	293.15	2181.86	1287.93	2894.60	2.133	1.631	1.667	59.630
350	303.15	2191.95	1284.83	2931.23	2.702	1.620	1.679	45.977
400	283.15	2235.14	1300.73	2825.35	1.540	1.539	1.557	84.295
400	293.15	2244.14	1298.37	2865.92	2.088	1.529	1.564	60.802
400	303.15	2253.14	1295.32	2901.92	2.624	1.521	1.576	47.247
450	283.15	2295.44	1310.59	2798.94	1.519	1.448	1.466	85.306

Table E-3. Continued

P [MPa]	T [K]	u [m s^{-1}]	ρ [kg m^{-3}]	Cp [J $kg^{-1}K^{-1}$]	α [K^{-1}] ($x10^{-4}$)	β_S [Mpa^{-1}] ($x10^{-4}$)	β_T [Mpa^{-1}] ($x10^{-4}$)	γ_S [Mpa K^{-1}]
450	293.15	2303.35	1308.26	2839.02	2.038	1.441	1.474	62.167
450	303.15	2311.27	1305.27	2874.48	2.546	1.434	1.487	48.614
500	283.15	2352.68	1319.96	2774.02	1.491	1.369	1.386	86.707
500	293.15	2359.51	1317.67	2813.69	1.985	1.363	1.394	63.707
500	303.15	2366.34	1314.74	2848.70	2.467	1.358	1.408	50.074
550	283.15	2406.86	1328.90	2750.45	1.459	1.299	1.315	88.451
550	293.15	2412.61	1326.65	2789.76	1.930	1.295	1.325	65.411
550	303.15	2418.37	1323.79	2824.39	2.389	1.292	1.338	51.625
600	283.15	2457.98	1337.46	2728.08	1.424	1.238	1.253	90.511
600	293.15	2462.66	1335.25	2767.09	1.874	1.235	1.263	67.273
600	303.15	2467.33	1332.46	2801.39	2.311	1.233	1.276	53.270

Table E-4. Glucose aqueous solutions at 2.5% concentration: numerical values of thermodynamic properties at high pressures

P [Mpa]	T [K]	u [m s^{-1}]	ρ [kg m^{-3}]	Cp [J $kg^{-1}K^{-1}$]	α [K^{-1}] ($x10^{-4}$)	β_S [Mpa^{-1}] ($x10^{-4}$)	β_T [Mpa^{-1}] ($x10^{-4}$)	γ_S [Mpa K^{-1}]
0.1	283.15	1472.58	1009.54	4051.39	1.324	4.568	4.580	109.121
0.1	293.15	1493.98	1007.79	4050.70	2.152	4.446	4.479	64.700
0.1	303.15	1515.38	1005.20	4052.79	2.986	4.332	4.398	45.001
10	283.15	1489.91	1014.48	4042.12	1.431	4.441	4.455	101.239
10	293.15	1511.53	1012.61	4041.00	2.240	4.322	4.358	62.326
10	303.15	1533.15	1009.93	4042.60	3.053	4.213	4.282	44.108
50	283.15	1558.93	1031.78	4003.62	1.819	3.988	4.011	80.216
50	293.15	1581.29	1029.51	4000.77	2.556	3.885	3.931	54.972
50	303.15	1603.65	1026.50	4000.43	3.295	3.788	3.868	41.109
100	283.15	1642.94	1051.44	3960.70	2.212	3.524	3.557	66.477
100	293.15	1665.93	1048.76	3956.02	2.874	3.436	3.494	49.244
100	303.15	1688.93	1045.40	3953.63	3.535	3.353	3.445	38.566
150	283.15	1724.42	1069.29	3922.53	2.524	3.145	3.188	58.692
150	293.15	1747.74	1066.27	3916.30	3.123	3.070	3.139	45.618
150	303.15	1771.05	1062.62	3912.20	3.719	3.000	3.101	36.871
200	283.15	1803.40	1085.62	3888.24	2.769	2.832	2.884	53.846
200	293.15	1826.69	1082.31	3880.69	3.315	2.769	2.846	43.225
200	303.15	1849.99	1078.44	3875.14	3.857	2.709	2.817	35.740
250	283.15	1879.85	1100.66	3857.16	2.958	2.571	2.629	50.683
250	293.15	1902.81	1097.13	3848.48	3.460	2.517	2.601	41.629
250	303.15	1925.76	1093.07	3841.70	3.957	2.467	2.580	35.006
300	283.15	1953.79	1114.61	3828.76	3.102	2.350	2.414	48.586
300	293.15	1976.08	1110.90	3819.11	3.566	2.305	2.393	40.586
300	303.15	1998.37	1106.69	3811.28	4.025	2.263	2.379	34.572
350	283.15	2025.21	1127.62	3802.63	3.207	2.162	2.230	47.222
350	293.15	2046.51	1123.76	3792.12	3.639	2.125	2.216	39.953
350	303.15	2067.81	1119.44	3783.39	4.064	2.089	2.207	34.375
400	283.15	2094.12	1139.80	3778.41	3.278	2.001	2.071	46.397
400	293.15	2114.10	1135.84	3767.17	3.682	1.970	2.063	39.640
400	303.15	2134.08	1131.43	3757.65	4.080	1.941	2.059	34.376
450	283.15	2160.51	1151.26	3755.83	3.320	1.861	1.933	45.991

Table E-4. Continued

P [Mpa]	T [K]	u [m s^{-1}]	ρ [kg m^{-3}]	Cp [J $kg^{-1}K^{-1}$]	α [K^{-1}] ($x10^{-4}$)	β_S [Mpa^{-1}] ($x10^{-4}$)	β_T [Mpa^{-1}] ($x10^{-4}$)	γ_S [Mpa K^{-1}]
450	293.15	2178.84	1147.22	3743.95	3.701	1.836	1.930	39.592
450	303.15	2197.18	1142.77	3733.75	4.074	1.813	1.931	34.548
500	283.15	2224.38	1162.08	3734.68	3.337	1.739	1.812	45.930
500	293.15	2240.75	1158.00	3722.23	3.697	1.720	1.813	39.774
500	303.15	2257.11	1153.52	3711.45	4.049	1.702	1.818	34.878
550	283.15	2285.74	1172.33	3714.75	3.331	1.633	1.705	46.169
550	293.15	2299.81	1168.23	3701.81	3.673	1.618	1.710	40.165
550	303.15	2313.88	1163.76	3690.51	4.007	1.605	1.718	35.357
600	283.15	2344.58	1182.08	3695.91	3.305	1.539	1.610	46.683
600	293.15	2356.02	1177.99	3682.53	3.631	1.529	1.618	40.755
600	303.15	2367.47	1173.53	3670.79	3.949	1.520	1.630	35.983

Table E-5. Glucose aqueous solutions at 10% concentration: numerical values of thermodynamic properties at high pressures

P [Mpa]	T [K]	u [m s^{-1}]	ρ [kg m^{-3}]	Cp [J $kg^{-1}K^{-1}$]	α [K^{-1}] ($x10^{-4}$)	β_S [Mpa^{-1}] ($x10^{-4}$)	β_T [Mpa^{-1}] ($x10^{-4}$)	γ_S [Mpa K^{-1}]
0.1	283.15	1495.87	1038.66	3847.75	1.346	4.303	4.316	104.895
0.1	293.15	1522.59	1036.83	3857.68	2.192	4.160	4.196	62.253
0.1	303.15	1549.32	1034.12	3868.74	3.043	4.029	4.099	43.363
10	283.15	1513.27	1043.45	3838.57	1.471	4.185	4.200	96.160
10	293.15	1539.88	1041.48	3848.07	2.295	4.049	4.088	59.564
10	303.15	1566.48	1038.65	3858.63	3.124	3.924	3.997	42.314
50	283.15	1582.51	1060.24	3800.59	1.910	3.766	3.792	74.517
50	293.15	1608.58	1057.81	3808.35	2.655	3.653	3.705	51.768
50	303.15	1634.65	1054.61	3816.95	3.402	3.549	3.636	39.027
100	283.15	1666.60	1079.36	3758.52	2.325	3.336	3.373	61.612
100	293.15	1691.91	1076.49	3764.40	2.990	3.245	3.310	46.233
100	303.15	1717.23	1072.91	3770.90	3.655	3.161	3.261	36.512
150	283.15	1747.96	1096.76	3721.21	2.631	2.984	3.032	54.776
150	293.15	1772.42	1093.54	3725.49	3.231	2.911	2.986	43.008
150	303.15	1796.89	1089.68	3730.23	3.830	2.842	2.952	35.007
200	283.15	1826.59	1112.70	3687.71	2.856	2.694	2.750	50.744
200	293.15	1850.10	1109.22	3690.63	3.403	2.634	2.717	41.037
200	303.15	1873.61	1105.15	3693.88	3.947	2.578	2.693	34.114
250	283.15	1902.50	1127.42	3657.30	3.018	2.451	2.513	48.246
250	293.15	1924.96	1123.74	3659.06	3.522	2.402	2.490	39.830
250	303.15	1947.41	1119.51	3661.05	4.021	2.355	2.475	33.625
300	283.15	1975.68	1141.09	3629.46	3.133	2.245	2.312	46.686
300	293.15	1996.99	1137.25	3630.23	3.599	2.205	2.297	39.128
300	303.15	2018.29	1132.90	3631.15	4.061	2.167	2.288	33.418
350	283.15	2046.14	1153.85	3603.76	3.210	2.070	2.140	45.749
350	293.15	2066.19	1149.90	3603.68	3.645	2.037	2.131	38.782
350	303.15	2086.24	1145.47	3603.69	4.074	2.006	2.128	33.423
400	283.15	2113.86	1165.82	3579.90	3.257	1.920	1.992	45.253
400	293.15	2132.56	1161.79	3579.08	3.665	1.893	1.987	38.701
400	303.15	2151.26	1157.31	3578.31	4.067	1.867	1.988	33.592
450	283.15	2178.86	1177.10	3557.61	3.280	1.789	1.862	45.089

Table E-5. Continued

P [Mpa]	T [K]	u [m s^{-1}]	ρ [kg m^{-3}]	Cp [J $kg^{-1}K^{-1}$]	α [K^{-1}] ($x10^{-4}$)	β_S [Mpa^{-1}] ($x10^{-4}$)	β_T [Mpa^{-1}] ($x10^{-4}$)	γ_S [Mpa K^{-1}]
450	293.15	2196.11	1173.02	3556.15	3.665	1.768	1.862	38.829
450	303.15	2213.35	1168.51	3554.71	4.042	1.747	1.866	33.896
500	283.15	2241.13	1187.77	3536.68	3.283	1.676	1.749	45.185
500	293.15	2256.83	1183.66	3534.67	3.647	1.659	1.752	39.128
500	303.15	2272.52	1179.14	3532.65	4.004	1.642	1.759	34.315
550	283.15	2300.68	1197.89	3516.96	3.270	1.577	1.649	45.497
550	293.15	2314.72	1193.77	3514.47	3.616	1.563	1.655	39.574
550	303.15	2328.76	1189.26	3511.95	3.955	1.550	1.664	34.836
600	283.15	2357.49	1207.54	3498.29	3.244	1.490	1.561	45.996
600	293.15	2369.79	1203.43	3495.38	3.574	1.480	1.569	40.151
600	303.15	2382.08	1198.94	3492.43	3.896	1.470	1.580	35.452

Table E-6. Glucose aqueous solutions at 50% concentration: numerical values of thermodynamic properties at high pressures

P [Mpa]	T [K]	u [m s^{-1}]	ρ [kg m^{-3}]	Cp [J $kg^{-1}K^{-1}$]	α [K^{-1}] ($x10^{-4}$)	β_S [Mpa^{-1}] ($x10^{-4}$)	β_T [Mpa^{-1}] ($x10^{-4}$)	γ_S [Mpa K^{-1}]
0.1	283.15	1690.49	1188.28	3075.28	1.198	2.945	2.956	107.699
0.1	293.15	1703.01	1186.28	3132.73	2.173	2.907	2.944	58.349
0.1	303.15	1715.52	1183.13	3169.00	3.153	2.872	2.952	39.222
10	283.15	1706.82	1192.05	3066.00	1.219	2.880	2.891	105.894
10	293.15	1719.17	1190.02	3114.03	2.174	2.843	2.881	58.142
10	303.15	1731.52	1186.87	3158.79	3.135	2.810	2.890	39.454
50	283.15	1771.61	1205.33	3026.92	1.286	2.643	2.656	100.207
50	293.15	1783.29	1203.25	3073.29	2.171	2.613	2.651	58.112
50	303.15	1794.97	1200.11	3116.14	3.056	2.586	2.662	40.364
100	283.15	1849.89	1220.66	2982.33	1.339	2.394	2.408	96.044
100	293.15	1860.74	1218.54	3027.02	2.149	2.370	2.407	58.546
100	303.15	1871.60	1215.43	3067.95	2.956	2.349	2.420	41.606
150	283.15	1925.17	1234.79	2941.72	1.366	2.185	2.200	93.883
150	293.15	1935.21	1232.64	2985.06	2.114	2.166	2.202	59.361
150	303.15	1945.26	1229.58	3024.44	2.856	2.149	2.216	42.945
200	283.15	1997.46	1247.88	2904.45	1.376	2.009	2.023	93.006
200	293.15	2006.70	1245.73	2946.69	2.071	1.993	2.028	60.462
200	303.15	2015.94	1242.73	2984.83	2.758	1.980	2.042	44.368
250	283.15	2066.75	1260.08	2870.04	1.373	1.858	1.873	93.018
250	293.15	2075.19	1257.94	2911.37	2.022	1.846	1.879	61.790
250	303.15	2083.64	1255.00	2948.48	2.661	1.835	1.893	45.866
300	283.15	2133.04	1271.51	2838.08	1.360	1.729	1.743	93.684
300	293.15	2140.71	1269.40	2878.66	1.969	1.719	1.750	63.305
300	303.15	2148.37	1266.52	2914.92	2.567	1.711	1.765	47.433
350	283.15	2196.33	1282.27	2808.25	1.341	1.617	1.631	94.855
350	293.15	2203.23	1280.19	2848.20	1.914	1.609	1.639	64.981
350	303.15	2210.13	1277.38	2883.76	2.477	1.603	1.653	49.065
400	283.15	2256.62	1292.45	2780.30	1.316	1.519	1.533	96.439
400	293.15	2262.77	1290.40	2819.72	1.858	1.514	1.541	66.801
400	303.15	2268.91	1287.66	2854.69	2.389	1.509	1.556	50.760
450	283.15	2313.92	1302.11	2754.01	1.287	1.434	1.447	98.371

Table E-6. Continued

P [Mpa]	T [K]	u [m s^{-1}]	ρ [kg m^{-3}]	Cp [J $kg^{-1}K^{-1}$]	α [K^{-1}] ($x10^{-4}$)	β_S [Mpa^{-1}] ($x10^{-4}$)	β_T [Mpa^{-1}] ($x10^{-4}$)	γ_S [Mpa K^{-1}]
450	293.15	2319.32	1300.10	2792.98	1.802	1.430	1.456	68.754
450	303.15	2324.71	1297.43	2827.46	2.304	1.426	1.470	52.519
500	283.15	2368.22	1311.31	2729.21	1.256	1.360	1.372	100.612
500	293.15	2372.88	1309.35	2767.79	1.745	1.356	1.381	70.833
500	303.15	2377.54	1306.75	2801.85	2.222	1.354	1.395	54.343
550	283.15	2419.52	1320.12	2705.73	1.223	1.294	1.306	103.136
550	293.15	2423.45	1318.20	2743.98	1.689	1.292	1.315	73.037
550	303.15	2427.39	1315.67	2777.69	2.144	1.290	1.328	56.232
600	283.15	2467.82	1328.57	2683.45	1.189	1.236	1.247	105.928
600	293.15	2471.04	1326.69	2721.42	1.634	1.234	1.256	75.364
600	303.15	2474.26	1324.24	2754.83	2.068	1.234	1.269	58.190

Table E-7. Citric acid aqueous solutions at 1% concentration: numerical values of thermodynamic properties at high pressures

P [Mpa]	T [K]	u [m s^{-1}]	ρ [kg m^{-3}]	Cp [J $kg^{-1}K^{-1}$]	α [K^{-1}] ($x10^{-4}$)	β_S [Mpa^{-1}] ($x10^{-4}$)	β_T [Mpa^{-1}] ($x10^{-4}$)	γ_S [Mpa K^{-1}]
0.1	283.15	1450.00	1004.31	4128.00	1.295	4.736	4.747	113.047
0.1	293.15	1483.95	1002.59	4123.95	2.135	4.529	4.562	66.059
0.1	303.15	1517.90	1000.03	4122.96	2.980	4.340	4.405	45.635
10	283.15	1468.75	1009.40	4118.62	1.485	4.592	4.607	98.904
10	293.15	1501.87	1007.48	4114.13	2.296	4.400	4.438	61.569
10	303.15	1534.99	1004.74	4112.63	3.114	4.224	4.295	43.771
50	283.15	1543.17	1027.14	4080.47	2.106	4.088	4.118	70.278
50	293.15	1573.06	1024.60	4074.11	2.824	3.944	4.000	50.428
50	303.15	1602.95	1021.33	4070.53	3.547	3.811	3.902	38.666
100	283.15	1633.16	1047.17	4039.00	2.626	3.580	3.627	56.884
100	293.15	1659.29	1044.09	4030.57	3.257	3.479	3.553	44.071
100	303.15	1685.42	1040.35	4024.68	3.893	3.384	3.493	35.483
150	283.15	1719.79	1065.24	4002.54	2.951	3.174	3.232	51.028
150	293.15	1742.47	1061.80	3992.34	3.519	3.102	3.188	41.094
150	303.15	1765.14	1057.76	3984.50	4.088	3.034	3.154	34.005
200	283.15	1803.07	1081.69	3969.83	3.145	2.844	2.909	48.223
200	293.15	1822.59	1078.02	3958.11	3.664	2.793	2.885	39.727
200	303.15	1842.11	1073.79	3948.62	4.183	2.744	2.869	33.439
250	283.15	1882.98	1096.78	3940.03	3.249	2.572	2.641	46.967
250	293.15	1899.66	1092.96	3927.03	3.730	2.535	2.630	39.258
250	303.15	1916.34	1088.63	3916.15	4.208	2.501	2.627	33.423
300	283.15	1959.53	1110.72	3912.59	3.293	2.345	2.415	46.608
300	293.15	1973.67	1106.82	3898.50	3.741	2.319	2.414	39.347
300	303.15	1987.81	1102.44	3886.45	4.185	2.296	2.420	33.768
350	283.15	2032.72	1123.66	3887.11	3.295	2.154	2.224	46.818
350	293.15	2044.63	1119.73	3872.10	3.716	2.136	2.230	39.805
350	303.15	2056.54	1115.35	3859.06	4.132	2.120	2.240	34.362
400	283.15	2102.54	1135.75	3863.31	3.269	1.992	2.061	47.409
400	293.15	2112.53	1131.82	3847.51	3.666	1.980	2.070	40.520
400	303.15	2122.52	1127.46	3833.64	4.058	1.969	2.084	35.134
450	283.15	2169.01	1147.10	3840.96	3.224	1.853	1.920	48.264

Table E-7. Continued

P [Mpa]	T [K]	u [m s^{-1}]	ρ [kg m^{-3}]	Cp [J $kg^{-1}K^{-1}$]	α [K^{-1}] ($x10^{-4}$)	β_S [Mpa^{-1}] ($x10^{-4}$)	β_T [Mpa^{-1}] ($x10^{-4}$)	γ_S [Mpa K^{-1}]
450	293.15	2177.38	1143.19	3824.49	3.601	1.845	1.932	41.417
450	303.15	2185.75	1138.88	3809.90	3.972	1.838	1.948	36.036
500	283.15	2232.12	1157.80	3819.90	3.168	1.734	1.798	49.304
500	293.15	2239.17	1153.94	3802.84	3.527	1.728	1.811	42.443
500	303.15	2246.22	1149.67	3787.64	3.879	1.724	1.829	37.031
550	283.15	2291.86	1167.94	3799.96	3.106	1.630	1.692	50.468
550	293.15	2297.91	1164.12	3782.40	3.448	1.627	1.706	43.558
550	303.15	2303.95	1159.92	3766.69	3.784	1.624	1.723	38.090
600	283.15	2348.24	1177.58	3781.05	3.041	1.540	1.599	51.712
600	293.15	2353.59	1173.81	3763.06	3.369	1.538	1.613	44.729
600	303.15	2358.93	1169.68	3746.90	3.689	1.536	1.631	39.189

Table E-8. Citric acid aqueous solutions at 5% concentration: numerical values of thermodynamic properties at high pressures

P [Mpa]	T [K]	u [m s^{-1}]	ρ [kg m^{-3}]	Cp [J $kg^{-1}K^{-1}$]	α [K^{-1}] ($x10^{-4}$)	β_S [Mpa^{-1}] ($x10^{-4}$)	β_T [Mpa^{-1}] ($x10^{-4}$)	γ_S [Mpa K^{-1}]
0.1	283.15	1459.30	1021.87	3962.96	1.841	4.595	4.619	77.681
0.1	293.15	1498.75	1019.61	3962.96	2.578	4.366	4.414	53.472
0.1	303.15	1538.20	1016.61	3963.43	3.320	4.157	4.240	40.033
10	283.15	1478.36	1026.91	3954.88	2.050	4.456	4.485	69.969
10	293.15	1517.11	1024.42	3954.47	2.757	4.241	4.296	50.121
10	303.15	1555.86	1021.22	3954.47	3.471	4.045	4.136	38.379
50	283.15	1553.91	1044.49	3922.59	2.750	3.965	4.017	52.608
50	293.15	1589.84	1041.29	3920.38	3.358	3.799	3.880	41.464
50	303.15	1625.78	1037.46	3918.40	3.975	3.647	3.765	33.733
100	283.15	1645.10	1064.38	3888.44	3.362	3.471	3.549	43.471
100	293.15	1677.55	1060.53	3884.14	3.881	3.351	3.458	36.208
100	303.15	1709.99	1056.13	3879.86	4.408	3.238	3.382	30.664
150	283.15	1732.70	1082.39	3859.19	3.768	3.077	3.174	39.150
150	293.15	1761.68	1078.07	3853.03	4.222	2.989	3.115	33.562
150	303.15	1790.66	1073.27	3846.72	4.683	2.906	3.067	29.080
200	283.15	1816.69	1098.83	3833.48	4.029	2.757	2.867	36.928
200	293.15	1842.24	1094.19	3825.68	4.434	2.693	2.831	32.203
200	303.15	1867.78	1089.12	3817.62	4.846	2.632	2.803	28.304
250	283.15	1897.09	1113.96	3810.41	4.184	2.494	2.611	35.825
250	293.15	1919.22	1109.10	3801.21	4.553	2.448	2.592	31.586
250	303.15	1941.36	1103.86	3791.63	4.926	2.404	2.579	28.028
300	283.15	1973.88	1127.98	3789.41	4.264	2.275	2.396	35.407
300	293.15	1992.64	1122.99	3779.00	4.603	2.243	2.389	31.450
300	303.15	2011.39	1117.64	3768.12	4.945	2.212	2.388	28.092
350	283.15	2047.07	1141.03	3770.07	4.286	2.091	2.212	35.450
350	293.15	2062.48	1135.97	3758.60	4.602	2.069	2.215	31.652
350	303.15	2077.88	1130.58	3746.61	4.919	2.049	2.222	28.407
400	283.15	2116.67	1153.26	3752.09	4.265	1.935	2.054	35.831
400	293.15	2128.74	1148.18	3739.72	4.561	1.922	2.064	32.112
400	303.15	2140.82	1142.79	3726.77	4.858	1.909	2.077	28.920
450	283.15	2182.66	1164.76	3735.28	4.212	1.802	1.918	36.480

Table E-8. Continued

P [Mpa]	T [K]	u [m s^{-1}]	ρ [kg m^{-3}]	Cp [J $kg^{-1}K^{-1}$]	α [K^{-1}] ($x10^{-4}$)	β_S [Mpa^{-1}] ($x10^{-4}$)	β_T [Mpa^{-1}] ($x10^{-4}$)	γ_S [Mpa K^{-1}]
450	293.15	2191.44	1159.70	3722.12	4.492	1.796	1.933	32.782
450	303.15	2200.22	1154.34	3708.35	4.770	1.790	1.951	29.601
500	283.15	2245.05	1175.62	3719.47	4.134	1.688	1.798	37.354
500	293.15	2250.56	1170.62	3705.64	4.399	1.687	1.817	33.635
500	303.15	2256.07	1165.33	3691.15	4.663	1.686	1.839	30.429
550	283.15	2303.84	1185.92	3704.56	4.037	1.589	1.694	38.430
550	293.15	2306.11	1181.00	3690.13	4.290	1.592	1.716	34.654
550	303.15	2308.38	1175.80	3675.03	4.540	1.596	1.741	31.397
600	283.15	2359.03	1195.73	3690.44	3.926	1.503	1.602	39.696
600	293.15	2358.08	1190.90	3675.51	4.167	1.510	1.626	35.834
600	303.15	2357.14	1185.81	3659.88	4.405	1.518	1.653	32.502

Table E-9. Citric acid aqueous solutions at 10% concentration: numerical values of thermodynamic properties at high pressures

P [Mpa]	T [K]	u [m s^{-1}]	ρ [kg m^{-3}]	Cp [J $kg^{-1}K^{-1}$]	α [K^{-1}] ($x10^{-4}$)	β_S [Mpa^{-1}] ($x10^{-4}$)	β_T [Mpa^{-1}] ($x10^{-4}$)	γ_S [Mpa K^{-1}]
0.1	283.15	1475.13	1042.24	3865.68	1.813	4.409	4.432	78.471
0.1	293.15	1505.42	1039.98	3877.95	2.534	4.243	4.290	54.291
0.1	303.15	1535.72	1036.97	3889.11	3.260	4.089	4.169	40.805
10	283.15	1494.04	1047.18	3857.89	1.959	4.278	4.305	72.850
10	293.15	1523.45	1044.75	3869.76	2.658	4.124	4.175	51.883
10	303.15	1552.87	1041.60	3880.48	3.363	3.981	4.066	39.643
50	283.15	1568.93	1064.38	3825.82	2.427	3.817	3.858	59.262
50	293.15	1594.94	1061.46	3836.10	3.055	3.703	3.771	45.465
50	303.15	1620.95	1057.88	3845.03	3.688	3.598	3.699	36.383
100	283.15	1659.11	1083.84	3790.32	2.801	3.352	3.406	51.789
100	293.15	1681.25	1080.50	3798.83	3.364	3.274	3.355	41.622
100	303.15	1703.38	1076.56	3805.82	3.929	3.201	3.316	34.397
150	283.15	1745.48	1101.42	3758.58	3.019	2.980	3.042	48.429
150	293.15	1764.16	1097.82	3765.58	3.532	2.927	3.015	39.922
150	303.15	1782.84	1093.66	3770.93	4.046	2.877	2.997	33.622
200	283.15	1828.03	1117.44	3729.70	3.133	2.678	2.745	46.981
200	293.15	1843.68	1113.68	3735.43	3.608	2.642	2.733	39.334
200	303.15	1859.33	1109.41	3739.40	4.081	2.607	2.729	33.530
250	283.15	1906.76	1132.17	3703.11	3.179	2.429	2.498	46.578
250	293.15	1919.81	1128.32	3707.76	3.622	2.405	2.497	39.399
250	303.15	1932.86	1123.99	3710.58	4.063	2.381	2.501	33.864
300	283.15	1981.68	1145.78	3678.41	3.180	2.222	2.290	46.804
300	293.15	1992.54	1141.91	3682.16	3.597	2.206	2.296	39.874
300	303.15	2003.41	1137.57	3684.01	4.010	2.190	2.306	34.476
350	283.15	2052.78	1158.46	3655.32	3.153	2.048	2.115	47.427
350	293.15	2061.89	1154.58	3658.30	3.547	2.037	2.125	40.617
350	303.15	2071.00	1150.27	3659.33	3.936	2.027	2.139	35.275
400	283.15	2120.07	1170.32	3633.63	3.109	1.901	1.965	48.305
400	293.15	2127.84	1166.47	3635.96	3.483	1.893	1.977	41.535
400	303.15	2135.61	1162.20	3636.30	3.851	1.887	1.993	36.197
450	283.15	2183.54	1181.49	3613.16	3.056	1.775	1.837	49.336

Table E-9. Continued

P [Mpa]	T [K]	u [m s^{-1}]	ρ [kg m^{-3}]	Cp [J $kg^{-1}K^{-1}$]	α [K^{-1}] ($x10^{-4}$)	β_S [Mpa^{-1}] ($x10^{-4}$)	β_T [Mpa^{-1}] ($x10^{-4}$)	γ_S [Mpa K^{-1}]
450	293.15	2190.40	1177.68	3614.93	3.412	1.770	1.850	42.559
450	303.15	2197.26	1173.46	3614.70	3.762	1.765	1.866	37.193
500	283.15	2243.19	1192.06	3593.79	2.999	1.667	1.727	50.447
500	293.15	2249.56	1188.29	3595.08	3.340	1.663	1.739	43.635
500	303.15	2255.94	1184.13	3594.36	3.673	1.659	1.755	38.225
550	283.15	2299.03	1202.10	3575.39	2.943	1.574	1.631	51.577
550	293.15	2305.34	1198.37	3576.28	3.269	1.570	1.643	44.720
550	303.15	2311.65	1194.27	3575.14	3.588	1.567	1.658	39.259
600	283.15	2351.05	1211.68	3557.87	2.890	1.493	1.548	52.674
600	293.15	2357.72	1208.00	3558.41	3.203	1.489	1.559	45.773
600	303.15	2364.39	1203.95	3556.92	3.509	1.486	1.573	40.263

LIST OF REFERENCES

Abe, F., Kato, C., and Horikoshi, K. 1999. Pressure-Regulated Metabolism in Microorganism. *Trends in Microbiology* 7 (11):447-453.

Acree, W.E. 1984. *Thermodynamic Properties of Nonelectrolyte Solutions*. Orlando, US: Academic Press, pp. 30-57.

Aleman, G. D., Farkas, D. F., Torres, J.A., Wilhelmsen, E., and Mcintyre, S. 1994. Ultra High Pressure Pasteurization of Fresh Cut Pineapple. *Journal of Food Protection* 57 (10):931-934.

Aleman, G. D., Ting, E. Y., Mordre, S. C., Hawes, A. C.O., Walker, M., Farkas, D. F., and Torres, J. A. 1996. Pulsed Ultra High Pressure Treatments for Pasteurization of Pineapple Juice. *Journal of Food Science* 61 (2):388-390.

Anese, M., Nicoli, M.C., Dall'Aglio, G., and Lerici, C.R. 1995. Effect of High Pressure Treatments on Peroxidase and Polyphenoloxidase Activities. *Journal of Food Biochemistry* 18:285-293.

Arroyo, G., Sanz, P.D., and Prestamo, G. 1997. Effect of High Pressure on the Reduction of Microbial Populations in Vegetables. *Journal of Applied Microbioloby* 82:735-742.

Asaka, M., Aoyama, Y., Nakanishi, R., and Hayashi, R. 1994. Purification of a Latent Form of Polyphenoloxidase from La France Pear Fruit and its Pressure-Activation. *Bioscience, Biotechnology & Biochemistry* 58 (8):1486-1489.

Asano, T., and Le Noble, W.J. 1978. Activation and Reaction Volumes in Solution. *Chemical Reviews* 78:407-489.

Ashie, I.N.A., and Lanier, T.C. 1999. High Pressure Effects on Gelation of Surimi and Turkey Breast Muscle Enhanced by Microbial Transglutaminase. *Journal of Food Science* 64 (4):704-708.

Ashie, I.N.A., Lanier, T.C., and MacDonald, G.A. 1999. Pressure-Induced Denaturation of Muscle Proteins and its Prevention by Sugars and Polyols. *Journal of Food Science* 64 (5):818-822.

Ashie, I.N.A., and Simpson, B.K. 1996. Application of High Hydrostatic Pressure to Control Enzyme Related Fresh Seafood Texture Deterioration. *Food Research International* 29 (5/6):569-575.

Athes, V., Lange, R., and Combes, D. 1998. Influence of Polyols on the Structural Properties of *Kluyveromyces lactis* β-galactosidase Under High Hydrostatic Pressure. *European Journal of Biochemistry* 255:206-212.

Balaban, M. O. 2001. Real Time Temperature Data Acquisition v. 1.2. University of Florida, Gainesville, FL, US.

Balasubramaniam, V.M. 1999. Role of Temperature on Inactivation of Bacterial Spores during High Pressure Processing of Foods. Paper presented at AIChE Annual Meeting, 1999, at New York, 64C - New Technologies.

Ballestra, P., and Cuq, J-L. 1998. Influence of Pressurized Carbon Dioxide on the Thermal Inactivation of Bacterial and Fungal Spores. *Lebensmittel-Wissenshaft-und-Technologie* 31 (1):84-88.

Banipal, P.K., Banipal, T.S., Lark, B.S., and Ahluwalia, J.C. 1997. Partial Molar Heat Capacities and Volumes of Some Mono-, Di- and Tri-Saccharides in Water at 298.15, 308.15, and 318.15 K. *Journal of the Chemical Society, Faraday Transactions* 93 (1):81-87.

BeMiller, J.N., and Whistler, R.L. 1996. Carbohydrates. In *Food Chemistry*, O. R. Fennema. New York, US: Marcel Dekker, 158-221.

Bernasconi, C. F. 1986. *Investigation of Rates and Mechanisms of Reactions, part II*: Wiley-Interscience Pub.,

Bett, K. E., Palavra, A.M.F., Retsina, T., Richardson, S.M., and Wakeham, W.A. 1989. A Vibrating-Rod Densimeter. *International Journal of Thermodynamics* 10 (4):871-883.

Bevington, P.R. 1969. *Data Reduction and Error Analysis for the Physical Sciences*. New York, US: McGraw-Hill, pp. 1-9, 56-65.

Beyer, R.T., and Letcher, S.V. 1969. *Physical Ultrasonics*. New York, US: Academic Press, 38-64, 65-90.

Bignon, J., and Lebas, J.M. 1997. New Trends in High Pressure Equipment: Example of a Semi-Continuous Hyperbar Pasteurizer for Citrus Juice. In *High Pressure Research in the Biosciences and Biotechnology*, K. Heremans, C. Balny, J. Frank, R. Hayashi, M. Hendrickx and H. Ludwig. Leuven: Leuven University Press, 479-482.

Blandamer, M.J. 1973. *Introduction to Chemical Ultrasonics*. London, UK: Academic Press, 65-121.

Blandamer, M.J. 1998. Equilibrium, Frozen, Excess and Volumetric Properties of Dilute Solutions. *Chemical Society Reviews* 27:73-79.

Blandamer, M.J., Davis, M.I., Douheret, G., and Reis, J.C.R. 2001. Apparent Molar Isentropic Compressions and Expansions of Solutions. *Chemical Society Reviews* 30:8-15.

Bobik, M. 1978. Thermodynamic Quantities for Liquid Benzene: 1. Sound Velocities Between 283 and 463 K and up to 62 MPa. *Journal of Chemical Thermodynamics* 10:1137-1146.

Braddock, R.J., Parish, M.E., and Goodner, J.K. 1998. High Pressure Pasteurization of Citrus Juices. Paper presented at Transactions of the 1998 Citrus Engineering Conference, 1998, at Lakeland, Florida,

Breazeale, M.A., and Cantrell Jr., J.H. 1981. Ultrasonics. In *Ultrasonics*, 19, edited by P. D. Edmonds. New York, US: Academic Press, 67-137.

Bridgman, P.W. 1912. Water, in the Liquid and Five Solid Forms, Under Pressure. *Proceedings of the American Academy of Arts and Sciences* 47:441-558.

Bridgman, P.W. 1914. The Coagulation of Albumen by Pressure. *The Journal of Biological Chemistry* 19:511-512.

Bridgman, P.W. 1931. *The Physics of High Pressure*. London: G. Bells & Sons, 1-29, 143-145, 307-329.

Brul, S.; Rommens, A.J.M.; Verrips, C.T. 2002. Mechanistic Studies on the Inactivation of Microorganisms by High Pressure. Paper presented at IFT Annual Meeting, at Anaheim, California,

Butz, P., and Tauscher, B. 1998. Food Chemistry Under High Hydrostatic Pressure. In *High Pressure Food Science, Bioscience and Chemistry*, N. S. Isaacs. Reading, UK: The Royal Society of Chemistry, 133-144.

Calik, H., Morrissey, M.T., Reno, P.W., and An, H. 2002. Effect of High-Pressure Processing on *Vibrio parahaemolyticus* Strains in Pure Culture and Pacific Oysters. *Journal of Food Science* 67 (4):1506-1510.

Cano, M.P., Hernandez, A., and De Ancos, B. 1997. High Pressure and Temperature Effects on Enzyme Inactivation in Strawberry and Orange Juice. *Journal of Food Science* 62 (1):85-88.

Cano, P.M., Hernandez, A., and De Ancos, B. 1999. Combined High Pressure/Temperature Treatments for Quality Improvement of Fruit-Derived Products. In *Processing of Foods: Quality Optimization and Process Assessment*, F. A. R. Oliveira, J. C. Oliveira, M. E. Hendrickx, D. Knorr and L. G. M. Gorris. Boca Raton, US: CRC Press, 301-324.

Castellari, M., Arfelli, G., Riponi, C., Carpi, G., and Amati, A. 2000. High Hydrostatic Pressure Treatments for Beer Stabilization. *Journal of Food Science* 65 (6):974-977.

Chalikian, T.V., and Breslauer, K.J. 1996. Compressibility as a Means to Detect and Characterize Globular Protein States. *Proceedings of the National Academy of Sciences USA* 93:1012-1014.

Chalikian, T.V., Gindikin, V.S., and Breslauer, K.J. 1995. Volumetric Characterizations of the Native, Molten Globule and Unfolded States of Cytochrome c at Acidic pH. *Journal of Molecular Biology* 250:291-306.

Chalikian, T.V., Sarvazyan, A.P., and Breslauer, K.J. 1994. Hydration and Partial Compressibility of Biological Compounds - Review. *Biophysical Chemistry* 51:89-109.

Chang, R. F., and Moldover, M. R. 1996. High-Temperature High-Pressure Oscilating Tube Densimeter. *Review of Scientific Instruments* 67 (1):251-256.

Chaplin, M.F. 1999. A Proposal for the Structuring of Water. *Biophysical Chemistry* 83:211-221.

Cheftel, J.C. 1991. Applications des Hautes Pressions en Technologie Alimentaire. *Industrie Alimentaires et Agricoles* 108 (3):141-153.

Cheftel, J-C. 1992. Effects of High Hydrostatic Pressure on Food Constituents: An Overview. In *High Pressure and Biotechnology*, 224, edited by C. Balny, R. Hayashi, K. Heremans and P. Masson. La Grande Motte: John Libbey Eurotext/INSERM, 195-224.

Chen, C.S. 1989. Water Activity - Concentration Models for Solutions of Sugars, Salts, and Acids. *Journal of Food Science* 54 (5):1318-1321.

Coleman, H.W., and Steele, W.G. 1999. *Experimental and Uncertainty Analysis for Engineers*. 2nd ed. New York, US: Wiley-Interscience, pp. 1-15, 47-82, 242-257.

Colman, P. 1997. High Pressure Food Processing Equipment With and Without Low Temperature Control. In *High Pressure Research in the Biosciences and Biotechnology*, K. Heremans, C. Balny, J. Frank, R. Hayashi, M. Hendrickx and H. Ludwig. Leuven, Belgium: Leuven University Press, 475-478.

Contreras, N. I., Fairley, P., McClements, D. J., and Povey, M. J. W. 1992. Analysis of Sugar Content of Fruit Juices and Drinks using Ultrasonic Velocity Measurements. *International Journal of Food Science and Technology* (27):515-529.

Corwin, H., and Shellhammer, T.H. 2002. Combined Carbon Dioxide and High Pressure Inactivation of Pectin Methylesterase, Polyphenol Oxidade, *Lactobacillus plantarum* and *Escherichia coli*. *Journal of Food Science* 67 (2):697-701.

Daridon, J. L. 1994. Mesure de la Vitesse du Son dans des Fluides Sous Pression Composes de Constituants Gazeux et Liquides. *Acustica* 80:416-419.

Davis, J.R. 2000. *Alloy Digest Source Book - Stainless Steels*. Materials Park, OH, US: ASM International - The Materials Information Society, 69-70.

Davis, L. A., and Gordon, R. B. 1967. Compression of Mercury at High Pressure. *The Journal of Chemical Physics* 46 (7):2650-2660.

De Cordt, S., Ludikhuyze, L.R., Van den Broeck, I., Weemaes, C.A., and Hendrickx, M.E. 1997. A Scientific Basis for Assessment, Design and Optimization of High Pressure/Thermal Processes. Paper presented at 7th International Congress on Engineering and Food, 1997, at London,

De Nevers, N. 2002. *Physical and Chemical Equilibrium for Chemical Engineers*. New York, US: Wiley-Interscience, pp. 130-159.

Denys, S., Van Loey, A. M., De Cordt, S., Hendrickx, M., and Tobback, P. P. 1997. Modeling of High Pressure Assisted Freezing and Thawing. In *High Pressure Research in the Biosciences and Biotechnology*, K. Heremans, C. Balny, J. Frank, R. Hayashi, M. Hendrickx and H. Ludwig. Leuven, Belgium: Leuven University Press, 351-354.

Deplace, G. 1995. Vessel Design. In *High Pressure Processing of Foods*, D. A. Ledward, D. E. Johnston, R. G. Earnshaw and A. P. M. Hasting. Nottingham: Nottingham University Press, 137-154.

Deplace, G., and Mertens, B. 1992. The Commercial Applications of High Pressure Technology in the Food Processing Industry. In *High Pressure and Biotechnology*, 224, edited by C. Balny, R. Hayashi, K. Heremans and P. Masson. La Grande Motte: John Libbey Eurotext / INSERM, 469-478.

Deuchi, T., and Hayashi, R. 1992. High Pressure Treatments at Subzero Temperature: Application to Preservation, Rapid Freezing and Rapid Thawing of Foods. In *High Pressure and Biotechnology*, 224, edited by C. Balny, R. Hayashi, K. Heremans and P. Masson. La Grande Motte: John Libbey Eurotext / INSERM, 353-355.

Diaz-Pena, M., and McGlashan, M.L. 1959. An Apparatus for the Measurement of the Isothermal Compressibility of Liquids. The Compressibility of Mercury, of Carbon Tetra-Chloride, and of Water. *Transactions of the Faraday Society* 55:2018-2024.

Dix, M., Fareleira, J.M.N.A., Takaishi, Y., and Wakeham, W.A. 1991. A Vibrating-Wire Densimeter for Measurements in Fluids at High Pressures. *International Journal of Thermodynamics* 12 (2):357-371.

Douheret, G., Davis, L. A., Reis, J.C.R., and Blandamer, M.J. 2001. Isentropic Compressibilities - Experimental Origin and the Quest for their Rigorous Estimation in Thermodynamically Ideal Liquid Mixtures. *ChemPhysChem* 2:148-161.

Douheret, G., and Davis, M.I. 1993. Measurement, Analysis, and Utility of Excess Molar - $(\delta V/\delta P)_S$. *Chemical Society Reviews* 44:43-50.

Douheret, G., Moreau, C., and Viallard, A. 1985. Excess Thermodynamic Quantities in Binary Systems of Non Electrolytes. I. Different Ways of Calculating Excess Compressibilities. *Fluid Phase Equilibria* 22:277-287.

Douzals, J.P., Marechal, P.A., Coquile, J.C., and Gervais, P. 1996. Comparative Study of Thermal and High Pressure Treatments Upon Wheat Starch Suspensions. In *High Pressure Bioscience and Biotechnology*, 13, edited by R. Hayashi and C. Balny. Amsterdam, NE: Elsevier Science, 433-438.

Dowling, A.P., and Ffwocs-Williams, J.E. 1983. *Sound and Sources of Sound*. Chischester, UK: Ellis Horwood, 11-35.

Drljaca, A., Hubbard, C.D., Van Eldik, R., Asano, T., Basilevsky, M.V., and Le Noble, W.J. 1998. Activation and Reaction Volumes in Solution. 3. *Chemical Reviews* 98 (6):2167-2289.

Dumay, E.M., Kalichevsky, T., and Cheftel, J.C. 1994. High Pressure Unfolding and Aggregation of β-Lactoglobulin and the Baroprotective Effects of Sucrose. *Journal of Agriculture and Food Chemistry* 42 (9):1861-1868.

Dumoulin, M., Ozawa, S., and Hayashi, R. 1998. Textural Properties of Pressure-Induced Gels of Food Proteins Obtained under Different Temperatures Including Subzero. *Journal of Food Science* 63 (1):92-95.

Dunne, P., and Kluter, R.A. 2001. Emerging Non-Thermal Processing Technologies: Criteria for Success. *The Australian Journal of Dairy Technology* 56 (2):109-112.

Dymond, J.H., Robertson, J., and Isdale, J.D. 1982. (P, ρ, T) of Some Pure n-Alkanes and Binary Mixtures of n-Alkanes in the Range 298 to 373 K and 0.1 to 500 MPa. *Journal of Chemical Thermodynamics* 14:51-59.

Dymond, J.H., Young, K.J., and Isdale, J.D. 1979. P, ρ, T Behavior for n-Hexane + n-Hexadecane in the Range 298 to 373 K and 0.1 to 500 MPa. *Journal of Chemical Thermodynamics* 11:887-895.

Earnshaw, R.G. 1995. High Pressure Microbial Inactivation Kinetics. In *High Pressure Processing of Foods*, D. A. Ledward, D. E. Johnston, R. G. Earnshaw and A. P. M. Hasting. Loughborough, UK: Nottingham University Press, 37-*46.

Earnshaw, R.G., Appleyard, J., and Hurst, R.M. 1995. Understanding Physical Inactivation Processes: Combined Preservation Opportunities Using Heat, Ultrasound and Pressure. *International Journal of Food Microbiology* (28):197-219.

Eggers, F. 1992. Ultrasonic Velocity and Attenuation Measurements in Liquids with Resonators, Extending the MHz Frequency Range. *Acustica* 76:231-240.

Eggers, F., and Funck, T. 1973. Ultrasonic Measurements with Milliliter Liquid Samples in the 0.5-100 MHz Range. *Review of Scientific Instruments* 44 (8):969-977.

Eggers, F., and Kaatze, U. 1996. Broad-Band Ultrasonic Measurement Techniques for Liquids. *Measurement Science and Technology* 7 (1):1-19.

Eley, E. 1992. Under Pressure. *Food Processing* 61 (4):23-24.

Enomoto, A., Nakamura, K., Hakoda, M., and Amaya, N. 1997a. Lethal Effect of High Pressure Carbon Dioxide on a Bacterial Spore. *Journal of Fermentation and Bioengineering* 83 (3):305-307.

Enomoto, A., Nakamura, K., Nagai, K., Hashimoto, T., and Hakoda, M. 1997b. Inactivation of Food Microorganisms by High Pressure Carbon Dioxide Tretament with or without Explosive Decompression. *Bioscience, Biotechnology & Biochemistry* 61 (7):1133-1137.

Farkas, D.F., and Hoover, D.G. 2000. Kinetics of Microbial Inactivation for Alternative Food Processing Technologies - High Pressure Processing. *Journal of Food Science - Supplement* 65 (6):47-64.

Farr, D. 1990. High Pressure Technology in the Food Industry. *Trends in Food Science & Technology* 01:14-16.

Fennema, O.R. 1996. Water and Ice. In *Food Chemistry*, O. R. Fennema. New York: Marcel Dekker, 17-94.

Fernandes, P., Cofrades, S., Solas, M.T., Carballo, J., and Jimenez Colmenero, F. 1998. High Pressure-Cooking of Chicken Meat Batters with Starch, Egg White, and Iota Carrageenan. *Journal of Food Science* 63 (2):267-271.

Fernandez-Martin, F., Otero, L., Solas, M.T., and Sanz, P.D. 2000. Protein Denaturation and Structural Damage During High-Pressure-Shift Freezing of Porcine and Bovine Muscle. *Journal of Food Science* 65 (6):2000.

Fine, R.A., and Millero, F. J. 1973. Compressibility of Water as a Function of Temperature and Pressure. *The Journal of Chemical Physics* 59 (10):5529-5536.

Firestone, F.A., and Frederick, J.R. 1946. Refinements in Supersonic Reflectoscopy, Polarized Sound. *The Journal of the Acoustical Society of America* 19 (1):200-211.

Franks, F., and Reid, D.S. 1973. Thermodynamic Properties. In *Water: A Comprehensive Treatise*, Vol. 2: Water in Crystalline Hydrates Aqueous Solutions of Simple Nonelectrolytes, edited by F. Franks. London, UK: Plenum Press, 323-380.

Freeman, M. 1997. Development of High Pressure Systems for Research and Development. In *High Pressure Research in the Biosciences and Biotechnology*, K. Heremans, C. Balny, J. Frank, R. Hayashi, M. Hendrickx and H. Ludwig. Leuven, Belgium: Leuven University Press, 491-494.

Freeman, M. 1998. Equipment & Systems for High Pressure. In *High Pressure Food Science Bioscience and Chemistry*, N. S. Issacs. Reading, UK: The Royal Society of Chemistry, 501-505.

Fuchigami, M., Kato, N., and Teramoto, A. 1996. Effect of Pressure-Shift Freezing on Texture, Pectic Composition and Histological Strucutre of Carrots. In *High Pressure Bioscience and Biotechnology*, R. Hayashi and C. Balny. Amsterdam, NE: Elsevier Science, 379-386.

Fuchigami, M., and Teramoto, A. 1996. Texture and Cryo-Scanning Electron Micrographs of Pressure-Shift-Frozen Tofu. In *High Pressure Bioscience and Biotechnology*, R. Hayashi and C. Balny. Amsterdam, NE: Elsevier Science, 411-414.

Funtenberger, S., Dumay, E., and Cheftel, J.C. 1995. Pressure-Induced Aggregation of β-Lactoglobulin in pH 7.0 Buffers. *Lebensmittel-Wissenshaft-und-Technologie* 28 (4):410-418.

Furukawa, S.;, Noma, S.;, Shimoda, M.;, and Hayakawa, I. 2002. Effect of Initial Concentration of Bacterial Suspensions on their Inactivation by High Hydrostatic Pressure. *International Journal of Food Science and Technology* 37:573-577.

Galazka, V.B, Ledward, D.A., Dickinson, E., and Langley, K.R. 1995. High Pressure Effects on Emulsifying Behavior of Whey Protein Concentrate. *Journal of Food Science* 60 (6):1341-1343.

Galema, S.A., and Hoiland, H. 1991. Stereochemical Aspects of Hydration of Carbohydrates in Aqueous Solutions. 3. Density and Ultrasound Measurements. *Journal of Physical Chemistry* 95 (13):5321-5326.

Ganzle, M.G., Ulmer, H.M., and Vogel, R.F. 2001. High Pressure Inactivation of *Lactobacillus plantarum* in a Molde Beer System. *Journal of Food Science* 66 (8):1174-1181.

Gekko, K, and Yamagami, K. 1991. Flexibility of Food Proteins as Revealed by Compressibility. *Journal of Agriculture and Food Chemistry* 39 (1):57-62.

Gekko, K. 1992. Effects of Pressure on the Sol-Gel Transition of Food Macromolecules. In *High Pressure and Biotechnology*, 224, edited by C. Balny, R. Hayashi, K. Heremans and P. Masson. La Grande Motte: John Libbey Eurotext / INSERM, 105-113.

Gekko, K., and Hasegawa, Y. 1986. Compressibility-Structure Relationship of Globular Proteins. *Biochemistry* 25 (21):6563-6571.

Gibbs, J.H. 1971. Nature of the Glass Transition and Vitreous State. In *Modern Aspects of the Vitreous State*, J. D. MacKenzie. London, UK: Butterworths, pp. 152-187.

Gibson, R.E. 1937. The Compressions of Solutions of Certain Salts in Water, Glycol and Methanol. *Journal of the American Chemical Society* 59:1521-1528.

Goldman, K. 1958. Determinaion of Density of Liquids Under Elevated Gas Pressure. *British Journal of Applied Physics* 9:40-42.

Goodner, J.K, Braddock, R.J., and Parish, M.E. 1998. Inactivation of Pectinesterase in Orange and Grapefruit Juices by High Pressure. *Journal of Agriculture and Food Chemistry* 46 (5):1997-2000.

Gould, G.W., and Sale, J.H. 1972. Role of Pressure in the Stabilization and Destabilization of Bacterial Spores. Paper presented at Symposia of the Society for Experimental Biology, at Cambridge, 147-157.

Gucker Jr., F.T. 1933. The Compressibility of Solutions. I. The Apparent Molal Compressibility of Strong Electrolytes. *Journal of the American Chemical Society* 55:2709-2719.

Hashizume, C., Kimura, K., and Hayashi, R. 1995. Kinetic Analysis of Yeast Inactivation by High Pressure Treatment at Low Temperatures. *Bioscience, Biotechnology & Biochemistry* 59 (8):1455-1458.

Hashizume, C., Kimura, K., and Hayashi, R. 1996. High Pressure Inactivation of Yeast Cells in Saline and Strawberry Jam at Low Temperature. In *High Pressure Bioscience and Biotechnology*, 13, edited by R. Hayashi and C. Balny. Amstredam, NE: Elsevier Science, 423-428.

Hayakawa, I, Linko, Y-Y., and Linko, P. 1996. Mechanism of High Pressure Denaturation of Proteins. *Lebensmittel-Wissenshaft-und-Technologie* 29 (8):756-762.

Hayakawa, I., Kanno, T., and Fujio, Y. 1994a. Study of High Pressure Effect on Inactivation of *Bacillus stearothermophilus* Spores. In *Developments in Food Engineering*, 2, edited by T. Yano, R. Matsumo and K. Nakamura. London: Blackie Academic & Professional, 867-869.

Hayakawa, I., Kanno, T., and Fujio, Y. 1994b. Study of the High Pressure Effect on Inactivation of *Bacillus stearothermophilus* Spores. Paper presented at 6th International Congress on Engineering and Food, 1994, pp. 867-869.

Hayakawa, I., Linko, Y-Y., and Linko, P. 1997. High Pressure Technology in Sterilization of Biomass by Adiabatic Expansion of Water. In *Engineering & Food at ICEF 7*, Part I, edited by R. Jowitt. London: Sheffield Academic Press, D9-D16.

Hayashi, R. 1995. Advances in High Pressure Food Processing Technology in Japan. In *Food Processing : Recent Developments*, A. G. Gaonkar. Amsterdam: Elsevier Science, 185-195.

Hayashi, R., Kinsho, T., and Ueno, H. 1998. Combined Application of Sub-Zero Temperature and High Pressure on Biological Materials. In *High Pressure Food Science, Bioscience and Chemistry*, N. S. Isaacs. Rading, UK: The Royal Society of Chemistry, 166-174.

Hayert, M., Perrier-Cornet, J.M., and Gervais, P. 1999. A Simple Method for Measuring the pH of Acid Solutions Under High Pressure. *Journal of Physical Chemistry A* 103 (12):1785-1789.

Hayward, A. T. J. 1971a. How to Measure the Isothermal Compressibility of Liquids Accurately. *Journal of Physics D: Applied Physics* 4:938-950.

Hayward, A. T. J. 1971b. Precise Determination of the isothermal Compressibility of Mercury at 20^{o}C and 192 bar. *Journal of Physics D: Applied Physics* 4:951-955.

He, H., Adams, R.M., Farkas, D.F., and Morrissey, M.T. 2002. Use of High-Pressure Processing for Oyster Shucking and Shelf-Life Extension. *Journal of Food Science* 67 (2):640-645.

Heinz, V., and Knorr, D. 1996. High Pressure Inactivation Kinetics of *Bacillus subtillis* Cells by a Three-State-Model Considering Distribution Resistance Mechanism. *Food Biotechnology* 10:149-161.

Hendrickx, M.E., Ludikhuyze, L.R., Van den Broeck, I., and Weemaes, C.A. 1998. Effects of High Pressure on Enzymes Related to Food Quality. *Trends in Food Science and Technology* 9:197-203.

Heremans, K. 1995. High Pressure Effects on Biomolecules. In *High Pressure Processing of Foods*, D. A. Ledward, D. E. Johnston, R. G. Earnshaw and A. P. M. Hasting. Loughborough, UK: Nottingham University Press, 81-97.

Heremans, K., Meersman, F., Rubens, P., Smeller, L., Snauwaert, J., and Vermeulen, G. 1999. A Comparison Between Pressure and Temperature Effects on Food Constituents. In *Processing of Foods: Quality Optimization and Process Assessment*, F. A. R. Oliveira, J. C. Oliveira, M. E. Hendrickx, D. Knorr and L. G. M. Gorris. Boca Raton, US: CRC Press, 269-280.

Heremans, K., Rubens, P., Smeller, L., Vermeulen, G., and Goossens, K. 1996. Pressure Versus Temperature Behavior of Proteins: FT-IR Studies With the Diamond Anvil Cell. In *High Pressure Bioscience and Biotechnology*, 13, edited by R. Hayashi and C. Balny. Amsterdam, NE: Elsevier Science, 127-134.

Heydemann, P. 1971. Ultrasonic Measurements at Very High Pressures. In *Physical Acoutics*, Vol. VIII, edited by W. P. Mason and R. N. Thurston. New York, US: Academic Press, 203-236.

Hinrichs, J., and Kessler, H.G. 1997. Reaction Kinetics of Whey Protein Denaturation Induced by Ultra High Pressure Treatment. Paper presented at 7th International Congress on Engineering and Food, 1997, D1-4.

Hite, B.H. 1899a. The Effect of Pressure in the Preservation of Milk. *Bulletin of the West Virginia Agricultural Experiment Station* 58:13-35.

Hite, B.H. 1899b. The Effect of Pressure in the Preservation of Perishable Food Stuffs. 22th Annual Report of the West Virginia Agricultural Experiment Station. Fairmont, 21-25.

Hite, B.H., Giddings, N.J., and Weakley-Jr., C.E. 1914. The Effect of Pressure on Certain Microrganisms Encountered in the Preservation of Fruits and Vegetables. *Technical Bulletin of the West Virginia University Agricultural Experimental Station* (146):1-66.

Hoiland, H. 1973. Pressure Dependence of the Volume of Ionization of Carboxylic Acids at 25, 35 and 45^{o}C and 1-1200 bar. *Journal of the Chemical Society Faraday I* 70:1180-1185.

Hoiland, H. 1986. Partial Molar Volumes of Biochemical Model Compounds in Aqueous Solution (ch.1). Partial Molar Compressibilties of Organic Solutes in Water (ch.2). In *Thermodynamics Data for Biochemistry and Biotechnology*, H.-J. Hinz. Berlin, GE: Springer-Verlag, 17-44, 129-147.

Hoiland, H., and Holvik, H. 1978. Partial Molal Volumes and Compressibilities of Carbohydrates in Water. *Journal of Solution Chemistry* 7 (8):587-597.

Hoover, D.G., Metrick, C., Papineau, M., Farkas, M., and Knorr, D. 1989. Biological Effects of High Hydrostatic Pressure on Food Microorganisms. *Food Technology* 43 (3):99-107.

Hori, K., Manabe, Y., Kaneko, M., Sekimoto, T., Sugimoto, Y., and Yamane, T. 1992. The Development of High Pressure Processor for Food Industries. In *High Pressure and Biotechnology*, 224, edited by C. Balny, R. Hayashi, K. Heremans and P. Masson. La Grande Motte: John Libbey Eurotext / INSERM, 499-507.

Horvath-Szabo, G., Hoiland, H., and Hogseth, E. 1994. An Automated Apparatus for Ultrasound Velocity Measurements Improving the Pulse-Echo-Overlap Method to a Precision Better than 0.5 ppm in Liquids. *Review of Scientific Instruments* 65 (5):1644-1648.

Hsu, K-C., and Ko, W-C. 2001. Effect of Hydrostatic Pressure on Aggregation and Viscoelastic Properties of Tilapia (*Orechromis niloticus*) Myosin. *Journal of Food Science* 66 (8):1158-1162.

Hui Bon Hoa, G., Di Primo, C., and Douzou, P. 1992. The Role of Electrostriction in the Control of Reaction Volumes of Biochemical Processes. In *High Pressure and*

Biotechnology, 224, edited by C. Balny, R. Hayashi, K. Heremans and P. Masson. La Grande Motte: John Libbey Eurotex/INSERM, 139-144.

Iametti, S., Donnizzelli, E., Vecchio, G., Rovere, P.P., Gola, S., and Bonomi, F. 1998. Macroscopic and Structural Consequences of High Pressure Treatment of Ovalbumin Solutions. *Journal of Agriculture and Food Chemistry* 46 (9):3521-3527.

Indrawati, S.D., Ludikhuyze, L.R., Van Loey, A.M., and Hendrickx, M.E. 2000. Lipoxygenase Inactivation in Green Beans (*Phaseolus vulgaris L.*) Due to High Pressure Treatment at Subzero and Elevated Temperatures. *Journal of Agriculture and Food Chemistry* 48 (5):1850-1859.

Indrawati, S.D., Van Loey, A.M., Ludikhuyze, L.R., and Hendrickx, M.E. 1999. Single, Combined, or Sequential Action of Pressure and Temperature on Lipoxygenase in Green Beans (*Phaseolus vulgaris L.*): A Kinetic Inactivation Study. *Biotechnology Progress* 15 (2):273-277.

Isaacs, N. S. 1981. *Liquid Phase High Pressure Chemistry*. Chichester, UK: John Wiley & Sons, 63-135.

Isaacs, N.S., Chilton, P., and Mackey, B. 1995. Studies on The Inactivation by High Pressure of Microorganisms. In *High Pressure Food Processing*, D. A. Ledward, D. E. Johnston, R. G. Earnshaw and A. P. M. Hasting. Loughborough, UK: Nottingham University Press, 65-79.

ISO, International Organization of Standardization. 1993. *Guide to the Expression of Uncertainty in Measurement*. Geneva: ISO,

Itoh, S., Yoshioka, K., Terakawa, M., and Nagano, I. 1996. Continuous High Pressure System for Liquid Food. In *High Pressure Bioscience and Biotechnology*, 13, edited by R. Hayashi and C. Balny. Amsterdam, NE: Elsevier, 455-462.

Itoh, S.; Yoshioka, K.; Terakawa, M.; Nagano, I. 1996. Debelopment of Pulsatile High Pressure Equipment. In *High Pressure Bioscience and Biotechnology*, 13, edited by R. Hayashi and C. Balny. Amsterdam, NE: Elsevier, 463-471.

Iwahashi, H., Obuchi, K., Fujii, S., Fujita, K., and Komatsu, Y. 1997. The Reason Why Trehalose is More Important for Barotolerance than hsp104 in *Saccharomyces cerevisiae*. In *High Pressure Research in the Biosciences and Biotechnology*, K. Heremans, C. Balny, J. Frank, R. Hayashi, M. Hendrickx and H. Ludwig. Leuven: Leuven University Press,

Kalichevsky, M.T., Knorr, D., and Lillford, P.J. 1995. Potential Food Applications of High Pressure Effects on Ice-Water Transitions. *Trends in Food Science & Technology* 6:253-259.

Kanda, T., Yamauchi, T., Naoi, T, and Inoue, Y. 1992. Present Status and Future Prospects of High Pressure Food Processing Equipment. In *High Pressure and*

Biotechnology, 224, edited by C. Balny, R. Hayashi, K. Heremans and P. Masson. La Grande Motte: John Libbey Eurotext / INSERM, 521-524.

Kapsalis, J.G. 1987. Influences of Hysteresis and Temperature on Moisture Sorption Isotherms. In *Water Activity: Theory and Application to Food*, L. B. Rockland and L. R. Beuchat. New York, US: Marcel Dekker, pp. 173-213.

Kaufman, M. 2002. *Principles of Thermodynamics*. New York, US: Marcel Dekker, pp. 212-272.

Kauzmann, W. 1948. The Nature of the Glassy State and the Behavior of Liquids at Low Temperatures. *Chemical Reviews* 43:219-256.

Kell, G. S. 1974. Thermodynamic and Transport Properties of Fluid Water. In *Water A Comprehensive Treatise*, F. Franks. London: Plenum Press, 363-412.

Kharakoz, D.P. 1991. Volumetric Properties of Proteins and Their Analogues in Diluted Water Solutions. 2. Partial Adiabatic Compressibilities of Amino Acids at 15-70^{o}C. *The Journal of Physical Chemistry* 95 (14):5634-5642.

Kharakoz, D.P. 1997. Partial Volumes and Compressibilities of Extended Polypeptide Chains in Aqueous Solution: Aditivity Scheme and Implication of Protein Unfolding at Normal and High Pressure. *Biochemistry* 36 (33):10276-10285.

Kharakoz, D.P., and Sarvazyan, A.P. 1993. Hydration and Intrinsic Compressibilities of Globular Protein. *Biopolymers* 33:11-26.

Kinsler, L. E., and Frey, A. R. 1962. *Fundamentals of Acoustics*. 2 ed. New York: John Wiley & Sons,

Kiyohara, O., Grolier, J-P. E., and Benson, G. C. 1974. Excess Volumes, Ultrasonic Velocities, and Adiabatic Compressibilities for Binary Cycloalkanol Mixtues at 25^{o}C. *Canadian Journal of Chemistry* 52:2287-2293.

Knorr, D. 1999a. Novel Approaches in Food Processing Technology: New Technologies for Preserving Foods and Modifying Function. *Food Biotechnology* 10:485-491.

Knorr, D. 1999b. Process Assessment of High Pressure Processing of Foods: An Overview. In *Processing of Foods: Quality Optimization and Process Assessment*, F. A. R. Oliveira, J. C. Oliveira, M. E. Hendrickx, D. Knorr and L. G. M. Gorris. Boca Raton, US: CRC Press, 249-268.

Knorr, D., Schlueter, O., and Heinz, V. 1998. Impact of High Hydrostatic Pressure on Phase Transitions of Foods. *Food Technology* 52 (9):42-45.

Ko, W-C., Tanaka, M., Nagashima, Y., Taguchi, T., and Amano, K. 1991. Effect of Pressure Treatment on Actomyosin ATPases from Flying Fish and Sardine Muscles. *Journal of Food Science* 56 (2):338-340.

Kortbeek, P.J., Trappeniers, N.J., and Biswas, S.N. 1988. Compressibility and Sound Velocity Measurements on N_2 up to 1 GPa. *International Journal of Thermophysics* 9 (1):103-116.

Kozak, J.J., Knight, S., and Kauzmann, W. 1968. Solute-Solute Interactions in Aqueous Solutions. *The Journal of Chemical Physics* 48 (2):675-690.

Kubota, H., Tanaka, M., and Makita, T. 1987. Volumetric Behavior of Pure Alcohols and Their Water Mixtures Under High Pressure. *International Journal of Thermophysics* 8 (1):47-70.

Kunugi, S. 1992. Effect of Pressure on Activity and Specificity of Some Hydrolytic Enzymes. In *High Pressure and Biotechnology*, 224, edited by C. Balny, R. Hayashi, K. Heremans and P. Masson. La Grande Motte: John Libbey Eurotext / INSERM, 129-137.

Lainez, A., Miller, J.F., Zollweg, J.A., and Streett, W.B. 1987. Volumetric and Speed of Sound Measurements for Liquid Tetrachloromethane Under Pressure. *Journal of Chemical Thermodynamics* 19:1251-1260.

Laplace, M. 1816. Sur la Vitesse du Son dans l'Air et dans l'Eau. *Annales de Chimie et de Physique* 3:238-241.

Lazarus, D. 1949. The Variation of the Adiabatic Elastic Constants of KCl, NaCl, CuZn, Cu, and Al with Pressure to 10,000 bars. *Physical Review* 76 (4):545-553.

Lechowich, R. V. 1993. Food Safety Implications of High Hydrostatic Pressure as a Food Processing Method. *Food Technology* 47 (6):170-172.

Lee, E.Y., and Park, J. 2002. Pressure Inactivation Kinetics of Microbial Transglutaminase from *Streptoverticillum mobaraense*. *Journal of Food Science* 67 (3):1103-1107.

Levelt-Sengers, J.M.H. 1965. The Experimental Determination of the Equation of State of Gases and Liquids at Low temperatures. In *Physics of High Pressures and the Condensed Phase*, A. Van Itterbeek. Leuven, Belgium: North Holland, 60-98.

Lewis, G.N., and Randall, M. 1923. *Thermodynamics and the Free Energy of Chemical Substances*. New York, US: McGraw-Hill Book Company, pp. 31-46.

Li, B., and Sun, D-W. 2002. Novel Methods for Rapid Freezing and Thawing of Foods - A Review. *Journal of Food Engineering* 54:175-182.

Linton, M., and Patterson, M.F. 2000. High Pressure Processing of Foods for Microbiological Safety and Quality. *Acta Microbiologica et Immunologica Hungarian* 47 (2/3):175-181.

Ludemann, H-D. 1992. Water and Aqueous Solutions Under High Pressure. In *High Pressure and Biotechnology*, 224, edited by C. Balny, R. Hayashi, K. Heremans and P. Masson. La Grande Motte: John Libbey Eurotext / INSERM, 371-379.

Ludikhuyze, L.R., Indrawati, S.D., Van den Broeck, I., Weemaes, C.A., and Hendrickx, M.E. 1998a. Effect of Combined Pressure and Temperature on Soybean Lipoxygenase. 1. Influence of Extrinsic and Intrinsic Factors on Isobaric - Isothermal Inactivation Kinetics. *Journal of Agriculture and Food Chemistry* 46 (10):4074-4080.

Ludikhuyze, L.R., Indrawati, S.D., Van den Broeck, I., Weemaes, C.A., and Hendrickx, M.E. 1998b. Effect of Combined Pressure and Temperature on Soybean Lipoxygenase. 2. Modeling Inactivation Kinetics under Static and Dynamic Conditions. *Journal of Agriculture and Food Chemistry* 46 (10):4081-4086.

Ludikhuyze, L.R., Ooms, V., Weemaes, C.A., and Hendrickx, M.E. 1999. Kinetic Study of the Irreversible Thermal and Pressure Inactivation of Myrosinase from Broccoli (*Brassica oleracea L. Cv. italica*). *Journal of Agriculture and Food Chemistry* 47 (5):1794-1800.

Ludikhuyze, L.R., Van den Broeck, I., Weemaes, C.A., and Hendrickx, M.E. 1997. Kinetic Parameters for Pressure-Temperature Inactivation of Bacillus subtilis α-Amylase under Dynamic Conditions. *Biotechnology Progress* 13 (5):617-623.

Ludwig, H., and Schreck, C. 1997. The Inactivation of Vegetative Bacteria by Pressure. In *High Pressure Research in the Biosciences and Biotechnology*, K. Heremans, C. Balny, J. Frank, R. Hayashi, M. Hendrickx and H. Ludwig. Leuven: Leuven University Press, 221-224.

Ludwig, H., van Almsick, G., and Schreck, C. 2002. The Effect of Hydrostatic Pressure on the Survival of Microorganisms. In *Biological Systems Under Extreme Conditions - Structure and Function*, Y. Taniguchi, H. E. Stanley and H. Ludwig. Berlin: Springer Verlag, 239-256.

Lullien-Pellerin, V., Popineau, Y., Meersman, F., Morel, M.H., Heremans, K., Lange, R., and Balny, C. 2001. Reversible Changes of Wheat γ46 Gliadin Conformation Submitted to High Pressures and Temperatures. *European Journal of Biochemistry* 268:5705-5712.

Machado, J.R.S., and Streett, W.B. 1983. Equation of State and Thermodynamic Properties of Liquid Methanol from 298 to 489 K and Pressures to 1040 bar. *Journal of Chemical and Engineering Data* 28 (2):218-223.

Makita, T. 1992. Application of High Pressure and Thermophysical Properties of Water to Biotechnology. *Fluid Phase Equilibria* 76:87-95.

Malhotra, R., Price, W. E., Woolf, L. A., and Easteal, A. J. 1990. Thermodynamic and Transport Properties of 1,2-Dichloroethane. *International Journal of Thermodynamics* 11 (5):835-861.

Malhotra, R., and Woolf, L. A. 1993. An Automated Volumometer: Thermodynamic Properties of 1,1-Dichloro-2,2,2-Trifluoroethane (R123) for Temperatures of 278.15 to 338.15 K and Pressures of 0.1 to 380 MPa. *International Journal of Thermophysics* 14 (5):1021-1038.

Masson, P. 1992. Pressure Denaturation of Proteins. In *High Pressure and Biotechnology*, 224, edited by C. Balny, R. Hayashi, K. Heremans and P. Masson. La Grande Motte: John Libbey Eurotext / INSERM, 89-100.

McClements, D.J. 1997. Ultrasonic Characterization of Foods and Drinks: Principles, Methods, and Applications. *Critical Reviews in Food Science and Nutrition* 37 (1):1-46.

McClements, D.J., and Fairley, P. 1991. Ultrasonic Pulse Echo Reflectometer. *Ultrasonics* 29:58-62.

McSkimin, H.J. 1957. Ultrasonic Pulse Technique for Measuring Acoustic Losses and Velocities of Propagation in Liquids as a Function of Temperature and Hydrostatic Pressure. *The Journal of the Acoustical Society of America* 29 (11):1185-1192.

Mertens, B. 1995. Hydrostatic Pressure Treatment of Food: Equipment and Processing. In *New Methods of Food Preservation*, G. W. Gould. London: Blackie Academic & Professional, pp. 135-158.

Mertens, B., and Deplace, G. 1993. Engineering Aspects of High Pressure Technology in the Food Industry. *Food Technology* 47 (6):164-169.

Mertens, B., and Knorr, D. 1992. Developments of Nonthermal Processes for Food Preservation. *Food Technology* (May):124-133.

Messens, W., Van Camp, J., and Huyghebaert, A. 1997. The Use of High Pressure to Modify the Functionality of Food Proteins. *Trends in Food Science & Technology* 8 (April):107-112.

Millero, F. J. 1980. Review of the Experimental and Analytical Methods for the Determination of the Pressure-Volume-Temperature Properties of Electrolytes. In *Thermodynamics of Aqueous Systems with Industrial Applications*, S. A. Newman, H. E. Barner, M. Klein and S. I. Sandler. Washington-DC, US: American Chemical Society, 581-622.

Millero, F. J., Curry, R. W., and Drost-Hansen, W. 1969. Isothermal Compressibility of Water at Various Temperatures. *Journal of Chemical and Engineering Data* 14 (4):422-425938-950.

Millero, F. J., Ward, G.K., Lepple, F.K., and Hoff, E.V. 1974. Isothermal Compressibility of Aqueous Sodium Chloride. Magnesium Chloride, Sodium, and Magnesium Sulfate Solutions From 0 to 45^{o} at 1 atm. *The Journal of Physical Chemistry* 78 (16):1636-1643.

Millero, F.J. 1971. The Molal Volumes of Electrolytes. *Chemical Reviews* 71 (2):147-176.

Millet, M., and Jenner, G. 1970. Etude des Relations P-V-T des Bromures D'Alcoyle Primaires. I. Dispositif et Techniques Experimentales. *Journal de Chimie Physique* 67 (7-8):1667-1670.

Missen, R.W. 1969. Use of the Term "Excess Function". *Industrial Engineering and Chemical Fundamentals* 8:81-84.

Miyawaki, O., Saito, A., Matsuo, T, and Nakamura, K. 1997. Activity and Activity Coefficient of Water in Aqueous Solutions and their Relationships with Solution Structure Parameters. *Bioscience, Biotechnology and Biochemistry* 63 (3):446-469.

Moelwyn-Hughes, E.A., and Thorpe, P.L. 1964. The Physical and Thermodynamic Properties of Some Associated Solutions. II. Heat Capacities and Compressibilities. *Proceedings of the Royal Society of London Ser. A* 278:574-587.

Moreau, C. 1995. Semi-Continuous High Pressure Cell for Liquid Processing. In *High Pressure Processing of Foods*, D. A. Ledward, D. E. Johnston, R. G. Earnshaw and A. P. M. Hasting. Nottingham: Nottingham University Press, 181-198.

Moriyoshi, T., and Inubushi, H. 1977. Compressions of Some Alcohol and their Aqueous Binary Mixtures at 298.15 K and at Pressures up to 1400 atm. *Journal of Chemical Thermodynamics* 9:587-592.

Morris, C.E. 2000. FDA Regs Spur Non-Thermal R&D. *Food Engineering* (July-August):1-4.

Mozhaev, V. V., Heremans, K., Frank, J., Masson, P., and Balny, C. 1994. Exploiting the Effects of High Hydrostatic Pressure in Biotechnological Applications. *Trends in Biotechnology* 12:493-501.

Mozhaev, V. V., Kudryashova, E.V., and Bec, N. 1996a. Modulation of Enzyme Activity and Stability by High Pressure. In *High Pressure Bioscience and Biotechnology*, R. Hayashi and C. Balny. Amsterdam, NE: Elsevier Science, 221-226.

Mozhaev, V.V., Heremans, K., Frank, J., Masson, P., and Balny, C. 1996b. High Pressure Effects on Protein Structure and Function. *Proteins: Structure, Function, and Genetics* 24:81-91.

Muringer, M.J.P., Trappeniers, N.J., and Biswas, S.N. 1985. The Effect of Pressure on the Sound Velocity and Density of Toluene and n-Heptane up to 2600 bar. *Physical Chemistry of Liquids* 14:273-296.

Nakagawa, T., Inubushi, H., and Moriyoshi, T. 1981. Compression of Water + t-butanol mixtures at 298.15 K and Pressures up to 142 MPa. *Journal of Chemical Thermodynamics* 13:171-178.

Nath, J. 1998. Speeds of Sound and Isentropic Compressibilities of (n-butanol + n-pentane) at T=298.15 K, and (n-butanol + n-hexane, or n-heptane, or 2,2,4-trimethylpentane) at T-303.15 K. *Journal of Chemical Thermodynamics* 30:885-895.

Newitt, D.M., and Weale, K.E. 1951. Pressure-Volume-Temperature Relations in Liquids and Liquid Mixtures. Part II. The Compression Isotherms of Some Organic Liquids up to 1000 Atmospheres, and Compressions of Some Aqueous and Non-Aqueous Binary Liquid Mixtures. *Journal of the Chemical Society*:3092-3098.

Newton, I. 1686. Philosophiae Naturalis Principia Mathematica. De Motucorporum. Liber Secundus. Sect I: De Motu corporum quibus refiftur in ratione velocitatis. Prop. XLVII. Theor. XXXVI. Pulsuum in Fluido Elastico propagatorum velocitates sunt in ratione composita ex dimidiata ratione vis Elastica directe e dimidiata ratione densitatis inverse; si modo Fluidi vis Elastica ejusdem condensationi proportionalis esse supponatur. *Londini, Juffu Societatis Regie ac Typis Josephi Streater* Jul. 5:354-372.

NOAA, National Climate Data Center -. *Surface Data: Daily (Temperature, Precipitation, Winds, Pressure, Snow, Etc) / Data Files and Graphics: Mean Sea Level Pressure*. Department of Commerce, National Oceanic and Atmospheric Administration (NOAA), and the National Environmental Satellite, Data and Information Service (NESDIS) 2002 [cited. Available from http://www.ncdc.noaa.gov/wdcamet.html.

Norrish, R.S. 1966. An Equation for the Activity Coefficients and Equilibrium Relative Humidities of Water in Confectionery Syrups. *Journal of Food Technology* 1:25-39.

Nozdrev, V.F. 1963. *Application of Ultrasonics in Molecular Physics*. New York, US: Gordon and Breach,

O'Connor, C.J., Odell, A.L., and Bailey, A.A.T. 1983. Mutarotation of D(+)-Glucose. II. Volumes of Activation for the Uncatalysed and Copper(II)-Catalysed Rates. *Australian Journal of Chemistry* 36:279-287.

O'Donnell, M., Busse, L.J., and Miller, J.G. 1981. Piezoelectric Transducers. In *Methods of Experimental Physics: Ultrasonics*, 19, edited by P. D. Edmonds. New York US: Academic Press, 29-66.

Ogawa, H., Fukuhisa, K., Kubo, Y., and Fukumoto, H. 1990. Pressure Inactivation of Yeasts, Molds, and Pectinesterase in Satsuma Mandarin Juice: Effects of Juice Concentration, pH, and Organic Acids, and Comparison with Heat Sanitation. *Agriculture, Biology and Chemistry* 54 (5):1219-1225.

Ohshima, T., Nakagawa, T., and Chiaki, K. 1992. Effect of High Hydrostatic Pressure on the Enzymatic Degradation of Phospholipids in Fish Muscle during Storage. In *Seafood Science and Technology*, E. Graham Bligh. Halifax: Fishing News Books, 64-75.

Olsson, S. 1995. Production Equipment for Commercial Use. In *High Pressure Processing of Foods*, D. A. Ledward, D. E. Johnston, R. G. Earnshaw and A. P. M. Hasting. Nottingham: Nottingham University Press, 167-180.

Olsson, S. 1997. HP Food Production Equipment. In *High Pressure Research in the Biosciences and Biotechnology*, K. Heremans, C. Balny, J. Frank, R. Hayashi, M. Hendrickx and H. Ludwig. Leuven, Belgium: Leuven University Press, 483-486.

O'Neill, M.J. 1966. Measurement of Specific Heat Functions by Differential Scanning Calorimetry. *Analytical Chemistry* 38 (10):1331-1336.

Otero, L., Martino, M., Zaritzky, N., Solas, M.T., and Sanz, P.D. 2000. Preservation of Microstructure in Peach and Mango During High-Pressure-Shift Freezing. *Journal of Food Science* 65 (3):466-470.

Paci, E., and Marchi, M. 1996. Constant-Pressure Molecular Dynamics Techniques Applied to Complex Molecular Systems and Solvated Proteins. *Journal of Physical Chemistry* 100 (10):4314-4322.

Paljk, S., Klofutar, C., and Kac, M. 1990. Partial Molar Volumes and Expansibilities of Some D-Pentoses and D-Hexoses in Aqueous Solutions. *Journal of Chemical and Engineering Data* 35 (1):41-43.

Palou, E., Lopez-Malo, A., Barbosa-Canovas, G.V., Welti-Chanes, J., and Swanson, B.G. 1997a. High Hydrostatic Pressure as a Hurdle for *Zygosaccharomyces bailii* Inactivation. *Journal of Food Science* 62 (4):855-857.

Palou, E., Lopez-Malo, A., Barbosa-Canovas, G.V., Welti-Chanes, J., and Swanson, B.G. 1997b. Kinetic Analysis of *Zygosaccharomyces bailii* Inactivation by High Hydrostatic Pressure. *Lebensmittel-Wissenshaft-und-Technologie* 30 (7):703-708.

Palou, E., Lopez-Malo, A., Welti-Chanes, J., Barbosa-Canovas, G.V., and Swanson, B.G. 1999. Importance of Water in Foods Preserved by High Hydrostatic Pressure. In *Water Management in the Design and Distribution of Quality Foods - Isopow 7*, Y. H. Roos, R. B. Leslie and P. J. Lillford. Lancaster: Technomic Pub., 481-501.

Palou, E.; Lopez-Malo, A.; Barbosa-Canovas, G.V.; Welti-Chanes, J. 2000. High Hydrostatic Pressure and Minimal Processing. In *Minimally Processed Fruits and Vegetables*, S. M. Alzamora, M. S. Tapia and A. Lopez-Malo. Gaithersburg: Aspen, 205-222.

Papadakis, E.P. 1967. Ultrasonic Phase Velocity by the Pulse Echo Overlap Method Incorporating Diffraction Phase Corrections. *The Journal of the Acoustical Society of America* 42 (1045-1051).

Papadakis, E.P., Lynnworth, L.C., Fowler, K.A., and Carnevale, E.H. 1972. Ultrasonic Attenuation and Velocity in Hot Specimens by the Momentary Contact Method with

Pressure Coupling, and Some Results on Steel to 1200°C. *The Journal of the Acoustical Society of America* 52 (3):850-857.

Parbrook, H.D. 1953. An Acoustic Interferometer for High Fluid Pressure. *Acustica* 3 (2):49-54.

Pares, D., Saguer, E., Toldra, M., and Carretero, C. 2000. Effect of High Pressure Processing at Different Temperatures on Protein Functionality of Porcine Blood Plasma. *Journal of Food Science* 65 (3):486-490.

Park, S.J., Lee, J.I., and Park, J. 2002. Effects of a Combined Process of High Pressure Carbon Dioxide and High Hydrostatic Pressure on the Quality of Carrot Juice. *Journal of Food Science* 67 (5):1827-1834.

Povey, M. J. W. 1989. Ultrasonics in Food Engineering. Part II: Applications. *Journal of Food Engineering* 9:1-20.

Povey, M. J. W., and Mason, T. J. 1998. *Ultrasound in Food Processing*. London: Blackie Academic & Professional,

Povey, M. J. W., and McClements, D. J. 1988. Ultrasonics in Food Engineering. Part I: Introduction and Experimental Methods. *Journal of Food Engineering* 8:217-245.

Povey, M.J.W. 1997. *Ultrasonic Techniques for Fluids Characterization*. Leeds, UK: Academic Press, 1-10, 11-46.

Prehoda, K.E., Mooberry, E.S., and Markley, J.L. 1998. Pressure Denaturation of Proteins: Evaluation of Compressibility Effects. *Biochemistry* 37 (17):5785-5790.

Prigogine, I. 1957. *The Molecular Theory of Solutions*. Amsterdam, NE: North Holland, pp. 44-60.

Prigogine, I., and Defay, R. 1965. *Chemical Thermodynamics*. Translated by D. H. Everett. London, UK: Longmans, pp. 262-290, 311-331.

Reis, J.C.R. 1982. Theory of Partial Molar Properties. *Journal of the Chemical Society, Faraday Transactions 2* 78:1595-1608.

Reis, J.C.R. 1998. New Thermodynamic Relations Concerning Apparent Molar Isentropic Compression and Apparent and Partial Isentropic Compressibilities. *Journal of the Chemical Society, Faraday Transactions* 94 (16):2385-2388.

Richards, T.W., and Chadwell, H.M. 1925. The Densities and Compressibilities of Several Organic Liquids and Solutions, and the Polymerization of Water. *Journal of the American Chemical Society* 47:2283-2302.

Rodriguez, E.L. 1988. Adiabatic Heating in Poly(Methyl Methacrylate) at High Hydrostatic Pressures. *Journal of Polymer Science: Part B: Polymer Physics* 26:459-462.

Roger, M.H. 1895. Action des Hautes Pressiones sur Quelques Bacteries. *Archives de Physiologie Normale et Pathologique* 7:12.

Rosenbaum, E.J. 1970. *Physical Chemistry*. New York, US: Appleton-Century-Crofts, Meredith Corporation, pp. 539-594.

Rouille, J., Lebail, A., Ramaswamy, H.S., and Leclerc, L. 2002. High Pressure Thawing of Fish and Shellfish. *Journal of Food Engineering* 53:83-88.

Rowlinson, J. S., and Swinton, F.L. 1981. *Liquids and Liquid Mixtures*. London, UK: Butterworth Scientific, 11-58.

Sage, B.H. 1965. *Thermodynamics of Multicomponent Systems*. New York, US: Reinhold Publishing, 88-103, 139-168, 226-244.

Saldo, J., Sendra, E., and Guamis, B. 2000. High Hydrostatic Pressure for Accelerating Ripening of Goat's Milk Cheese: Proteolysis and Texture. *Journal of Food Science* 65 (4):636-640.

Sarvazyan, A.P. 1982. Development of Methods of Precise Ultrasonic Measurements in Small Volumes of Liquids. *Ultrasonics* 20:151-154.

Sarvazyan, A.P. 1991. Ultrasonic Velocimetry of Biological Compounds. In *Annual Review of Biophysics and Biophysical Chemistry*, 20, edited by D. M. Engelman, C. R. Cantor and T. D. Pollard. Palo Alto, US: Annual Reviews, 321-342.

Saul, A., and Wagner, W. 1989. A Fundamental Equation for Water Covering the range from the Melting Line to 1273 K at Pressures up to 25 000 MPa. *Journal of Physical and Chemical Reference Data* 18 (4):1527-1564.

Schlueter, O., Heinz, V., and Knorr, D. 1998. Freezing of Potato Cylinders During High Pressure Treatment. In *High Pressure Food Science, Bioscience and Chemistry*, N. S. Isaacs. Reading, UK: The Royal Society of Chemistry, 315-324.

Seyderhelm, I., Boguslawski, S., Michaelis, G., and Knorr, D. 1996. Pressure Induced Inactivation of Selected Food Enzymes. *Journal of Food Science* 61 (2):308-383.

Shampine, L.F., and Reichelt, M.W. 1997. The MatLab ODE Suite. *SIAM Journal on Scientific Computing* 18 (1):1-22.

Shariaty-Niassar, M., Hozawa, M., and Tsukada, T. 2000. Development of Probe for Thermal Conductivity Measurement of Food Materials Under Heated and Pressurized Conditions. *Journal of Food Engineering* 43:133-139.

Shiio, H. 1958. Ultrasonic Interferometer Measurements of the Amount of Bond Water. Saccaharides. *Journal of the American Chemical Society* 80:70-73.

Shimada, K, Sakai, Y., Nagamatsu, K, Hori, T., and Hayashi, R. 1996. Measurement of the Gel-Point Temperature Under High Pressure by a Hot-Wire Method. In *High Pressure Bioscience and Biotechnology*, 13, edited by R. Hayashi and C. Balny. Amsterdam: Elsevier, 451-454.

Sionneau, M., Vasseur, J., Bouix, M., and Pontvianne, P.M. 1997. Continuous High Pressure Treatment of Milk. In *High Pressure Research in the Biosciences and Biotechnology*, K. Heremans, C. Balny, J. Frank, R. Hayashi, M. Hendrickx and H. Ludwig. Leuven, Belgium: Leuven University Press, 451-454.

Smeller, L., and Heremans, K. 1997a. *In situ* Observations of the Pressure-Induced Changes in Proteins With Infrared Spectroscopy in the Diamond Anvil Cell. In *High Pressure Research in the Biosciences and Biotechnology*, K. Heremans. Leuven: Leuven University Press, 131-134.

Smeller, L., and Heremans, K. 1997b. Some Thermodybamic and Kinetic Consequences of the Phase Diagram of Protein Denaturation. In *High Pressure Research in the Biosciences and Biotechnology*, K. Heremans. Leuven: Leuven University Press, 55-58.

Smeller, L., and Heremans, K. 1997c. Some Thermodynamics and Kinetic Consequences of the Phase Diagram of Protein Denaturation. In *High Pressure Research in the Biosciences and Biotechnology*, K. Heremans, C. Balny, J. Frank, R. Hayashi, M. Hendrikx and H. Ludwig. Leuven: Leuven University Press, 55-58.

Smelt, J.P.P.M. 1998. Recent Advances in the Microbiology of High Pressure Processing. *Trends in Food Science & Technology* 9:152-158.

Smelt, J.P.P.M., Hellemons, J.C., Wouters, P.C., and van Gerwen, S.J.C. 2002. Physiological and Mathematical Aspects in Setting Criteria for Decomtamination of Foods by Physical Means. *International Journal of Food Microbiology* (78):57-77.

Smith, D., Galazka, V.B., Wellner, N., and Sumner, I.G. 2000. High Pressure Unfolding of Ovalbumin. *International Journal of Food Science and Technology* 35:361-370.

Smith, D.E., and Winder, W.C. 1983. Effects of Temperature, Concentration and Solute Structure on the Acoustic Properties of Monosaccharide Solutions. *Journal of Food Science* 48:1822-1825.

Snauwaert, J., Rubens, P., Vermeulen, G., Hennau, F., and Heremans, K. 1998. *In situ* Microscopic Observation of Pressure-Induced Gelatinization of Starch in the Diamond Anvil Cell. In *High Pressure Food Science, Bioscience and Chemistry*, N. S. Issacs. Reading, UK: The Royal Society of Chemistry, 457-466.

Soto, A., Arce, A., and Khoshkbarchi, M.K. 1998. Experimental Data and Modeling of Apparent Molar Volumes, Isentropic Compressibilities and Refractive Indices in Aqueous Solutions of Glycine + NaCl. *Biophysical Chemistry* 74:165-173.

Stoforos, N.G., Crelier, S., Robert, M.C., and Taoukis, P.S. 2002. Kinetics of Tomato Pectin Methylesterase Inactivation by Temperature and High Pressure. *Journal of Food Science* 67 (3):1026-1031.

Stokes, R.H., and Robinson, R.A. 1966. Interactions in Aqueous Nonelectrolyte Solutions. I. Solute-Solvent Equilibria. *The Journal of Physical Chemistry* 70 (7):2126-2131.

Stolt, M., Stoforos, N.G., Taoukis, P.S., and Autio, K. 1999. Evaluation and Modeling of Rheological Properties of High Pressure Treated Waxy Maize Starch Dispersions. *Journal of Food Engineering* 40:293-298.

Sun, T.F., Kortbeek, P.J., Trappeniers, N.J., and Biswas, S.N. 1987. Acoustic and Thermodynamic Properties of Benzene and Cyclohexane as a Function of Pressure and Temperature. *Physical Chemistry of Liquids* 66:163-178.

Swalin, R.A. 1972. *Thermodynamics of Solids*. New York, US: Wiley-Interscience, pp. 21-45, 53-84.

Symons, M.C.R. 2001. Water Structure: Unique but not Anomalous. *Philosophycal Transactions of The Royal Society of London A* 359:1631-1646.

Tait, M.J., Suggett, A., Franks, F., and Ablett, S. 1972. Hydration of Monosaccharides: A Study by Dielectric and Nuclear Magnetic Relaxation. *Journal of Solution Chemistry* 1 (2):131-151.

Takagi, T., and Teranishi, H. 1986. Ultrasonic Speeds in Liquid Phase of Dichlorotetrafluorethane (R114) Under High Pressure. *Journal of Chemical and Engineering Data* 31 (1):105-107.

Takeo, T., Kinugasa, H., and Ishihara, M. 1994. Application of Sterilization Technique by Hydrostatic High Pressure for Green Tea Drink. In *Developments in Food Engineering*, 2, edited by T. Yano, R. Matsumo and K. Nakamura. London: Blackie Academic Professional, 864-866.

Tammann, G., and Schwarzkopf, E. 1928. Die Anderung der Temperatur des Volumenminimuns von Wasser in Abhangigkeit vom Druck, Verglichen mit der von Losungen in Abhangigkeit vom der Konzentration. *Zeitschrif fur Anorganische und Allegemeine Chemie* 174:216-224.

Tanaka, Y., Yamamoto, T., Satomi, Y., Kubota, H., and Makita, T. 1977. Specific Volume and Viscosity of Ethanol-Water Mixtures Under High Pressure. *The Review of Physical Chemistry of Japan* 47 (1):12-24.

Taniguchi, Y., and Takeda, N. 1992. Pressure-Induced Secondary Structure of Proteins Studies by FT-IR Spectroscopy. In *High Pressure and Biotechnology*, 224, edited by R. Hayashi and C. Balny. La Grande Motte: John Libbey Eurotext / INSERM, 115-122.

Tauscher, B. 1995. Pasteurization of Food by Hydrostatic High Pressure: Chemical Aspects. *Lebensmittel -Untersuchung und -Forschung* 200:3-13.

Tewari, G. 2000. Under Pressure to Keep Food Fresher. *Resource* 7 (Nov.):11-12.

Tewari, G., Jayas, D.S., and Holley, R.A. 1999. High Pressure Processing of Foods: An Overview. *Sciences des Aliments* 19:619-661.

Ting, E., Balasubramaniam, V.M., and Raghubeer, E. 2002. Determining Thermal Effects in High Pressure Processing. *Food Technology* 56 (2):31-35.

Ting, E., and Farkas, D.F. 1995. Cost of Ultrahigh Pressure Food Pasteurization. In *High Pressure Technology*, W. A. L. a. L. Picqueur. New York: McGraw-Hill, 75-85.

Traff, A. 1998. New Development of High Pressure Equipment Reduces Processing Cost. In *High Pressure Food Science Bioscience and Chemistry*, N. S. Isaacs. Reading, UK: The Royal Society of Chemistry, 236-241.

Traff, A., and Bergman, C. 1992. High Pressure Equipment for Food Processing. In *High Pressure and Biotechnology*, 224, edited by C. Balny, R. Hayashi, K. Heremans and P. Masson. La Grande Motte: John Libbey Eurotext / INSERM, 509-513.

Urbani, R., Sussich, F., Prejac, S., and Cesaro, A. 1997. Enthalpy Relaxation and Glass Transition Behavior of Sucrose by Static and Dynamic DSC. *Thermochimica Acta* 304/305:359-367.

Van Dael, W., and Van Itterbeek, A. 1965. The Velocity of Sound in Dense Fluids. In *Physics of High Pressures and the Condensed Phase*, A. V. Itterbeek. Leuven, Belgium: North Holland, 297-357.

Van den Broeck, I., Ludikhuyze, L.R., Van Loey, A.M., and Hendrickx, M.E. 2000. Inactivation of Orange Pectinesterase by Combined High Pressure and Temperature Treatments: A Kinetic Study. *Journal of Agriculture and Food Chemistry* 48 (5):1960-1970.

Van den Broeck, I., Ludikhuyze, L.R., Van Loey, A.M., Weemaes, C.A., and Hendrickx, M.E. 1999. Thermal and Combined Pressure-Temperature Inactivation of Orange Pectinesterase: Influence of pH and Additives. *Journal of Agriculture and Food Chemistry* 47 (7):2950-2958.

Van Eldik, R., Asano, T., and Le Noble, W.J. 1989. Activation and Reaction Volumes in Solution. 2. *Chemical Reviews* 89 (3):549-688.

Van Itterbeek, A. 1965. *Physics of High Pressure and the Condensed Phase*. Amsterdam: North-Holland Pub.,

Van Ness, H.C. 1964. *Classical Thermodynamics of Non-Electrolyte Solutions*. New York, US: The MacMillan Co., 69-79, 87-110.

Van Riel, A., Rubens, P., Heremans, K., and Engelborghs, Y. 1997. Pressure and Temperature Stability of Holo- Apo-Form of *Nereis* Sarchoplasmic Calcium-Binding Protein Studied by Fourier-Transform Infrared Spectroscopy. In *High Pressure Research in Biosciences and Biotechnology*, K. Heremans. Leuven: Leuven University Press, 63-66.

Vardag, T., and Korner, J.P. 1997. Design and Configuration of Plants for The High Pressure Processing of Foods. In *High Pressure Research in the Biosciences and Biotechnology*, K. Heremans, C. Balny, J. Frank, R. Hayashi, M. Hendrickx and H. Ludwig. Leuven: Leuven University Press, 487-490.

Vermeulen, G., and Heremans, K. 1997. FTIR Study of Pressure and Temperature Stability of Proteins in Emulsions and Reversed Micelles. In *High Pressure Research in Biosciences and Biotechnology*, K. Heremans. Leuven: Leuven University Press, 67-70.

Wagner, W., and Pruβ, A. 1993. International Equations for the Saturation Properties of Ordinary Water Substance. Revised According to the International Temperature Scale of 1990. *Journal of Physical and Chemical Reference Data* 22 (3):783-787.

Wagner, W., Saul, A., and Pruβ, A. 1994. International Equation for the Pressure Along the Melting and Along the Sublimation Curve of Ordinary Water Substance. *Journal of Physical and Chemical Reference Data* 23 (3):515-525.

Walstra, P. 1996. Dispersed Systems: Basic Considerations. In *Food Chemistry*, O. R. Fennema. New York: Marcel Dekker, 95-156.

Weemaes, C. A., Ludikhuyze, L. R., Van Den Broeck, I., and Hendrickx, M. 1999a. Kinetic Study of Antibrowning Agents and Pressure Inactivation of Avocado Polyphenoloxidase. *Journal of Food Science* 64 (5):823-826.

Weemaes, C. A., Ludikhuyze, L. R., Van Den Broeck, I., and Hendrickx, M. E. 1998a. Effect of pH on Pressure and Thermal Inactivation of Avocado Polyphenol Oxidase: A Kinetic Study. *Journal of Agriculture and Food Chemistry* 46 (7):2785-2792.

Weemaes, C.A., De Cordt, S.V., Ludikhuyze, L.R., Van den Broeck, I., Hendrickx, M.E., and Tobback, P. P. 1997. Influence of pH, Benzoic Acid, EDTA, and Glutathione on the Pressure and/or Temperature Inactivation Kinetics of Mushroom Polyphenoloxidade. *Biotechnology Progress* 13 (1):25-32.

Weemaes, C.A., Ludikhuyze, L.R., Van Den Broeck, I., and Hendrickx, M.E. 1998b. High Pressure Inactivation of Polyphenoloxidases. *Journal of Food Science* 63 (5):873-877.

Weemaes, C.A., Ludikhuyze, L.R., Van den Broeck, I., and Hendrickx, M.E. 1999b. Influence of pH, Benzoic Acid, Glutathione, EDTA, 4-Hexylrsorcinol, and Sodium Chloride on the Pressure Inactivation Kinetics of Mushroom Polyphenol Oxidase. *Journal of Agriculture and Food Chemistry* 47 (9):3526-3530.

Wilson, W. D. 1959. Speed of Sound in Distilled Water as a Function of Temperature and Pressure. *The Journal of the Acoustical Society of America* 31 (8):1067-1072.

Yamagushi, T., Yamada, H., and Akasaka, K. 1996. High Pressure NMR Study of Protein Unfolding. In *High Pressure Bioscience and Biotechnology*, 13, edited by R. Hayashi and C. Balny. Amsterdam, NE: Elseveier Science, 141-152.

Yasuda, A., and Mochizuki, K. 1992. The Behavior of Triglycerides Under High Pressure: The High Pressure Can Stably Crystallize Cocoa Butter in Chocolate. In *High Pressure and Biotechnology*, C. Balny, R. Hayashi, K. Heremans and P. Masson. La Grande Motte: John Libbey Eurotex / INSERM, 255-260.

Yuste, J.; Pla, R.; Capellas, M.; Sendra, E.; Beltran, E.; Mor-Mur, M. 2001. Oscillatory High Pressure Processing Applied to Mechanically Recovered Poultry Meat for Bacterial Inactivation. *Journal of Food Science* 66 (3):482-484.

Zhang, W., Biswas, S.N., and Schouten, J.A. 1992. Compressibility Isotherms of Helium-Nitrogen Mixtures at 298.15 K and up to 10 kbar. *Physica A* 182:353-364.

Zhao, Y., A., Flores R., and Olson, D. G. 1998. High Hydrostatic Pressure Effects on Rapid Thawing of Frozen Beef. *Journal of Food Science* 63 (2):272-275.

Zimmerman, F., and Bergman, C. 1993. Isostatic High Pressure Equipment for Food Preservation. *Food Technology* 47 (6):162-163.

BIOGRAPHICAL SKETCH

Roger Darros Barbosa was born in Campinas, State of São Paulo, Brazil on April 04, 1957. He received his bachelor's degree in food engineering at the State University of Campinas (UNICAMP) in 1979. After a 5-year period working for the food industry, including the cereal, candy and chocolate sectors, he returned to academics and completed his master's degree in food engineering at UNICAMP. He was then appointed at Paulista State University (UNESP) in the city of São José do Rio Preto, State of São Paulo, Brazil, as Teaching Assistant in 1987; and then in 1993 as Assistant Professor at the same university, where he taught food engineering-related courses such as Unit Operations for the Food Industry and Industrial Plant Design. In 1998, Roger came to the University of Florida to pursue a doctoral degree in food science with emphasis in food engineering. Roger joined Dr. Balaban and Dr. Teixeira's research group to work with the 'hidden' fundamentals of high-pressure food processing. After earning his doctoral degree at UF he will rejoin the teaching and research team in food engineering at UNESP.